Metabolism in Vascular Endothelial Cells: Effects of Hyperglycaemia, Pro-Inflammatory Cytokines and Polyphenols

Besim Ozyel, M.Sc

Institute of Food Research

A thesis submitted to the University of East Anglia for the degree of Doctor of Philosophy

September 2013

Abstract

<u>Hypothesis:</u> Dietary polyphenols can overcome the deleterious effects of hyperglycaemic or inflammatory conditions on the vascular endothelium by modulating endothelial cell metabolism.

<u>Results:</u> First, the effects of high-glucose concentrations, inflammatory cytokines and polyphenols on markers of endothelial cell function in HUVECs were explored. Hyperglycaemic conditions did not significantly affect cell proliferation or cell adhesion molecule expression (CAM), whereas TNF-α and IL1-β caused significant increases in cell adhesion molecule expression by HUVECs. Different polyphenols induced different responses, pro- and anti-inflammatory, depending on the concentration and period of exposure. Pre-treatment with the flavonol quercetin significantly reduced CAM expression in HUVECs.

Next, the ability of quercetin to overcome the pro-inflammatory effects of hyperglycaemia and cytokine treatments in HUVECs was investigated using a metabolomics approach with a view to understand the effects at a mechanistic level. As a result, significant changes in HUVEC metabolome in response to treatment with high-glucose concentrations or TNF-α have been demonstrated. Increases in lactate concentrations occurred under inflammatory conditions. Further, it was shown that quercetin could shift the lactate concentrations back towards that of the resting cells and also increase inosine concentrations, which is in keeping with an anti-inflammatory action. Quercetin treatments alone were shown to reduce concentrations of the pro-inflammatory metabolites ATP and ADP and, in parallel, increase concentrations of the anti-inflammatory metabolites adenosine and inosine.

Subsequently, quercetin metabolites inside the cells and in the culture medium after quercetin treatments were identified, and their effects on the activities of enzymes involved in purine metabolism enzymes were investigated. The inhibition of adenosine deaminase and CD73 activities with physiological cellular concentrations of quercetin was consistent with the elevations observed in adenosine and AMP levels.

<u>Conclusions:</u> Quercetin treatments reversed the effects of high-glucose and TNF-α on energy metabolite profiles. Quercetin was shown to enter the cells, and quercetin and its metabolites inhibited enzymes involved in purine metabolism, which is likely the underlying mechanism.

List of Contents

List of Figures

List of Tables

Abbreviations

ADA	Adenosine deaminase
ADP	Adenosine 5'-diphosphate
AFM	Atomic force microscopy
AKA	Adenosine kinase
AICAR	5-aminoimidazole-4-carboxamide-1-β-D-ribofuranoside
AMP	Adenosine 5'-monophosphate
APC	Allopyhycocyanin
ApoE -/-	Apolipoprotein E deficient
ATP	Adenosine 5'-triphosphate
BSA	Bovine serum albumin
BrdU	Bromodeoxy uridine
CAEC	Coronary artery endothelial cell
CAM	Cell adhesion molecule
CBG	Cystolic β-glucosidase
CD	Cluster of differentiation
CE	Cappillary Electrophoresis
COMT	Catechol-O-methyl transferases
DAD	Diode Array Detection
DMSO	Dimethyl sulfoxide
DP	Degree of polymerization
EDTA	Ethylenediaminetetraacetic acid
ELISA	Enzyme-linked immunoabsorbent assay

FITC	Fluorescein isothiocyanate
GlcA	Glucuronide
GSPE	Grape seed proanthocyanidin extract
HAEC	Human Arterial Endothelial Cell
HDL	High-density lipoprotein
HMDB	Human Metabolite Databank
HILIC	Hydrophilic Interaction Chromatography
HUVEC	Human umbilical vein endothelial cell
ICAM-1	Intercellular adhesion molecule 1
IL1-β	Interleukin 1-beta
IsoR	Isorhamnetin
LC -DAD	Liquid Chromatography
LDL	Low-density lipoprotein
LPS	Lipopolysaccharide
MS	Mass spectrometry
MRM	Multiple reaction-monitoring
NAD	Nicotinamide adenine dinucleotide
NO	Nitric oxide
NOS	Nitric oxide synthase
NMR	Nuclear magnetic resonance
PBS	Phosphate buffered saline
PC	Pyruvate carboxylase
PC	Principal component

PCA	Principal component analysis
PE	Phycoerythrin
PF	Photofrin
PI	Propidium iodide solution
PI3K	Phosphoinoside 3-kinase
PNP	Purine nuceleoside phosphorylase
PPM	Parts per million
PKCβ2	Protein kinase C β2
Q	Quercetin
SEM	Scanning electron microscopy
SBwE	*Sasa borealis* bamboo extract
SLGT-1	Sodium dependent glucose transporter-1
SULT	Sulfotransferase
SVEC	Saphenous vein endothelial cells
STZ	Streptozotocin
TNF-α	Tumor necrosis factor-alpha
TSP	Trimethylsilyl propionic acid
UGT	UDP-glucuronosyl transferases
VCAM-1	Vascular cell adhesion molecule 1
WHO	World health organization
2D	Two-dimensional

Symbols

D_2O	Deuterium oxide
g	Gram
h	Hour
^1H	Proton
IC_{50}	Half-maximal inhibitory concentration
MeCN	Acetonitrile
mg/g	Milligram per gram
mg/kg	Milligram per kilogram
mg/ml	Milligram per millilitre
mg/ 100 ml	Milligram per 100 millilitre
min	Minute
mM	Millimolar
ng/ml	Nanogram per millilitre
nM	Nanomolar
nm	Nanometre
Na_2HPO_4	Disodium phosphate
NaH_2PO_4	Sodium dihydrogen phosphate
NH_4OH	Ammonium hydroxide
rlu/s	Relative light units per second
μg	Microgram
μl	Microlitre
μg/ml	Microgram per millilitre

v/v   Volume per volume

w/w   Weight per weight

List of Publications and Prizes

Papers

In preparation.

Posters

Ozyel B., Kroon P. A. (2010). Effects of grape seed polyphenols on high-glucose-treated HUVECs, Norwich, UK, *Annual IFR Student Science Showcase*, May 2010

Ozyel B., Le Gall G., Colquhoun I., Bongaerts R., Kroon P. A. (2011). Investigation of protective roles of polyphenols in stressed vascular endothelial cells, Norwich, UK, *Annual IFR Student Science Showcase*, June 2011

Ozyel B., Le Gall G., Colquhoun I., Bongaerts R., Winterbone M., Kroon P. A. (2011). Evaluating the effects of polyphenols on hyperglycaemia- and inflammatory cytokine-challenged HUVECs using non-targeted ^{1}H NMR metabolic profiling, *Sitges, Spain, 5th International Conference on Polyphenols and Health, 16 - 20th Oct 2011*

Ozyel B., Le Gall G., Colquhoun I., Bongaerts R., Winterbone M., Kroon P. A. (2013). The effects of hyperglycaemia, inflammatory cytokines and dietary polyphenols on the HUVEC metabolome were assessed using non-targeted ^{1}H NMR metabolic profiling, Clermont-Ferrand, France, *2nd International Congress of Translational Research in Human Nutrition*

Ozyel B., Le Gall G., Philo M., Colquhoun I. J., Kroon P. A. (2013) Metabolism in vascular endothelial cells: effects of hyperglycaemia, pro-inflammatory cytokines and polyphenols, *Food and Health ISP Inaugural Annual Symposium*

Ozyel B., Le Gall G., Philo M., Colquhoun I. J., Kroon P. A. (2013). Evaluating the Effects of Polyphenols on Hyperglycaemia- and Inflammatory Cytokine-Challanged HUVECs: A Metabolomic Approach, Edinburgh, *National Institutes of Bioscience Conference*

Oral Presentations

Ozyel B. (2012). The effects of hyperglycaemia, inflammatory cytokines and dietary polyphenols on the human vascular endothelial cell metabolome assessed using non-targeted ^{1}H NMR profiling. Nantes, France, *6th French Network of Metabolomics and Fluxomics Meeting, 21st-24th May 2012*

Ozyel B. (2012). Investigation of Protective Roles of Polyphenols in Stressed Vascular Endothelial Cells. Norwich, UK, *Annual IFR Student Science Showcase*, 19th July 2012

Prizes

Travel grant from French Network of Metabolomics and Fluxomics to give an oral presentation at the *6th French Network of Metabolomics and Fluxomics Meeting*.

Travel grant from Nutrigenomics Organisation (NuGO) to present a poster at the *2nd International Congress of Translational Research in Human Nutrition*.

Acknowledgements

First of all, I would like to acknowledge and express my heartfelt gratitude to my supervisor   Dr Paul Kroon. I am indebted to him for allowing me to develop myself as an independent scientist while supporting me with his guidance, encouragement, and knowledge in the background during this project. He is a perfect role model for someone who wants to pursue a career in scientific world and bring impact to the field. I would like to thank also to my secondary supervisor Professor Richard Mithen for evaluating my work and contributing with his invaluable advices on the way.

The big part of the project involved metabolomics, and I would like to thank to IFR Metabolomics Team. Especially, the efforts of Dr Gwenealle Le Gall for introducing the essentials of metabolomics to me and her contributions to my personal development are well appreciated.

The Polyphenols and Health group have shown me how friendship and scientific collaboration should be during my time at IFR. I would like to thank to Mark Winterbone for his helps especially during my first days at IFR, to Dr Shikka Saha for her helps that made me confident using HPLC systems and to Dr Paul Needs for his extremely explanatory approaches in any chemistry related issues I had. Also, I would like to acknowledge the BBSRC for providing the funding that made the project possible.

When I left Cyprus at the age of 17, I promised to develop myself as a fully independent scientist. In the past 8 years, I always felt the support of my close friends on the way. Therefore, it is necessary to acknowledge my dudes Cangil, Cagri, Cemil, Dogkan, Dervis, Emrah ,Huseyin, Mertkan, Osman, Sevket, and my dudette Ezgi.

Finally, I would like to acknowledge the most valuable people in my life, my parents and my little brother. My mother protected me from everything and everyone since I was born. My father was always there whenever and wherever I needed him. My little brother is usually a pain, but being another fanatic Fenerbahce supporter makes him bearable.

CHAPTER 1: General Introduction

1.1 Scope of the Project and Structure of the Thesis

The research project described in this thesis was an investigation of the ability of selected dietary polyphenols to overcome the deleterious effects of hyperglycaemia and inflammatory cytokines on vascular endothelial cells, with a particular focus on elucidating underlying mechanisms. At the beginning of the project, the effects of hyperglycaemic conditions and inflammatory cytokines on established physiological markers of endothelial function and the ability of selected polyphenols to prevent these negative changes were assessed (Chapter 2). In the subsequent results chapters (Chapters 3-5) the research followed a logical path but the approaches were quite distinct. As a result, the thesis is presented with a general introduction that explains the relationship between diabetes/metabolic syndrome and atherosclerosis, and to introduce polyphenols (Chapter 1) and then a series of four results chapters that each contains an 'Introduction' section (to describe the state of the art and develop a hypothesis) and a 'Materials and Methods' section detailing the distinct methods used in the research. The thesis is completed with a 'General Discussion' chapter.

1.2 Diabetes, Metabolic Syndrome and Atherosclerosis

Many people around the world suffer from morbidity and mortality caused by cardiovascular disease (CVD). According to the World Health Organization (WHO) statistics, ≈17.3 million people died from CVDs in 2008 (Causes of death 2008, WHO). Coronary heart disease (heart attack) and cerebrovascular disease (stroke) were responsible for the 7.3 million and 6.2 million of the deaths, respectively. However, the key fact underlying these two diseases is the atherosclerotic disease.

1.2.1 Atherosclerosis

Atherosclerosis is the disease of large- and medium-sized arteries which involves the formation of atherosclerotic plaques in the arterial vessel walls over many

years as a result of complex pathological processes. These plaques contain endothelial cells, smooth muscle cells, leukocytes, foam cells, connective tissue elements, cholesterol, calcium and cell debris, which gradually leads to the focal thickening of the intima (innermost layer of the artery) disturbing the blood flow (Stary et al., 1994, Steinberg, 2002, Bobryshev, 2006, Ross, 1993, Ross, 1999). The atherosclerotic plaque bears the risk to break down forming blood clots that may enter coronary artery or brain leading to a heart attack or a stroke, respectively. The metabolic risk factors of atherosclerosis include hypertension, diabetes, high-cholesterol and obesity (Steinberger and Daniels, 2003, Selvin et al., 2005).

The complex nature of atherosclerosis indicates that the components of the vascular, metabolic and immune systems work in a harmony to modulate the development and progression of the disease. Atherosclerosis was originally considered as an ordinary lipid storage disorder (Libby et al., 2002). However, the studies that have been carried out in the last decade have underlined the promoting role of inflammation on the development and progression of atherosclerosis (Ross, 1999, Mannarino and Pirro, 2008). The initiation of atherosclerosis involves the accumulation of low-density lipoproteins (LDL) in the intima of the arteries which leads to the activation of the endothelium initiating an inflammation cascade that recruits circulating leukocytes and induces production of growth factors augmenting cell migration and proliferation (Berliner et al., 1995). The activation of endothelial cells stimulates the expression of cell adhesion molecules on the cell surface that favours the adhesion of circulating leukocytes to the site of activation. The attachment follows migration of the cells into the subendothelial space due to the increased chemokine production. Once the monocytes are in the intima, they differentiate into machorphages which express high levels of scavenger and Toll-like receptors. Scavenger receptors are responsible for the uptake of oxidized-LDL (oxLDL) into the macrophages together with apoptotic cell fragments that leads to foam cell formation. At the same time, Toll-like receptors modulate macrophage activation and production of pro-inflammatory cytokines, proteases and radical molecules. T lymphocytes (T cells) also accumulate in the atherosclerotic plaques, and they differentiate mainly into T-helper 1 cells. T-helper 1 cells produce interferon-ϒ (IFN-γ) that in turn stimulates pro-inflammatory cytokine production such as tumor necrosis factor-α

(TNF-α) and interleukin-1β (IL-1β). Therefore, all these processes contribute to the progression of the inflammatory state, and they are triggered by damage to the endothelial layer. Both diabetes and insulin resistance bear the potential to impair endothelial function.

1.2.2 Diabetes Mellitus and/or Metabolic Syndrome Are Risk Factors for CVD

Diabetes mellitus and metabolic syndrome patients are particularly at high risk to experience morbidity and mortality due to atherosclerosis and CVD (Haffner et al., 1998, Beckman et al., 2002, Lakka et al., 2002).

The characteristic feature of diabetes is hyperglycaemia. Insulin is a hormone that is produced by β-cells in pancreas, and it regulates blood glucose levels. Consequently, a defect in insulin production, action or both leads to diabetes mellitus. Danaei and co-workers estimated that overall 347 million people worldwide have diabetes according to the data obtained from health examination surveys and epidemiological studies (370 country-years and 2.7 million participants) (Danaei et al., 2011). WHO estimated that 3.4 million people died from consequences of fasting high blood glucose in 2004 (Global health risks, 2009), and anticipated that diabetes will be the 7th leading cause of death in 2030 (Global status report on noncommunicable diseases, 2010).

On the other hand, metabolic syndrome signifies a group of metabolic disorders including obesity, microalbuminuria, dyslipidemia, glucose intolerance and hypertension in addition to insulin resistance that is remarked as the main component of the disease (Roche et al., 2005, Cersosimo and DeFronzo, 2006). The metabolic syndrome is frequently observed also in people with type 2 diabetes (Navar et al, 2012), and it contributes to the risk of CVD (Alexander et al., 2003). Interestingly, the CVD risk with diabetes type 2 is greater than metabolic syndrome alone (Alexander et al., 2003). Furhermore, the existence of CVD risk with diabetes type 1 (Mangar et al., 2001) which lacks the additional risk factors of metabolic syndrome indicated that the hyperglycaemia is responsible for the CVD risk.

Therefore, the remarkable point is that the pathogenesis of atherosclerosis and CVD is the same regardless of the presence of hyperglycaemia and/or insulin resistance in individuals. Nevertheless, diabetes and metabolic syndrome effectively accelerate the pathogenesis of atherosclerosis and thus elevate the rate at which underlying atherosclerosis leads to cardiovascular events such as heart attacks and strokes (Reusch and Draznin, 2007, Ginsberg, 2000). In consequence, this provides a strong rationale for undertaking research concerned with determining the molecular/biochemical processes by which metabolic disorders (diabetes and metabolic syndrome) affect the development and progression of atherosclerosis to be able to develop suitable drugs or natural products that are capable of preventing atherosclerosis or diabetes/metabolic syndrome induced increases in the rate of disease development.

1.2.3 Endothelial Dysfunction Initiates Atherosclerotic Plaque Formation

The endothelium is a barrier lining all the blood vessels in the body and it plays essential roles in regulating vascular tone and structure by controlling the interaction between the blood and tissues (Landmesser et al., 2004). The endothelium lines a number of different types of vessels each with distinct functions and, accordingly, the functions of the endothelium vary according to which type of vessels it is lining. The aorta and the carotid/coronary/brachial/femoral arteries represent conduit arteries where the endothelium is required to maintain a limited activation of clotting and pro-inflammatory factors to inhibit the release of chemokines/cytokines/ growth factors and to prevent the adhesion of platelets and monocytes to the vascular endothelium (Cersosimo and DeFronzo, 2006). Furthermore, the endothelium contributes to the regulation of blood flow and the systemic blood pressure in the resistant arteries and to the transport and distribution of nutrients and hormones in the precapillary arterioles. Therefore, significant endothelial dysfunction may lead to the development and progression of the atherosclerosis at any levels in the arterial system (Cersosimo and DeFronzo, 2006).

Diabetes and metabolic syndrome are two disorders which have the capacity to damage the endothelium leading to the development and progression of atherosclerosis. The hyperglycaemic conditions experienced during diabetes

mellitus induce vascular endothelial cell apoptosis and this is thought to disrupt the integrity and functions of the endothelium and lead to vascular endothelial dysfunction. Vascular endothelial dysfunction is associated with atherosclerosis and is an independent risk factor for CVD (Hansson, 2005). The vascular endothelium is a dynamic structure that modulates vasodilation through endothelium derived relaxation factors nitric oxide (NO), prostacyclin and endothelium derived hyperpolarization factor (EDHF) under normal circumstances, and endothelial dysfunction is often reflected as the reduced bioavailability and therefore impaired vasodilator effect of these endothelium-derived relaxation factors together with increased endothelin-1 which is a potent vasoconstrictor known with pro-inflammatory effects (Böhm and Pernow, 2007).

Vascular endothelial dysfunction is believed to be modulated and enhanced by the reactive oxygen species (ROS), and it is therefore likely that the negative effects of hyperglycaemia on the endothelium are at least in part due to its effect of increasing free radical production (Tesfamariam, 1994). Progressive oxidation of glucose under physiological conditions yields hydrogen peroxide (H_2O_2) together with several reactive intermediates including hydroxyl-free radicals (Wolff and Dean, 1987). Thus, oxidative stress provides a link between diabetes and endothelial cell dysfunction (Cosentino et al., 1997, Son, 2007). Hyperglycaemia leads to alterations in several biochemical pathways such as glucose oxidation, generation of advanced glycation end-products (AGE), and activation of polyol pathways that all may be linked to the gradually elevated ROS generation; this eventually appears as an increased oxidative stress leading to endothelial dysfunction due to the triggering of the stress-sensitive intracellular pathways unless the endogenous antioxidants are able to balance the condition (Hink et al., 2001, Son, 2007, Ceriello, 2003).

The potent vasodilator, nitric oxide, is produced by nitric oxide synthase (NOS) enzymes, and it is essential for maintaining vascular function and structure (Son, 2007). According to published clinical studies, diabetes has an adverse effect on endothelium-dependent vasodilation (Williams et al., 1996). Superoxide is an effective enhancer of endothelial oxidative stress, and is produced by NAD(P)H oxidases and uncoupled endothelial nitric oxide synthase (eNOS) (Son, 2007). The activity of NAD(P)H oxidases is enhanced by hyperglycaemia, AGE, and

oxidized LDL (oxLDL); protein kinase C (PKC) is involved in the activation of NAD(P)H oxidases by hyperglycaemia and non-esterified free fatty acids (FFA) (Chisolm and Steinberg, 2000, Evans et al., 2002). Also, it has previously been reported that superoxide generation is elevated in vessels isolated from diabetic patients compared to non-diabetic control subjects, and at the same time increased expression of several NAD(P)H oxidase protein subunits were detected supporting the observation that NAD(P)H oxidases are more active in diabetes (Guzik et al., 2002). Beside leading to oxidative stress by itself, superoxide, is also capable of reacting with nitric oxide (NO$^\bullet$) yielding peroxynitrite (Milstien and Katusic, 1999). This may appear as reduced tetrahydrobiopterin (BH$_4$) concentrations if peroxynitrite reacts with BH$_4$ causing its oxidation. As a consequence, this would limit availability of BH$_4$ for eNOS coupling and lead to superoxide generation because eNOS would transfer electrons to molecular oxygen instead of generating NO$^\bullet$ by transferring electrons to L-arginine (Milstien and Katusic, 1999, Guzik et al., 2002). There are several literature reports of the presence of uncoupled eNOS in diabetic subjects and also decreased BH$_4$ availability in diabetic rats. Guzik and co-workers demonstrated the presence of uncoupled eNOS in diabetic vessels by incubating the vessels with the eNOS inhibitor; NG-nitro-L-arginine methyl ester (L-NAME) (Guzik et al., 2002). After incubation, the observed reduction in superoxide generation supported the notion that eNOS was uncoupled in the diabetic vessels. Further, supplementation of diabetic patients with BH$_4$ was shown to maintain endothelial function (prevent diabetes-induced endothelial dysfunction), thus supporting a role for uncoupled eNOS in endothelial dysfunction (Vásquez-Vivar et al., 1998, Milstien and Katusic, 1999, Guzik et al., 2002). In another study which compared normal mice with transgenic mice over-expressing GTP-cyclohydrolase I (GTPCH), which is the rate limiting enzyme for BH$_4$ synthesis, showed that endothelial function was maintained after treating mice with streptozotocin (STZ) to induce diabetes whereas endothelial function was not maintained in the diabetic rats that had low BH$_4$ availability (Vásquez-Vivar et al., 1998). Kim and co-workers further investigated the effects of high-glucose on the replication of large-vessel endothelium and showed a glucose-induced delay that could be overcome by superoxide dismutase, catalase and reduced glutathione, indicating the significance of oxidative stress in diabetes (Kim et al., 2002).

1.3 Polyphenol Consumption and CVD Risk

CVDs reduce the quality of life and the life span of individuals, and also have negative impacts on the national economies. According to the European Cardiovascular Disease Statistics 2012, over 1.9 million people per year die due to CVD in the European Union (EU), which accounts for the 40% of all deaths in the EU. The total burden of CVD for the EU economy was estimated as €196 billion a year, which was distributed as 54% to health care costs, 24% to productivity losses and 22% to the informal care of people with ongoing CVD (Nichols M, 2012). The report also indicated that fruit and vegetable consumption has increased across Europe in recent decades, while overall fat consumption has remained stable. Although fat consumption remained the same, increased fruit consumption was an optimistic observation that may lead to beneficial consequences since the epidemiological studies reported in the literature indicated that there is an association between diets rich in fruit and vegetables and a reduction in the incidence of CVD (Knekt et al., 2002, Bendinelli et al., 2011, Buijsse et al., 2010). For example, Buijsse and co-workers investigated the association of chocolate consumption with measured blood pressure and the incidence of CVD (Buijsse et al., 2010). Chocolate is a rich source of flavonoids (Corti et al., 2009), and the study has shown that low amounts of chocolate is associated with a lower risk of CVD that is reflected by a lower blood pressure. In another recent study, McCullough and co-workers investigated the association between flavonoid intake and CVD in a large, prospective cohort where a total of 38180 men and 60289 women were drawn from the subject population. 1589 CVD deaths in men and 1182 CVD deaths in women were observed during 7 years of follow up period. The authors concluded that the subjects with higher flavonoid intake possessed a lower risk of experiencing fatal CVD (McCullough et al., 2012). Also another prospective study which used postmenopausal women indicated that dietary intake of food rich in flavone, anthocyanidins and other flavonoids such as apples, bears, grapefruit, strawberries, chocolate and bran is associated with lower coronary heart disease and CVD risk (Mink et al., 2007).

Although the epidemiological studies indicated that there is an association between diets rich in fruit and vegetables and a reduction in the incidence of CVD, the degree of contribution and mechanisms of the individual fruit and vegetable

constituents with cardioprotective activities such as fibre, folate, potassium, antioxidants and phytochemicals such as carotenoids and polyphenols to the reduction in the incidence of CVD are not fully elucidated. Daily polyphenol intake is ~1 g, and that represents the highest intake value among all the phytochemicals (Scalbert and Williamson, 2000), and the human intervention studies further supported that increased polyphenol consumption is associated with reduced biomarkers of CVD such as blood pressure, platelet, function and blood lipid profiles (Hooper et al., 2008, Chong et al., 2010). For example, Erlund and co-workers investigated the effects of berry consumption which are rich in polyphenol content on hemostatic function, serum lipids, and blood pressure in middle-aged subjects with cardiovascular risk factors (Erlund et al., 2008). The subjects consumed 2 portions of berries daily for 8 weeks. According to the results, reduced blood pressure, increased HDL and prolonged PFA-100 CTs (inhibited platelet funtion) were observed indicating that regular berry consumption may improve vascular function preventing CVD. In, human intervention studies where the subjects were given tea and polyphenol rich extracts that contained mainly catechins, enhanced plasma antioxidant capacity and altered energy metabolism were observed (Gomikawa and Ishikawa, 2002, Dulloo et al., 1999). Similarly, in the human intervention studies where catechin and olimeric catechin rich food or extracts were given to subjects, increases in plasma antioxidant capacity together with other cardioprotective effects such as decreases in platelet aggregation, increases in nitric oxide (NO) production, decreased cell adhesion molecule expression and decreased LDL oxidation were observed (Pearson et al., 2002, Rein et al., 2000, Hollands et al., 2013).

Beside the intervention studies, there are numerous reports of in vitro studies concerned with the literature assessing the effects of polyphenols. In general, these provide some evidence that polyphenols have biological activities that are relevant in terms of preventing CVD. Nevertheless, the reported results need to be treated with some caution because most of these studies did not take bioavailability and metabolism factors into account (Kroon et al., 2004) and therefore the results may not reflect what occurs in vivo. The range of polyphenol concentrations reported to induce biological effects in vitro are across the range of 10-100 µM (Williamson and Manach, 2005). On the other hand, the physiological polyphenol concentration in plasma after a polyphenol-rich meal is unlikely to

reach 10 µM indicating that the concentrations used in the in vitro studies may be supraphysiological concentrations (Kroon et al., 2004). Therefore, bioavailability and metabolism of the polyphenol of interest should be carefully considered when devising in vitro studies and when interpreting the data arising from them.

1.4 Dietary Polyphenols

The plant kingdom members synthesize extensive amount of organic compounds. The compounds which aid the fundamental processes such as photosynthesis, respiration, growth and development fall into the group of plant primary metabolites (e.g. phytosterols, nucleotides and amino acids). On the other hand, plant secondary metabolites function in different manners such as protecting the plants from UV, acting as allelopathic agents and signalling molecules and also attracting attention which is particularly important for the plant protection and pollination (Crozier et al., 2006). The phytochemicals of particular interest in the studies reported here are the polyphenols. These are a very complex group of molecules that are ubiquitous secondary metabolites of plants (Scalbert et al., 2002, Shoji et al., 2005). They are synthesized in plants via shikimic acid pathway with an aromatic structure containing two or more hydroxyl groups (Arts and Hollman, 2005). This complex group of molecules are commonly consumed as part of the human diet since there are <100 polyphenols that have been identified in the plant food (Manach et al., 2004, Scalbert et al., 2005). Phenol-explorer (www.phenol-explorer.eu) is a comprehensive database on polyphenol content in foods, and Perez-Jimenez and co-workers used Phenol-explorer to estimate the individual polyphenol consumption of French adults in the diet of a cohort reporting a total number of 337 polyphenols consumed by the subjects (Pérez-Jiménez et al., 2011). Their carbon skeletons (number of phenol rings) and the structural elements involved in the binding of the phenol rings together are used to classify this group of molecules (D'Archivio et al., 2007). Phenolic acids, phenolic alcohols, flavonoids, stilbenes and lignans are the main classes of polyphenols (Figure 1.1).

Hydroxybenzoic acids

Hydroxycinnamic acids
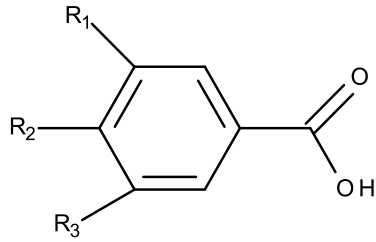
$R_1=R_2=OH, R_3=H;$ Protocatechuic acid
$R_1=R_2=R_3=OH;$ Gallic acid
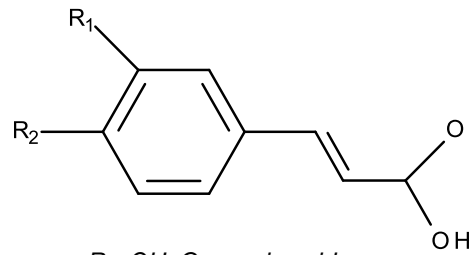
$R_1=OH;$ Coumaric acid
$R_1=R_2=OH;$ Caffeic Acid
$R_1=OCH_3, R_2=OH;$ Ferulic acid

Phenolic alcohols

Lignans

Secoisolariciresinol
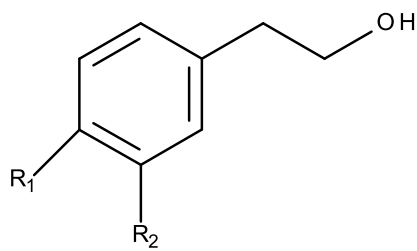
$R_1=OH, R_2=H;$ Tyrosol
$R_1=R_2=OH;$ Hydroxytyrosol
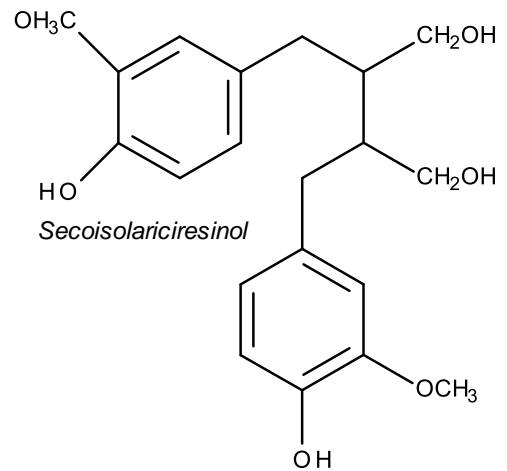
Stilbenes
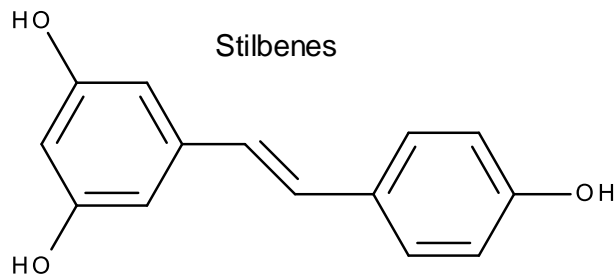
Resveratrol

Flavonoids
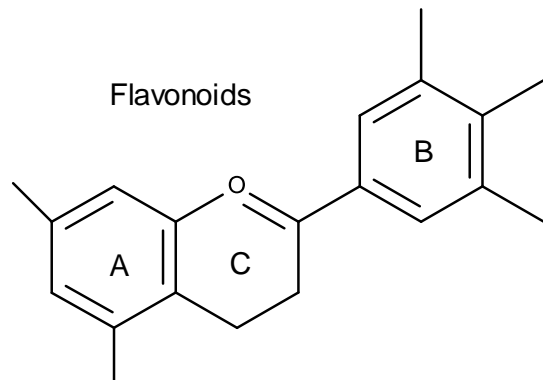
Figure 1.1: Chemical structures of main polyphenol classes.

Among these classes, flavonoids are the most abundant polyphenols in the plant kingdom (Crozier et al., 2006). Their structure involves a linear three-carbon chain binding two benzene rings (rings A and B) together (Figure 1.1). The three-carbon chain yields an oxygenated heterocycle (ring C), and according to its oxidation state flavonoids are divided into subclasses which are flavones, flavanones, isoflavones, flavonols, flavanols, and anthocyanidins (Figure 1.2) (Manach et al., 2004, D'Archivio et al., 2007).
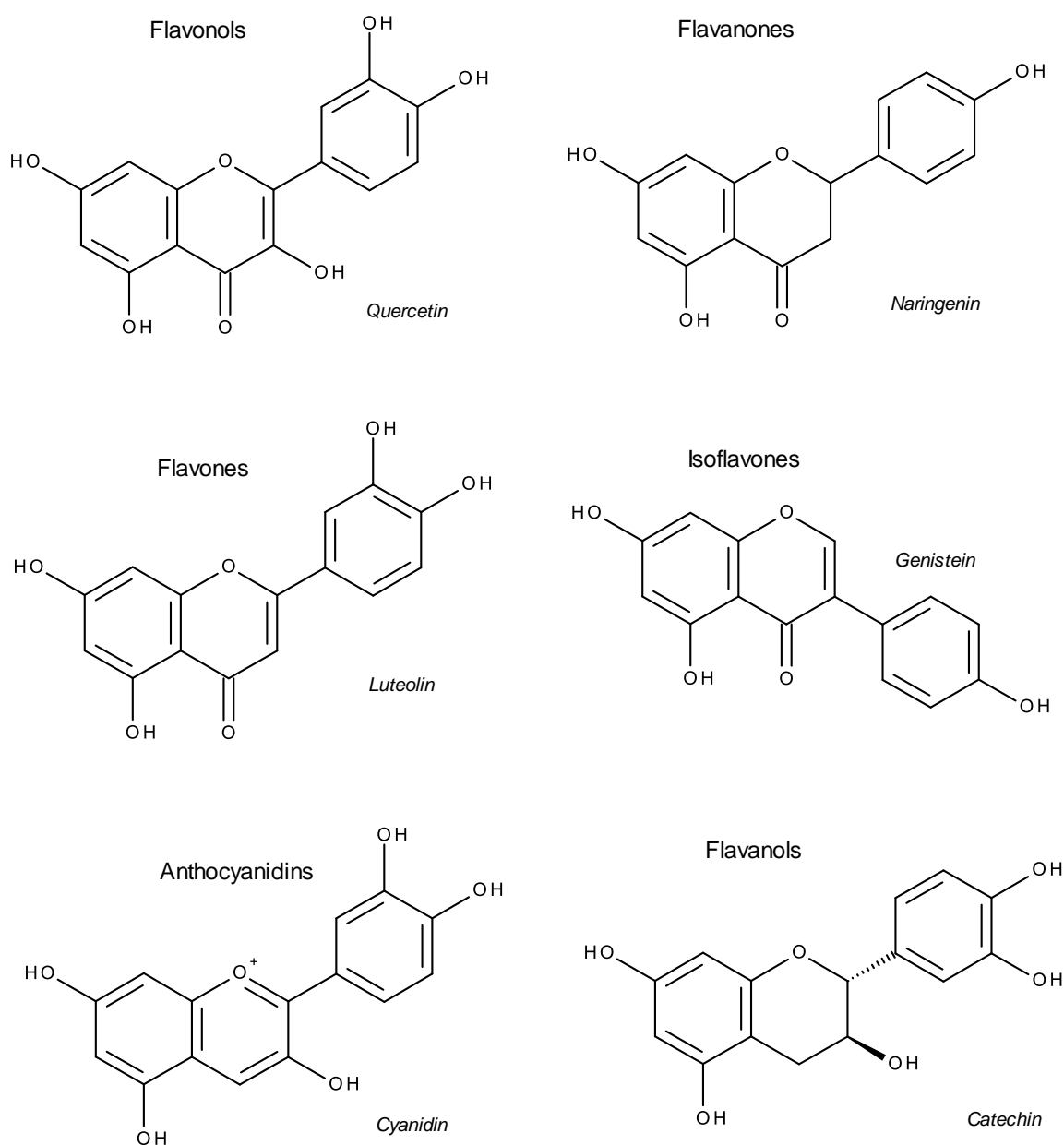
Figure 1.2: Flavonoid classes with example structures.

1.4.1 Bioavailablity, Absorption and Metabolism of Polyphenols

The generally acknowledged definition for bioavailability is simply the proportion of the polyphenol consumed that reaches the target tissue (D'Archivio et al., 2007). Dietary polyphenols are found in different chemical forms, and both their structures and chemical forms in the food affect the rate and extent of their absorption, metabolism and bioavailability in the circulation (Scalbert et al., 2005). They mostly exist in the form of esters, glycosides or polymers in the food. For example, all flavonoids (except flavanols) are found in the diet as glycosides. The glycosides that reach the small intestine are hydrolysed by lactase phloridzin hydrolase (LPH) in the brush border of intestinal epithelial cells which allows lipophilic aglycones to passively diffuse into the cells (Day et al., 1998, Day et al., 2000, Németh et al., 2003) or by the cytosolic β-glucosidase (CBG), depending on the nature of the sugar moiety attached to the polyphenol (Gee et al., 2000). It has been postulated that flavonoid glycosides could enter the cells via the sodium dependent glucose transporter-1 (SLGT1) (Hollman et al., 1995, Gee et al., 2000). Nevertheless, not all the flavonoids are absorbed in the small intestine. For example, flavonol glycosides such as rutin (a rhamnose group attached to quercetin) are not absorbed from the small intestine and pass the colon where they are hydrolysed by the colonic microbiota prior to absorption (Del Rio et al., 2013).

The newly formed aglycones are further modified as a result of the activities of sulfotransferases, catechol-O-methyl transferases and UDP-glucuronosyl transferases in the small intestine or liver before entering into the systemic circulation (Mullen et al., 2006). The sulfotransferases (SULT) are responsible for the addition of a sulfate moiety by substituting a hydroxyl group on the polyphenol to form a flavonoid-O-sulfate. The catechol-O-methyl transferases (COMT) are responsible for the addition of methyl groups to the polyphenols, but are only able to methylate catechol functional groups (adjacent hydroxyl groups on a benzene ring). Finally, UDP-glucuronosyl transferases (UGT) are responsible for catalysing the O-substitution of glucuronic acid to polyphenols. All three of the enzymes have been reported to be active in the small intestine (Murota and Terao, 2003, Chen et al., 2003). After conjugation in the small intestine, polyphenols are either released back to the intestinal lumen or enter into the portal circulation and are transported to the liver where they are further metabolized (Olthof et al., 2003, Crozier et al., 2006, Del Rio et al., 2013). Finally, the conjugated polyphenols enter the systemic

circulation. In addition, the liver can secrete flavonoid conjugates via bile which may result in further deconjugation in the small intestine or metabolization in the colon by the colonic microflora. The metabolized polyphenols are then reabsorbed or excreted in the faeces or urine (Crozier et al., 2006, D'Archivio et al., 2007).
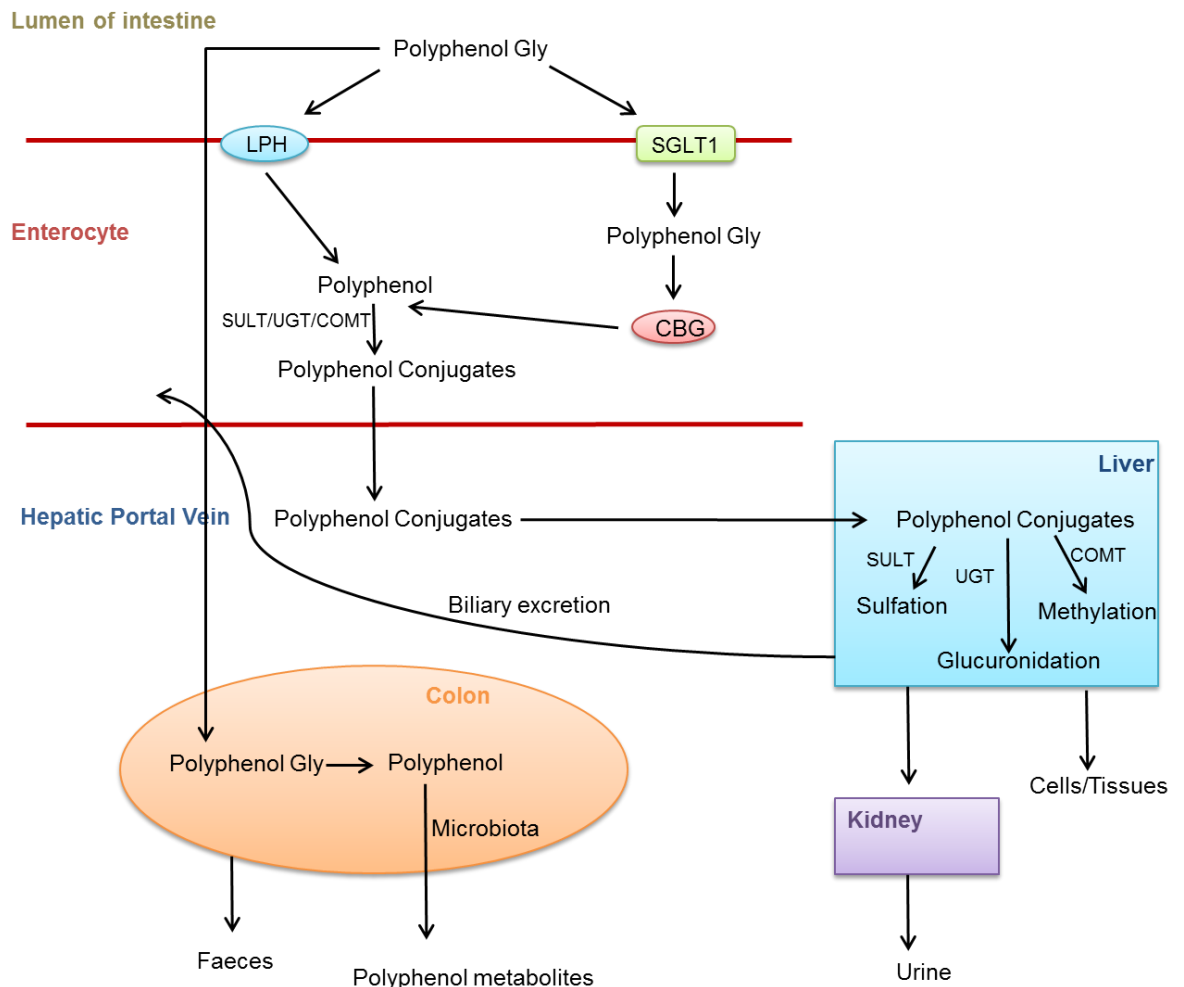
Figure 1.3: Absorption and metabolism of polyphenols. Sugar moieties are removed from the polyphenol glycosides in the small intestine or colon. The aglycones are conjugated by the enzymes SULT, UGT and COMT in the small intestine or hydrolysed by colon microbiota into smaller molecules. The conjugates from the small intestine pass into the liver for further conjugation. After being modified further in the liver, polyphenol conjugates are either secreted into systemic circulation or excreted by the kidneys via urine. SULT: sulfotransferase, UGT: UDP-glucuronosyl transferase, COMT: catechol-O-methyl transferases

1.4.2 Flavanols

The three-carbon chain is saturated in flavanols, and a hydroxyl group is attached to the 3-position (Figure 1.2). They are the most complex group of flavonoids, which are found both as monomers and polymers. The monomers are (+)-catechin and its isomer (−)-epicatechin. These monomers can be further hydroxylated in the B-ring yielding gallocatectins or esterified with gallic acid through the 3-position yielding a catechin gallate. The polymeric forms of flavonols are called proanthocyanidins (condensed tannins) which can be found as dimers, oligomers and polymers of the various flavanol monomer types which gives rise to different types of proanthocyanidins including procyanidins (polymers of catechin and epicatechin) and prodelphinidins (polymers of gallocatechin and epigallocatechin) according to the flavanol units present (BartolomÈ et al., 1996, Shoji et al., 2005, Gabetta et al., 2000).

In this project, the main interest was in the grape seed extracts. Grape seeds contain mainly catechin, epicatechin, procyanidins and their polymers and galloylated and gallated derivatives, which is equivalent to approximately 5% to 8% of the total grape seed weight (Ricardo da Silva et al., 1991, Prieur et al., 1994). The monomers catechin, epicatechin and epicatechin-3-O-gallate favour the formation of oligomeric procyanidins and higher polymers (Shi et al., 2003, Shoji et al., 2005). Procyanidin dimers and trimers are usually defined as B-series (procyanidin B1, B2, B3, B4 and B5) and C-series (procyanidin C1 and C2) respectively (Shi et. al., 2003). Several studies have shown that the degree of polymerization (dp) in procyanidins may reach quite high numbers. For example, procyanidins of up to a dp of 16 units were revealed using gel permeation chromatography and normal-phase HPLC by Prieur and co-workers (Prieur et al., 1994). However, the higher polymers may also be the products of the oxidative polymerization due to the extraction process (Shi et al., 2003). The higher the dp of procyanidins, the harder it becomes to separate, detect and identify the structure of the longer polymers (Robbins et al., 2009).

Polyhenols are antioxidants and reducing agents largely because their hydroxyl (OH⁻) groups are capable of donating hydrogen and they can gain an oxygen atom as they are singlet oxygen quenchers (Yao et al., 2004, Shi et al., 2003). At the same time, the antioxidant capacity of these free radical scavenger molecules is

also dependent on their solubilities (Rice-Evans et al., 1996) of which catechins are more lipid-soluble and procyanidins are more water-soluble (Shi et al., 2003). The bioavailability of the polyphenols may be correlated with the antioxidant capacity of the plasma as an indirect measurement of the degree of bioavailability (Scalbert and Williamson, 2000). Several studies showed the increased antioxidant capacity in the plasma following the intake of polyphenol-rich food (Duthie et al., 1998, Young et al., 1999, Rietveld et al. 2003). However more accurate investigation of the bioavailability of polyphenols involves the direct measurement of their concentrations in plasma and in urine (Scalbert and Williamson, 2000).

The absorption and metabolism of proanthocyanidins are not yet fully understood. Nevertheless, there is conflicting data on the absorption and metabolism of the flavonols and their polymers obtained by animal and human studies (Tsang et al., 2005). It has been shown that monomers and procyanidin dimers have much higher absorption efficiency through the gut whereas oligomers with higher dp are substantially less well absorbed (Sano et al., 2003, Baba et al., 2002, BladÈ et al., 2010). Kahle and co-workers investigated the metabolism of apple juice polyphenols in healthy ileostomy subjects (Kahle et al., 2007). Procyanidin profile in the content of ileostomy effluent represented the expected content that would be accumulated in the colon under physiological conditions. According to their observations, 90.3% of the procyanidins in the apple juice were recovered. The average dp of procyanidins was reduced compared to the procyanidins in the apple juice (dp 3.4 compared to dp 5.7, 2 hours after consumption). Also, a further study by the same group indicated that none of the dimeric procyanidins could be detected in the ileostomy content (Kahle et al., 2005). Therefore these observations alongside the study carried out by (Deprez et al., 2001) in which intestinal epithelial Caco-2 cells were used showing the retention of the procyanidin polymers (>dp3) on the Caco-2 cell layer whereas the monomers and dp2 and dp3 procyanidins were transferred across the monolayers of human intestinal epithelial Caco-2 cells, may indicate that the procyanidin polymers are cleaved to smaller oligomers and monomers and they are either absorbed through the small intestine or directed to the colon. Caco-2 cells form a monolayer, which mimics the function of the normal ileal enterocytes (Deprez et al., 2001).

Human microbiata have important functions in procyanidin metabolism. The higher dp procyanidins which are accumulated in the colon are subject to digestion by the colon microorganisms (Appledorn *et al.*, 2009). Although the microbial action in procyanidin metabolism has not been fully revealed yet, the degradation of the monomers (catechin and epicatechin) into phenolic acids which have been observed in the urine samples of people that consumed food containing high amounts of procyanidins signifies the importance of microbial digestion of procyanidins in the colon since the biological activities of procyanidins might be exerted via these metabolites (Gonthier et al., 2003, Appeldoorn et al., 2009). 2-(3,4-dihydroxyphenyl)acetic acid and 5-(3,4-dihydroxyphenyl)-γ-valerolactone represent the major metabolites produced by the digestion of procyanidins by gut microbiota (Appeldoorn et al., 2009).

The fraction of procyanidins that is not absorbed through the gut is also found to be effective in several aspects. Gulgun and co-workers administrated 100 mg/kg proanthocyanidin until the animals were intraperitoneally injected with methotrexate (20 mg/kg) to induce damage to the guts of the rats (Gulgun et al., 2010). The results revealed the possible antioxidant capacity of the proanthocyanidins in the gut as decreased jejunal damage and malondialdehyde levels, which may indicate an injury in the small intestine, were observed. Beside their antioxidant and anti-carcinogenic roles, proanthocyanidins which were not absorbed efficiently from the gut, were found to be effective immunomodualtors and anti-inflammatory agents (Ramiro-Puig and Castell, 2009, Romier et al., 2009) and to have antibacterial properties (Mayer et al., 2008).

1.4.3 Flavonols

Flavonols are the biggest contributor to flavonoid intake. The onions, curly kale, leeks, broccoli, and blueberries are rich sources for flavonols. Perez-Jimenez and co-workers reported that total polyphenol content of tea is 89-102 mg /100 ml according to the study where they determined the 100 richest sources of dietary polyphenols using Phenol-Explorer database (www.phenol-explorer.eu) (Perez-Jimenez et al., 2010). The authors referred black and green tea as the 52nd and 54th richest food, respectively. Generally the levels of flavonols in tea are up to 45 mg flavanols/L (Manach et al., 2004), and it has been reported that it is the main

source of flavonols in countries such as the UK and Netherlands where tea consumption is very high, tea is a major source of flavonols in the diet (Hertog et al., 1993). Red wine has been reported to contain up to 30 mg flavonols/L and is another important contributor to flavonol intakes (Manach et al., 2004). The flavonols are present in glycosylated forms (mainly with a glucose and/or rhamnose sugar attached). There is variation in flavonol contents of fruits from the same tree and even in the different sides of the same fruit since flavonol biosynthesis is stimulated by light (Manach et al., 2004, Crozier et al., 2006, D'Archivio et al., 2007). The main dietary flanovols (in order of abundance) quercetin, kaempferol, isorhamnetin and myricetin, and among these flavonols, quercetin is the flavonol of interest in the present study.

There are a very large number of published reports describing investigations of the potential physiological effects of quercetin. These range from chemical studies concerned with its ability to act as an antioxidant in aqueous and lipidic environments, through cell culture based experiments to determine its ability to affect cellular biomarkers that are thought to be related to disease risk or maintenance of healthy function, and feeding studies using animal models of human diseases, to human intervention studies where the impact of consuming quercetin on established disease risk factors/biomarkers has been assessed. (Egert et al., 2009, Tribolo et al., 2008, Galindo et al., 2012). These studies have shown that quercetin has the potential to induce a very large number of biological effects. For example, Dias and co-workers worked with streptozotocin-induced diabetic rats, and they observed decreases in oxidative stress, NF-κB activation, and also iNOS overexpression in liver after treating the rats with quercetin (150 μmol/kg, daily intraperitoneal injection) for 8 weeks (Dias et al., 2005). Nair and co-workers had observed a dose dependent inhibition of TNF-α production and gene expression in normal peripheral blood nuclear cells by preventing NF-κB activation, therefore, revealing anti-inflamatory properties of quercetin (Nair et al., 2006). Davis and co-workers demonstrated anti-pathogenic activities of quercetin. They assessed the effect of quercetin on exercise stress associated upper respiratory tract infection by feeding mice daily with 12.5 mg/kg quercetin for 7 days prior to infecting them with influenza. The results have shown that quercetin fed animals were less prone to respiratory infection (Davis et al., 2008). Erk and co-workers explored the alterations in the gene expression of Caco-2 cells after

quercetin treatments (5 µM). The results revealed alterations in the expression of genes involved in cell cycle and differentiation, apoptosis, tumor suppressor genes and oncogenes, cell adhesion and cell-cell interaction, transcription, signal transduction and energy metabolism. Furthermore, quercetin treatment downregulated cell proliferation and induced apoptosis in Caco-2 cells exposing the anti-carcicogenic potential of quercetin (Erk et al., 2005). Finally, several studies reported in the literature indicated the cardioprotective potential of quercetin. Chen and co-workers demonstrated that quercetin treatment protected cardiomyocytes (H9C2 cells) against the effects of ischemia/reperfusion injury. Quercetin achieved this by regulating Src kinase, FAK (focal adhesion kinase), and STAT3 (signal transducer and activator of transcription 2) that led to inhibition of inflammatory responses and maintaining cell physiology, including morphology, redox status, and metabolism (Chen et al., 2013).

All the studies mentioned above have tested the effects of quercetin aglycone. Nevertheless, quercetin is present in glycosylated forms in plants and food. Furthermore quercetin glycosides are modified upon absorption and then they are efficiently conjugated before entering the peripheral blood. There are several reports of the pharmacokinetics of quercetin in humans, and to date quercetin aglycone has not been detected in human plasma. Mullen and co-workers fed healthy human subjects lightly fried onions with a total polyphenol content of 275 µM (mainly quercetin 4'-glucoside and quercetin 3,4'-diglucoside) and collected plasma and urine samples over 24 h (Mullen et al., 2006). HPLC-MS analysis of plasma samples revealed that quercetin was metabolized to a number of quercetin conjugates with the three most abundant being quercetin 3'-O-sulfate (Q 3'-O-S), quercetin 3-O-glucuronide (Q 3-O-GlcA), isorhamnetin 3-O-glucuronide (IsoR 3-O-GlcA). A quercetin O-diglucuronide and a quercetin O-glucuronide-O-sulfate were also detected in the plasma samples, but their molecular structures were not identified. The metabolites were present in the circulatory system within 30 min of ingestion. Therefore, that indicated the removal of the glucose moieties in the gastrointestinal tract which was followed by the conjugations in the enterocytes with the activities of sulfotransferase, catechol O-methyl transferase and uridine-5'-diphosphate glucuronosyl-transferases prior to the release into the circulatory system. Another short-term human study, Egert and co-workers compared the effectiveness of quercetin enriched cereal bars and quercetin powder-filled hard

capsules in increasing plasma quercetin concentrations (Egert et al., 2012). Similarly, they observed an increase in plasma quercetin concentration in the first 30 min. However, they measured only the quercetin aglycone and methylquercetin aglycone levels since they treated the samples with a mixture of β-glucuronidase/sulfatese in order to hydrolyse any glucuronidated or sulfated conjugates prior to the HPLC analysis. Quercetin, isorhamnetin (3' O-methylquercetin) and tamarixetin (4' O-methyquercetin) were identified in the extracted plasma samples. On the other hand, a long-term study by Cialdella-Kam and co-workers assessed the dose-response to 3 months of quercetin-containing supplements on quercetin conjugation in adults (Cialdella-Kam et al., 2013). The supplements containing quercetin, vitamin C and niacin were given to the healthy adults as a soft chew to ingest twice a day for 3 months. Isorhamnetin 3'-O-glucuronide, quercetin 3'-O-glucuronide, quercetin 3'-O-sulfate and quercetin diglucuronide were the conjugates present in the plasma of the subjects supplemented with quercetin for 3 months.

Beside the effects of quercetin aglycone, its metabolites were also demonstrated to have beneficial effects. Day and co-workers assessed the effects of quercetin glucuronides on the xanthine oxidase and lipoxygenase activities (Day et al., 2000). Quercetin 4'-O-glucuronide was found to be a potent inhibitor of xanthine oxidase which was followed by quercetin 3'-O-glucuronide, quercetin 7-O-glucuronide and quercetin 3-O-glucuronide. Therefore, quercetin glucuronides may be effective in diminishing reactive oxygen species (ROS) production. Quercetin aglycone is a potent antioxidant, and also quercetin metabolites were observed to possess antioxidant activities. Shiari and co-workers showed that quercetin 3-O-glucuronide pre-treatment inhibited H_2O_2-induced production of intracellular ROS in mouse fibroblast 3T3 cultured cells (Shirai et al., 2002). Similarly, Loke and co-workers showed that quercetin and its metabolites (3'-O-methylquercetin and quercetin 3-glucuronide) had antioxidant activities at physiologically relevant concentrations (Loke et al., 2008). Neutrophil-mediated peroxidation of LDL was inhibited by quercetin (IC_{50}=1 μM) and its metabolites (IC_{50}= 2 to 4 μM). Therefore, a reduction in the inhibitory activity was observed when quercetin was conjugated. Lotito and co-workers investigated whether quercetin metabolites retain anti-inflammatory properties of the quercetin aglycone (Lotito et al., 2011). They measured the effects of quercetin metabolites on the

TNF-α-induced cell adhesion molecule expression in human aortic endothelial cells (HAECs). 3'-O-methyquercetin and 4'-O-methylquercetin were shown to inhibit expression of ICAM-1 at physiological concentrations. On the other hand, E-selectin expression was inhibited weakly and VCAM-1 expression was not affected. The other metabolites tested (quercetin 3-O-glucuronide and quercetin 3'-O-sulfate) did not retain the anti-inflammatory properties of quercetin. Similarly, Tribolo and co-workers showed that quercetin and its metabolites (Q 3'-O-S, Q 3-O-GlcA, IsoR 3-O-GlcA and the mixture of all metabolites) inhibited VCAM-1 at physiological concentrations (2 µM) in LPS/TNF-α stimulated HUVECs (Tribolo et al., 2008). However, ICAM-1 expression was inhibited only by quercetin (2 µM) and the mixture of all metabolites (10 µM). In contrast, quercetin metabolites (Q 3'-O-S, Q 3-O-GlcA and IsoR 3-O-GlcA) did not affect cell adhesion molecule expression in TNF-α activated human artery smooth muscle cells (Winterbone et al., 2009).

1.4.4 Stilbenes

In contrast to flavonols, stilbenes are present in relatively small quantities in the human diet and are only found in a very restricted number of foods. They are phytoalexins (self-defence agents) which are synthesised by plants in response to various infections (e.g. fungal, bacterial and viral) and also in response to several stress conditions (Crozier et al., 2006). Resveratrol is the most extensively studied stilbene which exists as both *cis* and *trans* isomers, and it appears mostly as *trans* resveratrol 3-O-glucoside (piceid) in plant tissues.

According to Burkon and Somoza, the resveratrol human metabolites identified in human plasma after feeding human subjects with a polyphenol-rich diet for 48 h were resveratrol 3-O-sulfate, resveratrol 3-O-glucuronide, resveratrol 4'-O-glucuronide, resveratrol diglucuronides and resveratrol disulfates (Burkon and Somoza, 2008). Furthermore, Bode and co-workers showed that after feeding human subjects with an oral dose of 0.5 mg *trans*-resveratrol/kg body weight, a portion of the unabsorbed *trans*-resveratrol was metabolized by colon microbiota (Bode et al., 2013). The identified metabolites were dihydroresveratrol, 3,4'-dihydroxy-*trans*-stilbene and 3,4'-dihydroxybibenzyl (lunularin). However, they observed that there were interindividual differences in metabolite production.

There are various in vitro studies demonstrating antioxidant, anti-carcinogenic and anti-inflammatory properties of resveratrol. Gulcin (2010) showed the in vitro antioxidant and radical scavenging power of resveratrol by employing several in vitro antioxidant assays including H_2O_2 scavenging activities, total antioxidant activity, reducing abilities, and Fe^{2+} chelating activities. Tang and co-workers demonstrated anti-carcinogenic effects of resveratrol on esophageal squamous cell carcinoma (ESCC) (Tang et al., 2013). They showed that 100 µM resveratrol treatments for 24 h significantly diminished ESCC cell growth and induced apoptosis. Furthermore, Storniolo and Moreno showed that resveratrol human metabolites retain the anti-carcinogenic effects of resveratrol aglycone. Resveratrol 3-O-sulfate, resveratrol 3-O-glucuronide and resveratrol 4'-O-glucuronide reduced Caco-2 proliferation dose-dependently (1-50 µM), and also induced apoptosis (Storniolo and Moreno, 2012). Wakabayashi and Takeda demonstrated anti-inflammatory effects of resveratrol using human coronary artery smooth muscle cells (HCASMCs) (Wakabayashi and Takeda, 2013). Resveratrol (1-50 µM) treatments dose-dependently diminished basal levels of monocyte chemoattractant prorein-1 (MCP-1), interleukin-6 (IL-6) and IL-8 which are important in the initiation of atherosclerotic plaque formation. Furthermore, the resveratrol treatments decreased the production of MCP-1, IL-6 and IL-8 also in the IFN-γ-stimulated HCASMCs.

There are several reported in vivo animal and human studies indicating the potential beneficial health effects of resveratrol. Baur and co-workers showed that resveratrol improves health and survival of mice on a high-calorie diet by inducing alterations such as increased insulin sensitivity, reduced insulin-like growth factor-1 (IGF-1) levels, increased AMP-activated protein kinase (AMPK) and peroxisome proliferator-activated receptor-γ coactivator 1α (PGC-1α) activity, increased mitochondrial number, and improved motor function (Baur et al., 2006). Brasnyo and co-workers assessed the effects of resveratrol on human type 2 diabetic patients. Patients were supplemented with 5 mg resveratrol twice daily for 4 weeks. The final assessments revealed a decrease in insulin resistance and urinary ortho-tyrosine excretion, and at the same time elevated the pAkt:Akt ratio in platelets. The authors concluded that resveratrol enhances insulin sensitivity in humans by regulating insulin signalling via Akt pathway as a consequence of a possible decrease in oxidative stress (Brasnyó et al., 2011).

1.5 The Potential of Polyphenols in the Prevention and Treatment of Diabetes and Metabolic Syndrome

A limited number of pre-clinical research studies using cell culture and animal models and clinical studies have reported the potential effects of the polyphenols in the prevention and treatment of diabetes and metabolic syndrome.

For example, Basu and co-workers investigated the effects of pomegranate polyphenols on both healthy and type 2 diabetic volunteers. The study involved consumption of 2 pomegranate capsules rich in ellagic acid (743 mg polyphenols each) daily for 4 weeks. Interestingly, pomegranate capsule supplementation caused a reduction in lipid peroxidation in diabetic subjects whereas there were no significant alterations in healthy subjects (Basu et al., 2013). In another study, Rizza and co-workers supplemented subjects with metabolic syndrome with flavonone hesperitin (500 mg/d orally for 3 weeks), and they observed that hesperetin caused anti-inflammatory effects reflected as reductions in circulating high-sensitivity C-reactive protein, serum amyloid A protein, soluble E-selectin (Rizza et al., 2011). Furthermore, hesperetin supplementation increased flow-mediated dilation in the patients indicating the anti-atherogenic effects of the polyphenol.

El-Alfy and co-workers focused on the protective effects of red grape seed proanthocyanidins against the oxidative stress which is assumed to be a promoting factor in the induction of diabetes due to pancreatic β-cell destruction by reactive oxygen species (ROS) (El-Alfy et al., 2005). Alloxan induced diabetic rats were given grape seed proanthocyanidins in normal saline by oral gavage. The grape seed proanthocyanidins treatment yielded a significant reduction in hyperglycaemia. Beside the decline in hyperglycaemia, an elevation in pancreatic glutathione levels and a reduction in lipid peroxidation that is the rate-limiting step in atherosclerosis implied that the anti-diabetic properties of the grape seed proanthocyanidins might be due to its antioxidant properties. Another study was focused on the insulomimetic properties of the grape seed proanthocyanidins. Feeding diabetic rats with grape seed procyanidins revealed a decrease in the level of glycaemia. Glucose uptake was shown to be enhanced by procyanidins in two insulin-sensitive cell lines, L6E9 (myoblasts) and 3T3-L1 (adipocyte like cells),

demonstrating that procyanidins may affect insulin-sensitive tissues. At the same time, the phosphoinoside 3-kinase (PI3K) inhibition by wortmannin treatment of cultured cells eliminated the anti-glycaemic effects of the procyanidins, indicating the insulomimetic property of the grape seed procyanidins (Pinent et al., 2004).

Culturing HUVECs in media with high-glucose concentrations is a widely used model for investigating the effects of hyperglycaemia on endothelial cell apoptosis. HUVECs experience increased apoptosis in hyperglycaemic conditions and this is associated with variety of changes in the cells that are important in the initiation and development of atherosclerosis. Generation of advanced glycation end products (AGE) (Goldin et al., 2006) and reactive oxygen species (ROS), increased cell adhesion molecules (CAMs) expression (Altannavch T. S., 2004), decreased eNOS and NO production (Eckel et al., 2002), increased matrix metalloproteinase production (Lee et al., 2008b) together with the activation of JNK (Kaneto Hideaki, 2004) and MAPK pathways (Hsieh et al., 2007, Yang et al., 2008) have all been observed in high-glucose treated HUVECs. Several plant natural products are found to be effective in reversing some of the effects of hyperglycaemia in HUVECs (Choi et al., 2008, Lee et al., 2008a, Hsieh et al., 2007). There are a number of reports indicating that polyphenol-rich extracts such as those from tea, bamboo, *Buddleja officinalis*, and guava leaves can reduce the high-glucose-induced increases in apoptosis and protect endothelial cells from damage (Lee et al., 2008a, Lee et al., 2008b, Choi et al., 2008). *Sasa borealis* bamboo extract (SBwE) is believed to have an effect on the pathways involving the activation of protein kinase C β2 (PKCβ2) and NAD(P)H oxidase. PKCβ2 and NAD(P)H are affected by high glucose leading to the production of ROS including superoxide and hence oxidative stress in the endothelial cells (Li and Shah, 2003). The inhibition of NAD(P)H oxidase induced PKC-dependent peroxynitrite formation by SBwE is believed to be responsible for the observed reduction in HUVEC apoptosis (Choi et. al., 2008). On the other hand, together with its anti-apoptotic effects, guava leaf sap has a high polyphenol content which was shown to be effective in the inhibition of glycative and autoxidative reactions yielding glyoxal and methylglyoxal that induce ROS production (Hsieh et. al., 2007). Another report indicated that quercetin metabolites (a mixture of quercetin sulfates and glucuronides from rat plasma) effectively and dose-dependently inhibited the high-

glucose-induced increase in apoptosis in HUVECs by inhibiting JNK and caspase-3 activity (Chao et al., 2009).

1.6 Rationale and Aims of the Research Project

The anti-inflammatory, anti-atherogenic, anti-apoptotic and antioxidant effects of polyphenols mentioned above indicated that polyphenols have the potential to attenuate the deleterious effects of high-glucose conditions, which are associated with diabetes (and metabolic syndrome). However, the current data concerned with mechanisms is scarce and rather fragmented, and the reports concerned with determining the effects of polyphenols on high-glucose-stressed endothelial cells have all taken a selective / targeted approach. Since (1) the effects of increased glucose concentrations on endothelial cells is multifaceted, and (2) polyphenols have been shown to work through multiple mechanisms and elicit a variety of changes in the functions of cells to which they are exposed, non-targeted holistic approaches such as transcriptomics, proteomics and metabolomics are likely to be effective approaches for determining the full range of responses and providing insights into the underlying mechanisms of action. Considering that the most important direct consequence of diabetic and metabolic syndrome states is hyperglycaemia, it seems likely that the negative effects of hyperglycaemia in the endothelium may be mediated through changes in cell metabolism.

Furthermore, apart from the one report that concerned an investigation into the potential for quercetin conjugates (physiological metabolites of this dietary flavonoid) to counter the deleterious effects of high-glucose on vascular endothelial cells (Chao et al., 2009), nothing is known of how the metabolism of polyphenols (that occurs during the first pass) influences their ability to protect endothelial cells from the effects of high-glucose.

Therefore, the overall aim in the study was to determine the ability of quercetin to overcome the pro-inflammatory effects of hyperglycaemia and cytokine treatments in HUVECs, with a view to understand the effects at a mechanistic level on the entire system. In order to achieve this, the effects of high-glucose concentrations, inflammatory cytokines and polyphenols on markers of endothelial function in HUVECs were explored (Chapter 2). That was followed by optimizing a protocol,

which facilitated quick and effective freezing of cellular metabolism, extraction of metabolites and analysis of extracted metabolites by employing the global analysis approach using ^{1}H NMR (proton nuclear magnetic spectroscopy) to produce non-biased and reproducible results (Chapter 3). The optimized ^{1}H NMR protocol was then used to investigate the effects of hyperglycaemia, inflammatory cytokines and polyphenol treatments on HUVEC metabolite profiles, and HILIC mode LC-MS/MS analysis was used to provide supplementary data (Chapter 4). The final results chapter (Chapter 5) describes the identification of quercetin metabolites inside the cells and in the culture medium after quercetin treatments, and reports their effects on the activities of enzymes involved in purine metabolism, in tubo and using intact HUVECs, which provided a plausible explanation of the polyphenol-induced alterations in HUVEC metabolite profile identified in Chapter 4.

CHAPTER 2: Effects of high-glucose, pro-inflammatory cytokines and polyphenols on endothelial cell function: Targeted experiments to test effects of polyphenols on inflamed HUVECs

2.1 Abstract

Background: Chronic exposure of the vascular endothelium to high-glucose conditions and/or inflammatory cytokines decreases endothelial function and leads to damage which eventually manifests as atherosclerosis. There is some evidence that dietary polyphenols can protect against cardiovascular disease, but the mechanisms are not well understood.

Aim: To explore the effects of high-glucose concentrations, inflammatory cytokines and polyphenols on markers of endothelial function in HUVECs.

Approach/methods: Cultured HUVECs were used as a model, and the medium was supplemented with high-glucose concentrations, cytokines and/or with polyphenols in order to investigate the effects of hyperglycaemia and inflammation on vascular endothelial cell function, and the potentially protective effects of polyphenols. Cell proliferation and cell adhesion molecule (CAM) expression were assessed as markers of endothelial cell function.

Results: Hyperglycaemic conditions did not significantly affect cell proliferation or CAM expression, whereas the inflammatory cytokines TNF-α and IL1-β caused significant increases in ICAM-1 and VCAM-1 expression (all $p<0.001$). Three different classes of polyphenols were assessed for their ability to alter cell proliferation and CAM expression in resting and stimulated (hyperglycaemia, inflammatory cytokines) HUVECs; flavanols from grape, the flavonol quercetin and the stilbene resveratrol. A grape skin extract containing (+)-catechin, (-)-epicatechin and procyanidin oligomers and polymers significantly increased bromodeoxyuridine (BrdU) incorporation at lower concentrations and decreased it at higher concentrations compared to the control (all $p<0.05$), whereas a grape seed extract containing mainly flavanol monomers, dimers and trimers was ineffective. Interestingly, the grape seed and skin extracts had no effects alone,

but worked in synergy with IL1-β to induce significant increases in ICAM-1 and VCAM-1 expression, respectively; synergistic increases in ICAM-1 were also observed for the grape seed extract with IL1-β ($p<0.01$). Pre-treatments with quercetin (10 & 25 μM) for 2 h and 6 h (but not 45 min) significantly decreased TNF-α-induced VCAM-1 ($p<0.05$) but not ICAM-1 expression. Resveratrol had no significant effect on ICAM-1 or VCAM-1 expression alone, but acted in synergy with TNF-α to significantly increase expression of both CAMs ($p<0.05$). In contrast, two human resveratrol metabolites (3-O-sulfate,3,5-di-O-sulfate) had no effect on ICAM-1 expression.

<u>Conclusion:</u> The inflammatory cytokines TNF-α and IL1-β induced significant changes in CAM surface expression, and the different polyphenols induced different responses, pro- and anti-inflammatory, depending on concentration and period of exposure.

2.2 Introduction

Several studies have provided evidence to show that high-glucose concentrations can affect endothelial cell proliferation. This effect of high-glucose may be the outcome of changes in several metabolic pathways. Varma and co-workers reported the effects of incubation of the HUVECs with 20 mM or 40 mM glucose containing media (Varma et al., 2005). These high-glucose concentrations in the media reduced cell proliferation significantly according to the results obtained on culture day 8 which showed log-phase growth possibly due to an alteration in the phosphoinositide 3-kinase (PI3K) and Akt signalling pathways. The authors proposed that the inhibition of tyrosine phosphorylation of PI3K and threonine 308-phosphorylation of Akt by high-glucose might be responsible for the uncoupling of PI3K-Akt signalling leading to proliferative dysfunction in the HUVECs (Varma et al., 2005). On the other hand, Chen and co-workers reported the effects of the incubation of HUVECs for 24 hours in media containing 28.5 mM glucose (high-glucose conditions) (Chen et al., 2007). Also, they investigated the effects of high glucose concentrations on the expression of p15^{INK4} which is a member of INK4 family of cyclin-dependent kinase inhibitors. The reduction in cell proliferation with the increased expression of p15^{INK4} protein due to high-glucose and also the attenuation of the reduction in the cell proliferation by the antisense p15^{INK4} oligonucleotide indicated that the high glucose-induced reduction in HUVEC proliferation might be dependent on the p15^{INK4} expression (Chen et al., 2007).

Both of these studies revealed a significant reduction in cell proliferation with the incubation of cells with high-glucose containing media. This is important since a possible reduction in endothelial cell proliferation may gradually lead to vascular endothelial dysfunction and initiation of atherosclerotic plaque formation. Therefore, cell proliferation was chosen as a parameter to test the potential anti-atherogenic effects of polyphenols on HUVECs under high-glucose concentrations in this project.

Atherosclerosis was originally and for quite some time considered as an unremarkable lipid storage disorder (Libby et al., 2002). However the studies that have been carried out in the last decade have underlined the promoting role of inflammation which has helped to the identification of a number of possible cellular and molecular mechanisms affecting the development and progression of

atherosclerosis (Ross, 1999). For example, binding of leukocytes to healthy endothelium is not favoured whereas an atherogenic diet initiates expression of cell adhesion molecules that enables binding of leukocytes to the endothelium, which is an important initial step in the inflammation process in the vasculature (Libby et al., 2002). Therefore, another important parameter is the expression of cell adhesion molecules (CAM) since these "sticky" proteins are vital for the initiation of atherosclerosis. This is because the formation of atherosclerotic plaques requires the recruitment of leukocytes, which are the mediators of host defences and inflammation at these sites (Libby et. al., 2002). VCAM-1, ICAM-1 and E-selectin are the three cellular adhesion molecules that are expressed on endothelial cells and leukocytes in response to inflammatory factors during atherosclerotic plaque formation (Davies et al., 1993, Blankenberg et al., 2003). VCAM-1 is the most important cell adhesion molecule involved in atherosclerotic plaque formation. Its affinity for leukocytes, particularly monocytes and T-lymphocytes, which are present in the emerging atherosclerotic plaques, reveals the importance of this molecule in the initiation of atherosclerosis (Liyama *et al.*, 1999). Also, Cybulsky and co-workers showed that reduced VCAM-1 expression is effective in reducing atherosclerotic plaque formation in mice (Cybulsky et al., 2001). Beside VCAM-1, two other molecules, ICAM-1 and E-selectin, have important roles in the initiation of atherosclerotic plaque formation (Davies et. al., 1993).

Several studies reported increased CAM expression in the cells grown in high-glucose medium (Piconi et al., 2004, Baumgartner-Parzer et al., 1995, Altannavch T. S., 2004). Therefore, in this chapter the objective was to explore the effect of high-glucose, pro-inflammatory cytokines and polyphenols on endothelial function markers in HUVECs using targeted experiments to test the hypothesis that the polyphenols can overcome the deleterious effects of hyperglycaemic or inflammatory conditions on the vascular endothelium.

2.3 Materials & Methods

2.3.1 Materials

The Cell Proliferation ELISA (chemiluminescent) was purchased from Roche Applied Science (West Sussex, UK). Propidium iodide solution (PI), lipopolysaccharide (LPS), paraformaldehyde, phosphate buffered saline (PBS), ethylenediaminetetraacetic acid (EDTA), sodium azide, bovine serum albumin (BSA), dimethylsulfoxide (DMSO), D-glucose, D-mannitol, quercetin and epicatechin were purchased from Sigma-Aldrich® (Poole, UK). Dichloromethane, methanol, acetic acid were all HPLC grade and obtained from Fisher Scientific (Loughborough, UK). The grape skin extract was a crude extract used in the Kroon lab for method development and as a standard. Grape seed extracts were Leucoselect® Phytosome® from Indena® (France) and exGrape® from Groupe Grap'sud® (France). Monoclonal antibodies used for flow cytometry analysis were: phycoerythrin (PE)-anti-human ICAM-1 (clone HA58), PE-anti-human VCAM-1 (clone 51-10C9) and PE-anti-mouse IgG1 (isotype control; clone MOPC21), from BD Bioscience (Erembodegem, Belgium). FITC mouse anti-human CD62E antibody was purchased from Immunostep Research (Salamanca, Spain). TNF-α and IL1-β were purchased from R&D Systems (Abingdon, UK);, they were dissolved in PBS containing 1% BSA. Luna® 5-Silica(2) and Luna® 5-C18(2) columns were obtained from Phenomenex®. Clonetics® Trypsin (0.025%)/EDTA (0.01%) was obtained from Cambrex Bio Science (Cambrex, Wokingham, UK). Trans-resveratrol-O-sulfates were synthesized in the Kroon lab by Dr Paul Needs (Yu et al., 2002, Kawai et al., 2000). Resveratol was purchased from AK Scientific, Inc (USA).

2.3.2 Human Umbilical Vein Endothelial Cells (HUVECs)

2.3.2.1 Source

Human umbilical vein endothelial cells (HUVECs) were obtained from Cambrex Bio Science (Wokingham, England) and grown in EGM2 Bullet Kit (Lonza).

2.3.2.2 EGM2 Bullet Kit Medium

Supplements and growth factors (hydrocortisone, hEGF, FBS, VEGF, hFGF-B, R3-IGF-1, heparin and gentamicin/amphotericin-B).

2.3.2.3 Storage

The cells were kept in a liquid nitrogen tank in vials containing up to 10^6 cells in 1 ml of growth media with 10% DMSO. These vials were used to seed cells for experiments.

2.3.2.4 Freezing cells

When a plate of cells had reached confluence (single-layer of cells covering whole surface of the growth area), the cells were either sub-cultured onto another plate or frozen into vials to be stored in liquid nitrogen tank. These vials contained cells in 10% DMSO which was necessary for protecting cells from the formation of ice crystals that may disrupt the cell membrane.

2.3.2.5 Thawing and seeding cells

The number of vials containing the required amount of cells were removed from the liquid nitrogen tank. The cells were thawed and added into the growth medium. Then cells were seeded with a density of 2800-3000 cells/cm^2. All the experiments were carried out between passage number 4 and 5 (doubling population≤10). Cultures were maintained at 37°C and 5% CO_2.

2.3.3 HUVEC Proliferation Measurement

Cell proliferation was measured by using a bromodeoxyuridine (BrdU) incorporation type assay. A kit obtained from ROCHE$^®$ was used for the measurement. BrdU is a thymidine analogue. The dye incorporates into the cells and binds to the DNA during DNA replication. Hence the amount of proliferating

cells can be measured by an ELISA assay probing the dye with a chemiluminescent labelled anti-BrdU antibody.

HUVEC proliferation was investigated by using EGM$^®$ media with three different glucose concentrations of 5.5 mM (basal medium), 10 mM and 20 mM. HUVECs were cultured in black 96-well plates with clear bottom at 3500 cell/cm^2 by using basal medium in a final volume of 100 µl. Cultures were maintained at 37°C and 5% CO_2. After 24 hours of the seeding, the media were changed either to 10 or 20 mM glucose containing experimental media with/without polyphenol treatments. At the same time, EGM$^®$ media that contain equimolar concentrations of mannitol were used as controls against hyperosmolarity. HUVEC proliferation was measured at 24, 48 and 72 hours. The effects of grape skin and grape seed extracts (Leucoselect$^®$ Phytosome$^®$) on the proliferation of high-glucose treated HUVECs were assessed. Grape seed and grape skin extract solutions were prepared in dimethylsulfoxide (DMSO) at concentrations such that the final concentration of the solvent in cell suspension did not exceed 0.1% (v/v). 0.1% (v/v) DMSO was added into control treatments. At the end of the treatment periods, BrdU incorporation was allowed either for 4 h or 12 h by adding 10 µl BrdU labelling solution to each well (final concentration 10 µM BrdU). This was followed by fixing the cells with the FixDenat solution (200 µl/well, 30 min at room temperature) provided in the kit. The fixed cells were incubated with 100 µl anti-BrdU-POD/well for 1.5 h at room temperature. The chemiluminescence was then measured using a microplate luminometer (Luminoskan Ascent, Thermo Labsystems, Helsinki, FL).

2.3.4 High Performance Liquid Chromatography (HPLC)
HPLC was used for the qualitative analysis of grape skin extract and grape seed extract samples. The grape skin extract was initially analyzed by two different HPLC methods to obtain a favourable method; normal phase HPLC with fluorescence detection and reverse phase HPLC with UV diode array detection, whereas only normal phase HPLC with fluorescence detection was used for the analysis of grape seed extract samples.

Samples (40 mg, in triplicate) were extracted using 950 µl 70% aqueous ethanol at 70°C for 20 minutes. Each sample was then split between two HPLC vials ready

for analysis in normal and reverse phase HPLC by using 250 x 4.60 mm internal diameter 5 μm "Luna® 5-Silica(2)" and "Luna® 5-C18(2)" columns with pore sizes of 100Å respectively. Standard curves were prepared by injecting the instruments with different volumes of 0.1mg/ml epicatechin standard for each method to be able to determine the amount of epicatechin in grape skin/seed extract samples. Samples were eluted at a rate of 1 ml/min. Catechin and procyanidins were identified by comparing the retention times with the retention times of previously analysed standards and higher-chain length procyanidins in the Kroon Lab respectively. A mobile phase consisting of dichloromethane, 100% methanol and 50% acetic acid was used for normal phase analysis, whereas 0.1% trifluoro-aceticacid (TFA)/water and 0.1% TFA/acetonitrile were used in reverse phase HPLC over 65 min long analysis (Table 2.1 and 2.2). The injection volumes were 10 μl and 20 μl for normal phase and reverse phase analyses respectively.

2.3.4.1 Gradient Profiles

Table 2.1: Gradient profile of mobile phase in normal phase HPLC analysis over 65 minutes.

B: Dichloromethane **C:** Methanol **D:** 50% Acetic Acid

Time (min)	B %	C %	D %
30	82	14	4
45	67.5	28.4	4
50	56.8	39.2	4
55	10	86	8
65	82	14	4

Table 2.2: Gradient profile of mobile phase in reverse phase HPLC analysis over 65 minutes.

A: 0.1% TFA/Water   **B:** 0.1% TFA/Acetonitrile

Time (min)	A %	B %
0	3	97
5	3	97
15	17	83
17	17	83
22	25	75
30	35	65
35	50	50
40	100	0
50	100	0
55	3	97
65	3	97

2.3.5 Cell Adhesion Molecule Expression in HUVECs

Effects of experimental conditions on CAM expression were assessed by a flow cytometry based method using antibodies specific for VCAM-1 and ICAM-1 which are conjugated with two different fluorophores, one for each antibody. Phycoerythrin (PE) labelled antibody is used for VCAM-1 detection whereas allophycocyanin (APC) labelled antibody is used for ICAM-1 detection. The cell adhesion molecule (CAM) detection protocol was optimized prior to the experiments (Figure 2.1).

HUVECs were cultured in 6-well plates at 3500 cell/cm^2 by using basal medium (5.5 mM glucose). The experiments were performed with HUVECs in both an

unstimulated state and under inflammatory conditions induced by a mixture of LPS 10 µg/ml (Sigma-Aldrich®) and TNF-α 10 ng/ml (Sigma-Aldrich®), only by TNF-α 5 ng/ml (R&D Systems) or only by IL1-β 5 ng/ml (R&D Systems). All experiments were carried out between passage number 4 and 5 (doubling population ≤10) cells. Cultures were maintained at 37°C and 5% CO_2. The basal media were changed with experimental high-glucose media with or without polyphenol treatments for 18, 24 or 48 hours in each experiment when 90-95% confluency was reached to test the effect of high-glucose on cellular adhesion molecule expression.

After the treatments, confluent monolayers were washed with PBS and harvested using Clonetics® Trypsin (0.025%)/EDTA (0.01%) (Cambrex). Cells were re-suspended in PBS (pH 7.4) containing 0.1% BSA and 0.02 mmol/L NaN_3. Monoclonal antibodies were added to the cells and incubated in the dark at 4°C for 30 min. After washing in PBS containing 0.1% BSA, 4 mmol/L EDTA and 0.02 mmol/L NaN_3, cells were fixed with paraformaldehyde at 1% final concentration or stained with propidium iodide (PI) (Invitrogen®) just before the flow cytometry analysis. Propidium iodide is a membrane impermeant nucleic acid dye and generally excluded from viable cells. In membrane permeable/dead cells, PI will bind to nucleic acid upon entering the cells brightly fluorescent enabling the exclusion of dead or dying cells from the flow cytometry analysis.

The cell surface expression of the adhesion molecules (ICAM-1 and VCAM-1) was quantified using a Beckman Coulter Cytomics FC500 MPL flow cytometer with a 488nm and 635nm excitation laser. High-flow mode was obtained with a flow rate of 60 µl/min. A total of 15000 events were acquired for each sample. Appropriate APC-labeled mouse IgG1 isotypic control used for background fluorescence alongside with the ICAM-1 or VCAM-1 antibodies. Fluorescent detectors varied between fluorophores. FITC was detected using the FL1 detector and a 525/20nm bandpass filter. PE was detected using the FL2 detector using a 575/15nm bandpass filter. PI was detected using PMT FL3 quantifying light between 615-620nm, while APC was quantified using PMT FL4 and a 675/30nm bandpass filter. FlowJo® v.7.6.5 was used for data analysis. A forward scatter threshold was used.

Antibody Titration		
ICAM-1 APC	VCAM-1 PE	E-Selectin FITC

Stimulant Selection			
LPS	LPS/TNF-α	TNF-α	IL1-β

Cell Harvesting Method	
PBS/EDTA	Trypsin/EDTA

Dead/Alive Cells		
1% Paraformaldehyde	Propidium Iodide	LIVE/DEAD® Fixable Dead Cell Stain Kit

High-glucose treatments			
5.5 mM	10 mM	20 mM	28.5 mM

Cytokine Treatments	
TNF-α	IL1-β

Polyphenol Treatments			
Grape Seed/ Skin Extracts	Quercetin	Resveratrol	Resveratrol Human Metabolites

Figure 2.1: Cell adhesion molecule detection protocol optimization and experiments. CAM detection work began with antibody titration experiments, which were followed by the experiments to optimize the protocol. Trypsin/EDTA treatment was chosen as the detachment method of the cells. PI was used to stain dead cells in order to exclude them from analysis.

2.3.6 Statistical Analysis

Means and standard deviation values for the means were calculated using conventional methods. The differences in the cell proliferation and cell adhesion molecule measurements after particular treatments were statistically analyzed using 1 way analysis of variance (1-Way ANOVA) followed by Tukey post hoc test with the aid of GraphPad Prism 5.01 software. Significant differences in measurements were reflected with a p value less than 0.05 (* $p < 0.05$, ** $p < 0.01$, *** $p < 0.001$).

2.4 Results

2.4.1 Procyanidin Content of Grape Seed and Grape Skin Extracts

The amount of epicatechin in the crude grape skin extract was estimated as 31.25 mg/g (3.13% w/w) using normal phase HPLC with fluorescence detection (Figure 2.2) and 32.75 mg/g (3.28% w/w) by using reverse phase HPLC with UV diode array detection (Figure 2.3). These two values obtained by using two different HPLC methods for the amount of epicatechin in the grape skin extract are very similar and indeed were not significantly different (p>0.05).

There were two commercial grape seed extract samples, Leucoselect[®] Phytosome[®] and exGrape[®], with "guaranteed" procyanidin contents. Both of the samples were analyzed qualitatively using normal phase HPLC with fluorescence detection (Figure 2.4 and 2.5). The results revealed a profile of catechin, epicatechin, dimers (dp2) and a low amount of trimers (dp3) in both of the extracts. On the other hand, crude grape skin extract, which was chosen for the preliminary analysis, was shown to contain tetramers, pentamers and higher polymers as well as the monomers and smaller oligomers that were found in the grape seed extracts.
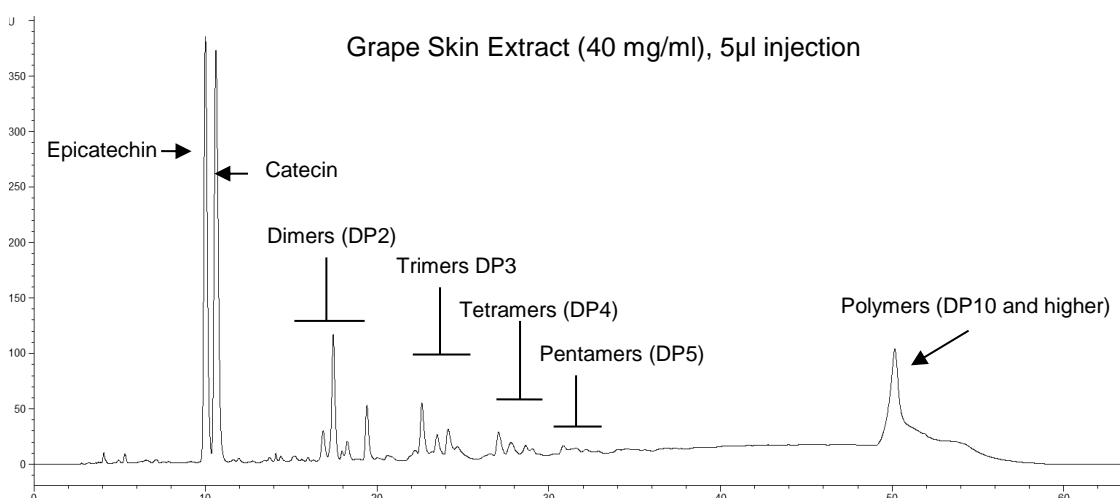
Figure 2.2: Chromatogram of crude grape skin extract sample obtained by using normal phase HPLC with fluorescence detection. Amount of epicatechin in the grape skin extract sample was determined as 32.75 mg/g (3.28% w/w).
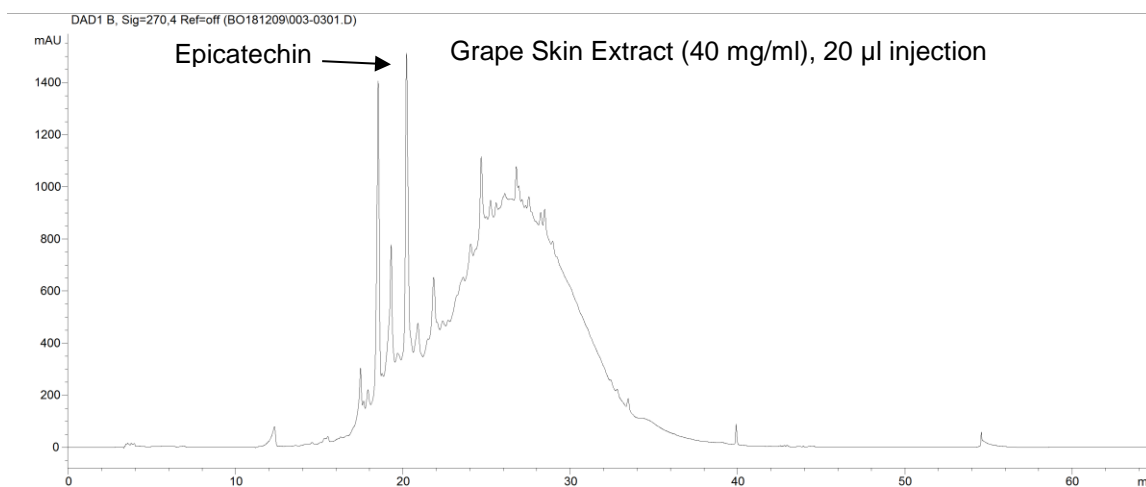
Figure 2.3: Chromatogram of crude grape skin extract obtained by using reverse phase HPLC with UV diode array detection (270 nm). Amount of epicatechin in the grape skin extract samples was determined as 31.25 mg/g (3.13% w/w).
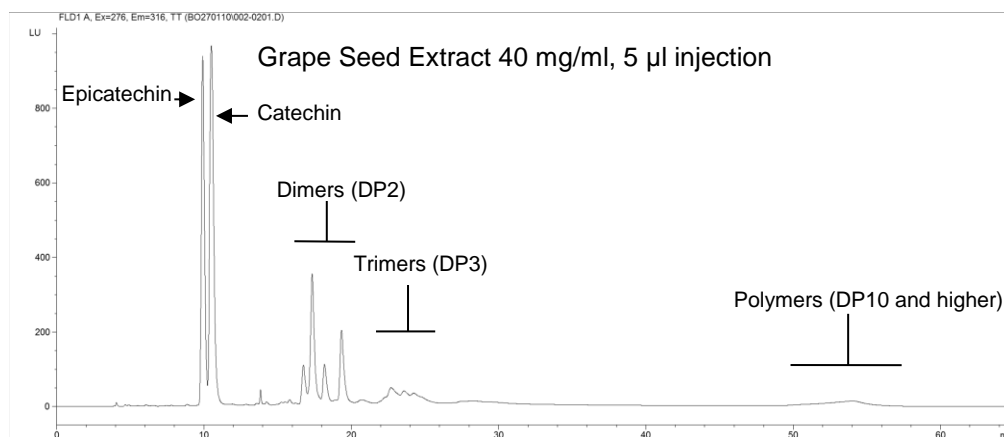
Figure 2.4: Chromatogram of grape seed extract sample (Leucoselect® Phytosome®) obtained by using normal phase HPLC with fluorescence detection. Amount of epicatechin in the grape seed extract sample was determined as 98 mg/g (9.8% w/w).
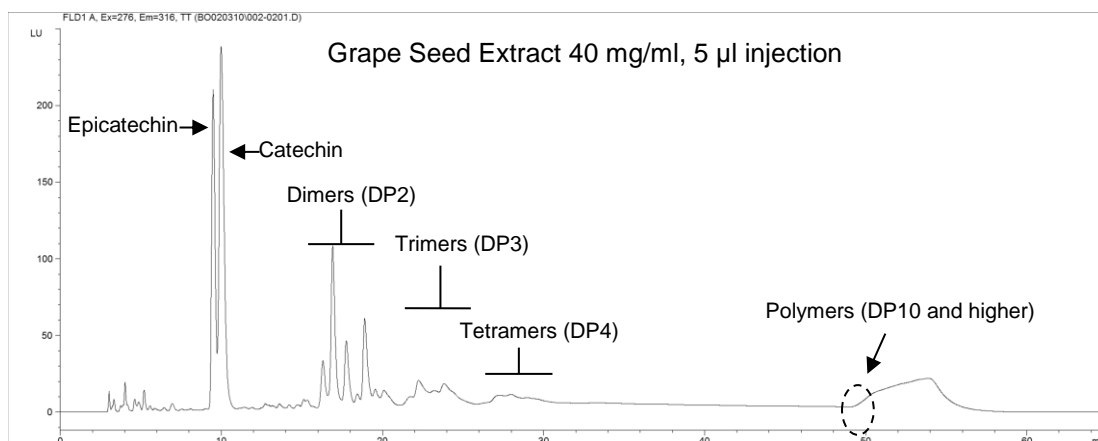
Figure 2.5: Chromatogram of grape seed extract sample (exGrape®) obtained by using normal phase HPLC with fluorescence detection. Amount of epicatechin in the grape seed extract sample was determined as 22.5 mg/g (2.25 % w/w).

2.4.2 Effect of High-Glucose and Grape Seed/Skin Extracts on HUVEC Proliferation

DNA synthesis was measured using BrdU incorporation assay to assess the effect of glucose and grape skin/seed extracts on HUVEC proliferation.

High-glucose (10 mM and 20 mM) did not affect cell proliferation over the first 24 h (Figure 2.6A). On the other hand, increased HUVEC proliferation was observed with high-glucose treatments after 48 h and 72 h (Figures 2.6B and 2.6C respectively). Nevertheless, this effect of high-glucose concentrations was not consistent throughout the study. Figure 2.9 indicated that there was not an alteration in HUVEC proliferation after high-glucose treatments for 48 h. In the experimetns where increased cell proliferation was observed after 48 h of high-glucose treatments, there was a threshold effect of high-glucose on cell proliferation rather than a dose-dependent effect since there was not a difference observed in proliferation of HUVECs treated with 10 mM and 20 mM glucose (Figure 2.6B). After 72 h treatment, 10 mM glucose did not affect cell proliferation, whereas 20 mM glucose moderately but significantly elevated the cell proliferation (Figure 2.6C). Mannitol (4.5 mM and 14.5 mM) treatments did not have an effect on cell proliferation at any time point (24h, 48h or 72h treatments; Figures 2.7A, 2.7B & 2.7C respectively).

Strong effects of grape skin extract treatments were observed. Relatively low concentrations of grape skin extract increased BrdU incorporation in HUVECs grown in all 5.5 mM, 10 mM and 20 mM glucose containing media (Figure 2.8A, 2.8B, 2.8C). BrdU incorporation started to decline in HUVECs grown under 5.5 mM glucose with 2.5 µg/ml grape skin extract treatment which is followed by the strong inhibition of proliferation with the 5 µg/ml grape skin extract treatment (Figure 2.8A). It was observed that the increase in glucose concentration lowers the grape skin extract concentration needed for a reduction in cell proliferation. 2 µg/ml grape skin extract decreased BrdU incorporation in HUVECs grown under 10 mM glucose medium by 19.9%, whereas similar concentration of grape skin extract was enough to completely inhibit proliferation of HUVECs grown under 20 mM glucose medium (Figure 2.8B and 2.8C).

In contrast, grape seed extract (Leucoselect[®] Phytosome[®]) did not increase cell proliferation. However, a small but significant reduction in proliferation was observed in HUVECs grown under high-glucose (10 mM and 20 mM) conditions with 1 µg/ml grape seed extract treatment (Figure 2.9).

A.

B.

C.
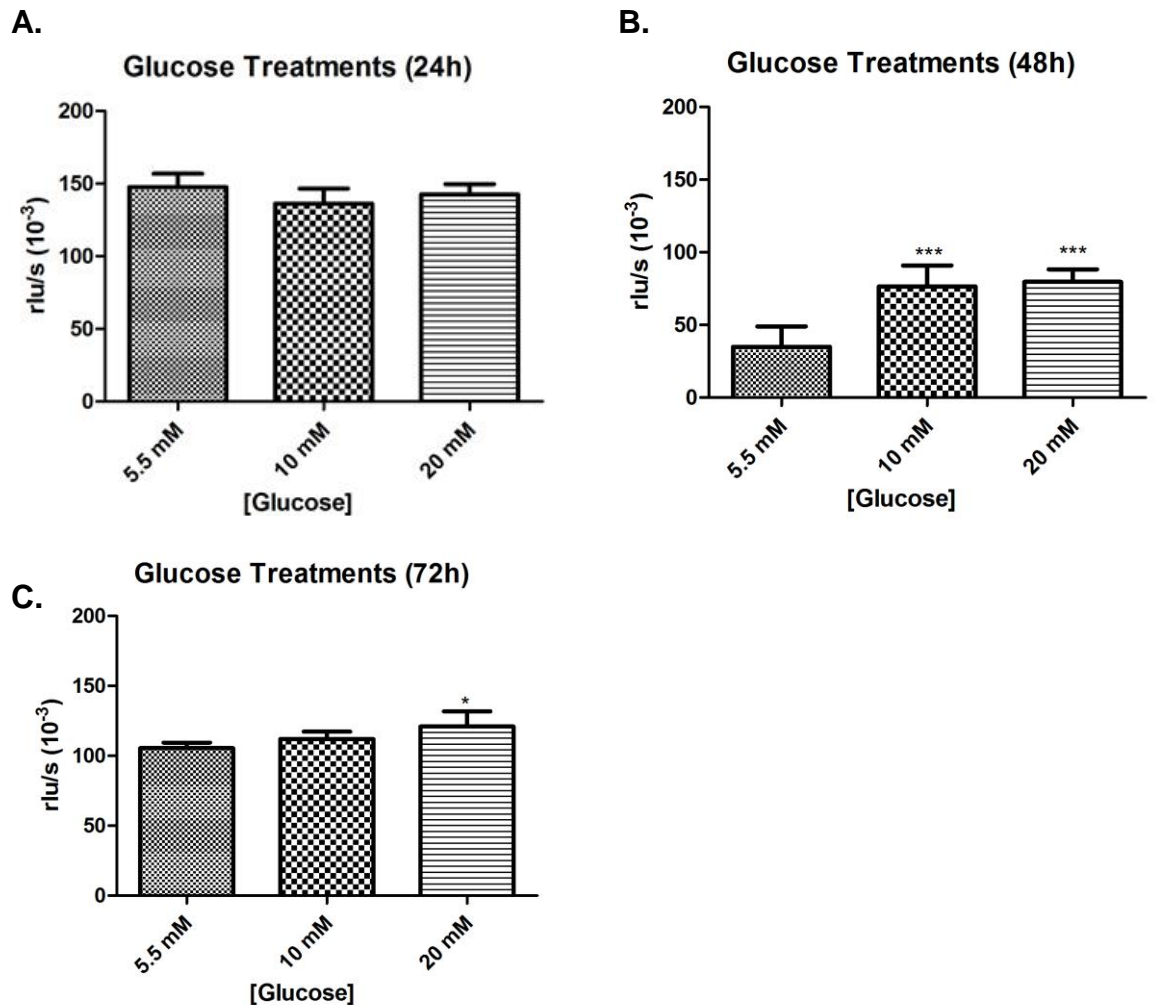
Figure 2.6: Measurement of proliferation of high-glucose treated HUVECs. BrdU incorporation was allowed for 4 h. **A.** High-glucose treatment for 24h (n=12). **B.** High-glucose treatment for 48 h (n=6). **C.** High-glucose treatment for 72 h (n=6).
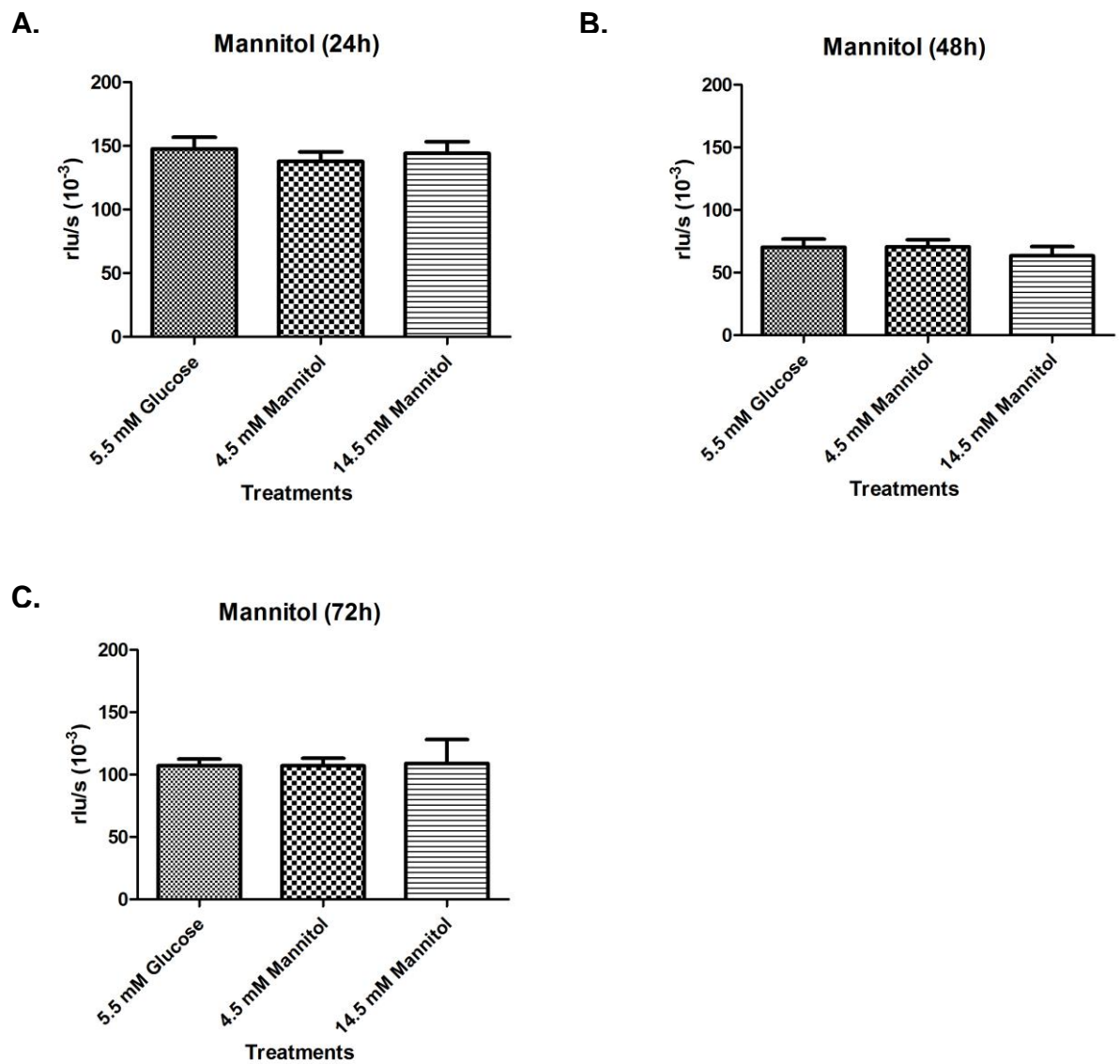
Figure 2.7: Measurement of proliferation of the mannitol treated HUVECs. BrdU incorporation was allowed for 4 h. **A.** Manitol treatment for 24h (n=6). **B.** Mannitol treatment for 48h (n=6). **C.** Mannitol treatment for 72h (n=6).

A.

5.5 mM Glucose

B.

10 mM Glucose

C.
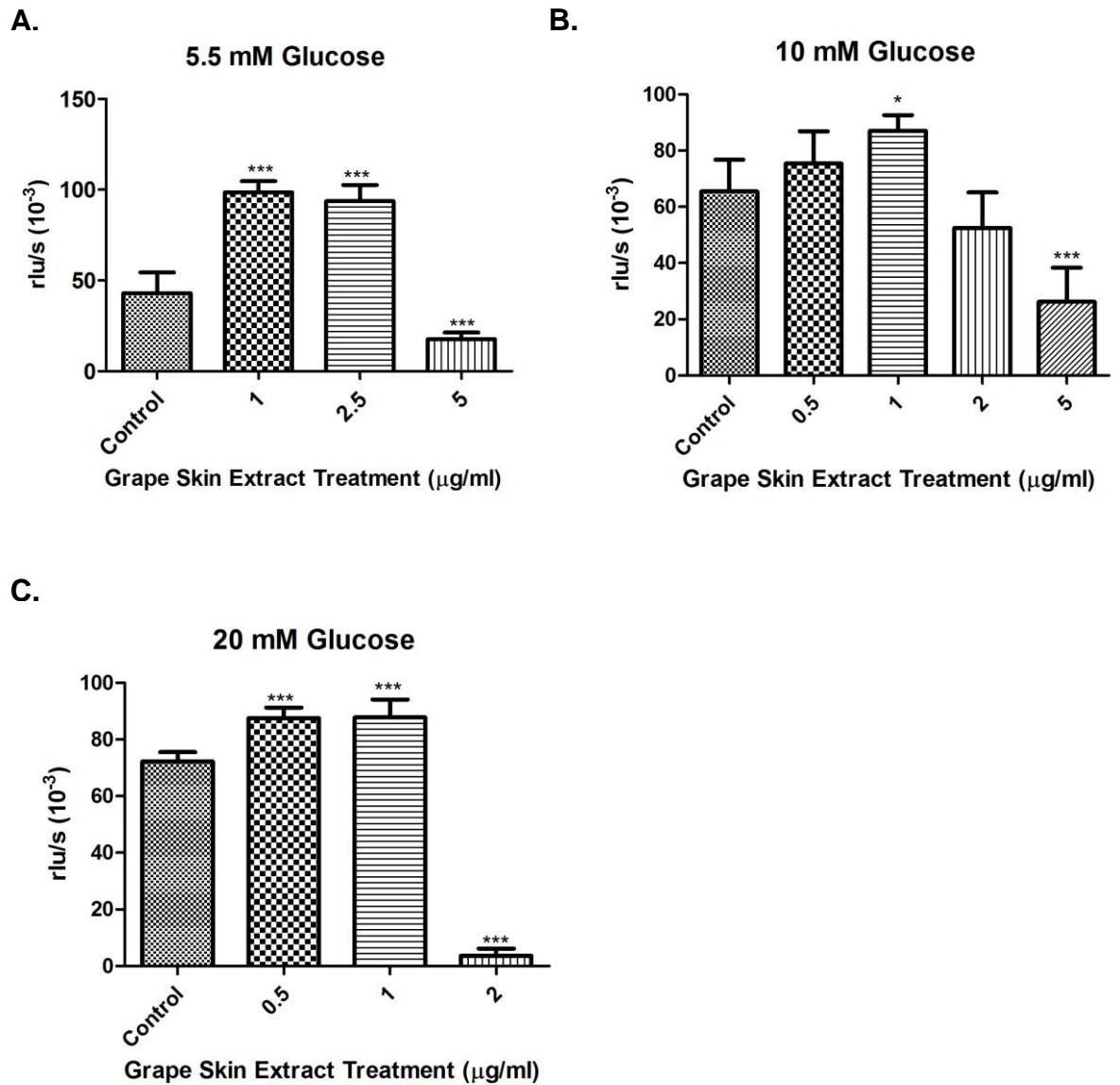
20 mM Glucose

Figure 2.8: Measurement of proliferation of grape skin extract treated HUVECs, which were grown under different glucose concentrations for 48 h. BrdU incorporation was allowed for 4 h. **A.** HUVECs grown under 5.5 mM glucose (basal medium) (n=6). **B.** HUVECs grown under 10 mM glucose (n=6). **C.** HUVECs grown under 20 mM glucose (n=6).

A.

B.

C.
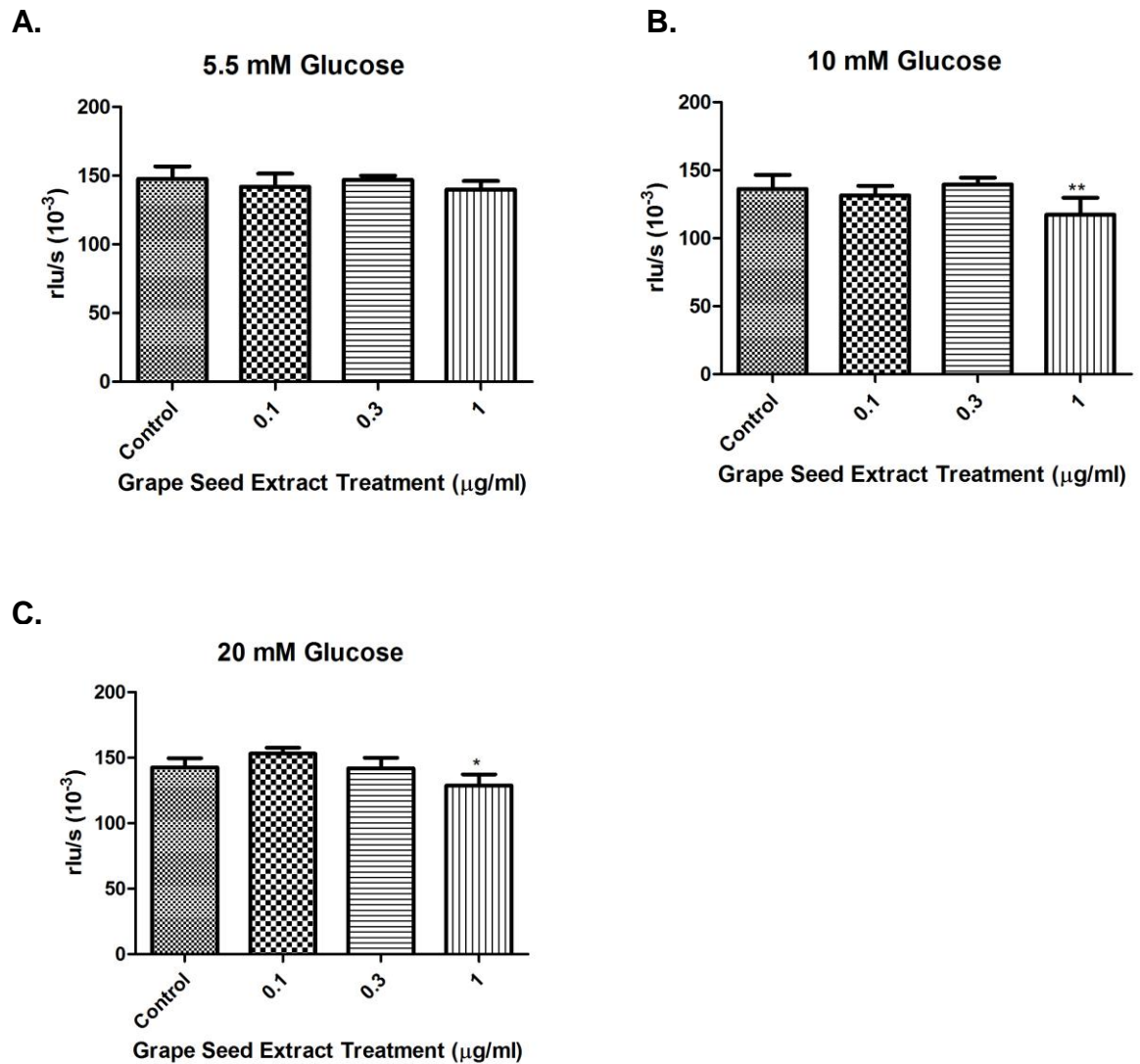
Figure 2.9: Measurement of proliferation of grape seed extract (Leucoselect® Phytosome®) treated HUVECs, which were grown under different glucose concentrations for 48 h. BrdU incorporation was allowed for 12 h. **A.** HUVECs grown under 5.5 mM glucose (basal medium) (n=6). **B.** HUVECs grown under 10 mM glucose (n=6). **C.** HUVECs grown under 20 mM glucose (n=6).

2.4.3 Cell Adhesion Molecule Measurement Protocol Optimization

The CAM quantification protocol involves harvesting cells, staining for the adhesion molecules and flow cytometry analysis. Preliminary development work was undertaken in order to test how several variable impacted on method, performance and to ensure that reliable results were obtained (Figure 2.1). First of all, three individual antibodies that were conjugated with different colours were tested. Phycoerythrin (PE) labelled antibody was used for VCAM-1 detection, allophycocyanin (APC) labelled antibody was used for ICAM-1 detection, and fluorescein isothiocyanate (FITC) labelled antibody was used for E-selectin detection. The antibodies used could detect VCAM-1 and ICAM-1 on LPS (10 µg/ml) and TNF-α (10 ng/ml) (24h) stimulated HUVECs (Figures 2.10A and 2.10B). However, E-selectin could not be detected neither after 4h nor 24h LPS (10 µg/ml) and TNF-α (10 ng/ml) stimulation (Figure 2.10C).
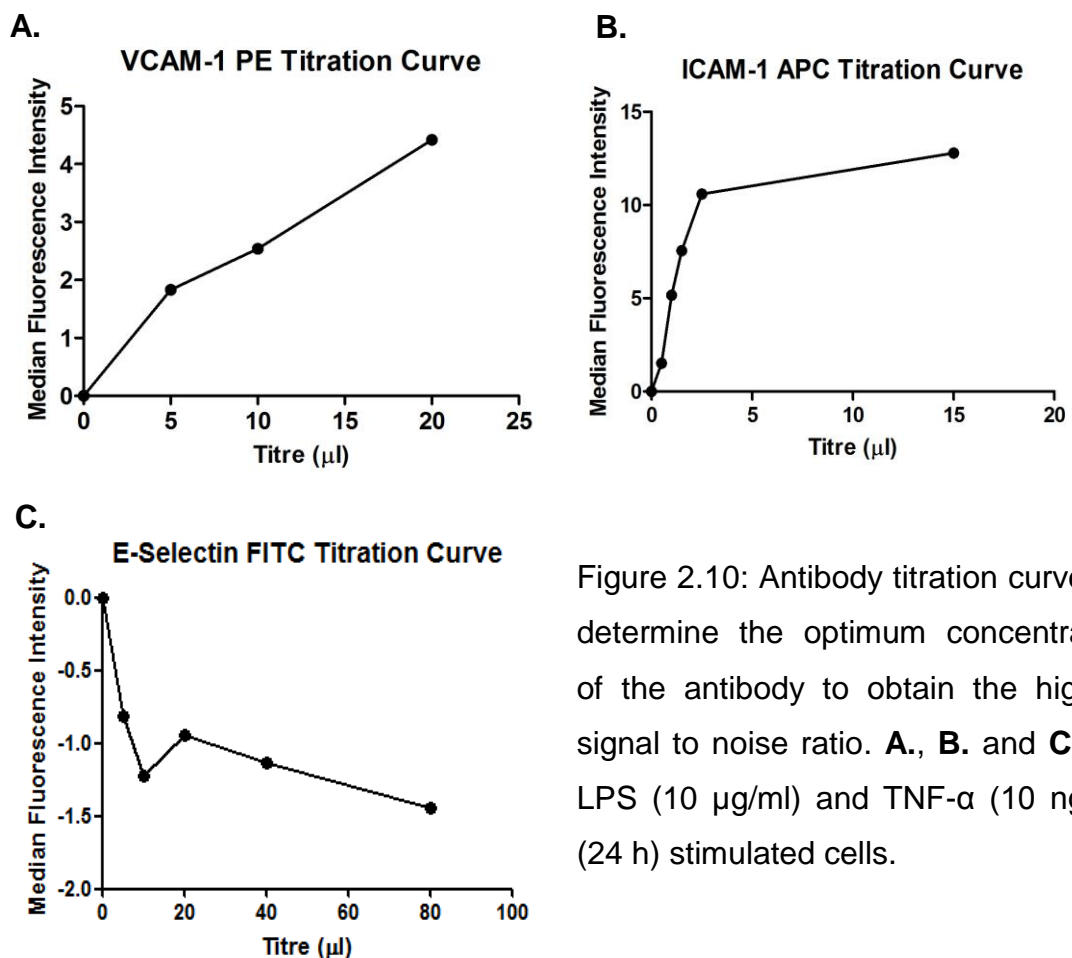
Figure 2.10: Antibody titration curves to determine the optimum concentration of the antibody to obtain the highest signal to noise ratio. **A.**, **B.** and **C.** are LPS (10 µg/ml) and TNF-α (10 ng/ml) (24 h) stimulated cells.

After optimizing the use of the antibodies, several different stimulants were tested to activate CAM expression by HUVECs. The cells were stimulated by treating them with LPS (10 µg/ml), a mixture of LPS (10 µg/ml) and TNF-α (10 ng/ml), TNF-α (10 ng/ml) or IL1- β (10 ng/ml). E-selectin was not activated by any of the tested stimulants. LPS (10 µg/ml) was the only treatment that did not activate VCAM-1 and ICAM-1 expression. Also, no synergy was observed when the cells were treated with a mixture of LPS (10 µg/ml) and TNF-α (10 ng/ml) observed (data not shown). Therefore, TNF-α and IL1- β were chosen to stimulate HUVECs subsequent experiments.

After the stimulation of the cells to express CAMs, they need to be detached by using a non-destructive method so as to not damage the CAM proteins. There are three options that are being widely used to harvest the cells prior to the CAM detection. These methods include the use of trypsin-EDTA, PBS-EDTA or mechanical detachment using a cell scraper. Preliminary experiments were performed of which both trypsin/EDTA and PBS/EDTA were used to harvest HUVECs. PBS/EDTA treatment for harvesting the cells yielded much lower cell counts and only ICAM-1 could be detected by flow cytometry. On the other hand, after trypsin-EDTA treatment much higher cell counts were achieved and ICAM-1 and VCAM-1 could be detected by flow cytometry. E-selectin could not be detected with either of the methods (Figure 2.10)**.**

HUVECs were fixed with paraformaldehye at 1% final concentration after they were stained, just before running the flow cytometry analysis for the preliminary experiments. However, it was not possible to exclude dead cells from the analysis when using this fixing method (Figure 2.11A). Propidium iodide staining was used to allow separation of live cells from dead cells using gating during analysis of flow data (Figure 2.11B). When the expression of CAMs by dead and live cells were compared, it was observed that dead cells express higher levels of ICAM-1 and VCAM-1 on the cell surface (Figure 2.11C). Beside propidium iodide treatment, another method was tried to be able to analyse live cells separately. This method involved the use of a fixable green fluorescent reactive dye obtained from "LIVE/DEAD® Fixable Dead Cell Stain Kits, Invitrogen®". This dye is capable of staining both intracellular and surface free amines in dead cells allowing the exclusion of live cells, as the dye is only capable of staining cell-surface amines of

live cells. The main difference between two methods is that the fixable dye allows the fixation of the cells with paraformaldhyde before the flow cytometry analysis giving flexibility in practical aspects prior flow cytometry analysis. The fixable stain was performed in parallel with propidium iodide treatment for a comparison. Although the green fluorescent reactive dye yielded stronger signals, the results obtained by these methods were similar (data not shown). Therefore, propidium iodide treatment was the chosen treatment to separate live cells for the analysis as it is a relatively cheaper method than the fixable dye method.
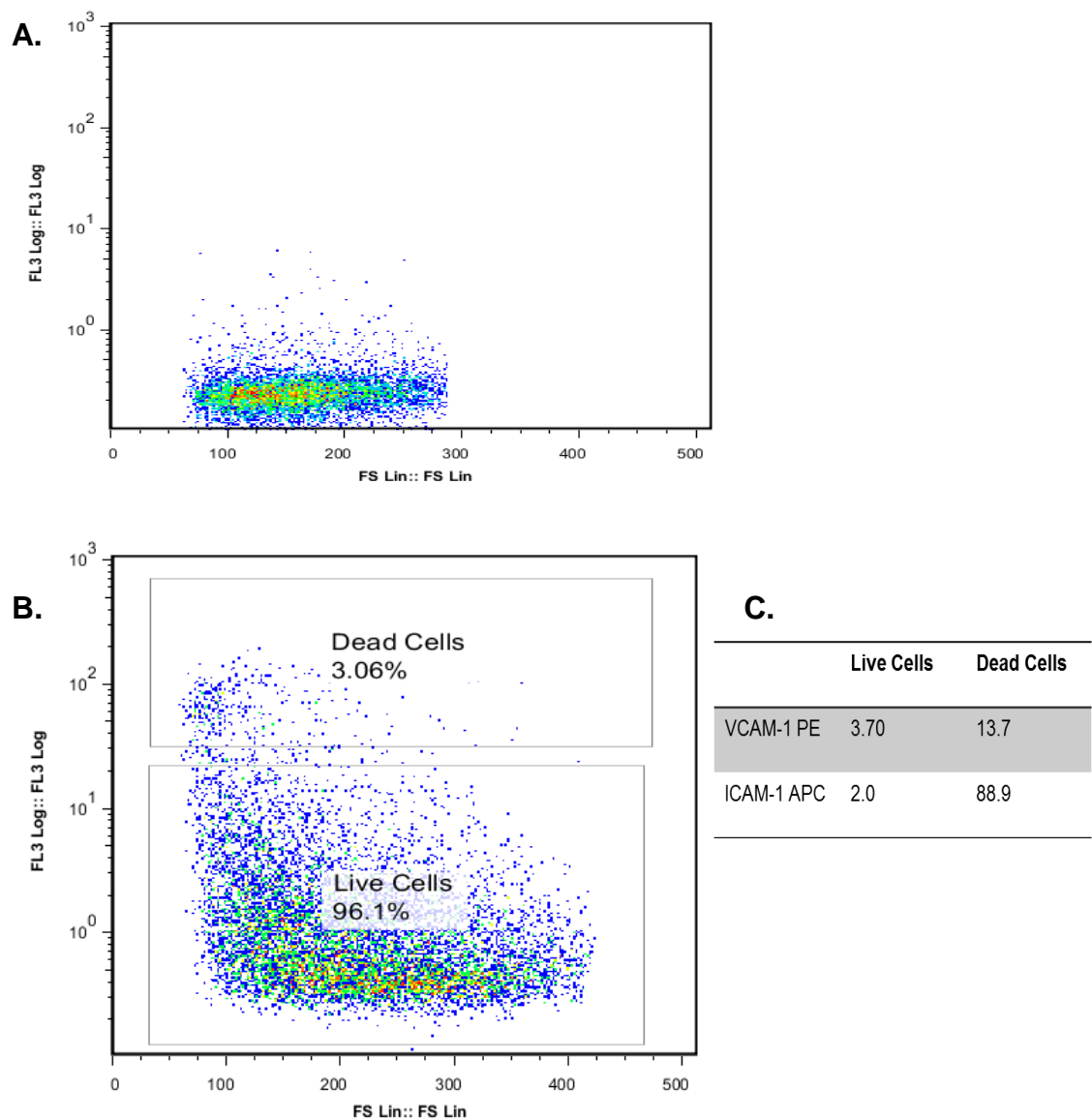
Figure 2.11: Gating live cells. **A.** Paraformaldehyde fixed cell population. Whole cell population was included in the analysis. **B.** Propidium iodide treated cell population. Propidium iodide negative cell population (live cells) was gated for further analysis. **C.** Median fluorescence intensities. Dead cells showed non-specific binding to antibodies.

2.4.4 Effect of High-Glucose Conditions on CAM Expression in HUVECs

High-glucose experiments involved the incubation of confluent HUVECs with four different glucose concentrations (10 mM, 20 mM, 28.5 mM and 35 mM) with or without TNF-α for 24 and 48 hours. High-glucose incubations did not induce CAM expression after either 24 or 48 hours (Figure 2.12). 10 ng/ml TNF-α treatments (10 ng/ml) induced both VCAM-1 and ICAM-1 expression, however, high-glucose co-treatment did not enhance the pro-inflammatory effect of TNF-α (data not shown).
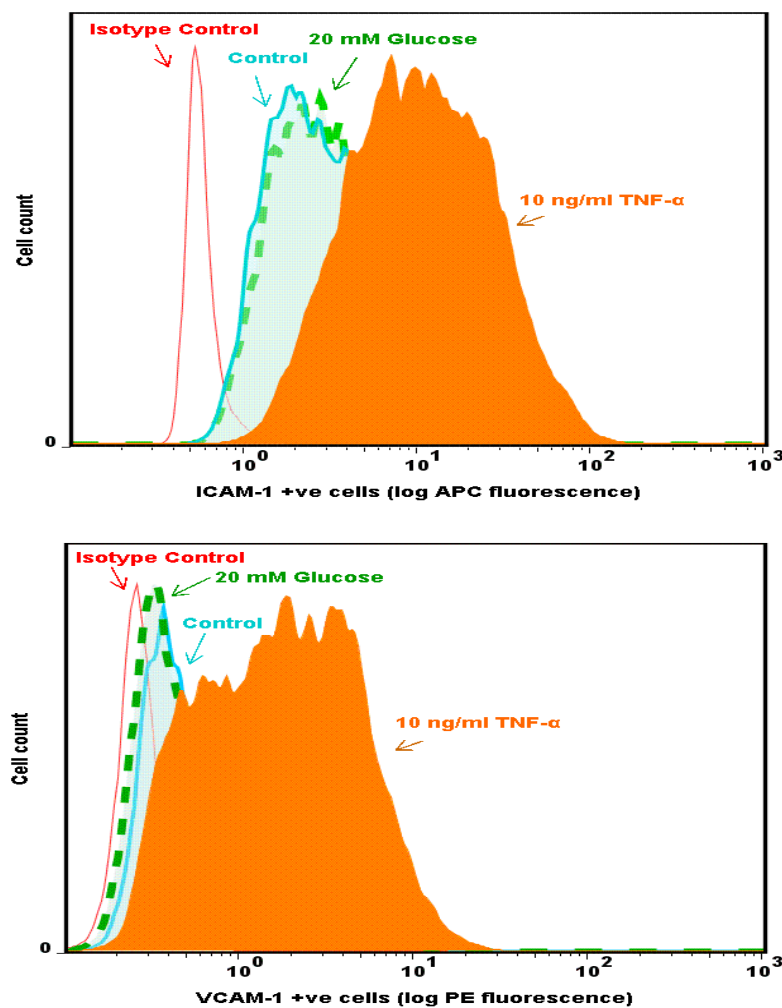
Figure 2.12: High-glucose treated HUVECs. Control cells have very low levels of VCAM-1 and ICAM-1 expression. TNF-α (10 ng/ml) activated the expression of both VCAM-1 and ICAM-1. However, 20 mM glucose did not activate the cells.

2.4.5 Effect of Inflammatory Mediators on CAM Expression in HUVECs

The pro-inflamatory cytokines, TNF-α and IL-1β, were used to activate HUVECs in order to be able to test the potential anti-inflammatory effects of selected polyphenols.

ICAM-1 is constantly expressed on cells at low concentrations whereas VCAM-1 and E-selectin expression requires activation by stimulants (Figure 2.13A). Both TNF-α and IL-1β effectively induced VCAM-1 and ICAM-1 expression in HUVECs (Figure 2.14). The cells were treated with these cytokines for a maximum of 18 hours prior to CAM measurement as the expression of CAMs start to decline after 18 hours according to reports in the existing literature (Lush et al., 2000, García-Conesa et al., 2009) HUVECs were treated with different concentrations of these agents to generate calibration curves (Figures 2.14A, 2.14B, 2.14C and 2.14D).

A.
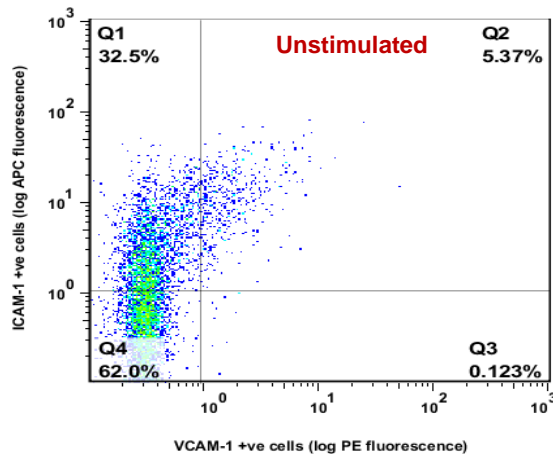
Figure 2.13: HUVEC stimulation. **A.** VCAM-1 and ICAM-1 expression in unstimulated HUVECs. **B.** IL1-β titration. IL1-β dose dependently stimulated HUVECs to express VCAM-1 and ICAM-1.

B.

A.

TNF-α Titration (VCAM-1)

B.

TNF-α Titration (ICAM-1)

C.

IL-1β Titration (VCAM-1)

D.

IL-1β Titration (ICAM-1)
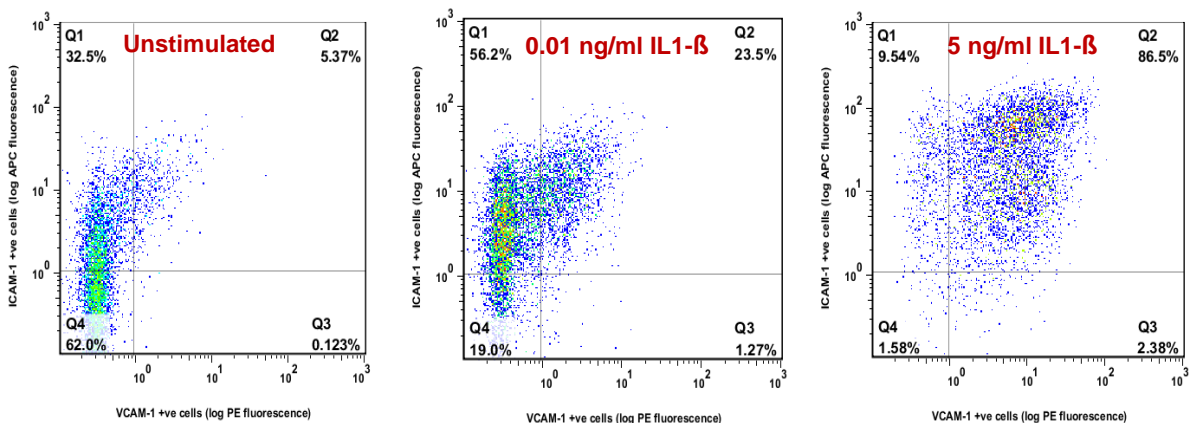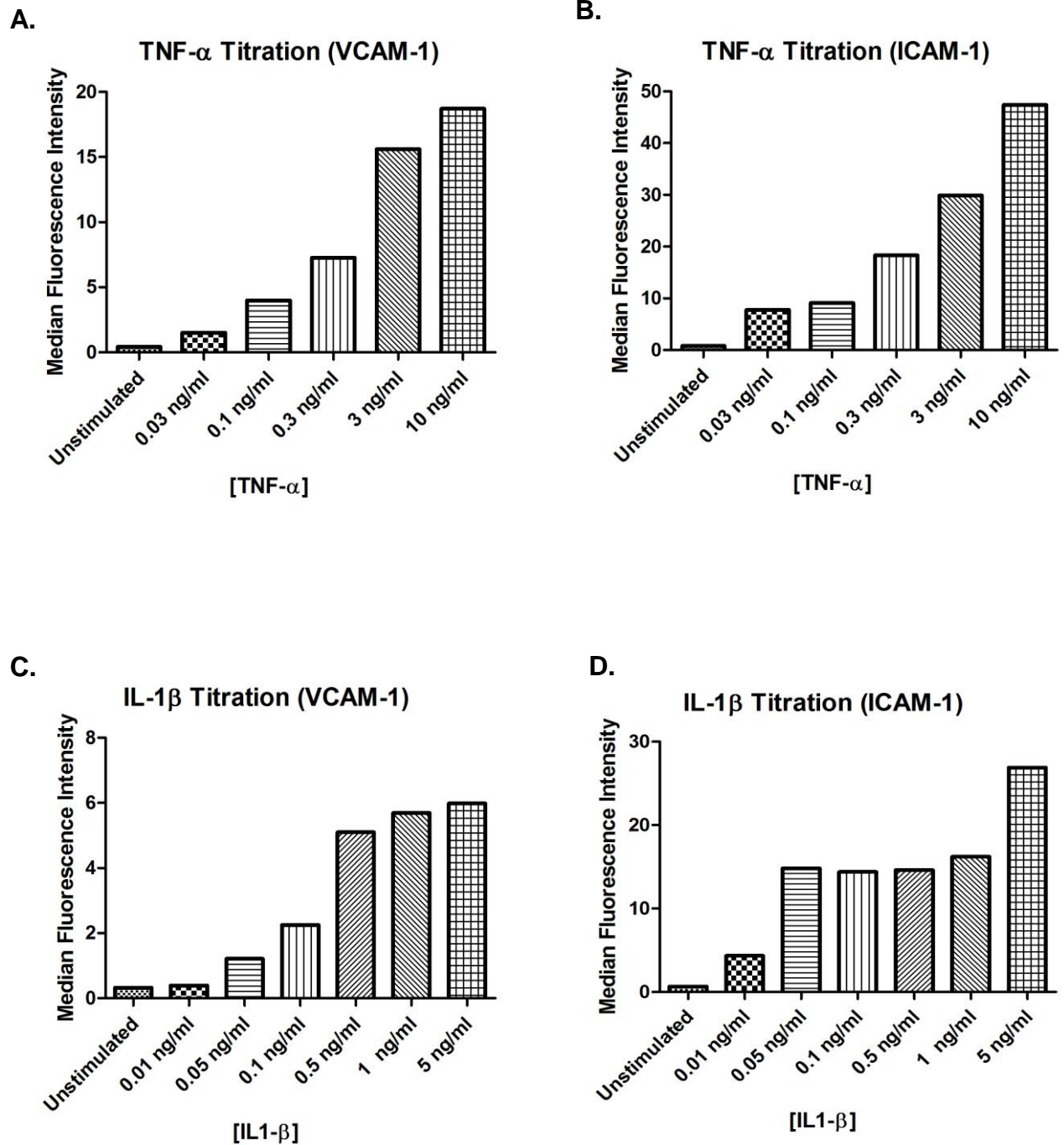
Figure 2.14: TNF-α and IL-1β titration curves. Confluent HUVECs were stimulated with different concentrations of TNF-α or IL-1β for 18 h. The flow cytometry analysis of live cells revealed that both of the cytokines increased VCAM-1 and ICAM-1 expression dose dependently.

2.4.6 Grape Seed/Skin Extract Treatments

Grape seed/skin extract treatments were applied to the cells either 45 minutes or 6 hours prior to the stimulation by IL-1β. After the pre-incubation period of the cells with the extracts, they were activated for either 6h or 18h with IL-1β. Concentrations used were 2.5, 5, 10 and 30 µg/ml grape seed extract and 0.5, 1, 2, 2.5, 10 and 30 µg/ml grape skin extract.

Grape seed and skin extracts became toxic to the cells at 20 and 30 µg/ml concentrations respectively; it was observed that the cells started to detach from the culture plates at these concentrations.

The experiments carried out in this study showed that neither grape seed nor grape skin extracts were effective in inhibiting pro-inflammatory cytokine-induced cell adhesion molecule expression (Figures 2.15, 2.16, 2.17 and 2.18). Pre-incubation with grape seed extract for 45 min and 6 h increased the expression of ICAM-1 and VCAM-1 respectively, (Figures 2.15 and 2.16). Interestingly, grape seed extract or grape skin extract treatments alone did not stimulate HUVECs to express CAMs (Figure 2.19). However, a synergistic increase in ICAM-1 expression was observed with grape seed extract or grape skin extract and IL1- β co-treatments (Figure 2.19).
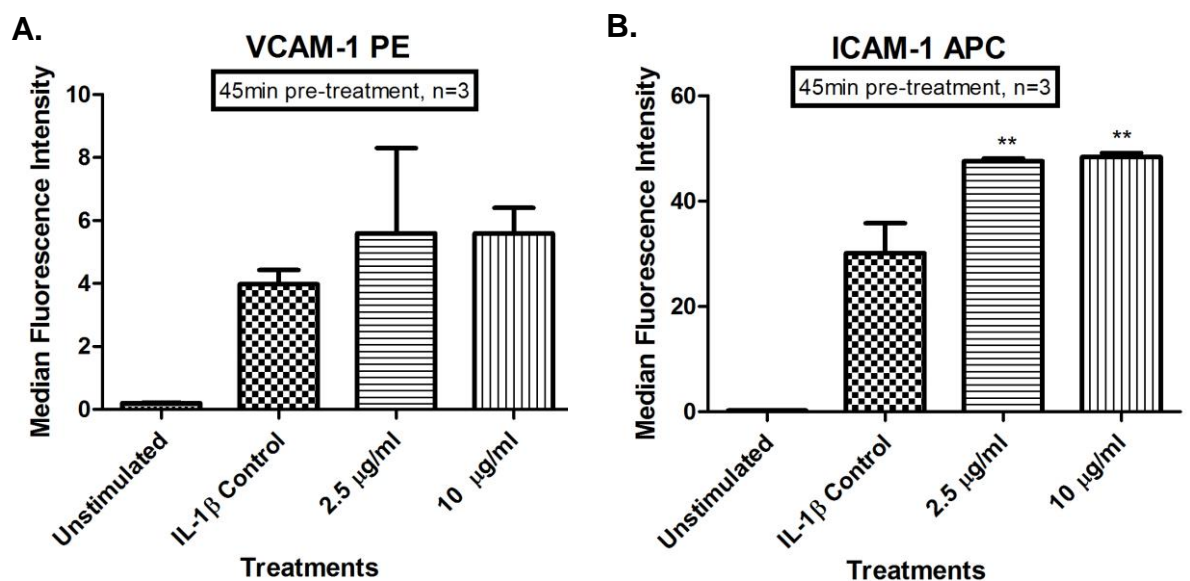
Figure 2.15: The effects of grape seed extract on IL1-β stimulated HUVECs. Cells were pre-incubated for 45min with different concentrations of grape seed extracts which was followed by IL1-β (5 ng/ml) activation for 18 hours.
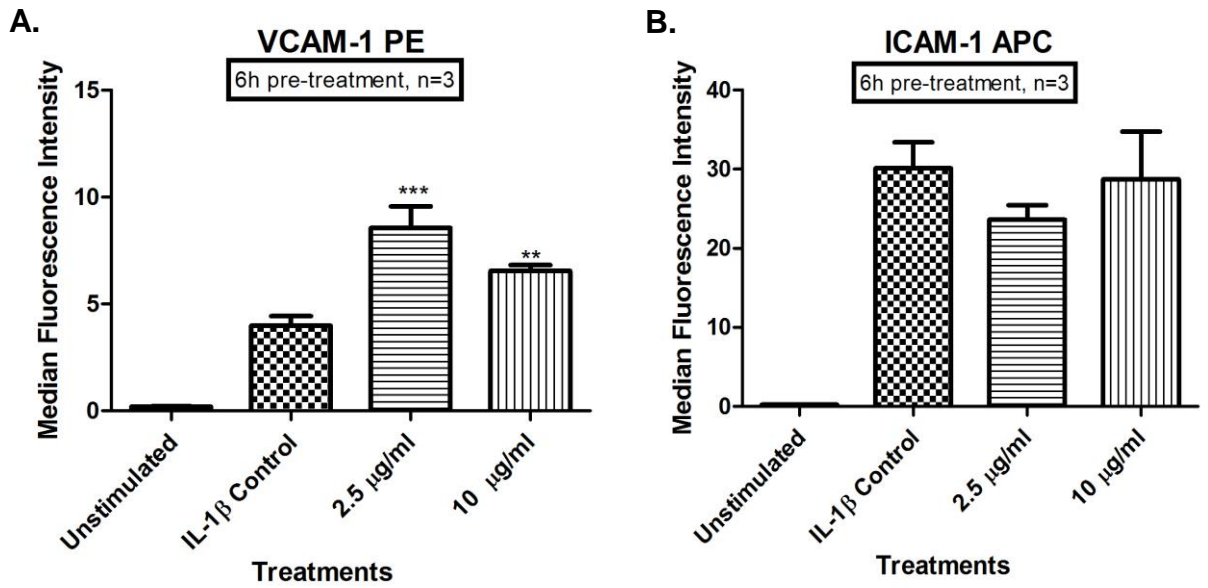
Figure 2.16: The effects of grape seed extract on IL1-β stimulated HUVECs. Cells were pre-incubated for 6 hours with different concentrations of grape seed extracts which was followed by IL1-β (5 ng/ml) activation for 18 h.
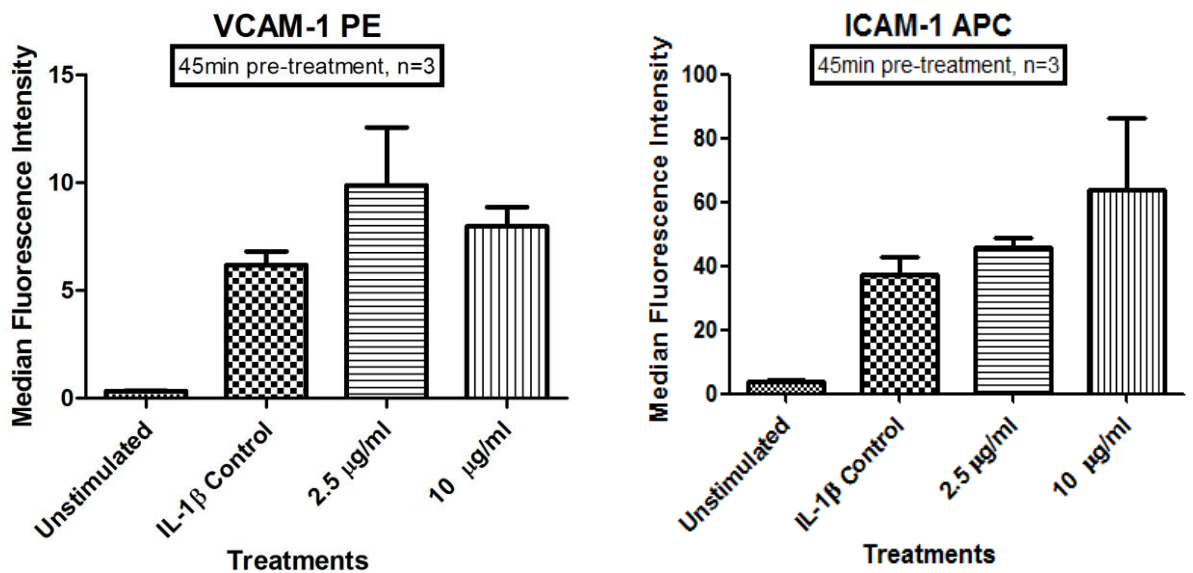
Figure 2.17: The effects of grape skin extract on IL1-β stimulated HUVECs. Cells were pre-incubated for 45 min with different concentrations of grape seed extracts which was followed by IL1-β (5 ng/ml) activation for 18 h.
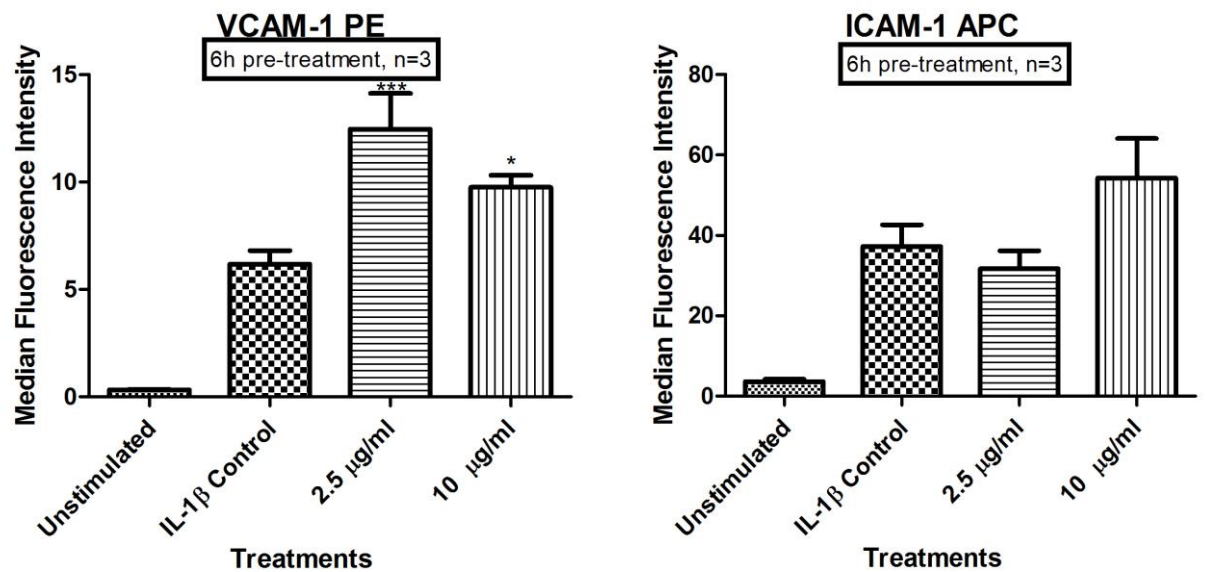
Figure 2.18: The effects of grape skin extract on IL1-β stimulated HUVECs. Cells were pre-incubated for 6h with different concentrations of grape seed extracts which was followed by IL1-β (5 ng/ml) activation for 18 hours.
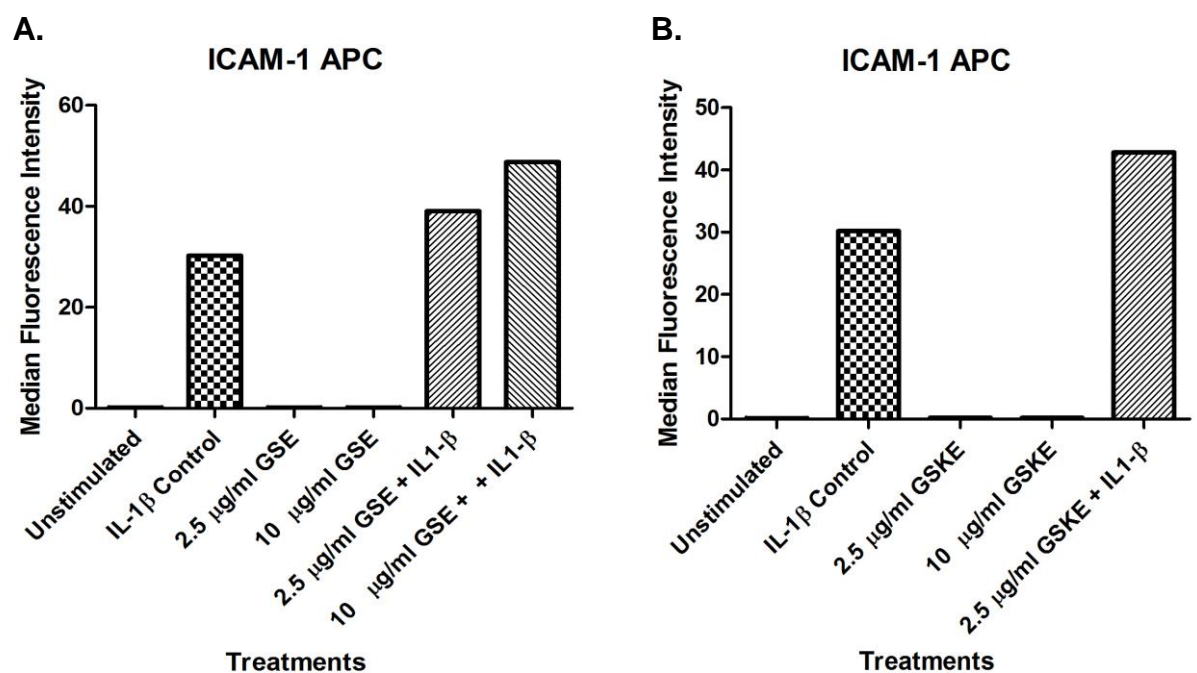
Figure 2.19: Up-regulatory effect of grape seed and grape skin extracts on IL-1β induced ICAM-1 expression. Cells were pre-incubated for 6 hours with different concentrations of extracts which was followed by IL1-β (5 ng/ml) activation for 18 hours. Grape seed (**A.**) or grape skin extract (**B.**) alone did not increase the expression of ICAM-1. However, a synergistic increase was observed with either grape seed or skin extract and IL-1β.

2.4.7 Quercetin Treatments

In this study, HUVECs were pre-incubated with quercetin (0.1μM, 1 μM, 10 & 25 μM) for 45 min or 6 h, which was followed by the activation of the cells with either TNF-α (5 ng/ml) or IL1-β (5 ng/ml). 45 min pre-incubation with quercetin did not show any effects on TNF-α (5 ng/ml) stimulated ICAM-1 or VCAM-1 expression in HUVECs (0.1μM to 25μM) (Figure 2.20). On the other hand, 6h pre-incubations with quercetin (10 and 25 μM) resulted in significant reductions in VCAM-1 expression compared to cells treated with TNF-α alone (p<0.01 and p<0.001 respectively) (Figure 2.21). Interestingly, quercetin (10 μM & 25 μM) was able to inhibit only TNF-α induced expression of VCAM-1 (Figure 2.21). Nevertheless, the same concentrations of quercetin could inhibit the expression of IL-1β-induced expression of VCAM-1 and ICAM-1 (Figure 2.22). Quercetin treatment alone did not induce CAM expression by HUVECs (data not shown).
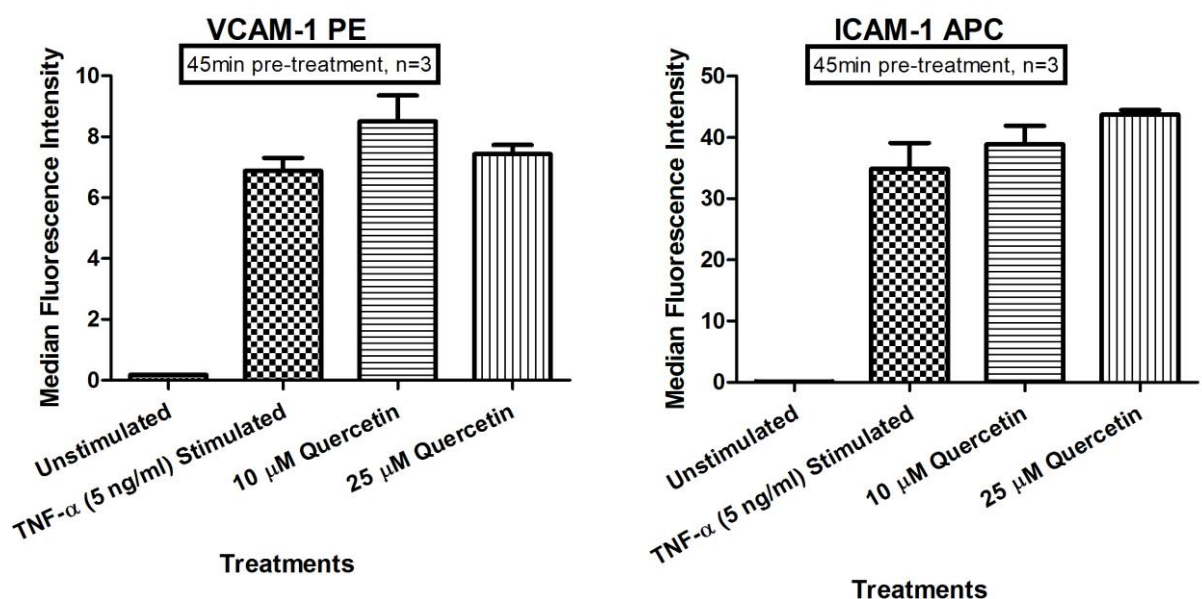
Figure 2.20: The effects of quercetin on TNF-α stimulated HUVECs. Cells were pre-incubated for 45 min with 10 μM and 25 μM quercetin which was followed by TNF-α (5 ng/ml) activation for 18 h.
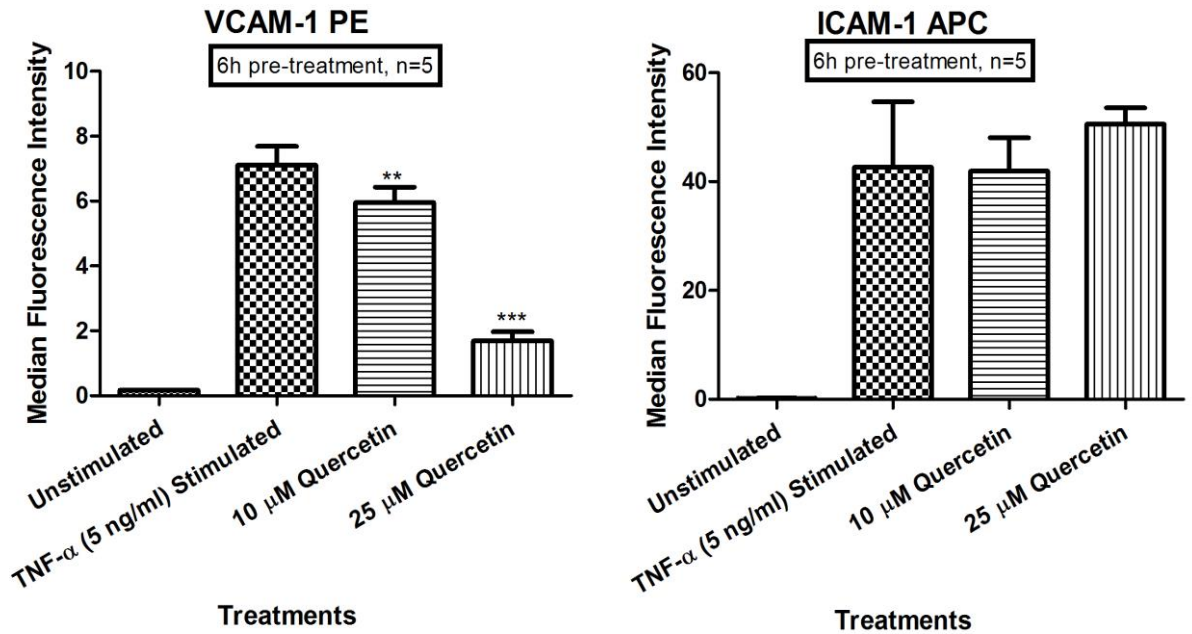
Figure 2.21: The effects of quercetin on TNF-α stimulated HUVECs. Cells were pre-incubated for 6 hours with 10 µM and 25 µM quercetin which was followed by TNF-α (5 ng/ml) activation for 18 hours. Quercetin inhibited VCAM-1 expression dose dependently.
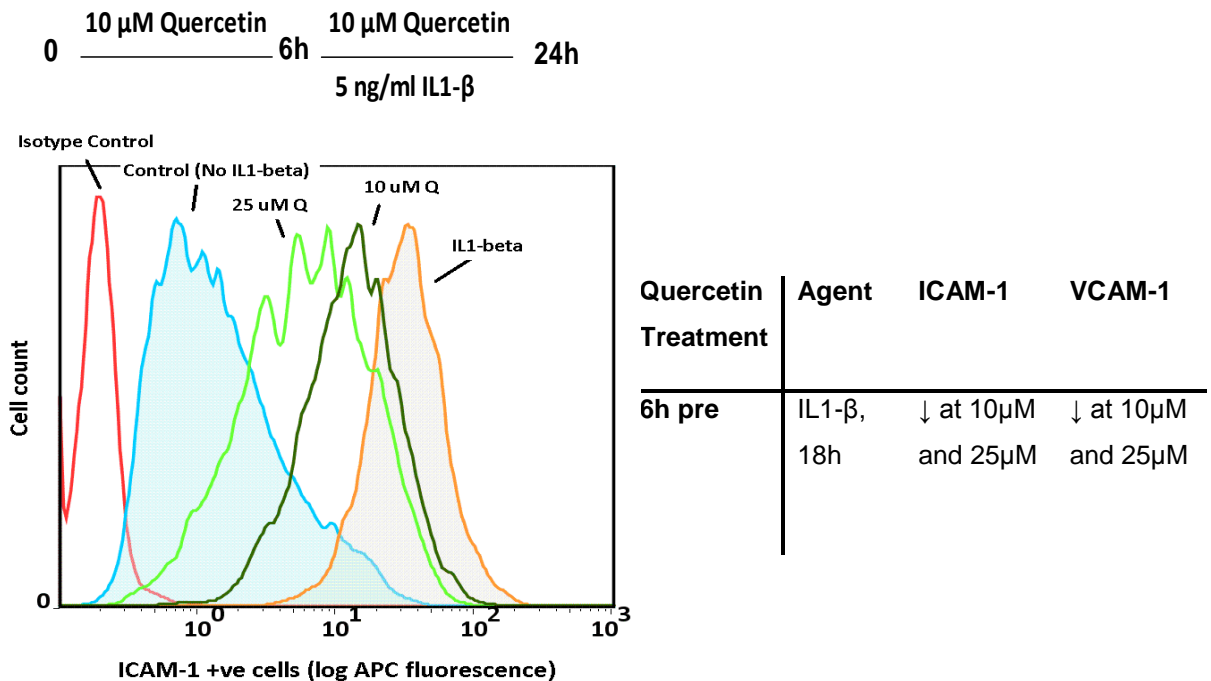
Figure 2.22: Representative histogram for the effects of quercetin on IL1-β stimulated HUVECs. Cells were pre-incubated for 6 hours with 10 µM and 25 µM quercetin which was followed by IL1-β (5 ng/ml) activation for 18 hours. Quercetin inhibited both VCAM-1 and ICAM-1 expression dose dependently.

2.4.8   Resveratrol and Resveratrol Human Metabolite Treatments

Effects of different resveratrol concentrations on HUVECs were tested after TNF-α or IL-1β stimulation. There were no significant changes in expression of VCAM-1 or ICAM-1 after the 2 h pre-incubation of HUVECs with resveratrol which was followed by 6h TNF-α (5 ng/ml) stimulation (Figures 2.23A and 2.23B). Longer pre-incubations (6h) with resveratrol followed by longer periods of stimulation with TNF-α (5 ng/ml) (18h) increased both VCAM-1 and ICAM-1 expression by HUVECs (Figures 2.23C and 2.23D). Quercetin was used as a positive control for CAM expression inhibition. Treatment with quercetin (10 µM) inhibited VCAM-1 and ICAM-1 expression after a 2 h pre-incubation which was followed by 6 h of TNF-α (5 ng/ml) stimulation (Figures 2.23A and 2.23B). As expected, quercetin was only able to strongly inhibit VCAM-1 expression when applied to the cells for 6 h pre-incubation before the 18 h TNF-α (5 ng/ml) stimulation (Figure 2.23C).

Effects of resveratrol, resveratrol human metabolites and resveratrol human metabolites mixture were also tested on IL1-β stimulated HUVECs. 2 h pre-incubation with these polyphenols was followed by 6 h stimulation with IL1-β (5 ng/ml) (Figures 2.24A and 2.24B). Resveratrol increased ICAM-1 expression, whereas its human metabolites, resveratrol 3-O-sulfate (10 µM), resveratrol 3,5-O-disulfate (10 µM) and mixtures (10 µM each metabolite) did not significantly alter CAM expression by HUVECs after IL1-β stimulation (Figure 2.24B). Resveratrol 3-sulfate (10 µM) and resveratrol 3,5-disulfate (10 µM) mixture also did not have an effect on CAM expression by TNF-α (5 ng/ml) stimulated HUVECs (Figures 2.24 & 2.25).
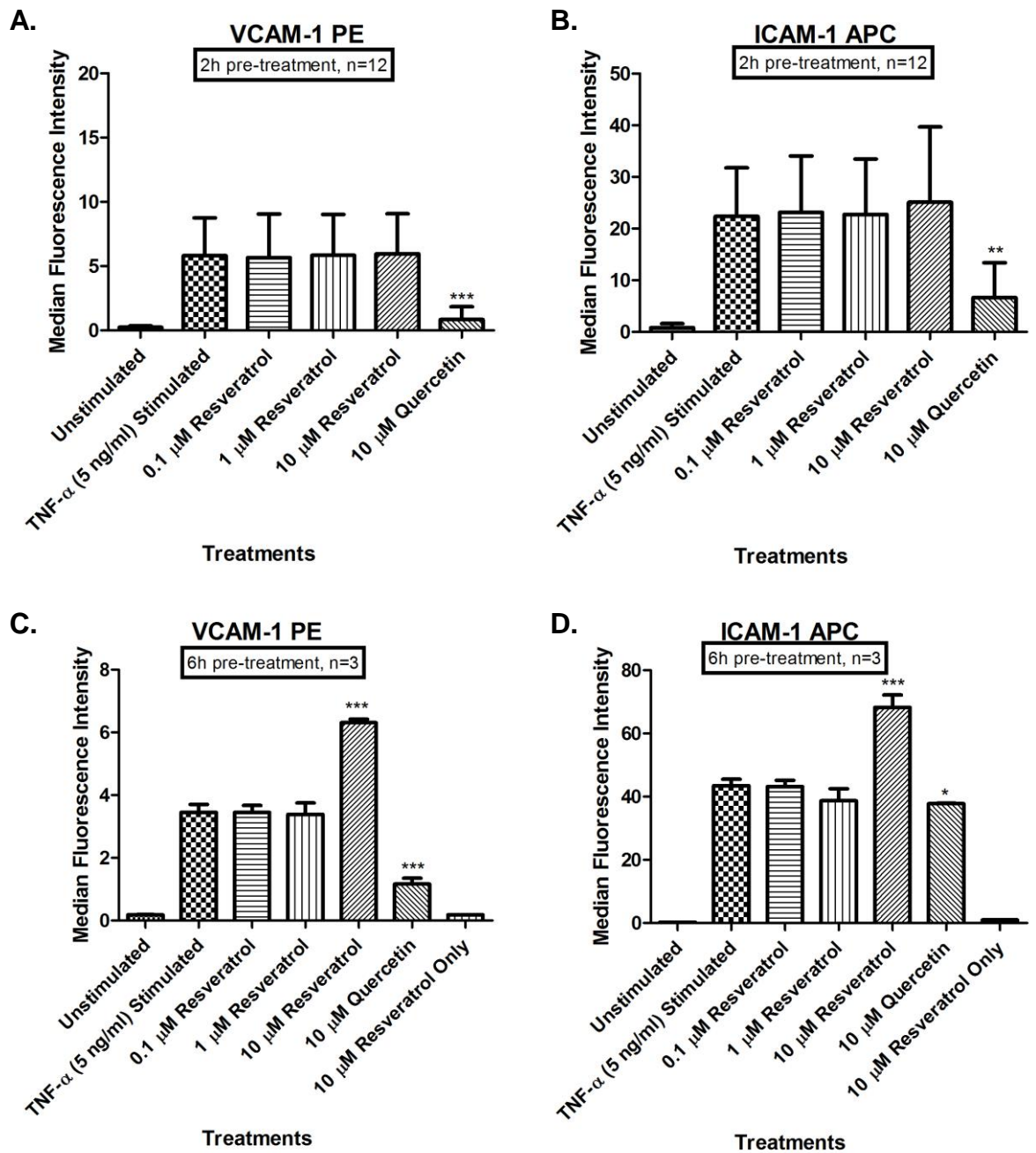
Figure 2.23: The effects of different resveratrol concentrations on TNF-α stimulated HUVECs. Cells were pre-incubated for 2 h or 6 h with 0.1 µM, 1 µM and 10 µM resveratrol which was followed by TNF-α (5 ng/ml) activation for 6 h or 18 h respectively.
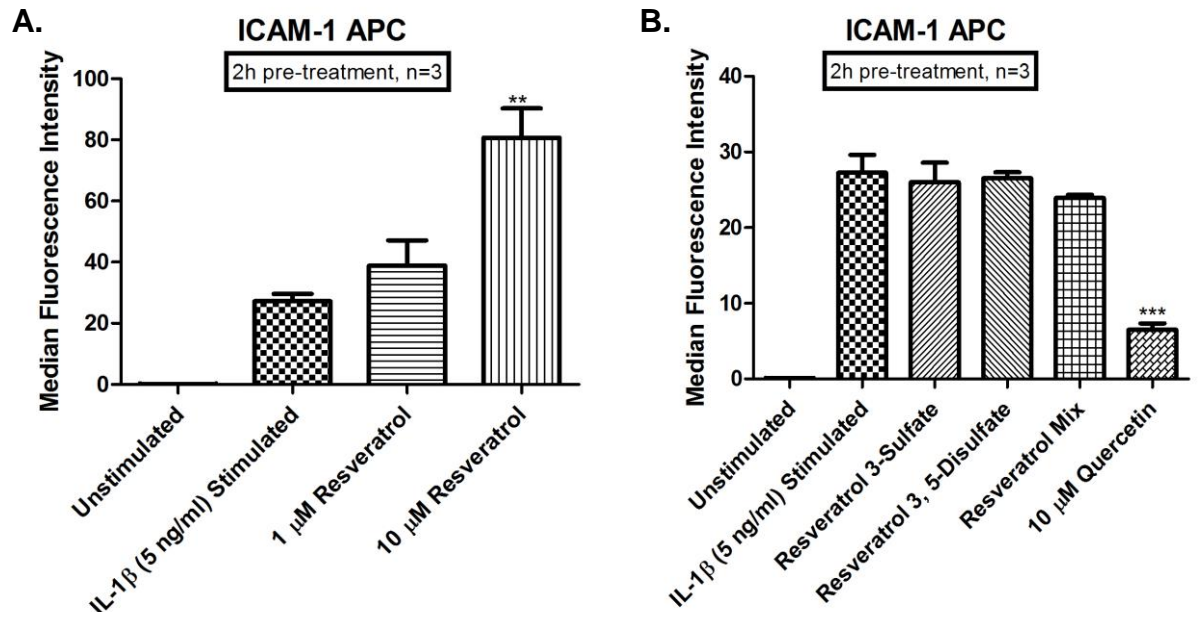
Figure 2.24: The effects of different resveratrol concentrations on IL1-β stimulated HUVECs. Cells were pre-incubated for 2 h with 10 µM resveratrol, resveratrol 3-sulfate, resveratrol 3,5-disulfate and resveratrol 3-sulfate/resveratrol 3,5-disulfate mixture which was followed IL1-β (5 ng/ml) activation for 6 h.
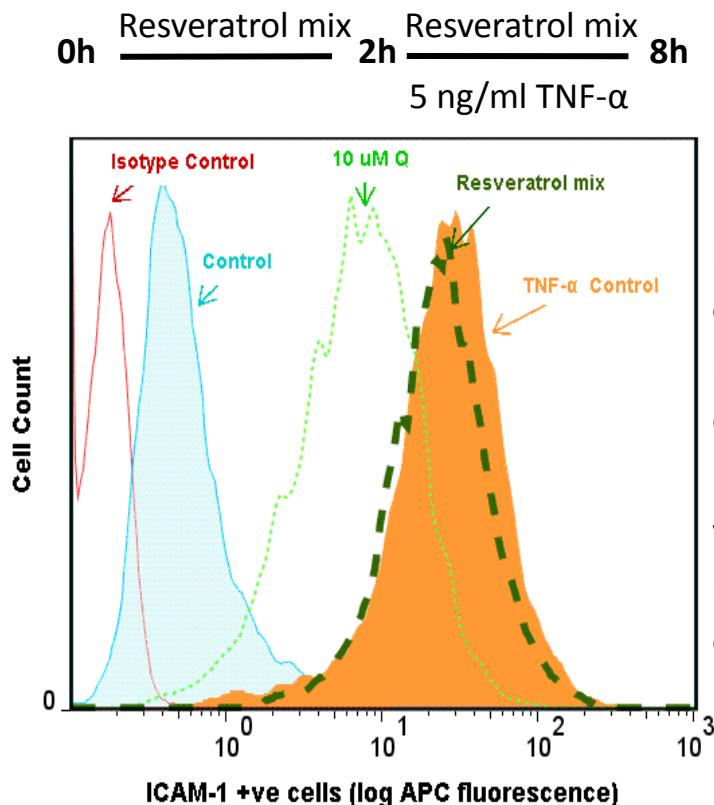
Figure 2.25: Representative histogram for the effect of quercetin and resveratrol human metabolite mixture on ICAM-1 expression. Quercetin effectively reduced ICAM-1 expression whereas resveratrol human metabolite mixture was not effective.

2.5 Discussion

In this study, the aim was to investigate the endothelial damaging and pro-inflammatory activities of high-glucose conditions and inflammatory cytokines, and the potential for polyphenols to overcome the observed deleterious effects.

Hyperglycaemic conditions did not significantly affect cell proliferation or CAM expression, whereas the inflammatory cytokines TNF-α and IL1-β caused significant increases in ICAM-1 and VCAM-1 expression (all p<0.001). Three different classes of polyphenols were assessed for their ability to alter cell proliferation and CAM expression in resting and stimulated (hyperglycaemia, inflamatory cytokines) HUVECS; flavan-3-ols from grape, the flavonol quercetin and the stilbene resveratrol. The different polyphenols induced different responses, pro- and anti-inflammatory, depending on concentration and period of exposure.

In the literature, the effect of high-glucose on HUVEC proliferation is well established indicating that high-glucose inhibits HUVEC proliferation (Selva et al., 1996, Chen et al., 2007, Varma et al., 2005, Chen et al., 2011b). Varma et al. (2005) and Chen et al. (2007) are key studies on the effect of glucose on HUVEC proliferation. Both of these studies revealed a significant reduction in cell proliferation with the incubation of cells with high-glucose containing media. However, Varma et. al. (2005), used trypan blue to measure cell proliferation. Tyrpan blue is a method more suitable for determining cell numbers, and it is not a direct measurement for the actively proliferating cells. Consequently, in the letter to editor, Davidson and Yellon (2006) raised the question whether high-glucose decreases cell proliferation or increases apoptosis. Nevertheless, Chen et al. (2007) used a relatively more effective method for cell proliferation measurement; the ^{3}H-thymidine incorporation assay that is capable of detecting actively proliferating cells by binding to the DNA during replication process. They have tested the effects of shorter glucose treatment (18.5-28.5 mM, 24 h) since the previous studies had shown that high-glucose start to induce HUVEC apoptosis after 48 h treatment (Baumgartner-Parzer et al., 1995, Ho et al., 2000). Previous studies also revealed that mannitol treatment induces vascular endothelial cell necrosis after 48-72 h (McGinn et al., 2003), and Chen et al. (2007) showed that 24 h mannitol treatment did not have an effect on cell proliferation. Therefore,

previous studies together with the findings observed by Varma et al. (2005) and Chen et al. (2007) showed that the reduction in cell numbers were not due to increases in apoptosis or necrosis, but were due to decreases in the rate at which the cells proliferated, and this was a specific effect of glucose itself and not due to secondary effects of high-glucose concentrations (e.g. through increased osmolarity).

In this study, the effects of high-glucose concentrations on HUVEC proliferation were not consistent. 24 h glucose treatment (10 mM and 20 mM) did not affect cell proliferation. 48 h and 72 h high-glucose treatments either did not affect or increased cell proliferation. Equimolar mannitol treatments did not have an effect on cell proliferation. Therefore, the potential increases in cell proliferation observed after high-glucose treatments in several experiments were not due to change in the osmolarity. Increased cell proliferation with high-glucose treatment was observed also in several other cell types, but the exact mechanism is not defined yet (Jeong et al., 2011, Sun et al., 2009, Han et al., 2011, Sun et al., 2010).

Prior to the investigation of effects of grape seed and skin extracts on HUVECs grown under high-glucose concentrations, procyanidin profiles of the two extracts were determined using the optimized normal phase method. Reverse phase HPLC is a routinely used method for the quantification of phenolics and flavonoids. However, reverse phase HPLC did not provide a good resolution for polymeric procyanidins (Figure 2.3). On the other hand, optimized normal phase method enabled the separation of the oligomeric and polymeric procyanidins with a higher resolution as in studies using similar methods (Gu et al., 2002, Prior and Gu, 2005). HPLC analysis of the extracts revealed that grape seed extract contains catechin, epicatechin and dimers only whereas grape skin extract contains trimers, tetramers, pentamers and higher polymers.

Grape skin extract treatment increased cell proliferation at low concentrations (Figures 2.8A, 2.8B and 2.8C). However, it was observed that this proliferation-inducing effect decreases under high-glucose conditions, and in parallel, anti-proliferative effects started to be observed at lower concentrations (Figures 2.8B and 2.8C). On the other hand grape seed extract showed only anti-proliferative properties. The difference between grape skin and grape seed extract treatments

was almost certainly due to the difference between the procyanidin profiles of these two different extracts.

Previous studies were mainly focused on the anti-proliferative effects of grape seed extracts on cancer cells (Cedó et al., 2013, Dinicola et al., 2012, Chatelain et al., 2011). Similarly, Agarwal and co-workers showed that 24 hours treatment with 10, 20, 50 μg/ml grape seed extract caused 65-76% inhibition in BrdU incorporation in HUVECs grown in basal media (5.5 mM glucose) (Agarwal C., 2004). The grape seed extract (Traco Labs Inc., IL, USA) by Agarwal and co-workers comprised mainly catechin and epicatechin together with small quantities of procyanidins of various chain lengths.

Therefore, the data presented here are important as it was shown that a grape skin extract containing a relatively small portion of monomers (3.28% w/w epicatechin) (Figure 2.2) and higher-chain length procyanidins was able to increase proliferation of HUVECs grown under high-glucose concentrations, whereas a grape seed extract (Leucoselect® Phytosome®) containing a greater proportion of monomers (9.8% w/w epicatechin) and shorter chain length procyanidins (up to dp4) caused an anti-proliferative effect (Figure 2.4). Hence, increase in the rate of proliferation of endothelial cells grown under high-glucose concentrations after grape skin extract treatment indicated anti-atherogenic properties of higher-chain length procyanidins showing that they may be capable of preventing possible impairment in endothelial cell proliferation, which gradually leads to vascular endothelial dysfunction initiating atherosclerotic plaque formation.

Cell proliferation measurements were followed by assessing the effect of high-glucose, inflammatory cytokines and polyphenols on cell adhesion molecule expression by HUVECs. CAM measurement method was optimized successfully after assessing a series of parameters. TNF-α and IL1-β were found to be most effective treatments to stimulate CAM expression by HUVECs, with both able to strongly induce VCAM-1 and ICAM-1 expression. It was shown in previous studies that E-selectin is sensitive to trypsin (Gräbner et al., 2000). This can be overcome by crosslinking the antibody to E-selectin before trypsinization process. However, this may be still not the best option as the antibodies are also proteins and they may be cleaved by the trypsin. There are several studies, which compare the cell

harvesting methods indicating cons and pros for each of them. According to Mutin and co-workers, the highest cell viability and the most effective method with the lowest disruption to the adhesion molecules is the trypsinization method, which is followed by the PBS-EDTA treatment (Mutin et al., 1996). Therefore, PBS/EDTA treatment was also tested to harvest the cells, as it is a less invasive method. Nevertheless, E-selectin could not be detected and cell yield was much lower compared to the trypsin/EDTA treatment (data not shown). Trypsin/EDTA treatment was chosen to be used in the experiments. However, it is an invasive method and may lead to cell death. Dead cells may behave differently leading to non-specific binding to the antibodies (Figure 2.11). Therefore, experiments were carried out using propidium iodide to include only the live cells into the analysis rather than using the traditional method to fix cells prior to the analysis using paraformaldehyde.

After CAM measurement method was optimized, the effects of high-glucose on CAM expression by HUVECs were tested. However, high-glucose was not effective in inducing CAM expression by HUVECs after treatments with different glucose concentrations for different durations (Figure 2.12). There are conflicting data in the literature concerning the effects of high-glucose on the expression of cellular adhesion molecules by HUVECs. The data varies between short-term glucose exposure and ≥24 h glucose exposure and also between reports for ≥24 h exposures. A short-term study which involved the incubation of a 3D in vitro human vascular tissue model with a high-glucose concentration (30 mM) for 9 h showed a significant increase in VCAM-1 expression compared to the cells grown in basal media (5.6 mM) (Gappa-Fahlenkamp and Shukla, 2009). However there were not significant increases in the expression levels of ICAM-1 and E-selectin with the high-glucose incubation over 9 h. TNF-α could activate ICAM-1 expression after 9 h treatment, but it did not have an effect in the expression levels of E-selectin after 9 h.

Several other studies that involved 24 h incubation of HUVECs with high-glucose media revealed an increase in the expression of VCAM-1, ICAM-1 and E-selectin (Piconi et al., 2004, Baumgartner-Parzer et al., 1995, Altannavch T. S., 2004). Therefore the time interval for the incubation of the cells at 37°C might be important and at least 24 h incubation with the high-glucose media might be

necessary for the induction of ICAM-1 and E-selectin expression. Also, there is inconsistency among reports of 24 h incubation with high-glucose for the expression of E-selectin. Altannavch and co-workers reported an increase in the expression of E-selectin as a result of the 24 h incubation of HUVECs with 16.5 mM glucose media (Altannavch T. S., 2004). In contrast, Taki and co-workers did not detect a significant increase in E-selectin expression after the 24 h incubation of HUVECs in 33 mM glucose (Taki et al., 1996).

An interesting study involved the treatment of HUVECs with sera from type 1 diabetic patients and non-diabetic people (Ramussen et al., 2002). 6 h incubation with the non-diabetic sera stimulated the cells to produce CAMs higher than basal levels. When the cells were incubated with the sera from diabetic patients, a significant increase was observed in VCAM-1 expression compared to the cells incubated in sera from non-diabetic people. In parallel, experiments involving the incubation of the cells with high-glucose (5.5 to 13.5 mM) media did not activate the cells to express CAMs. On the other hand, TNF-α treatment increased VCAM-1 and E-selectin expression by the cells. Therefore, this study suggested that the increase in the VCAM-1 expression after the incubation with diabetic sera might be due to a component in the sera rather than high-glucose itself. Previous reports in the literature showed that higher levels of inflammatory cytokines were observed in the circulation of diabetics compared to non-diabetics (Lechleitner et al., 2000, Rajarajeswari et al., 2011, Nilsson et al., 1998, Spranger et al., 2003) which is likely to explain the increase in CAMs due to a secondary effect of hyperglycaemia.

A recently published study by Azcuita and co-workers also investigated the effect of high-glucose on the expression of CAMs by endothelial cells. They incubated the cells in a high-glucose containing media with or without IL-1β or TNF-α (Azcutia et al., 2010). The high-glucose treatment could not induce CAM expression. However, incubation of the cells with high-glucose media in the presence of TNF-α caused a synergistic increase in the expression levels of ICAM-1 and VCAM-1. Therefore these two studies revealed that the high-glucose is not enough to activate HUVECs by itself, but it may have a synergistic effect to increase the CAM expression with pro-inflammatory cytokines.

In summary, effects of glucose on HUVECs may be affected by the conditions in different labs. Therefore, the study presented here continued to assess the effects

of polyphenols on CAM expression by HUVECs after stimulating them with either IL-1β or TNF-α.

Grape seed/skin extracts, quercetin, resveratrol and resveratrol human metabolites were tested for their abilities to inhibit cell adhesion molecule expression in HUVECs. All these polyphenols are well known for their anti-inflammatory properties (Altannavch T. S., 2004, Ferrero et al., 1998, Tribolo et al., 2008). Among the polyphenols tested, quercetin is the only polyphenol that inhibited pro-inflammatory cytokine induced VCAM-1 and ICAM-1 expression by HUVECs (Figure 2.22). Interestingly, grape seed/skin extracts increased cell adhesion proliferation synergistically with IL-1β and TNF-α (Figures 2.15 and 2.19). Sen and Bagchi showed that pre-incubation with a grape seed proanthocyanidin extract (GSPE) (1-5 µl/ml) inhibited the TNF-α (10 ng/ml, for 16 h) induced VCAM-1 expression (Sen and Bagchi, 2001). However, at the same time, this extract increased ICAM-1 expression. On the other hand, two consecutive studies by Zhang et al. (2006) and Ma et al. (2007) showed selective inhibition of VCAM-1 expression induced by advanced glycation end products (200 mg/L for 12 h or 24 h) by pre-incubation of HUVECs with grape seed proanthocyanidin extract (5, 15, 25 , 50 and 100 µg/ml) for 4 h. At the same time, Zhang et al. (2006) showed that GSPE did not have an effect on ICAM-1 expression. The GSPE extract used by Zheng et al. (2006) was reported to comprise at least 96% procyanidins, but the exact composition was not indicated. On the other hand, the GSPE used in other two reported studies were reported to contain mainly dimeric proanthocyanidins (>50% of the total) which is similar to the dimeric procyanidin content of the grape seed/skin extracts used in the study reported here.

The up-regulatory effect of grape seed/skin extracts on TNF-α or IL-1β induced VCAM-1 and ICAM-1 expression observed in this study was not due to cytotoxicity, since only the viable cells were included in the analysis, which was achieved by excluding propidium iodide stained cells (Figure 2.11B). Also, it was shown that this up-regulatory change was the synergistic effect of the inflammatory cytokines and the extracts, as the extracts alone did not induce the expression of VCAM-1 and ICAM-1 (Figure 2.19).

Several reports have provided evidence that resveratrol has anti-inflammatory properties (Ou et al., 2006). It has been shown that resveratrol is capable of inhibiting induced VCAM-1 and ICAM-1 expression in endothelial cells. Resveratrol (30 µM and 50 µM) pre-treatment for 1 h of phorbol 12-myristate 13-acetate activated (for 4 h) HT1080 endothelial cells inhibited the ICAM-1 expression (Park et al., 2009). Ferrero and co-workers showed that pre-incubation of HUVECs with resveratrol (100 nM-1 µM) inhibits TNF-α induced ICAM-1 expression (Ferrero et al., 1998). They also showed that 24 h pre-treatment of human saphenous vein endothelial cells inhibits LPS (4 mg/L, 4h) induced expression of VCAM-1. In an interesting study, Deng *et al.* (2010) showed that both resveratrol (0.1 µM -10 µM, 2h pre-incubation) and the resveratrol derivative, *trans*-3,5,4-trimethoxystilbene (0.1 µM -10 µM, 4 h pre-incubation) could inhibit TNF-α induced VCAM-1 and ICAM-1 expression. In these previous studies, the cells were activated for short time periods. Therefore both 6h and 24 h stimulation were tested in the experiments in this study. Also shorter resveratrol pre-treatment periods were tested. However, in this study, an anti-inflammatory effect of resveratol could not be established. It is observed that higher doses of resveratrol synergistically increased ICAM-1 expression with pro-inflammatory cytokines (Figures 2.23C and 2.23D). Data presented here shows that resveratrol is not pro-inflammatory by itself (Figures 2.23C and 2.23D). Two different resveratrol human metabolites and their mixture were also tested for their potential anti-inflammatory effects. However, there was no significant change in the induced expression of VCAM-1 and ICAM-1 after the pre-incubation of HUVECs with resveratrol human metabolites or their mixtures (Figure 2.24).

There are numerous reports that provide evidence of inhibitory effects of quercetin on induced VCAM-1 and ICAM-1 expression in endothelial cells. Kobuchi and co-workers showed the inhibition of TNF-α induced expression of ICAM-1 in ECV304 cells with the pre-incubation with quercetin (1-50 µM) (Kobuchi et al., 1999). Middleton and Anne also showed the inhibitory effect of quercetin (1-3 µM) on ICAM-1 expression in HUVECs activated by LPS (Middleton and Anne, 1995). On the other hand, Tribolo et al. (2008) showed that the pre-incubation of HUVECs with 10 µM and 50 µM quercetin for 45 minutes inhibited TNF-α /LPS induced VCAM-1 and ICAM-1 expression. Beside quercetin aglycon, it was also been shown that several quercetin human metabolites had the capacity to inhibit the

expression of these two cell adhesion molecules even though they were not as potent as quercetin aglycone. In the present study, it was shown that anti-inflammatory effects of quercetin were dependent on type and duration of the agent used to stimulate the cells (Figures 2.20, 2.21 and 2.22).

In conclusion, hyperglycaemic conditions did not significantly affect cell proliferation or CAM expression, the inflammatory cytokines TNF-α and IL1-β induced significant changes in CAM surface expression, and the different polyphenols induced different responses, pro- and anti-inflammatory, depending on concentration and period of exposure.

Since the effect of increased glucose concentrations and pro-inflammatory cytokines on endothelial cells is multifaceted, and polyphenols have been shown to work through multiple mechanisms and elicit a variety of changes in the functions of cells to which they are exposed, a non-targeted approach such as metabolomics would provide the ideal approach for determining the full range of responses. Therefore, the next chapter involved method development and model assessment for the proposed metabolomics study.

CHAPTER 3: Metabolomic Analysis of HUVECs: Method Development and Testing

3.1 Abstract

Background: There are very few reports describing metabolite profiling of adherent cells. The methods used for cell harvesting and metabolite extraction may have influence on the results as it was shown in previous studies that different harvesting or extraction methods yielded variable results, and there is not an optimal method for all the cell types. Metabolite profiling of HUVECs by ^{1}H NMR (proton nuclear magnetic spectroscopy) is a novel approach.

Aim: To develop and test a protocol that facilitates rapid arrest of cellular metabolism, efficient extraction of metabolites and analysis of extracted metabolites by ^{1}H NMR producing non-biased and reproducible results.

Approaches/methods: An initial protocol for extracting metabolites from cultured cells was established based on a review of the available literature. The protocol was then optimised to achieve maximum recovery of ^{1}H NMR metabolite signals and minimize medium carry-over. ^{1}H NMR spectroscopy was used to determine HUVEC metabolite profiles. The 2D NMR approaches of correlation spectroscopy (COSY) and heteronuclear single quantum correlation (HSQC) were used to identify metabolites. Six different sample preparation methods for profiling intracellular metabolites from HUVECs were compared for their effectiveness. Subsequently, the sensitivity and reproducibility of the selected method was assessed using samples from cells treated with lipopolysaccharide (LPS), malonate and growth factor-free medium (GF).

Results: Among the six different sample preparation methods, direct methanol extraction, yielded the strongest signals with the highest number of metabolites detected. Therefore, it was used to bring cellular metabolism to a halt and allow metabolite extraction in a single step avoiding any possible alterations in cellular metabolism prior to NMR analysis. NMR spectra obtained for the metabolite extracts showed adequate signal-to-noise ratio which allowed identification of 27 metabolites. LPS treatment did not induce any significant alterations in HUVEC metabolome. Removal of growth factors from culture medium led to a significant

decrease in the levels of aspartate ($p<0.01$), asparagine ($p<0.001$), tyrosine ($p<0.001$) and pyruvate ($p<0.01$). Malonate (10 mM, 6 h and 24 h) treatments disrupted cellular respiration causing reductions in intracellular ATP ($p<0.001$), glutamate ($p<0.01$), aspartate ($p<0.001$), lactate ($p<0.001$) and formate ($p<0.05$) levels, and elevations in glucose, pyruvate, inosine ($p<0.001$) and histidine ($p<0.001$) levels, and these observations are in keeping with the known effects of malonate as an inhibitor of Krebs cycle (inhibits succinate dehydrogenase). Also, succinate (50 mM) co-treatment prevented deleterious effects of malonate on HUVECs.

Conclusions: The protocol facilitated rapid and effective freezing of cellular metabolism and extraction of metabolites. The extracted metabolites were analysed using ^{1}H NMR, which produced non-biased and reproducible results when the effects of several known metabolic effectors on HUVECs were tested in the HUVEC model.

3.2 Introduction

High-glucose, pro-inflammatory cytokines and polyphenols have all been shown to work through multiple mechanisms and elicit a variety of changes in the functions of cells. However, these changes were mainly investigated using targeted approaches so far as in the Chapter 2 of the present study. For example, Hsieh and co-workers assessed the protective effects of polyphenol rich guava budding leaves on glucose stimulated HUVECs by measuring cell viability, ROS and NO productions (Hsieh et al., 2007). Wang and co-workers investigated the effects of grape seed proanthocyanidins on the proliferation of glucose stimulated vascular smooth muscle cells (Wang et al., 2010). In another study, Crespo and co-workers compared the effects of kaempferol and quercetin on cytokine-induced pro-inflammatory status of cultured human endothelial cells by measuring cell adhesion molecule expression (Crespo et al., 2008). Therefore, non-targeted approach metabolomics, was chosen as the ideal approach for further exploring effects of high-glucose, pro-inflammatory cytokines and polyphenols on HUVECs with a view to understanding the effects at a mechanistic level on the entire system. The metabolomics approach allows the identification of underlying disturbances in cellular metabolism after biological treatments that would not have been easily detected using targeted approaches, establishing more robust biomarkers of diseased states.

Metabolomics targets determination of all small molecule (<1 kDa) metabolites present in a biological medium (Sellick et al., 2008, Teng et al., 2009, Danielsson et al., 2010). In recent years, this global analysis approach has gained noticeable importance as it can be used to visualise alterations in metabolome during both healthy and diseased states in biological systems (Miccheli et al., 2006, El Ghazi et al., 2010, Martínez-Martín et al., 2012). This approach may provide an influential attitude to define the possible effects of different agents (biological or chemical) on cellular phenotype since the alterations in metabolome reflects the changes in phenotype, which discriminates it from the transcriptomics and proteomics approaches (Dunn et al., 2005, Dunn and Ellis, 2005) (Figure 3.1).
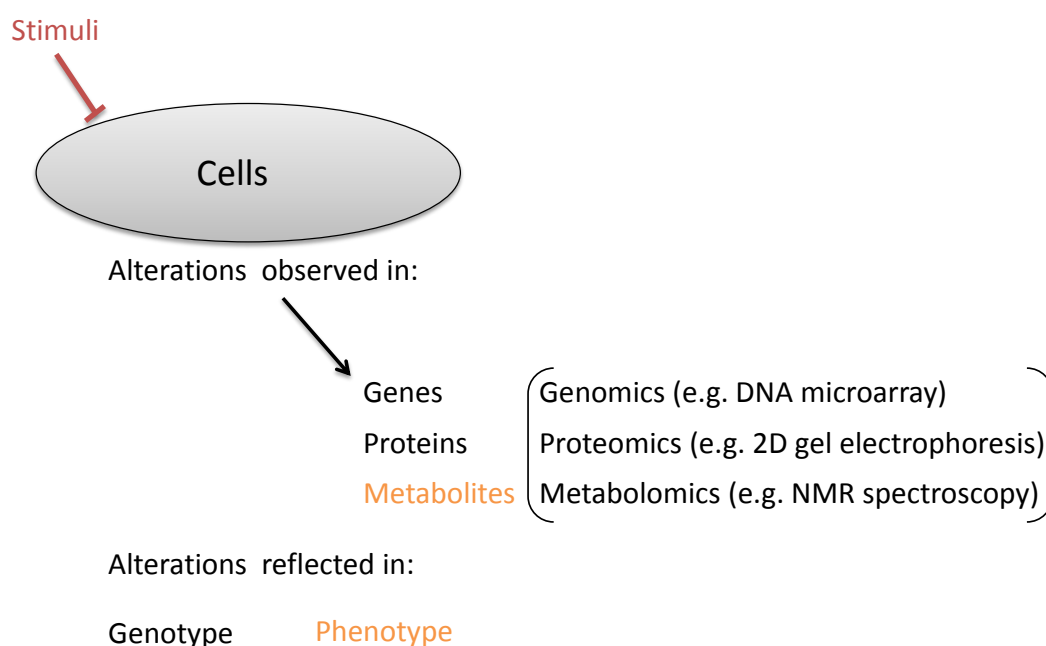
Figure 3.1: Global analysis approaches in response to external stimuli. Alterations in gene expression, protein and metabolite profiles of cells can be determined using different global approaches; however, alteration in metabolite profile is more proximal to alterations observed in cellular phenotype.

Gas chromatography (GC) or GC coupled to mass spectrometry (MS) were the initial analytical techniques used to detect metabolites. However, as NMR spectroscopy was improved it became the most popular analytical technique for metabolomics together with LC-MS. The improvements in the NMR spectroscopy were both in the hardware and in the methodologies which increased detection sensitivity enabling measurements of significantly smaller amounts of substances or spending less time for a fixed sample concentration. For example, two milestones in the hardware technology were the development of superconducting magnets up to 1 GHz providing higher field strength up to 23.5 Tesla (2.35 Tesla by iron magnet technology) and the cryoprobe technology which provides higher sensitivity and reduce signal-to-noise ratio at the given field strength (Kovacs et al., 2005). NMR spectroscopy is more practical compared to GC and MS since it requires minimal sample preparation and it is a non-destructive technique which enables further analysis of samples if necessary. On the other hand, GC and MS may require chemical or physical modification of samples since the metabolites in

the sample must be separated (e.g. liquid chromatography) before MS detection or made volatile before GC analysis. Nevertheless, MS detection is more sensitive and in most cases can detect lower concentrations of metabolites, and may be used to complement data from NMR spectroscopy (Duarte, 2011, Valdés et al., 2012).

Although there are several metabolomics studies reported in the literature which involved cell suspension and adherent cell types, metabolic profiling of HUVECs by ^{1}H NMR is a novel approach (Sellick et al., 2008, Duarte et al., 2010, El Ghazi et al., 2010, Dettmer et al., 2011). Therefore, a protocol was derived by reviewing existing reports in the literature to initiate experiments in the current study (Bennett et al., 2008, Teng et al., 2009, Martineau et al., 2011).

In metabolomics, appropriate sample preparation prior to analysis bears a great importance. As the cellular metabolites may degrade quickly due to environmental conditions, the state of dynamic cellular metabolism must be quenched as soon as possible. Otherwise, it is not possible to have unbiased measurements of metabolite concentrations as they will reflect the changes until metabolism is brought to a halt (Danielsson et al., 2010, Dietmair et al., 2010).

Therefore, in this study, a series of experiments were carried out to optimize a literature derived protocol which ultimately allowed quick and effective freeze of cellular metabolism, extraction of metabolites and analysis of extracted metabolites by employing ^{1}H NMR producing non-biased and reproducible results. This protocol was then further tested assessing the effects of lipopolysaccharide (LPS), growth medium without growth factors (GF) and malonate on HUVEC metabolome (metabolite profile).

3.3 Materials & Methods

3.3.1 Materials

Deuterium oxide (D_2O, D, 99.9%) was purchased from Cambridge Isotope Laboratories, Inc (USA). All other chemicals were obtained from Sigma-Aldrich (Poole,UK) unless specified. Centrifugation process used a Heraus Sepintech-Mega fuge 1.0R) and centrifugal evaporator (Jouan RC1022).

3.3.2 Quenching Metabolism and Extracting Metabolites (Literature Derived Protocol)

10 cm dishes were seeded with a density of 2800-3000 cells/cm^2. Cultures were maintained at 37°C and 5% CO_2. Growth medium was changed on the following day of seeding in order to remove DMSO from the medium. Thereafter, medium was changed every 2 days. Cells became confluent 5 days after seeding. The initial method used to quench metabolism and extract metabolites for subsequent NMR analysis was derived from the following existing literature reports; Bennett et al. (2008), Teng et al. (2010) and Martineau et al. (2011).

1. Remove the medium from confluent cells by aspiration

2. Quench cells with 3 ml of cold 80% HPLC grade methanol in water (-80°C)

3. Incubate the cells for 15 minutes on dry ice

4. Detach the cells and disrupt cell membranes using a cell scraper

5. Pipette the cells solution into centrifuge tubes

6. Centrifuge at 2000g for 5 min at 4°C

7. Save the supernatants on ice. Reconstitute the pellet in 0.5 ml 80% methanol (4°C).

8. Repeat steps 6-7

9. Pool the supernatants

10. Dry the sample using a centrifugal evaporator

11. Reconstitute the sample in an appropriate solvent according to the subsequent analytical procedure;

      i.   For NMR (<u>NMR Buffer</u>: 203 mM Na_2HPO_4, 40 mM NaH_2PO_4, 7.7 mM NaN_3, 145 µM TSP in D_2O)

      ii.   For MS (H_2O)

3.3.3 ^{1}H NMR Spectroscopy Recording and Statistical Analysis of ^{1}H NMR Data

High-resolution ^{1}H NMR spectra were recorded on a 600 MHz Bruker Avance spectrometer fitted with a 5 mm TCI cryoprobe and a 60 slot auto-sampler (Bruker, Rheinstetten, Germany). Sample temperature was controlled at 300°K. Each spectrum consisted of 128 scans of 32,768 complex data points with a spectral width of 13.3 ppm (acquisition time 2.05s). The *noesypr1d* pre-saturation sequence was used to suppress the residual water signal with low power selective irradiation at the water frequency during the recycle delay (D1 = 2s) and mixing time (D8 = 0.10s).

Spectra were transformed with 0.3 Hz line broadening and zero filling, manually phased and baseline corrected using the TOPSPIN 2.0 software. The NMR spectra were further analyzed using the Amix$^{®}$ software package (Bruker, Germany) to create buckets for signals within the range of 0.1-8.9 ppm (except the water signals, 4.60-5.0ppm). These buckets were of various widths, and each one encompassed singlets or multiplets that represented metabolites. The signal intensity for each bucket was integrated and a data matrix was obtained. Statistical multivariate analysis was performed using Matlab. The analysis involved principle component analysis (PCA), which is an unsupervised method. Data were scaled to unit variance (autoscaling) to compensate for large differences in intensity among metabolite signals. Buckets defined in a NMR spectrum form a single data point in PCA, and they are responsible for the separation observed in PCA plots. The contribution of each bucket to the separation in PCA plot can be visualised using the corresponding loading plot. In a loading plot, each bucket forms a data point.

Final analysis involved applying univariate statistical analysis to confirm the changes observed by multivariate analysis, and determining the significance of the

differences. Non-parametric Mann-Whitney tests were used, and p values less than 0.05 (* $p<0.05$, ** $p<0.01$, *** $p<0.001$) were accepted as a significant difference.

3.4 Results

3.4.1 Determination of Initial Metabolite Profiling Protocol for HUVECs

The aim was to (1) draw up an initial protocol based on the available literature, (2) identify the metabolites using this protocol and assess several method performance parameters, (3) investigate variations in the method parameters on method performance and select the best protocol, (4) test the use of the protocol with the HUVEC model that has been treated with a known metabolic poison and with strong biological effectors (i.e. characterize the system/model).

An initial protocol was formed according to the information obtained from the literature (Bennett et al, 2008, Teng et al., 2010, Martineau et al., 2011). Cold methanol/water buffer was selected as the solvent to quench cellular metabolism before extracting intracellular metabolites. Methanol (80% v/v, at -80°C) was added directly onto the cells immediately after the medium had been rapidly removed. The rapid addition of -80°C aqueous methanol to the cells causes an extremely rapid temperature drop in the cells and brings metabolism to a halt because enzymatic reactions are effectively terminated. In addition, the high concentration of methanol rapidly and effectively disrupts cell membranes and releases the cytosol into the bulk liquid extract phase and thus bypasses the need of an additional extraction step. After the addition of the cold methanol, cells were incubated on dry ice for 15 minutes to further disrupt cell membranes, and then the lysed cells/debris were scraped from the plastic surface using a cell scraper. After collecting the cell lysate, the cell debris was separated from the liquid phase by centrifugation, and the samples were dried using centrifugal evaporator. Dried metabolites were then re-suspended in appropriate buffers for subsequent analysis by NMR spectroscopy or MS.

Having established an initial protocol, further experiments were designed to test variations of the quenching and extraction methods with adherent HUVECs, in order to gain a better understanding of how variations in the method affected performance, and to select the most effective procedures for use in a final protocol. First, the effectiveness of quenching cellular metabolism and extracting metabolites with cold methanol was assessed. HUVECs were grown until confluence and metabolites were extracted by cold methanol addition. After the

NMR spectra were obtained for the samples, further analysis was performed using Amix$^®$ software. A typical ^{1}H NMR spectrum provides distinctive signals with particular splitting patterns for hydrogen-bearing molecules in a sample (Figure 3.2). Signal intensities are proportional to the concentration of the individual metabolites in the sample.

Amix$^®$ software was used to locate any differences in spectra visually and also for choosing and integrating the peaks (bucketing) to go into multivariate analysis (Figure 3.2). Multivariate analysis was performed on the data for intra- and extracellular metabolites (Figure 3.3).

Multivariate analysis showed a good separation between intra- and extracellular metabolite profiles. The first two principal components (PC) were plotted against each other (Figure 3.3A). The two types of sample scores separated easily along PC1. The intracellular scores formed a tight cluster on the negative side of PC1, therefore, the extraction method used was repeatable (Figure 3.3A). The extracellular scores were divided into a score on the upper right hand quadrant of the plot (the fresh medium or medium 0) and a group of scores on the right hand lower quadrant (spent medium replicates) (Figure 3.3A). The spent medium replicates clustered tightly.

The loading plot highlighted the buckets responsible for the separation on the score plot (Figure 3.3C). For example, the bucket 6.15 was located on the left hand side of the PC1 axis, which means that the intracellular extracts contained more of the signal at 6.15 ppm than the extracellular extracts as the intracellular extracts were located in the same side of the score plot (Figures 3.3A and 3.3B). Figure 3.3C shows the bucketing of signals for multivariate analysis. In the regions of the spectra that show the 6.15 ppm peak, there is a doublet at 6.15 ppm (ATP) present in the intracellular extracts but absent from the extracellular material which probably arose from a nucleotide entity and contributed to separation of these different sample groups.
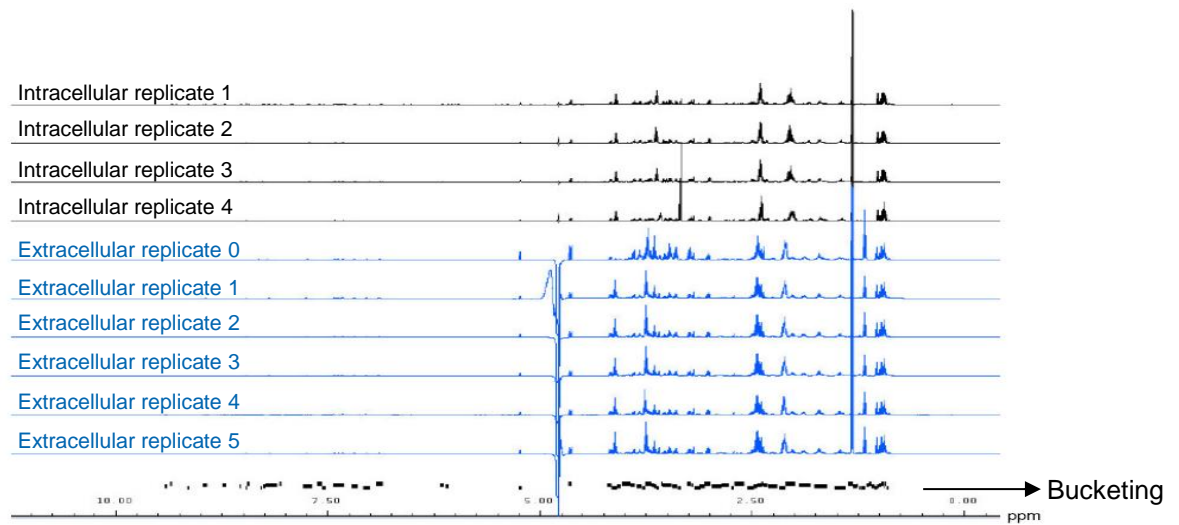
Figure 3.2: ^{1}H NMR spectra of the intracellular and extracellular extracts from HUVECs. Extracellular replicate 0 is fresh medium, 1-5, the spent medium on day 5 of the cell growth.
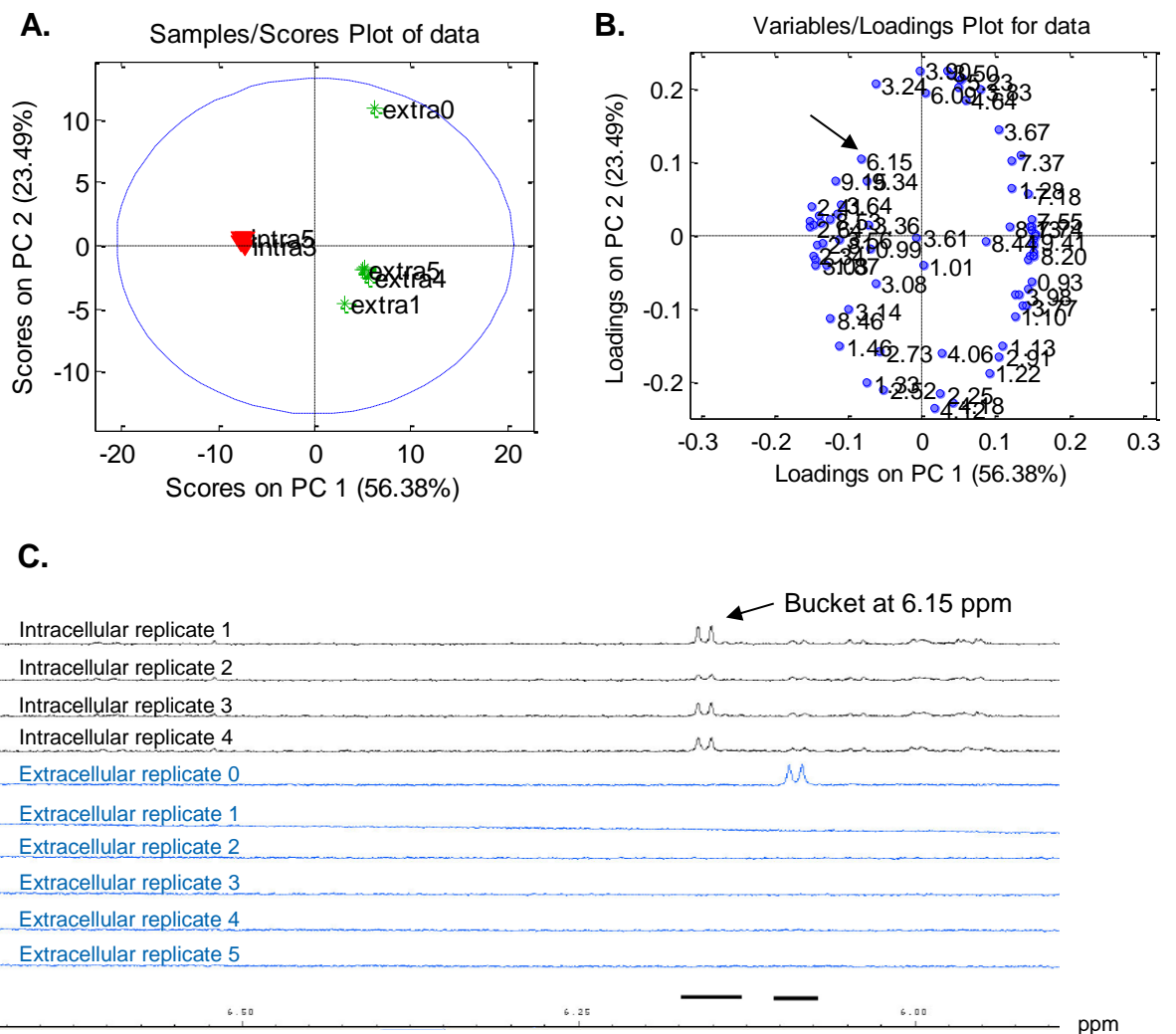
Figure 3.3: **A.** Score plot of the first two axes from the PCA on 10 samples (4 intracellular replicates, 5 extracellular replicates (spent media) and 1 fresh medium. **B.** Loading plot for samples highlighting buckets contributed to PCA result. **C.** Signals bucketed for multivariate analysis.

Selected areas (1.3-3.2 ppm for Figure 3.4A and 5.8-8.0 ppm for Figure 3.4B) of the ^{1}H NMR spectra of the intracellular and extracellular extracts from HUVECs highlighted the differences in the metabolite composition of the profiles. For example, in Figure 3.4A, glutamate was at higher concentration in the intracellular extracts, and glutamine was present at a much higher concentration in the extracellular extracts (spent media) and fresh medium. Some of the nucleosides/nucleotides were unique to the intracellular extracts.

The results obtained indicated that there was very little variation between replicate samples (good precision). When the spectra were investigated, most of the peaks were found to be common in the intra- and extracellular samples. After this observation, the extraction protocol was questioned, as the similarity in the spectra of intra- and extracellular samples might be due to medium carry-over although it is expected that media metabolites would be taken up by cells and cell metabolites would be excreted to the media. Therefore a series of experiments were performed in which additional cell wash steps were included prior to methanol extraction to investigate the possibility of bias caused by medium carry-over into cell samples.
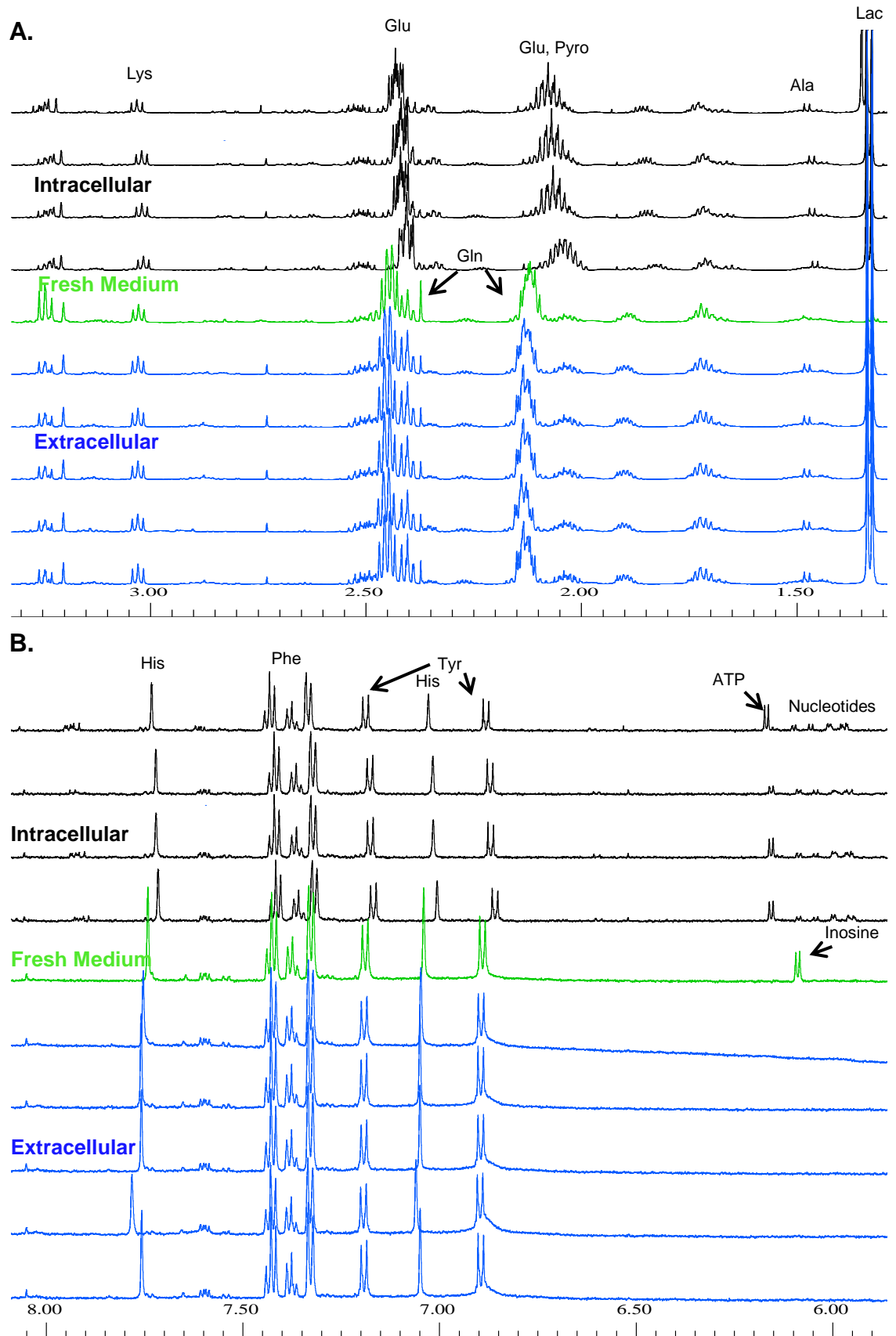
Figure 3.4: Selected areas (0.9-3.2 ppm for **A** and 5.8-8.0 ppm for **B**) of the ^{1}H NMR spectra of the intracellular and extracellular extracts from HUVECs.

3.4.2 Identification of Metabolites

The spectra from one-dimensional ^{1}H NMR analyses yielded overlapping signals for many metabolites (Figure 3.5A). Therefore, two-dimensional (2D) NMR experiments were performed also to confirm metabolite identities by obtaining more dispersed signals and uncovering molecular interactions. In this study, interactions between two nuclei through the bonds which connect them (J-coupling interaction) were assessed to obtain signal multiplicity and coupling constants. Metabolites in HUVECs were assigned by analyzing their ^{1}H/^{1}H (correlation spectroscopy, COSY) (Figure 3.5B) and ^{1}H/^{13}C (heteronuclear single quantum correlation, HSQC) spin system coupling patterns and comparing their ^{1}H NMR spectra chemical shifts with previously reported values (Teng et al., 2009), human metabolite databank [www.hmdb.ca]) and standard compounds. In total, 27 metabolites could be identified (Table 3.1).

A. [1]H spectrum for HUVECs (intracellular)
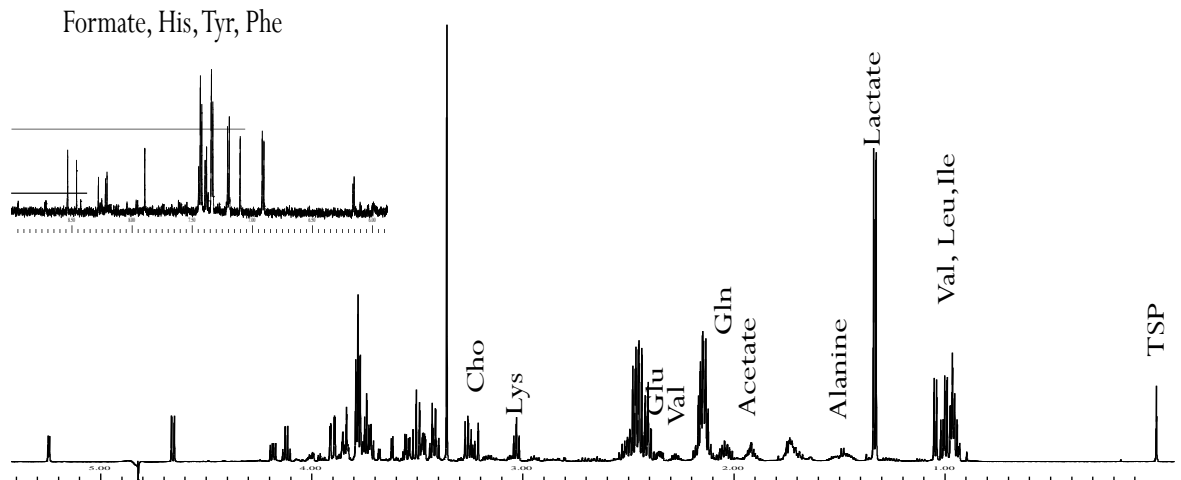
B. COSY (^{1}H/^{1}H) Experiment
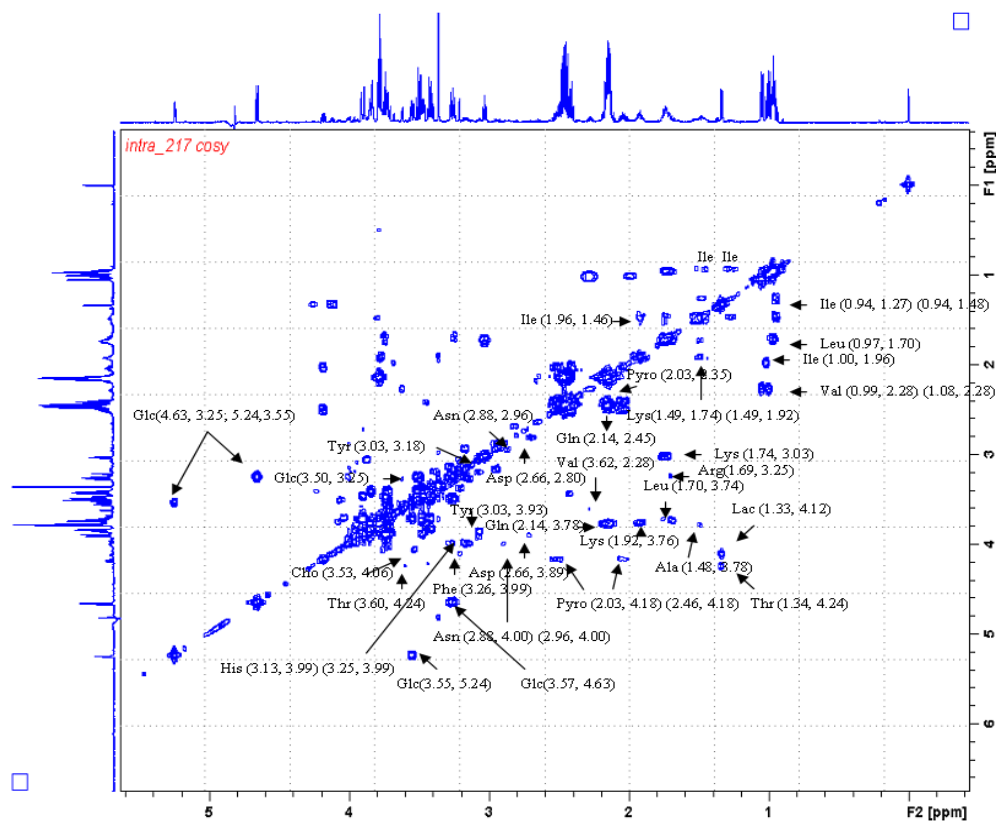
Figure 3.5: **A.** ^{1}H NMR spectrum of intracellular metabolite extract from HUVECs (8.50-0 ppm). Several metabolites are annotated to the responsible signals. **B.** COSY experiment with intracellular metabolite extract from HUVECs. Metabolites were assigned by analysing ^{1}H/^{1}H spin system coupling patterns.

Table 3.1: Intracellular metabolite list for HUVECs. 27 metabolites were identified of which 17 were amino acids.

No	Metabolites	Abbreviation	¹H NMR Signals
1	Leucine	Leu	0.97(t), 1.70(m), 3.74(m)
2	Isoleucine	Ile	0.94(t), 1.00(d), 1.27(m), 1.46(m), 1.96(m). 3.66(d)
3	Valine	Val	0.99(d). 1.08(d), 2.28(m), 3.62(d)
4	Threonine	Thr	1.34 (d), 3.60(d), 4.24(m)
5	Alanine	Ala	1.48(d), 3.78(q)
6	Lysine	Lys	1.49(m), 1.74(m), 1.92(m), 3.03(t), 3.76(t)
7	Arginine	Arg	1.67(m), 1.92(m), 3.25(t), 3.79(t)
8	Pyroglutamate	Pyro	2.03(m), 2.46(m), 2.35(m), 4.18(dd)
9	Glutamate	Glu	2.04(m), 2.14(m), 2.34(m), 3.75(dd)
10	Glutamine	Gln	2.14(m), 2.45(m), 3.78(t)
11	Pyruvate	Pyr	2.38(s)
12	Methionine	Met	2.14(m), 2.65(t), 3.85(dd)
13	Aspartate	Asp	2.66(dd), 2.80(dd), 3.89(dd)
14	Asparagine	Asn	2.88(m), 2.96(m), 4.00(m)
15	Tyrosine	Tyr	3.03(m), 3.18(m), 3.93(m), 6.89(m), 7.18(m)
16	Phenylalanine	Phe	3.10(dd), 3.26(dd), 3.99(dd), 7.32(d), 7.42(dd)
17	Histidine	His	3.13(dd), 3.25(dd), 7.10(dd), 7.90(dd)
18	Glycine	Gly	3.54(s)
19	Lactate	Lac	1.33(d), 4.12(q)
20	Acetate	-	1.92 (s)
21	Choline	Cho	3.12(s), 3.53(m), 4.05(m)
22	Glucose	Glc	3.25(dd), 3.41(m), 3.49(m), 3.55(dd), 3.75(m), 3.82(m), 3.91(dd), 4.63(d), 5.24(d)
23	Inosine	Ino	4.30(q), 4.44(q), 6.10(s), 8.25(s), 8.36(s),
24	Adenosine triphosphate	ATP	6.16(d), 8.24(s), 8.53(s)
25	Nicotinamide adenine dinucleotide	NAD	8.14 (s), 8.20(m), 8.41 (s), 8.51(s), 9.13(d), 9.33(s)
26	Adenosine diphosphate	ADP	5.94(m), 8.29(s), 8.54(s)
27	Formate	-	8.46 (s)

3.4.3 Comparison of HUVEC Metabolite Extraction Methods

After removal of cell medium by pipetting, it was possible to observe an unavoidable thin layer of medium still present on the cells. This situation might have caused bias in the determination of intracellular metabolites. To explore the potential for medium-to-cell carry over directly, culture media were spiked with two different concentrations of D-mannitol (1 mM and 11 mM) and, after a short period of incubation, cell and media samples were analysed by ^{1}H NMR. Since D-mannitol cannot cross biological membranes (non-permeable), it is suitable for use as a marker to indicate the degree of medium carry-over into intracellular extracts. The presence of the signals belonging to D-mannitol in the NMR spectra from cellular samples indicated that there was some medium carry-over for both of the concentrations of mannitol tested. Somewhat surprisingly, the mannitol signals remained in cell extracts produced from cells that were washed with ice-cold PBS prior to metabolite extraction (Figure 3.6).
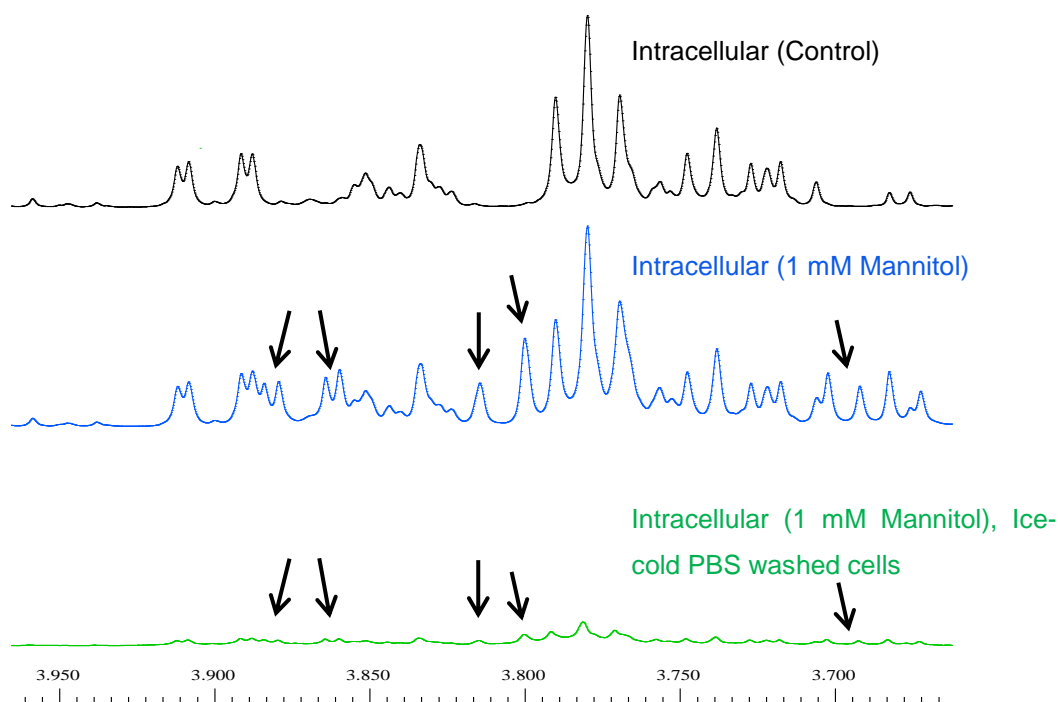
Figure 3.6: Assessment of medium metabolite carry-over by spiking growth medium with D-mannitol prior to metabolite extraction. D-mannitol signals in spectra were pointed-out using arrows

Previously, Teng *et al.* (2009) described spiking culture medium with 0.5 mM sucrose and establishing that there was no medium carry-over into the methanol extract after washing cells twice with ice-cold PBS.

Having shown that spiked mannitol was carried over into HUVEC extracts, 5 different sample preparation methods for profiling intracellular metabolites from HUVECs were compared for their effectiveness in avoiding medium carry-over into the cell extracts. These methods involved additional wash steps prior to methanol addition onto the cells (Table 3.2). Beside additional wash steps, culture plates with different dimensions were also compared for optimal results (10 cm dish; 55 cm^2 surface area vs 6-well plate; 9.4 cm^2 surface area).

Table 3.2: Wash steps prior to metabolite extraction with 80% methanol (-80$^°$C) treatment. Warm PBS, ice-cold PBS and warm NaCl (saline) were used to wash the cells in order to prevent medium carry-over.

Wash Steps
1X wash with <u>PBS at 37$^°$C</u>
3X wash with <u>PBS at 37$^°$C</u>
1X wash with <u>PBS – ice-cold</u>
1X wash with <u>NaCl (0.9% w/v) at 37$^°$C</u>
3X wash with <u>NaCl (0.9% w/v) at 37$^°$C</u>

The score plot resulting from multivariate analysis of all 84 samples which included both intra- and extracellular samples showed that the extracellular samples (spent medium) were packed together tightly whereas intracellular samples were scattered (Figure 3.7A). This observation is consistent with different wash steps being applied to the cell samples prior to extraction of intracellular metabolites whereas all the media samples were treated similarly. The most scattered set of data was observed at the right-bottom quadrant of the plot. These samples belong to the intracellular metabolite extraction from 6-well plates, which were nearly 6-

times smaller in surface area than the 10 cm dishes used for all extractions. NMR spectra for 6-well plate samples revealed that the metabolite concentrations were much lower for samples from 6-well plates compared to 10 cm dishes, and this is consistent with the increased variation (reduced precision) of the data. Therefore, 10 cm dishes appeared to be more practical to work with in future experiments since they provided stronger signals after metabolite extraction. The analysis of intracellular samples obtained with different cell pre-washing steps showed that the replicates from each pre-wash process had similar metabolite profiles, but there were differences between the different pre-washes tested. There was not a significant intra- or inter-day variation observed for extracts without a wash step (n=3 for 2 experiments performed on different days, n=6 in total). However, sample-to-sample variation was observed in the sample replicates with extra wash steps. The highest variation was observed with the "3X PBS (37°C)" wash step (Figure 3.7B). Also, the cells used in these experiments were grown using passage 4 cells frozen on different days to assess possible differences in metabolism of HUVECs grown up from different vials. Therefore, the results showed that cells grown up from different vials fell into the cluster of data for direct methanol extraction ("No wash") in PCA analysis indicating that they had similar metabolite profiles.
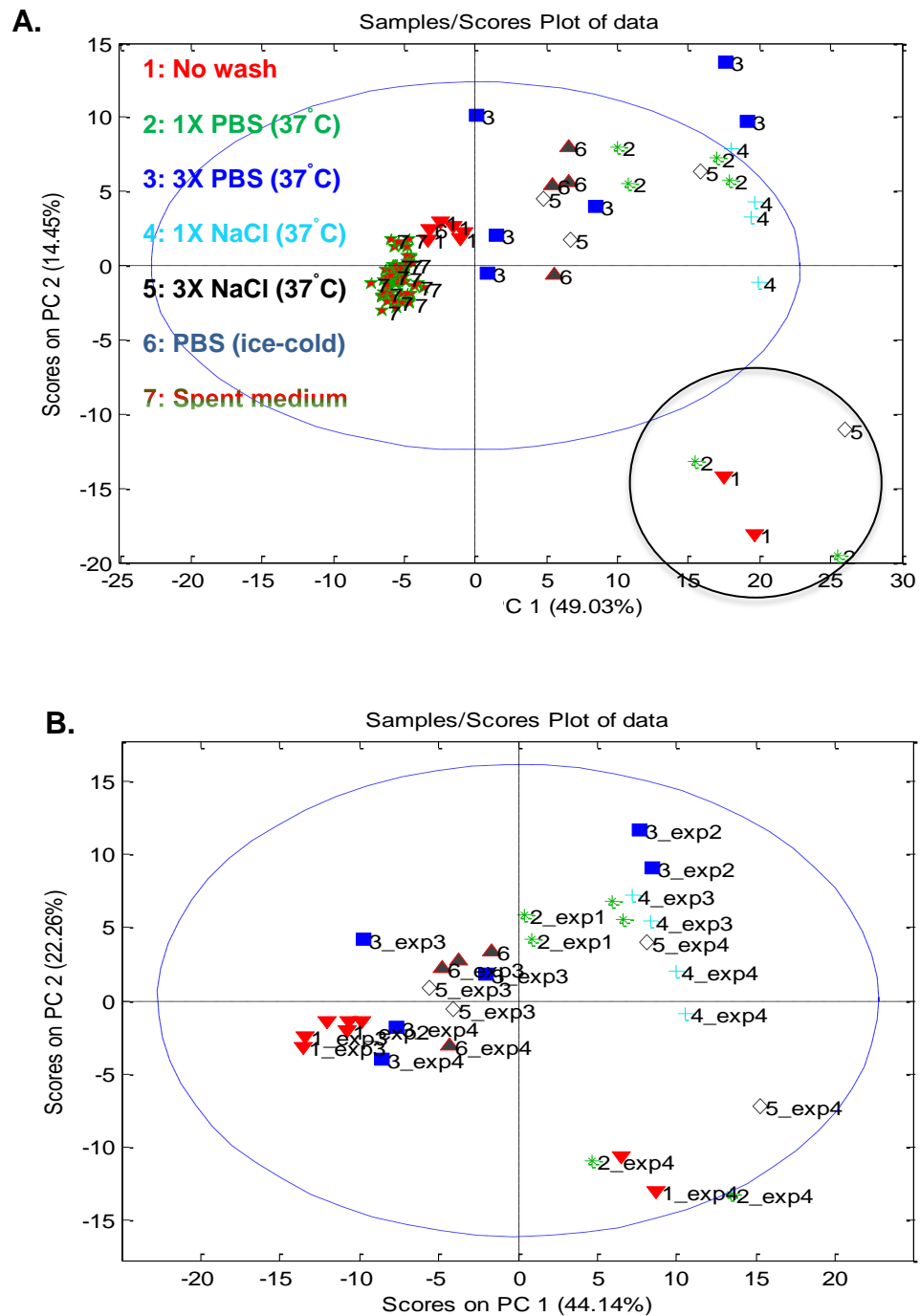
Figure 3.7: **A.** Score plot of the first two axes from the PCA on 84 samples, which include both intracellular and extracellular samples. The intracellular scores are scattered and the extracellular scores form a tight cluster (n=94). **B.** Intracellular samples with different wash steps (2 experiments n=3 each)

"1X PBS (37°C)", "3X PBS (37°C)", "1X NaCl (37°C)" and "3X NaCl (37°C)" yielded lower intensity signals compared to "No wash" and "1X PBS (ice-cold)" (Figures 3.8A and 3.9A). This may be explained as a loss of metabolites due to leakage or disruption to the cell membrane by the washing steps. The aim with this experimental series was to determine a suitable quenching and extraction method. A favourable method to quench cellular metabolism must be quick and reproducible in order to obtain unbiased metabolite concentrations. These experiments showed that direct extraction with methanol (-80°C) and extraction with methanol just after a single wash with ice-cold PBS yielded higher concentrations of metabolites than warm NaCl and PBS wash methods. This observation is probably explained by increased leakage of metabolites during the longer-lasting wash methods compared to the shorter times between removing media and extracting metabolites for direct methanol and single ice-cold PBS wash methods that should minimize the amount of leakage from the cells. However, it is also possible that extracts without a wash step generated higher intensity signals due to medium carry-over. Indeed, there is some evidence to support this notion; the more stringent cell washing methods produced more extensive relative reductions in the signals for amino acids such as histidine, tyrosine and phenylalanine than observed for ATP signals (6.15 ppm) (Figure 3.8B & 3.9B). Since ATP was only present in intracellular extracts but not in spent medium (Figure 3.4B), whereas the amino acids were present in both cell and media samples, this observation is consistent with increased wash steps leading to reductions in medium carry-over. Nevertheless, D-mannitol signals were still present also in intracellular extracts, which had received a 1X PBS (ice-cold) wash step prior to extraction (Figure 3.6). The mannitol signal intensity was lower, but this was not specific to the mannitol signal as all metabolites had lower intensity signals after the wash step compared to direct methanol extraction including the ATP signal at 6.15 ppm. Therefore, it could be concluded that the lower intensity of the signals was due to metabolite loss, at least to some degree.

Overall, these data favoured minimising processing and thus using direct methanol extraction in the subsequent experiments. However, without the wash steps, the probability of medium carry-over in the extracts remains.

A.
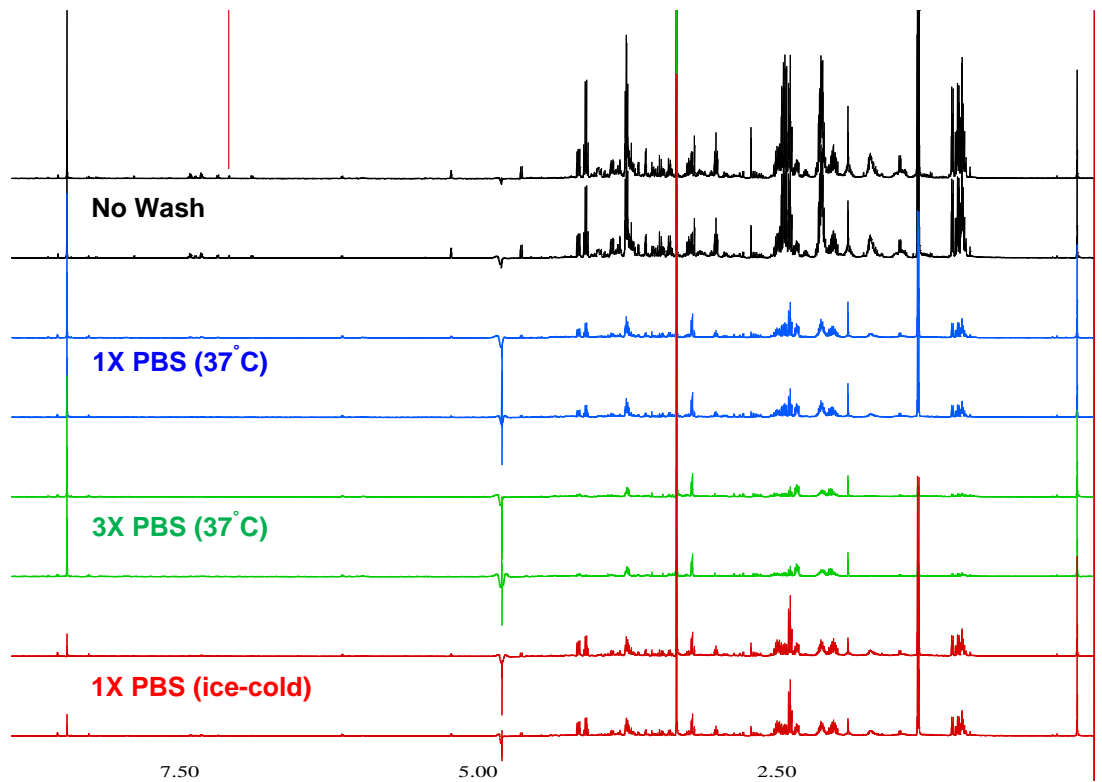
B.
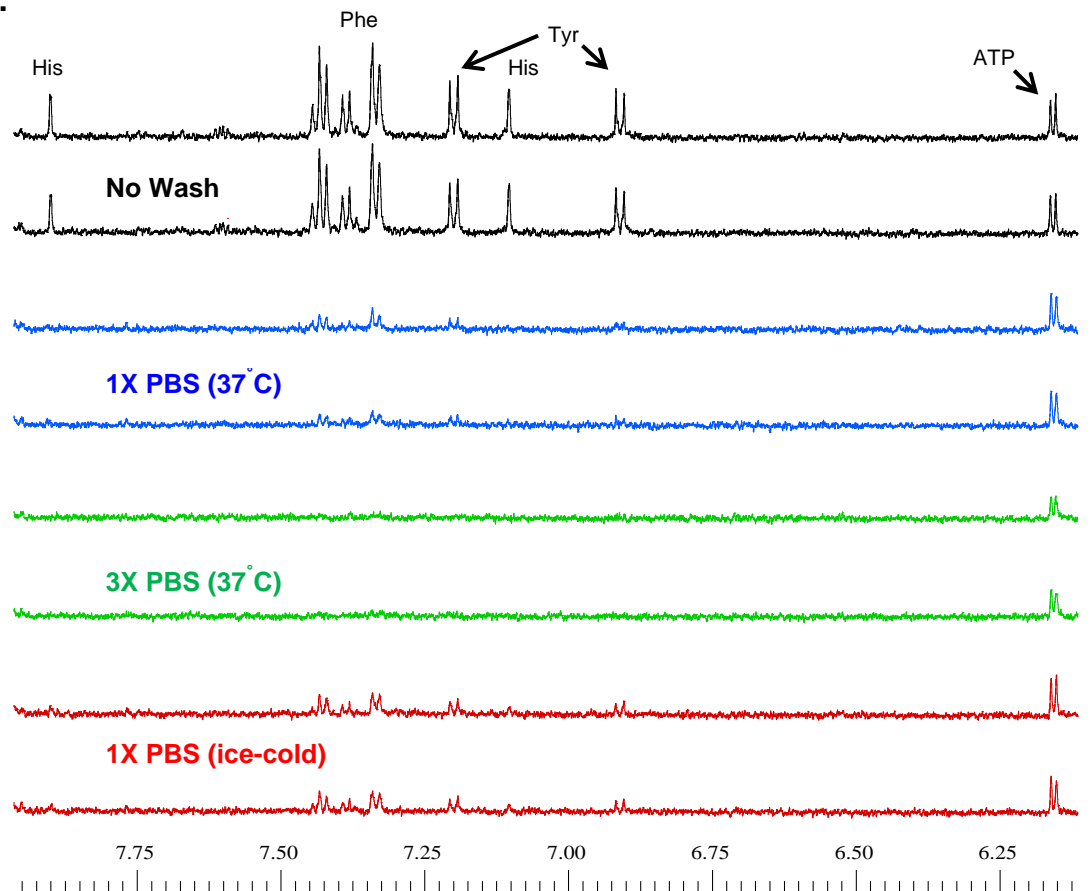
Figure 3.8: Different regions of ^{1}H NMR spectra of intracellular extracts after different wash steps. **A.** 8.00-2.40 ppm. **B.** 8.00-6.10 ppm.

A.

B.
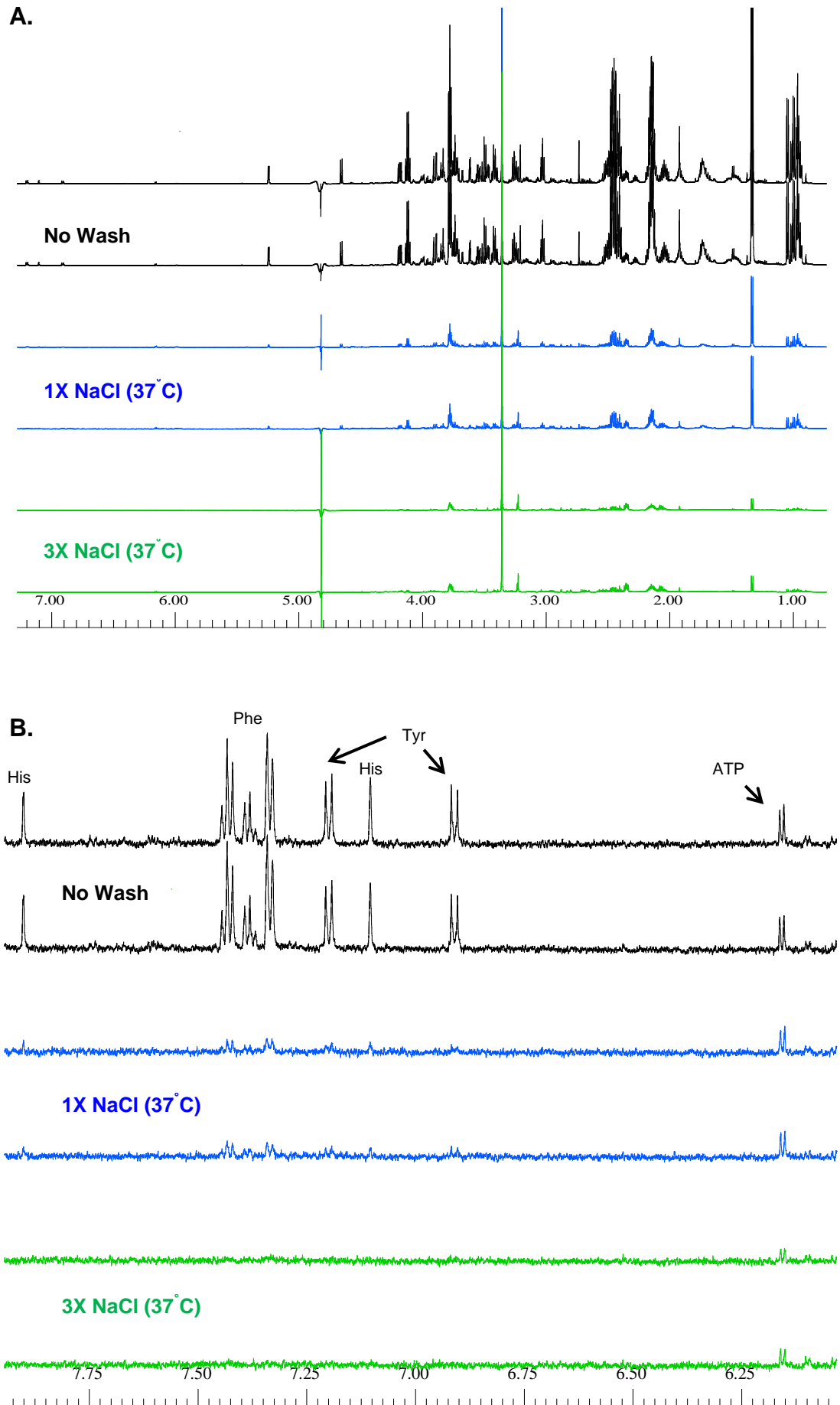
Figure 3.9: Different regions of ^{1}H NMR spectra of intracellular extracts after different wash steps. **A.** 7.00-1.00 ppm. **B.** 8.00-6.10 ppm.

3.4.4 Treatments to test method: LPS, malonate, medium without growth factors

As the medium carry-over seemed to be unavoidable direct methanol extraction that yielded higher concentrations of metabolites and gave low between-replicate variation was chosen as the method for the subsequent experiments. The next objective was to investigate the suitability of the method for detecting changes in metabolite profiles in cultured HUVECs in response to treatments that would be expected to alter the cell metabolome. After reviewing the literature, lipopolysaccharide (LPS), malonate and growth medium without growth factors (GF) were selected as suitable treatments to be tested for their effects on HUVEC metabolism.

Confluent HUVECs were treated with LPS (10 ng/ml) or growth medium without growth factors (GF) for 24 hours and with malonate (1 mM and 10 mM) for 6 h or 24 h. Subsequently, cellular metabolism was quenched with 80% methanol (-80°C) and the metabolites were extracted. The signals falling under a bucket were integrated, and statistical multivariate analysis was performed on these data using Matlab$^{®}$. The data was also transferred into Microsoft$^{®}$ Excel for further univariate analysis. It was observed that "10 mM Malonate" samples and "No GF" samples were separated from "Control" and "LPS" samples easily on the PCA plot (Figure 3.10). On the other hand, "1 mM Malonate" and "LPS" samples were similar to control samples. The close proximity of "10 mM Malonate" and "No GF" sample replicates on the PCA plot reflected the robustness of the cellular metabolism quenching and metabolite extraction protocol.
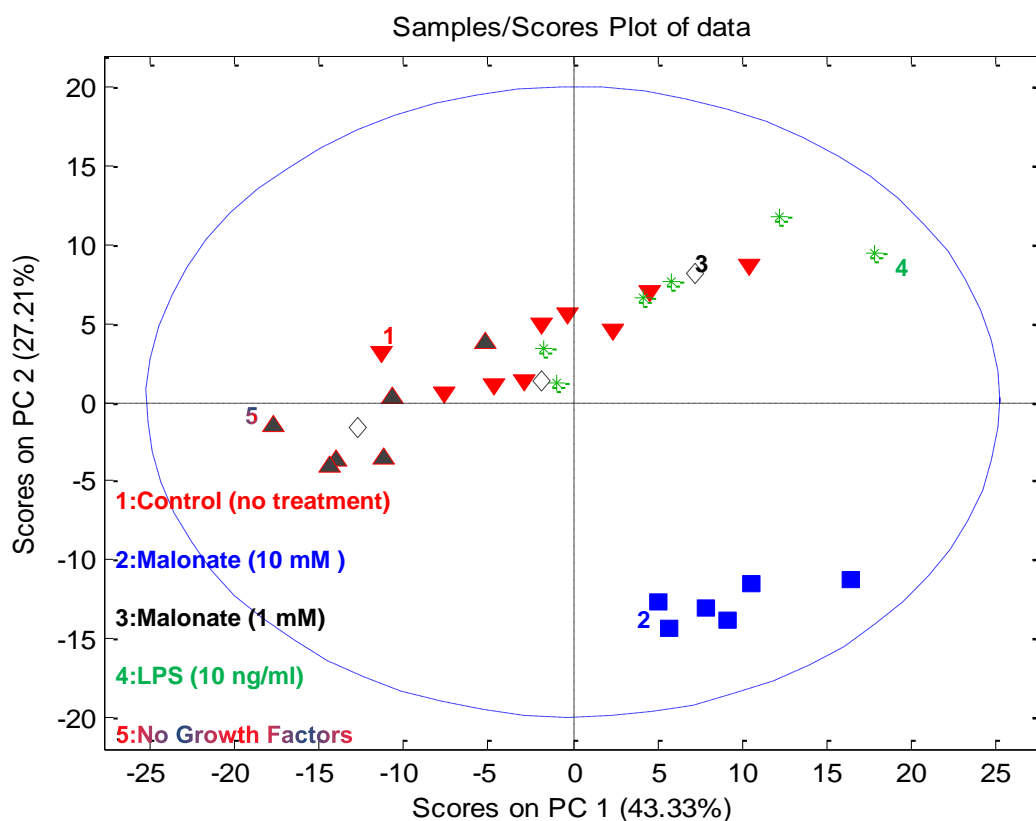
Figure 3.10: Score plot of the first two axes from the PCA on intracellular metabolite samples of non-treated cells (control), cells treated with no growth factor medium, LPS and malonate treated cells.

The differences observed in the score plot were consistent with the differences in the spectra of intracellular samples from cells treated with no growth factor containing medium and intracellular samples from cells treated with malonate (10 mM). Therefore, metabolite changes responsible for the separation in the PCA plot were identified after univariate statistical analyses (Mann-Whitney test, non-parametric). Removal of the growth factors from culture medium led to a decrease in the levels of several amino acids, namely aspartate ($p<0.01$), asparagine ($p<0.001$) and tyrosine ($p<0.001$) were the amino acids whose intracellular levels were significantly dropped. Alanine and phenylalanine levels were also reduced, however, the reductions were not statistically significant. Pyruvate was the other metabolite whose level was reduced significantly ($p<0.01$) after the removal of the growth factors from culture medium, together with non-significant reductions in ATP and acetate levels. Hence all these alterations in the metabolic profile contributed to separation in the PCA plot.

Malonate was selected to test the developed method because it is a Krebs cycle inhibitor and was expected to alter the profile of Krebs cycle intermediates (Figure 3.11). Several experiments were designed to further validate the developed HUVEC extraction protocol using malonate, succinate and fumarate.

Experimental set-up:

Malonate (10 mM) ;   6 h or 24 h

Malonate (10 mM) + Fumarate (20 mM) ; 24 h

Malonate (10 mM) + Succinate (50 mM) ; 6 h or 24 h
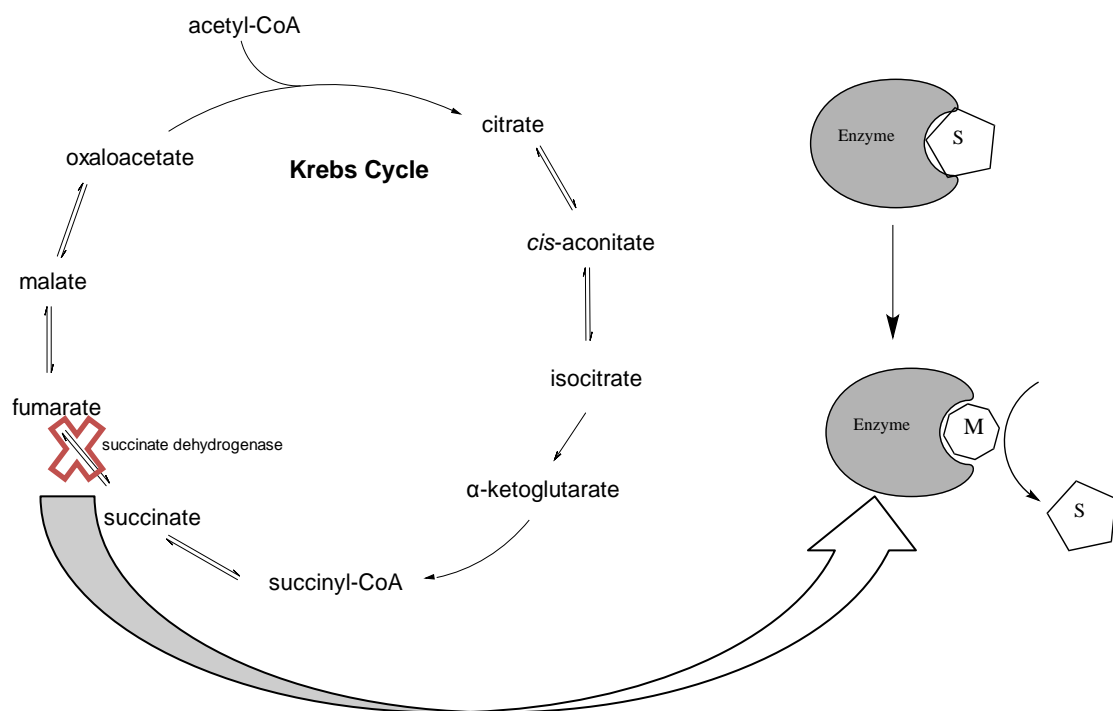
Figure 3.11: Malonate (M) is a competitive inhibitor of succinate dehydrogenase, which competes with substrate succinate (S) for the enzyme active site. Therefore, it can disrupt cellular respiration.

Cell culture medium was spiked with two different concentrations of malonate, 1 and 10 mM, for 6 h or 24 h in order to visualize possible changes in the HUVEC metabolite profile. These experiments were followed by malonate (10 mM) / fumarate (20 mM) and malonate (10 mM) / succinate (50 mM) co-treatments to observe whether fumarate and succinate can prevent malonate related changes in HUVEC metabolite profile.

1 mM malonate did not have any significant effects on HUVEC metabolite profile. On the other hand, 10 mM malonate addition into the culture medium caused significant reductions in intracellular ATP ($p < 0.001$), glutamate ($p < 0.01$), aspartate ($p < 0.001$), lactate ($p < 0.001$) and formate ($p < 0.05$) levels, and increase in glucose ($p < 0.05$), pyruvate ($p < 0.05$), inosine ($p < 0.001$) and histidine ($p < 0.001$) levels (Table 3.3) (Figure 3.12 and 3.13). These changes clearly indicated that the cellular metabolism was disrupted. These changes could be reverted by succinate co-treatment whereas fumarate co-treatment could not overcome the deleterious effects of malonate on HUVEC metabolism. In addition, increases in fumarate levels were observed with succinate co-treatment.

Table 3.3: The changes in HUVEC metabolite profile after malonate treatments for 6 h or 24 h and the ability of succinate to prevent these changes. Arrows indicated decrease or increase in particular metabolite concentrations (resting cells were compared with malonate treated cells; malonate treated cells were compared with malonate and succinate co-treated cells).

Malonate (10 mM); 6h & 24h		Malonate (10 mM) + Succinate (50 mM); 24h	Malonate (10 mM) + Succinate (50 mM); 6h
Glutamate	↓	↑	↑
Pyruvate	↑	↓	↓
Aspartate	↓	↑	↑
Glucose	↑	↓	↓
Inosine	↑	↓	↓
ATP	↓	↑	↑
Fumarate	-	↑	↑
Histidine	↑	↓	↓
Formate	↓	↑	↑

Fumarate co-treament did not prevent the negative effects of malonate on HUVECs. However, an elevation in malate levels was observed with the treatment (Figure 3.12). Krebs cycle was not recovered possibly due to the negative feedback effect of malate accumulation on the enzyme fumarase which converts fumarate to malate (Figure 3.11).

It could be observed that both of the treatments, 6 h and 24 h malonate, resulted in an unhealthy phenotype in HUVECs. However, succinate co-treatment partially prevented the change in the phenotype as reduced shrinkage was observed in the cells which indicated that the cells were less stressed since the cellular respiration was recovered (Figures 3.14A and 3.14B).
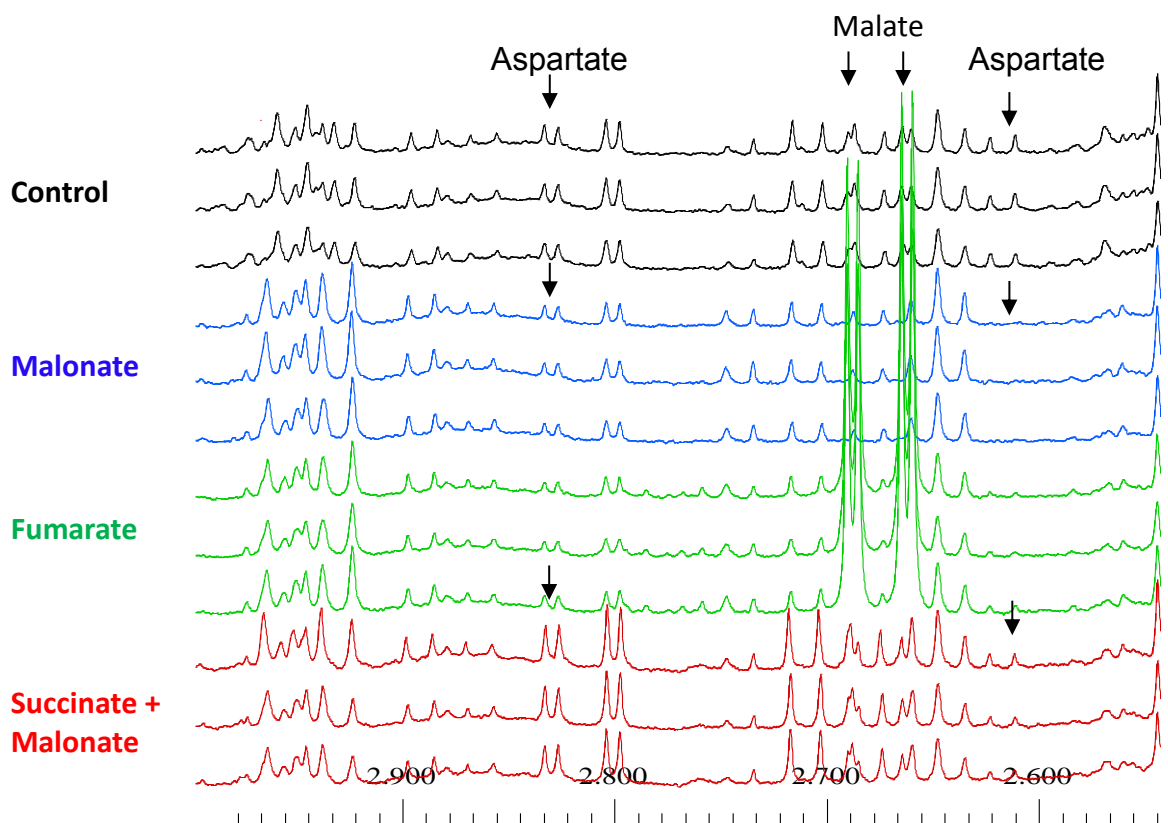
Figure 3.12: ^{1}H NMR spectra for 24 h treatments. Level of aspartate was lower with malonate (10 mM) treatment, but succinate (50 mM) co-treament prevented the decrease in intracellular aspartate concentration (2.60 and 2.80 ppm). A dublet of dublet is present with fumarate (20 mM) treatment around 2.70 ppm which belongs to malate.
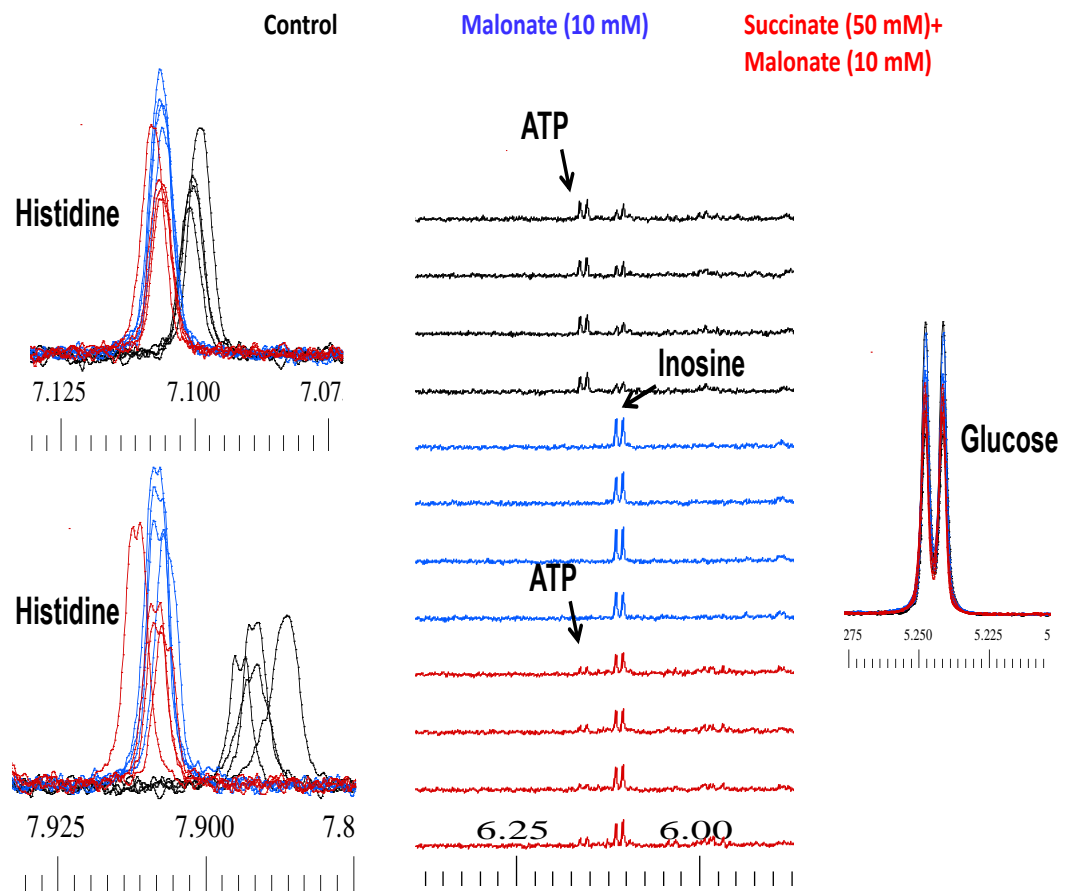
Figure 3.13: ^{1}H NMR spectra for 6 h treatments. Histidine level was increased with malonate treatment, but succinate co-treament prevents this increase. ATP generation by Krebs cycle was blocked with malonate treatment but succinate co-treatment managed to keep Krebs cycle active to generate ATP. Glucose was not used up by cells after malonate treatment, but with succinate co-treatment glucose was used up to generate energy.

A.
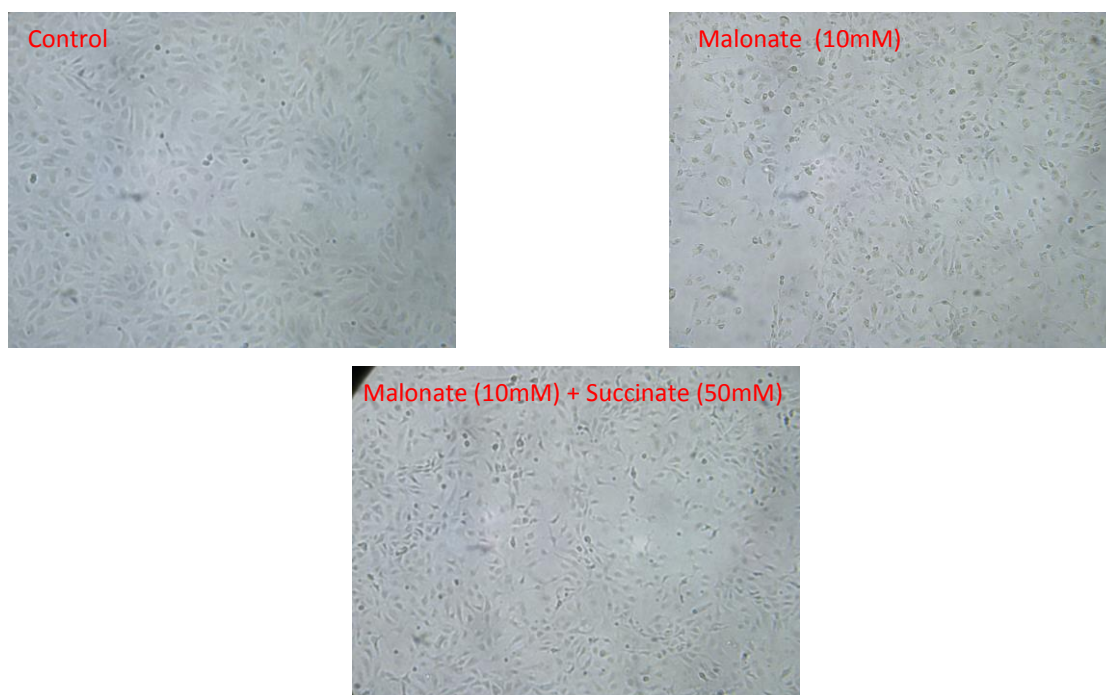
B.
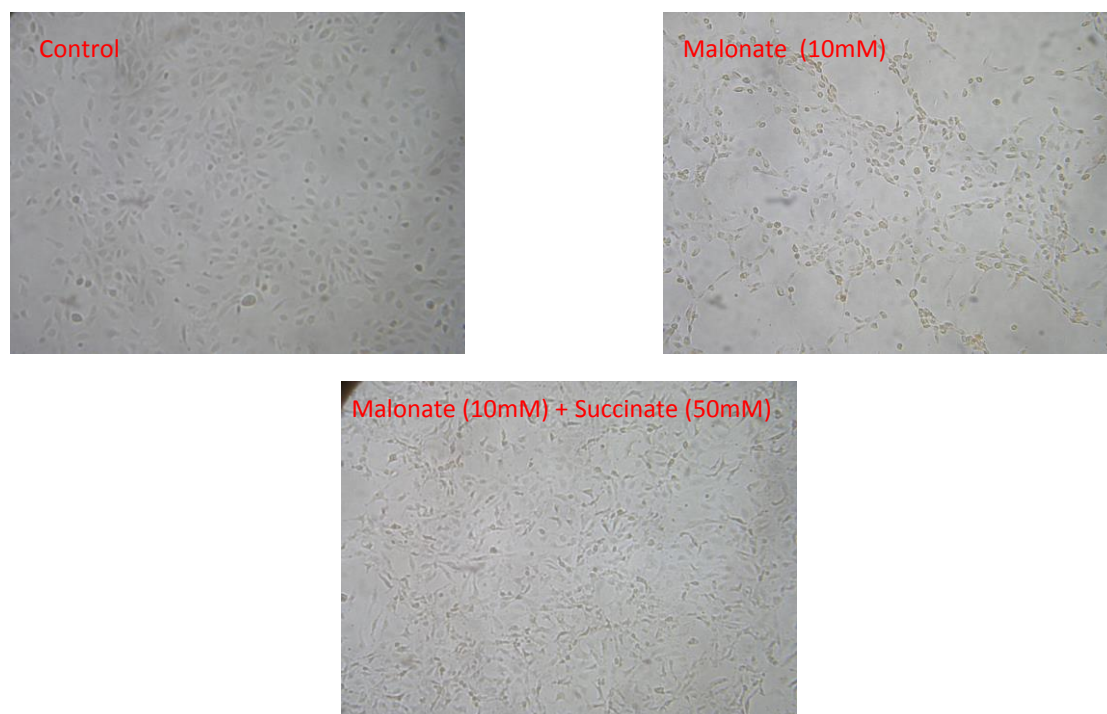
Figure 3.14: Malonate and malonate/succinate treatments. **A.** 6 h malonate treatment. **B.** 24 h malonate treatment. After both 6 h and 24 h malonate treatments HUVECs shrank and looked unhealthy. However, succinate co-treatment prevented the change in the phenotype.

3.5 Discussion

In this study a protocol that allowed quick and effective freezing of cellular metabolism, extraction of metabolites and analysis of extracted metabolites by employing ^{1}H NMR was developed. The protocol facilitated the generation of non-biased and reproducible data from ^{1}H NMR analyses and was shown to be suitable for detecting alterations in HUVEC metabolism induced by relatively strong treatments such as a metabolic poison (malonate) and removal of growth factors from the cell culture medium.

There are a few reports concerned with metabolite profiling of mammalian cells using ^{1}H NMR in the literature covering a few different adherent cell types (Duarte et al., 2010, Martineau et al., 2011, Martínez-Martín et al., 2012). However, there was not any information reported in the literature about the HUVEC metabolome until recently when in 2012 Martinez-Martin and co-workers carried out a study using NMR metabolomics on HUVECs. They had used high-resolution magic angle spinning (HR-MAS) magnetic resonance spectroscopy to test effects of AMPK activation by the adenosine analog, 5-aminoimidazole-4-carboxamide-1-β-D-ribofuranoside (AICAR), on the HUVEC metabolome. As a result, they observed alterations in energy metabolism and phospholipid biosynthesis. HR-MAS involves the analysis of semi-solid or viscous samples such as cell pellets. Detection of metabolites is achieved by spinning the sample at the magic angle 54.7°, which reduces line broadening effects observed due to chemical shift anisotropy, dipolar couplings and sample heterogeneity (Griffin et al., 2002). This technique was found to be useful in previous cell studies (Griffin et al., 2002, Shi et al., 2008, Weybright et al., 1998). However, Martinez-Martin et al. (2012) did not give any details about the metabolite extraction procedure. They had mentioned that the results were highly reproducible, but the method used for cell harvesting and metabolite extraction might have had influence on the results as it was shown in previous studies that different harvesting or extraction methods yielded variable results and there is not an optimal method for all the cell types (Sellick et al., 2008, Martineau et al., 2011).

An ideal protocol for extracting metabolites from HUVECs must include a quick method to quench the cellular metabolism that would not stress the cells. Freezing in liquid nitrogen, acid treatment, cold/hot phosphate buffered saline treatment,

cold saline treatment and using methanol buffer solutions are several examples of quenching methods that have been reported (Teng et al., 2009, Miccheli et al., 2006, Sellick et al., 2008). In this study, it was preferred to use cold methanol in a single step to quench cellular metabolism and extract metabolites. In CAM detection experiments (Chapter 2), trypsinization, which is a conventional method to harvest cells was used. However, in metabolomics experiments, trypsin would not be suitable to be used before quenching cellular metabolism as it mechanically cleaves the surface proteins that attach the cells to the culture plates stressing the cells. Also, this method requires repetitive and time-consuming wash/centrifuge steps that could cause metabolite carry-over (Dettmer et al., 2011, Teng et al., 2009). Instead of quenching cellular metabolism and extracting intracellular metabolites with a single solvent addition step, there are also various two-step extraction methods that have been used by researchers. These include treatments with cold/warm methanol or methanol/water solvents and acid or alkaline treatments (Sellick et al., 2008). However, an additional step may increase the chance of metabolite carry-over. Therefore, a method, which brought cellular metabolism to a halt and achieved metabolite extraction in a single step was used in this study in order to avoid any possible alterations in cellular metabolism prior to NMR analysis. NMR spectra obtained for the metabolite extracts showed adequate signal-to-noise ratio which allowed identification of 27 metabolites. Nevertheless, there was evidence of some medium-carry over in the extracts (e.g. after spiking medium with mannitol) even with an additional wash step. Therefore, the method provided good consistency (precision) but the absolute concentrations may not be accurate. However, this is expected to be similar between samples, and since the differences between treatments and controls are the particular interest, it would be possible to identify the alterations in the metabolites after the treatments with the developed method.

Experiments were designed to investigate the sensitivity and reproducibility of the technique being used. This was achieved by assessing the biological changes observed after treating cells with LPS, malonate, and medium without growth factors. LPS was tested for its effects on cell adhesion molecule expression in previous chapter. It did not induce VCAM-1 and ICAM-1 expression by HUVECs. Nevertheless, it is a well-known pro-inflammatory molecule (the gram-negative bacterial cell wall constituent) (Porter et al., 2010) and it was previously reported

that LPS could activate microglial cells by inducing changes in cellular metabolism including elevation in glutamate and lactate levels (Yawata et al., 2008, El Ghazi et al., 2010). Therefore, LPS was chosen as a treatment that could change NMR metabolic profile of HUVECs. However, LPS treatment did not induce any detectable significant alterations in HUVEC metabolome.

The second type of treatment tested for its ability to alter HUVEC metabolism was to remove growth factors from cell culture medium. The removed factors included human epidermal growth factor (hEGF), vascular endothelial growth factor (VEGF), human fibroblast growth factor B (hFGF-B) and insulin like growth factor (R3-IGF-1). Growth factor deprivation may disrupt cellular nutrient intake resulting in intracellular nutrient deficiency (Edinger and Thompson, 2002, Kan et al., 1994). This starvation due to the blockage of nutrient intake activates nutrient-sensing signalling pathways (Panieri et al., 2010), which may lead to initiation of autophagy (Lum et al., 2005). Autophagy can be defined as a catabolic mechanism, which involves sequestration and degradation of cytoplasmic components including long-lived proteins and dysfunctional organelles yielding nucleotides, amino acids and fatty acids that can favour cellular homeostasis by contributing to synthesis of macromolecules and ATP generation (Levine and Yuan, 2005, Han et al., 2012, Guo et al., 2013). The present data indicated that growth factor deprivation in cell culture medium led to an energy deficit in the cells that was reflected by the reduction observed in ATP and pyruvate levels. Similarly, Gottlieb and co-workers showed a reduction in the ATP/ADP ratio due to the defect in mitochondrial respiratory control in murine cell lines (Gottlieb et al., 2002). At the same time, observation of a reduction in the levels of amino acids which are all involved in feeding into the Krebs cycle indicated that autophagy almost certainly degraded intracellular contents to maintain ATP production promoting cell survival. Alanine, aspartate, asparagine, tyrosine and phenylalanine were the amino acids whose intracellular levels were reduced (Figure 3.15). Asparagine can be converted to aspartate with hydrolysis of the amide group, and aspartate can be converted to Krebs cycle intermediate oxaloacetate by a transamination reaction. Phenylalanine can be converted to tyrosine, and can be converted to the Krebs cycle intermediate fumarate. Alanine can be converted to pyruvate by a transamination reaction, which can be directed to the Krebs cycle. Therefore, it was shown that

alterations in HUVEC energy metabolism could be observed after treating cells with culture medium without growth factors using ^{1}H NMR spectroscopy.
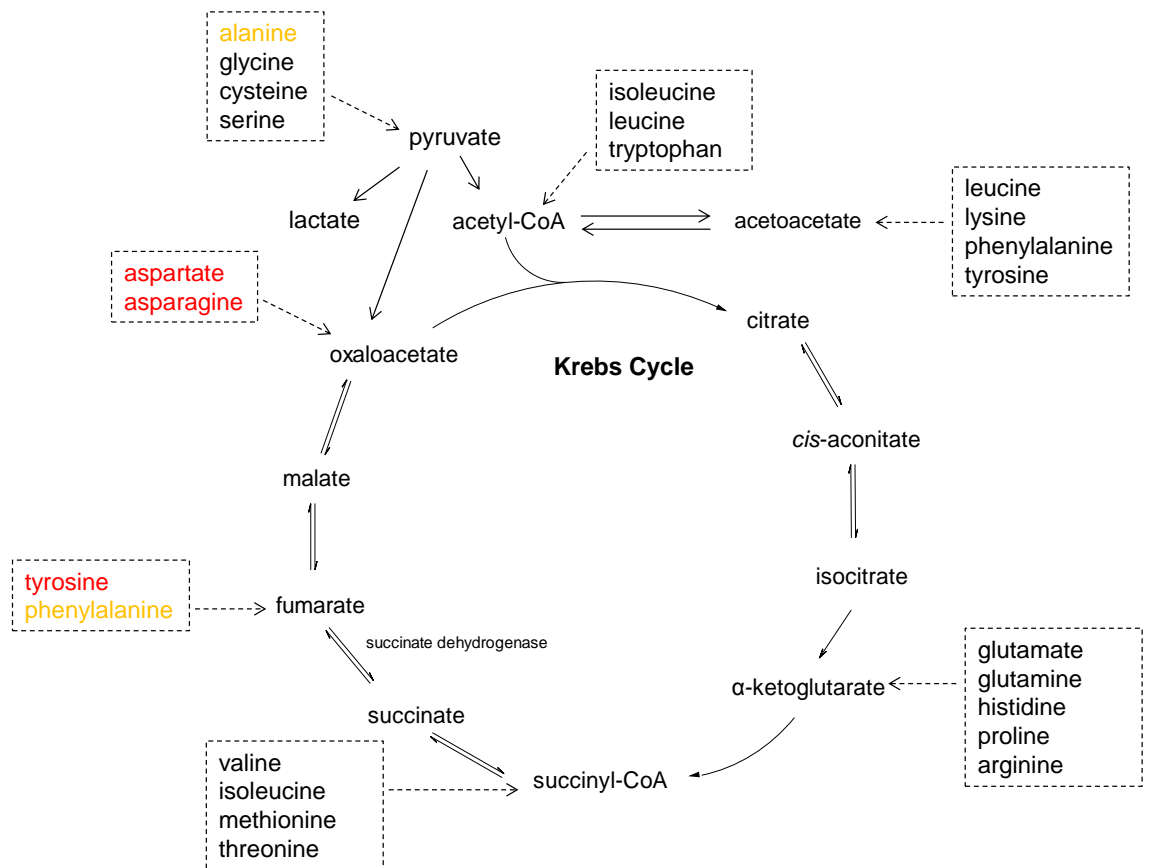
Figure 3.15: Amino acid carbon skeleton entry into Krebs cycle. Tyrosine, asparagine and aspartate levels significantly reduced after treating cells with culture medium without GF. Also, insignificant reductions were observed in alanine and phenylalanine levels. Therefore, it may be speculated that the reductions indicated Krebs cycle feeding to meet cellular energy demand.

Malonate is one of the metabolic effectors, which was used to test the developed method in view of the fact that it is a Krebs cycle inhibitor. It competes with succinate to bind to the active site of the enzyme succinate dehydrogenase (Figure 3.11). Excess intracellular malonate concentrations are expected to bring the Krebs cycle to a halt. This would disrupt cellular energy metabolism.

Therefore, theoretically, excess intracellular succinate concentrations would help to prevent the inhibition of the enzyme succinate dehydrogenase by malonate as it is a competitive inhibitor that does not react with the enzyme. Also, another option for overcoming the inhibitory effect of malonate on the Krebs cycle would be the addition of excess amount of fumarate, which is the product of succinate oxidation by succinate dehydrogenase that would enable the progress of reactions in the cycle (Figure 3.15).

It has been speculated that HUVECs produce energy mainly via glycolysis (Peters et al., 2009, Sweet et al., 2009). However, the results obtained here clearly demonstrated that the Krebs cycle is active even though the glycolysis is the major biochemical pathway to produce energy in HUVECs.

Cellular respiration, which is the most important biochemical reaction to produce cellular energy, starts with the conversion of glucose to pyruvate in glycolysis followed by the Krebs cycle in which NADH and $FADH_2$ are produced for ATP production via the electron transport chain. The data presented here (depletion in ATP levels together with glucose and pyruvate accumulation) after malonate treatments revealed that the pyruvate was not channelled into the Krebs cycle and cellular respiration was switched off (Figure 3.13). Glutamate might be channeled into the Krebs cycle after conversion to the Krebs cycle intermediate α-ketoglutarate. Accelerated glutamate transport into HUVECs provides a precursor for the biosynthesis of macromolecules and glutamine, which can be used up to produce energy in cultured cells (Pan et al., 1995). Although succinate could not be detected with ^{1}H NMR, its level was expected to increase with the malonate treatment, and intracellular accumulation of histidine may be related to inhibition of urucanate hydratase by excess succinate (Figure 3.13). Histidine is a glucogenic amino acid, which can be catabolized into glutamate through a multi-enzyme system that involves the activities of 4 enzymes. Urucanate hydratase is the second enzyme in this system, and generates imidazolone propionate by

hydration of urocanate. Hug and co-workers showed that succinate inhibited urocanate hydratase which resulted in urocanate accumulation in *Pseudomonas putida* (Hug et al., 1968). This caused a negative feedback in the enzyme, histidase, which led to histidine accumulation.

In conclusion, the developed protocol was sensitive enough to detect and quantify 27 metabolites in HUVECs by ^{1}H NMR. Previous studies reported in the literature used between 3-6 sample replicates in order to observe alterations in the metabolisms of different cells types with particular treatments (Teng et al., 2009, Duarte, 2011, Martineau et al., 2011). The present study has shown that 6 sample replicates gave consistent results between replicate samples, and it was suitable to detect changes in the HUVEC metabolome in response to a metabolic poison and removal of critical growth factors from the medium. In the next chapter, the protocol will be used to explore potential changes in HUVEC metabolite profiles in response to hyperglycaemia, inflammatory cytokine and polyphenol treatments.

CHAPTER 4: Effects of high-glucose, TNF-α and quercetin on endothelial cell primary metabolism: NMR and mass spectrometry analyses

4.1 Abstract

Background: The effect of increased glucose concentrations and pro-inflammatory cytokines on endothelial cells is multifaceted, and polyphenols have been shown to work through multiple mechanisms and elicit a variety of changes in the functions of cells to which they are exposed. However, studies reported in the literature are mainly focused on the effects of high-glucose and inflammatory cytokines on individual endothelial cell activation and function markers so far and there have been no studies reported on the effects of polyphenols on primary metabolism in endothelial cells. Therefore, a non-targeted approach such as metabolomics provided the ideal approach for determining the full range of responses at a mechanistic level on the metabolic system.

Aim: To demonstrate effects of quercetin on high-glucose and TNF-α stressed endothelial cells using non-targeted analysis approach metabolomics with a view to understanding the effects at a mechanistic level on the metabolic system.

Approaches/methods: ^{1}H NMR spectroscopy was used to determine HUVEC metabolite profile, and HILIC mode LC-MS/MS analysis was used to measure intra- and extracellular levels of ATP, ADP, AMP, adenosine, inosine and xanthine providing supplementary data.

Results: 18 h glucose (28.5 mM) treatment significantly increased intracellular lactate ($p < 0.01$) and glutamate ($p < 0.05$) concentrations compared to unstimulated cells. Interestingly, quercetin affected mainly the HUVEC energy metabolism. Increases in intracellular inosine and acetate concentrations were observed, whereas lactate ($p < 0.01$), ATP ($p < 0.01$) and NAD^+ ($p < 0.01$) concentrations were reduced with quercetin pre-treatment (2 h) prior to high-glucose treatment (18 h). TNF-α (10 ng/ml, 6 h) treatment led to an elevation in asparagine concentrations ($p < 0.05$) and a trend of elevation in pyroglutamate concentratins ($p = 0.0679$), whereas a reduction was observed in asparate concentrations ($p < 0.001$)

compared to unstimulated cells. On the other hand, the only significant change observed with quercetin (10 µM) pre-treatment (2 h) prior to TNF-α stimulation (6 h) was a reduction in pyruvate concentrations ($p < 0.05$). However, a trend of elevation in inosine ($p = 0.0566$) and a trend of decrease in aspartate ($p = 0.0569$) and ATP concentrations were observed. MS analyses revealed that pre-treatment with quercetin led to an increase in intracellular inosine and decrease in ATP ($p < 0.01$), ADP ($p < 0.05$) and NAD^+ ($p < 0.01$) concentrations, and increase in extracellular inosine ($p < 0.01$) and decrease in xanthine ($p < 0.05$) levels in high-glucose stimulated HUVECs. TNF-α stimulation (6h) increased intracellular AMP concentrations ($p < 0.05$) whereas it decreased adenosine ($p < 0.01$) and NAD^+ ($p < 0.01$) concentrations compared to unstimulated HUVECs. Quercetin pre-treatment increased intracellular inosine ($p < 0.001$) and adenosine ($p < 0.05$) concentrations in TNF-α stimulated HUVECs whereas it reduced ATP ($p < 0.05$) concentrations. It also increased extracellular inosine ($p < 0.01$) concentrations. Quercetin treatment alone was found to time-dependently increase intracellular pyroglutamate and lactate concentrations, whereas it reduced inosine concentrations time-dependently. Finally, MS analysis revealed that quercetin treatment alone decreased intracellular ATP and ADP concentrations, and increased AMP, adenosine and inosine concentrations depending on the treatment duration. Likewise, elevations in extracellular adenosine and inosine concentrationss were observed.

Conclusions: The prevention of deleterious increases in lactate, reductions in the concentrations of pro-inflammatory metabolites ATP and ADP and, in parallel, increased concentrations of anti-inflammatory metabolites adenosine and inosine are consistent with the anti-inflammatory properties of quercetin that protect vascular endothelial cells against inflammation-induced damage.

4.2 Introduction

Atherosclerosis has been characterized as a chronic inflammatory disease (Libby et al., 2002). Vascular endothelial dysfunction initiates formation of atherosclerotic plaques at sites of injury. Atherosclerotic plaque formation is associated with diabetes since the hyperglycaemic and pro-inflammatory conditions have the potential to activate endothelial cells and disrupt endothelial cell function due to the production of various vasoactive factors, growth factors and cytokines observed during diabetes (Guerci et al., 2001). Endothelial cells possess important functions such as regulating vessel permeability, inflammation and thrombosis (Galley and Webster, 2004). High-glucose concentrations and pro-inflammatory cytokines bear the potential to affect endothelial cell activation and function through multiple mechanisms, and polyphenols have been tested to investigate whether they have the potential to attenuate or completely prevent high-glucose and pro-inflammatory cytokine-induced conditions. So far, studies reported in the literature are mainly focused on the effects of high-glucose and inflammatory cytokines on individual endothelial cell activation and function markers. For example, Altannavch and co-workers reported that high-glucose concentrations and TNF-α induced cell adhesion molecule expression by HUVECs (Altannavch T. S., 2004). Chen and co-workers showed that the high-glucose concentrations reduced the endothelial cell proliferation rate (Chen et al., 2007). Sheu and co-workers suggested that the hyperglycaemic conditions induced human endothelial cell apoptosis by triggering caspase-3 activity through a phosphoinositide 3-kinase regulated cyclooxygenase-2 pathway, and also increases ROS production (Sheu et al., 2005). Rogers and co-workers showed that hypo- or hyperglycaemia lowers eNOS levels in HUVECs diminishing its cytoprotective effects (Rogers et al., 2013). Furthermore, Tribolo and co-workers reported that dietary polyphenol quercetin and its human metabolites prevented LPS/TNF-α induced expression of cell adhesion molecules by endothelial cells (Tribolo et al., 2008). Wahyudi and Sargowo showed that green tea polyphenols significantly reduced TNF-α expression by preventing oxLDL mediated NF-κβ activation (Wahyudi and Sargowo, 2007). Nevertheless, the reported literature regarding to the effects of polyphenols on hyperglycaemic conditions are very limited and targeted to particular aspects such as inhibitory activities against

cellular apoptosis and ROS productions (Chao et al., 2009, Hsieh et al., 2007, Choi et al., 2008)

After a literature review was carried-out, only a handful of published reports were observed that concerned with the effects of high-glucose concentrations, TNF-α or polyphenols on mammalian cell metabolism, and only a few using a non-targeted metabolomics approach to explore cellular primary metabolism. However, there were several interesting studies reported with regards to the effects of high-glucose or TNF-α on particular aspects of cellular metabolism. For example, Mortuza and co-workers assessed effects of chronic high-glucose concentrations on sirtuins (SIRTs), which is an important protein family in regulating aging process and metabolism that prevents aging-like process also in endothelial cells (Adams and Klaidman, 2007, Mortuza et al., 2013). They reported that high-glucose concentrations diminished SIRT-1 activity leading to alterations in mitochondrial function that accelerated an aging-like process (Mortuza et al., 2013). In another study, Iqbal and Zaidi demonstrated that TNF-α treatment time-dependently increased cellular NAD^+ levels in macrophages due to increased degradation of NAD^+ by NAD^+ metabolising enzymes (Iqbal and Zaidi, 2006).

Beside the targeted experiments, there were several non-targeted metabolomics studies reported in the literature. A study focussed on the effects of TNF-α on phospholipid metabolism in human breast cancer cells (MCF7) using ^{31}P and ^{13}C NMR spectroscopy (Bogin et al., 1998). It was revealed that TNF-α inhibited choline transport in MCF7 cells by affecting the kinetics of membrane bound enzymes leading to a reduction in cellular phosphocholine levels. These alterations in the cellular metabolism were associated with apoptosis initiation (Shih and Stutman, 1996). In another study, Ibanez and co-workers developed a multianalytical platform based on CE/LC-MS analysis in order to determine effects of rosemary polyphenols on colon cancer cell (HT29) proliferation. Significant alterations in the cellular metabolome were observed after polyphenol treatments, and the results suggested chemopreventive effects of rosemary polyphenols with the observation of elevations in the reduced glutathione/oxidized glutathione ratio and changes in cellular polyamine profiles (Ibáñez et al., 2012). The effects of rosemary were also tested on K562 leukemia cells by applying a global microarray approach together with a metabolomics approach employing an MS-based method

(Valdés et al., 2012). In parallel with their effects on colon cancer cells, rosemary polyphenols treatment altered the leukemia cell metabolome, and particularly the elevation in the intracellular reduced glutathione levels and the reduction in the hypoxanthine levels indicated their chemopreventive effects on cancer cells. Another study reported the effects of resveratrol on the HepG2 cells (a human hepatoblastoma cell line) metabolome, which were investigated using ^{1}H NMR analyses (Massimi et al., 2012). Resveratrol treatment caused significant changes in HepG2 metabolite profiles which were consistent with a switch in cellular energy metabolism was switched towards fat utilization to produce energy rather than using amino acids and glucose as cellular fuel.

Chapter 2 was focused on the effects of high-glucose, inflammatory cytokines and polyphenols on individual endothelial cell function markers. According to the results, glucose did not have an effect on HUVEC proliferation or surface expression of VCAM-1 and ICAM-1 by HUVECs. IL1-β and TNF-α induced CAM expression by HUVECs, and the effects were stronger for TNF-α compared to IL1-β. Quercetin was the only polyphenol that prevented CAM expression by HUVECs after cytokine stimulation.

Nevertheless, the effects of high-glucose concentrations, pro-inflammatory cytokines and polyphenols on the primary metabolism in endothelial cells have not been extensively studied so far. In chapter 3, a protocol was developed and tested which facilitated rapid and effective freezing of cellular metabolism and extraction of metabolites. The extracted metabolites were analysed using ^{1}H NMR, which produced reproducible results when the effects of several known metabolic effectors on HUVECs were tested in the HUVEC model. The examples above with regards to both endothelial cell function markers and endothelial metabolism indicated that the effect of high-glucose and pro-inflammatory cytokines on endothelial cells is multifaceted, and polyphenols have been shown to work through multiple mechanisms and elicit a variety of changes in the functions of cells to which they are exposed.

Therefore, the aim of the research presented in this chapter was to demonstrate effects of quercetin on high-glucose and TNF-α stressed endothelial cells using non-targeted analysis approach metabolomics with a view to understanding the effects at a mechanistic level on the metabolic system in order to test the

hypothesis that pro-inflammatory conditions alter the metabolome of HUVECs, and polyphenols are able to prevent some or all of the hyperglycaemia or inflammation-induced metabolic changes.

4.3 Materials & Methods

4.3.1 Materials

Deuterim oxide (D_2O, D, 99.9%) was purchased from Cambridge Isotope Laboratories, Inc (USA). All other chemicals were obtained from Sigma-Aldrich (Poole,UK) unless specified. Centrifuge (Heraus Sepintech-Mega fuge 1.0R). Centrifugal evaporator (Jouan RC1022). HPLC grade acetonitrile was obtained from Fisher Scientific (Loughborough, UK). Cambridge Soft BioDraw Ultra software trial version was used to draw biological diagrams.

4.3.2 Optimized Cell Quenching and Metabolite Extraction Method

Cell culture medium was quickly aspirated from the culture dish (10-cm) and 3 ml of 80% HPLC grade methanol (-80°C) was added to quench the cells. Then, the culture dish was incubated for 15 min on dry ice. Cells were then detached and cell membranes were disrupted by a cell-scraper. The methanol solution containing metabolites was transferred into a 5 ml centrifuge tube. The solution was centrifuged at 2000g for 5 minutes at 4°C. The supernatant was saved. The pellet was re-constituted in 0.5 ml of 80% HPLC grade methanol and centrifuged again. The supernatants were pooled and dried using a centrifugal evaporator.

4.3.3 ^{1}H NMR Spectroscopy Analysis of Intra- and Extracellular Metabolite Extracts

Dried intracellular extracts were re-constituted in a buffer containing Na_2HPO_4, NaH_2PO_4, NaN_3 and TSP in D_2O. Spent media were diluted in the same NMR buffer prior to NMR analsysis. NMR recording was carried out according to details mentioned in Chapter 3. The NMR spectra were further analysed by Amix[®] software.

All the signals were separated to form buckets. The signals falling under a bucket were integrated, and statistical multivariate analysis was performed on these data using Matlab®. The analysis involved principle component analysis (PCA), which is an unsupervised method. Buckets defined in a NMR spectrum form a single data point in PCA, and they are responsible for the separation observed in a PCA plot. The contribution of each bucket to the separation in PCA plot was visualized using the corresponding loading plot. In a loading plot, each bucket forms a data point. Final analysis involved applying univariate statistical analysis to confirm the changes observed by multivariate analysis, and determine the significance of the differences. Non-parametric Mann-Whitney test was used, and p value less than 0.05 ($p < 0.05$) accepted as a significant difference.

4.3.4 HILIC Mode LC-MS/MS Analysis of Extra- and Intracellular Metabolites

Levels of ATP, ADP, AMP, adenosine, inosine and xanthine were measured in both intra- and extracellular samples using the analytical method as published by Preinerstorfer et al. (2010). Intracellular metabolites were extracted following the protocol optimized for NMR spectrometry analysis. Prior to MS analysis, dried extracts were dissolved in H_2O. Extracellular samples (spent culture media) were analysed without any additional preparation steps.

An Agilent 1200 HPLC system (Agilent Technologies, Waldbronn, Germany) coupled to an Applied Biosystems 4000 QTrap triple quadrupole mass spectrometer was used. Data were processed with the Analyst 1.5 software (Applied Biosystems). During chromatographic runs, autosampler temperature was set to 5°C, temperature of the column compartment was 25°C and injection volume was 10 µl. Metabolites were separated using a ZIC-HILIC stationary phase (150 mm X 4.6 mm, 5 µm) purchased from Merck SeQuant (Marl, Germany) at a flow rate of 700 µl/min. Mobile phases were 20 mM ammonium acetate (adjusted to pH 7.5 for the neutral HILIC method), respectively, in (A) H_2O and (B) 90% acetonitrile (MeCN). Mobile phase pH was adjusted using ammonium hydroxide solution (NH_4OH). Gradient elution was performed as in Table 4.1.

A standard mixture was prepared which contained all of the 6 metabolites mentioned. Calibration curves were drawn for each metabolite using the standard mixture to quantify the levels of each metabolite in the samples.

Table 4.1: Gradient profile of mobile phase in HILIC Mode LC.

Time (min)	%A	%B
0	0	100
30	80	20
31	0	100
45	0	100

4.3.5 Post-hoc Analysis for Estimating Power of Analytical Method

The equation below (Equation 4.1) was used to estimate the magnitude of the effect that was necessary to observe a significant difference in the levels of a particular metabolite after a particular treatment.

Equation 4.1:

$$n = \frac{2 \times [Z_{(1-\alpha/2)} + Z_{(1-\beta)}]^2}{\Delta^2}$$

$$n = number\ of\ sample\ replicates$$

$$Z_{(1-\alpha/2)} = 1.96, \qquad \alpha = 0.05$$

$$Z_{(1-\beta)} = 1.282, \qquad \beta = 0.1$$

$$\Delta = \frac{differences\ in\ means}{standard\ deviation\ of\ differences}$$

4.4 Results

4.4.1 Effects of Hyperglycaemia and Quercetin Treatments on HUVEC Metabolome Using ^{1}H NMR

Effects of acute hyperglycaemia on HUVEC metabolite profiles were explored. Cells were grown under basal culture medium (5.5 mM glucose) until confluency, and then the medium was replaced with experimental high-glucose medium (28.5 mM glucose) for 18 h. Dietary polyphenol, quercetin (10 µM), was also tested for its potential to alter metabolite profile in the presence of hyperglycaemia. The experiments involved 2 h pre-treatment with quercetin (10 µM) followed by 18 h high-glucose (28.5 mM) treatment. After the treatments, cellular metabolism was quenched, metabolites were extracted and analysed using ^{1}H NMR by following the protocol validated in the previous chapter.

A multivariate analysis was carried out for the data obtained for unstimulated cells, high-glucose treated (18 h) cells and quercetin pre-treated (2h) cells which were further high-glucose stimulated (18 h) in order to reveal alterations in the HUVEC metabolome after the treatments. Score plots of PC5 and PC10 showed a strong separation indicating that the treatments had different effects on HUVEC metabolome (Figure 4.1A). The contribution of individual buckets (chemical shifts representing metabolites) to the separation in the PCA plot were visualised using a corresponding loading plot (Figure 4.1B). There were 185 buckets, and glucose signals were not included in the analysis as they would have contributed non-specifically to the separation. Furthermore, univariate analysis (Mann-Whitney test) was conducted for the buckets identified in the loading plot between unstimulated (n=30) and high-glucose (28.5 mM) treated (18 h, n=30), and also between high-glucose (28.5 mM) (18 h, n=20) treated and quercetin pre-treated samples (2 h quercetin + 18 h high-glucose, n=20) in order to confirm the significance of the changes observed.

Confirmation of alterations in lactate concentrations was given as an example to show how the analysis was performed to reveal statistically significant changes. First of all, the bucket at 4.12 ppm which represents lactate was identified as a data point in the loading plot indicating that the bucket had contributed significantly to the separation (Figure 4.1B). Therefore, the signal at 4.12 ppm was checked in

the related spectra (Figures 4.2A and 4.2B), which was followed by a Mann-Whitney test that confirmed the increase in intracellular lactate levels with high-glucose treatment compared to unstimulated cells (p<0.01) and the reduction with quercetin pre-treatment compared to high-glucose treated cells (p<0.01) (Figure 4.2C and 4.2D). Further, the minimum magnitude of effect that was necessary to observe a significant difference in lactate concentrations after quercetin treatment was estimated by employing Equation 4.1. The results revealed that a minimum of 9.9% alteration in lactate concentrations was necessary in order to observe a significant difference after the quercetin treatments when 20 sample replicates were analysed.

According to the loading plot analysis, the lactate, inosine, ATP, pyruvate, acetate, glutamate, aspartate, NAD^+ and asparagine buckets contributed significantly to the separation observed in the PCA plot (Figure 4.1B). A Mann-Whitney test confirmed that 18 h glucose treatment significantly increased intracellular lactate (p<0.01) and glutamate (p<0.05) levels compared to unstimulated cells (Table 4.2A). These data show that the main effect of quercetin treatment was to alter HUVEC energy metabolism. Increases in intracellular inosine and acetate levels were observed, whereas lactate (p<0.01), ATP (p<0.01) and NAD^+ (p<0.01) levels were reduced with quercetin pre-treatment (Table 4.2B). A trend of decrease in pyruvate level with quercetin pre-treatment was observed, but it was not statistically significant.

A.
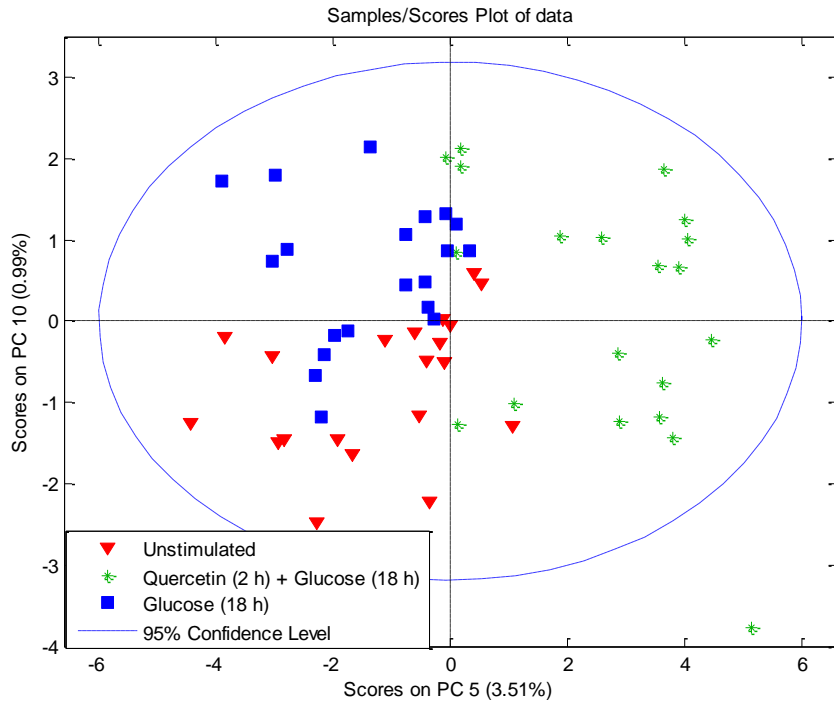
B.
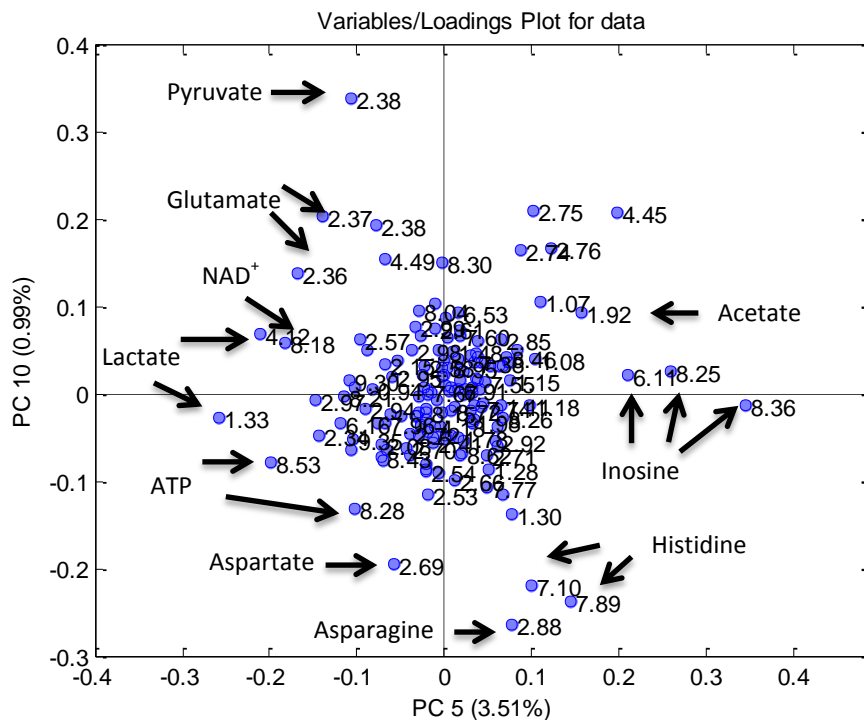
Figure 4.1: Multivariate analysis for the effects of hyperglycaemia on HUVEC metabolome. **A.** Score plot of PC5 and PC10 from the PCA. 3 different treatment groups separated from each other. **B.** Loading plot for samples highlighting the buckets contributed to the PCA result.

A.

B.

Control

28.5 mM Glucose

28.5 mM Glucose

Quercetin (10µM)

Lactate (4.12ppm)

C.

D.
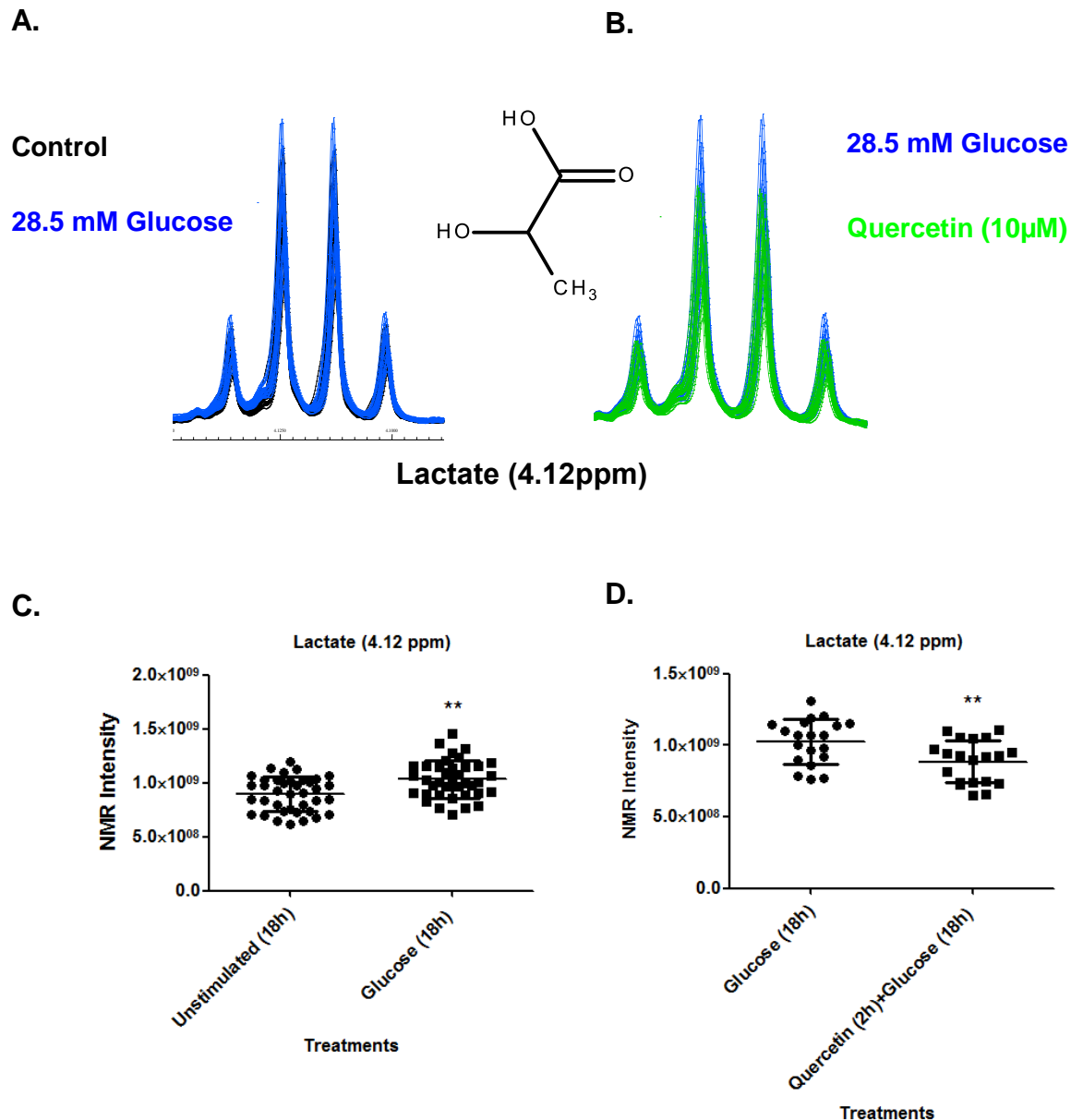
Figure 4.2: Changes in metabolite concentrations after selected treatments are represented by ^{1}H NMR spectra. **A.** 18 h treatment of confluent HUVECs with glucose (28.5 mM). Increase in lactate levels were observed compared basal glucose concentration. **B.** 2 h quercetin (10 µM) pre-treatment followed by 18 h glucose (28.5 mM) stimulation prevented high-glucose mediated lactate increases in HUVECs. **C. & D.** Statistical comparison of treatments using NMR intensity. **p<0.01, significant differences between two treatments by Mann-Whitney test.

Table 4.2: Statistically significant alterations in HUVEC metabolome after high-glucose and quercetin treatments. **A.** Alterations in HUVEC metabolome with high-glucose treatment. **B.** Effects of quercetin pre-treatment on metabolome of high-glucose stimulated HUVECs.

A.

Unstimulated vs High-glucose (18 h); n=38
Lactate ⬆ (p<0.01)
Glutamate ⬆ (p<0.05)

B.

High-glucose (18 h) vs Quercetin (2 h) + High-glucose (18 h); n=20
Inosine ⬆ (p<0.001)
Acetate ⬆ (p<0.05)
Lactate ⬇ (p<0.01)
ATP ⬇ (p<0.01)
NAD^+ ⬇ (p<0.01)
Pyruvate ⬇

4.4.2 Effects of TNF-α and Quercetin Treatments on HUVEC Metabolome Using ¹H NMR

In Chapter 2, TNF-α was shown to activate HUVECs to express cell adhesion molecules (CAMs), which are particularly important during inflammation. Quercetin prevented CAM expression after TNF-α stimulation depending on the durations of both pre-treatment with quercetin and stimulation with TNF-α. 2 h pre-treatment with quercetin (10 μM) was shown to inhibit both VCAM-1 and ICAM-1 by HUVECs after TNF-α stimulation (6 h) revealing anti-inflammatory properties of quercetin. Therefore, in the current study confluent HUVECs were stimulated with TNF-α (10 ng/ml) for 6 h to explore the alterations in HUVEC metabolome during the inflammatory state. Effects of quercetin on inflamed HUVECs were also investigated with 2 h pre-treatment with quercetin (10 μM) prior to stimulating cells for 6 h with TNF-α (10 ng/ml).

After the treatments, cellular metabolism was quenched, metabolites were extracted and analysed using ¹H NMR by following the protocol developed and tested in the previous chapter. A multivariate analysis was carried out for the data obtained for unstimulated cells, TNF-α stimulated (6 h) cells and quercetin pre-treated (2h) cells that were further TNF-α stimulated (6 h) to reveal potential alterations in the HUVEC metabolome caused by these treatments (Figure 4.3). Score plots of PC4 and PC7 showed separation of these three treatment groups indicating that they had different effects on the HUVEC metabolome (Figure 4.3A). The contribution of individual buckets to the separation in the PCA plot were visualised using the corresponding loading plot (Figure 4.3B).

According to the loading plot analysis pyruvate, NAD⁺, ATP, inosine, lactate, aspartate, asparagine and histidine were responsible for the separation observed in the PCA plot (Figure 4.3B). Furthermore, univariate analyses (Mann-Whitney test) were conducted for the buckets identified in the loading plot between unstimulated (n=17) and TNF-α stimulated (6 h, n=17), and also between TNF-α stimulated (6 h, n=11) and quercetin pre-treated samples (2 h quercetin + 6 h TNF-α, n=11) in order to confirm the significance of the changes observed. The Mann-Whitney tests confirmed that TNF-α (10 ng/ml) treatment caused an elevation in asparagine levels (p<0.05) and a trend of elevation in pyroglutamate levels (p=0.0679), whereas a reduction was observed in asparate levels (p<0.001)

(Table 4.3A). On the other hand, the only significant change observed with quercetin (10 µM) pre-treatment were reductions in pyruvate levels (p<0.05). However, a trend of elevation in inosine (p=0.0566) and a trend of decrease in aspartate (p=0.0569) and ATP levels were observed after loading plot and Mann-Whitney tests for individual experiments were analysed (Table 4.3B).

A.
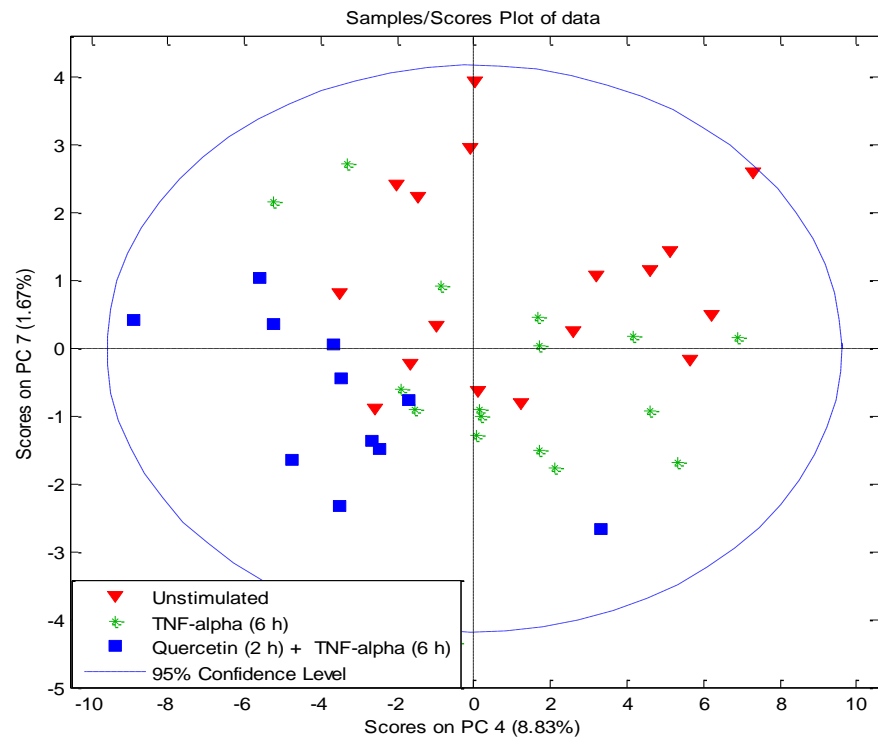
B.
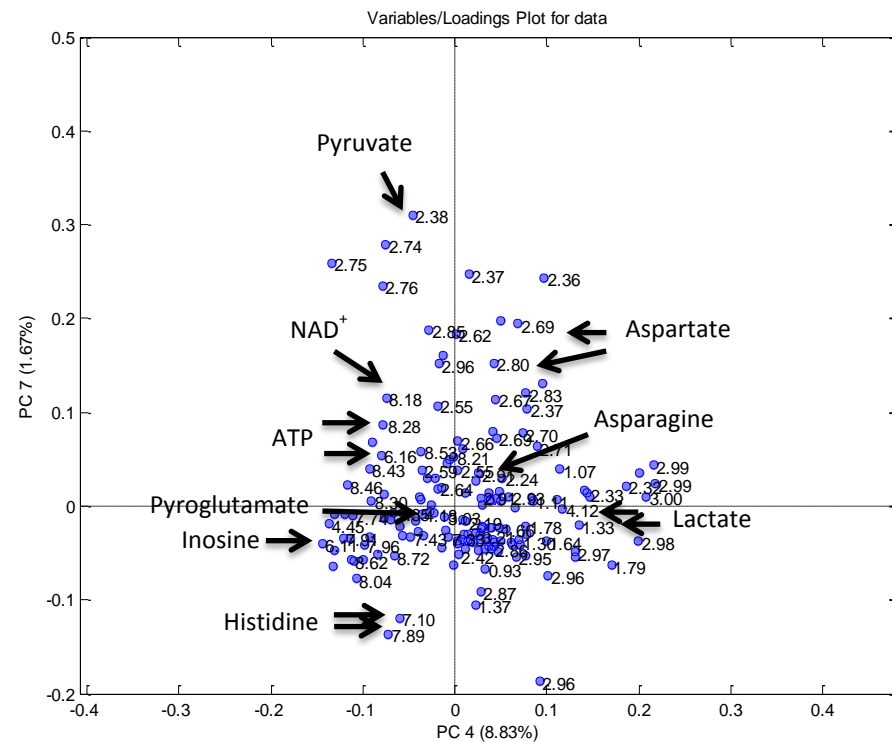
Figure 4.3: Multivariate analysis for the effects of TNF-α on the HUVEC metabolome. **A.** Score plot of PC4 and PC7 from the PCA. 3 different treatment groups sepereated from each other. **B.** Loading plot for samples highlighting the buckets contributed to PCA result.

Table 4.3: Statistically significant alterations in HUVEC metabolome after TNF-α and quercetin treatments. **A.** Alterations in HUVEC metabolome with TNF-α treatment. **B.** Effects of quercetin pre-treatment on metabolome of TNF-α stimulated HUVECs.

A.

Unstimulated vs TNF-α (6 h); n=17
Asparagine ⬆ (p<0.05)
Pyroglutamate ⬆ (p=0.0679)
Aspartate ⬇ (p<0.001)

B.

TNF-α vs Quercetin (2 h) + TNF-α (6h); n=11
Inosine ⬆ (p=0.0566)
Pyruvate ⬇ (p<0.05)
Aspartate ⬇ (p=0.0569)
ATP ⬇

4.4.3 LC-MS Analysis of Changes in HUVEC Energy Metabolites

NMR spectrometry results after high-glucose, TNF-α and quercetin treatments highlighted the alterations observed in HUVEC energy metabolism. Therefore, a multiple reaction-monitoring (MRM) based LC-MS analysis was used to measure both intracellular and extracellular concentrations for AMP, ADP, ATP, adenosine, inosine, xanthine and NAD^+ since mass spectrometry analysis was expected to be substantially more sensitive measuring for metabolite concentrations compared to ^1H NMR. However, extracellular concentrations for only adenosine, inosine and xanthine could be measured due to low extracellular concentrations for AMP, ADP, ATP and NAD^+.

There were no significant changes in the concentrations of measured metabolites with high-glucose treatment (18 h) compared to unstimulated cells. However, the

results confirmed the significant increases in intracellular inosine ($p<0.05$) and decreases in intracellular ATP ($p<0.01$), ADP ($p<0.05$) and NAD^+ ($p<0.01$) concentrations with quercetin pre-treatment (2 h) followed by high-glucose stimulation (18 h) (n=6) (Table 4.4). At the same time extracellular inosine ($299.7\pm24.5\%$ of high-glucose stimulated cells, $p<0.001$) concentrations were increased, whereas reductions were observed in xanthine ($94.3\pm2.48\%$ of high-glucose stimulated cells, $p<0.05$) concentrations with quercetin pre-treatment followed by high-glucose treatment (n=6). Quercetin pre-treatment led to an insignificant increase in adenosine concentrations ($107.1\pm4.76\%$ of high-glucose stimulated cells). Refer to supplementary information for metabolite concentrations (page 201).

TNF-α stimulation (6h) increased intracellular AMP concentrations ($p<0.05$) whereas it decreased adenosine ($p<0.01$) and NAD^+ ($p<0.01$) concentrations compared to unstimulated HUVECs. On the other hand, quercetin pre-treatment (2 h) followed by TNF-α stimulation (6 h) led to an elevation in inosine ($p<0.001$) and adenosine ($p<0.05$) concentrations and a reduction in ATP ($p<0.05$) concentrations (Table 4.5). The changes observed among the extracellular metabolites were increases in adenosine concentrations ($132.6\pm43.4\%$ of unstimulated cells) after TNF-α stimulation and quercetin pre-treatment prior to TNF-α stimulation ($133.3\pm50.8\%$ of unstimulated cells) and also increases in inosine concentrations ($159.5\pm6.89\%$ of TNF-α stimulated cells, $p<0.01$) after quercetin pre-treatment that was followed by TNF-α stimulation (n=6). Refer to supplementary information for metabolite concentrations (page 202).

Further, the minimum magnitude of the effect that was necessary to observe a significant difference in inosine concentrations after pre-treatment with quercetin prior to high-glucose stimulation of the cells was estimated by employing Equation 4.1. This would allow a comparison of the precision of ^{1}H NMR and HILIC mode LC-MS analyses since the inosine concentrations were measured using both NMR spectroscopy and LC-MS. The results revealed that a minimum of 33% alteration in inosine concentrations was necessary in order to observe a significant difference after the quercetin treatments when 20 sample replicates were analysed by ^{1}H NMR spectroscopy, whereas 29% alteration in inosine concentrations was

necessary when 6 sample replicates were analysed by LC-MS indicating that LC-MS provided more precise measurements.

Table 4.4: Statistically significant alterations in HUVEC metabolome after high-glucose and quercetin treatments.

High-glucose (18 h) vs Quercetin (2 h) + High-glucose (18 h); n=6	
Intracellular	**Extracellular**
Inosine (p<0.05) ↑	Inosine (p<0.01) ↑
ATP (p<0.01) ↓	Xanthine (p<0.05) ↓
ADP (p<0.05) ↓	
NAD^+ (p<0.01) ↓	

Table 4.5: Statistically significant alterations in HUVEC metabolome after TNF-α and quercetin treatments.

TNF-α vs Quercetin (2 h) + TNF-α (6h); n=6	
Intracellular	**Extracellular**
inosine (p<0.001) ↑	Inosine (p<0.01) ↑
adenosine (p<0.05) ↑	
ATP (p<0.05) ↓	

4.4.4 Time-Dependent Effects of Quercetin

The HUVEC metabolome was investigated post-addition of quercetin (10 µM) into the cell medium. This was achieved by analysing HUVEC extracts obtained 2 h, 4 h, 8 h and 20 h after treating cells with quercetin (10 µM) by NMR. Measurement of intracellular AMP, ADP, ATP, adenosine, inosine, xanthine and NAD^+ concentrations were carried out also by mass-spectrometry in MRM mode.

Pyroglutamate and lactate were the two metabolites whose concentrations were most significantly increased with time (Figures 4.4A and 4.4B, respectively). Aspartate and acetate concentrations (Figures 4.4C and 4.4D, respectively) were also increased post-quercetin treatment, but the proportion of increases for these metabolites after 4 h quercetin treatment were lower compared to the time-dependent effect of quercetin on pyroglutamate and lactate concentrations. At the same time, a time-dependent decrease was observed in inosine concentrations (Figure 4.4E).
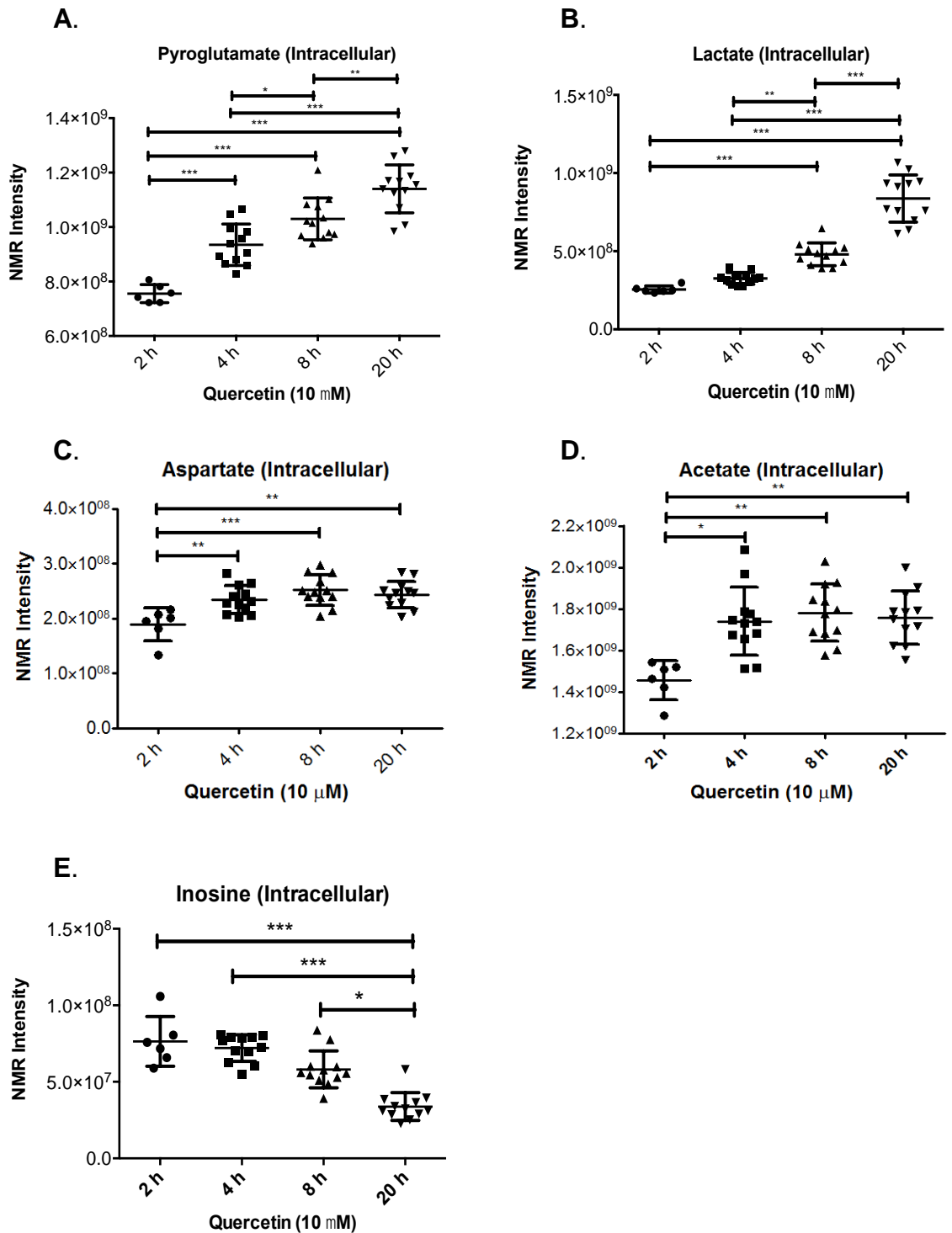
Figure 4.4: Quercetin treatments caused time-dependent changes in certain intracellular metabolites. **A.** Pyroglutamate concentrations were significantly increased with time. **B.** Lactate concentrations were significantly increased with time after 8 h. Aspartate (**C.**) and acetate (**D.**) concentrations were significantly increased after 4 h and there were no furher increase with time. **E.** Inosine concentrations were significantly decreased with time after 8 h.

LC-MS analyses (Table 4.6) revealed that intracellular ATP levels were significantly reduced after 8 h and 20 h quercetin treatments. Similarly, a significant reduction in ADP and NAD^+ concentrations were observed after 20 h quercetin treatment. 8 h and 20 h quercetin treatments increased both AMP and inosine concentrations, and 2 h and 20 h treatments also led to a significant increase in adenosine concentrations. Xanthine was the only metabolite measured which was not affected by quercetin treatments (Table 4.6A). On the other hand, 2 h quercetin treatment caused a significant increase in extracellular adenosine ($p<0.01$) concentrations (Table 4.6B). In parallel with the changes observed in intracellular inosine concentrations, quercetin time-dependently increased extracellular inosine concentrations. Finally, 20 h quercetin treatment caused a small but significant reduction in extracellular xanthine concentrations ($P<0.01$). Refer to supplementary information for metabolite concentrations (page 200).

Table 4.6: Effects of quercetin on energy metabolites in HUVECs. Metabolite levels were measured using mass spectrometry MRM mode. Values in the table represent percentage of intracellular (**A.**) or extracellular (**B.**) metabolite levels after quercetin treatment for each time point compared with metabolite levels in untreated cells for each time point (n=6).

A. Intracellular metabolites

	2 h	8 h	20 h
ATP	179.7±89.5%	55.6±15.6% (p<0.01)	70.7±14.2% (p<0.01)
ADP	-	-	71.57±21.0% (p<0.05)
AMP	96.5±14.2%	153.6±40.0% (p<0.05)	117.2±28.8%
Adenosine	286.2±187.6% (p<0.05)	72.8±29.8%	162.4±65.2% (p<0.05)
Inosine	122.4±22.1%	200.9±40.9% (p<0.01)	273.2±34.5% (p<0.01)
Xanthine	100.0±17.01%	102.8±20.3	109.8±12.5%
NAD$^+$	-	90.6±10.4	75.5±3.2% (p<0.01)

B. Extracellular metabolites

	2 h	8 h	20 h
Adenosine	112.5±5.95% (p<0.01)	105.8±16.2%	103.4±15.6%
Inosine	120.1±2.9% (p<0.01)	167.8±4.2% (p<0.01)	303.4±12.9% (p<0.01)
Xanthine	102.9±4.7%	104.2±10.6%	93.8±1.0% (p<0.01)

4.5 Discussion

NMR and MS analysis results revealed that high-glucose, TNF-α and quercetin treatments affected mainly HUVEC energy metabolism which was reflected as alterations in energy metabolites such as intracellular ATP, ADP, AMP, adenosine, inosine, lactate, pyruvate, NAD^+ and amino acids that feed into the Krebs cycle such as aspartate, asparagine and glutamate. Furthermore, it was shown that the effects of quercetin on certain metabolites were time-dependent.

Hyperglycaemic conditions caused elevations in intracellular glutamate and lactate levels compared to unstimulated cells. On the other hand, quercetin pre-treatment prior to high-glucose stimulation repressed the increase in intracellular lactate levels keeping its concentration closer to the level of unstimulated cells. The other interesting changes observed with quercetin pre-treatment were increases in inosine concentrations and reductions in ATP level. It is most likely that the reductions in lactate and ATP concentrations, and increases in inosine concentrations were associated with the anti-inflammatory properties of quercetin.

Physiological lactate concentrations in circulating blood are around 1-3 mM, whereas they are typically higher (around 5-15 mM) during tissue injury and inflammation (Sjöstrand et al., 2000, Ghani et al., 2004). In recent years, reports have been published showing that HUVECs produce cellular energy mainly via "aerobic glycolysis" yielding end-product lactate after utilization of glucose even in the presence of oxygen. This is in contrast to other non-malignant cell types, where the Krebs cycle provides auxiliary ATP production after glutamine utilization that supplies Krebs cycle intermediate α-ketoglutarate (Peters et al., 2009, Sweet et al., 2009). These reported observations are consistent with the elevation of intracellular lactate and glutamate levels reported here for HUVECs after high-glucose treatment since the increased level of glycolytic substrate glucose would shift energy production towards glycolysis limiting glutamate utilization for the production of the Krebs cycle intermediate α-ketoglutarate. It has been reported that dibabetic patients have higher blood lactate concentrations (Messana et al., 1998), and this is correlated (or associated with) with CVD risk (Crawford et al., 2010). Therefore, increased extra- and intracellular concentrations of lactate may have important implications on endothelial cell function even though the increase observed in this study was only ≈15%.

Since the extracellular lactate concentration bears importance in this circumstance, extracellular lactate levels were measured in the spent media by NMR spectroscopy confirming the elevated lactate concentrations ($\approx$10%, p<0.001, n=38) after high-glucose stimulation that were reduced by quercetin pre-treatment ($\approx$11%, p<0.01, n=20) in the present study. In a previous study, it was reported that isocapnic acidosis enhances HUVEC adhesiveness by increasing cellular adhesion molecule expression (Chen et al., 2011a). Therefore a potential reduction in pH caused by increased extracellular lactate concentrations has the potential to induce CAM expression in HUVECs. However, there was no increase observed in ICAM-1 and VCAM-1 after 5.5-28.5 mM glucose treatments for 18 hours in the present study. Exogenous lactate treatment was shown to induce vascular endothelial growth factor (VEGF) and vascular endothelial growth factor receptor 2 (VEGFR2) protein productions by HUVECs (Kumar et al., 2007, Beckert et al., 2006, Hunt et al., 2007). In contrast with other growth factors, VEGF was shown to induce expression of inflammatory genes including VCAM-1, ICAM-1, E-selectin and IL-8 in HUVECs (Schweighofer et al., 2009, Weston et al., 2002). Therefore, a potential increase in VEGF concentration due to increased lactate concentrations may have pro-atherogenic effects on HUVECs. Beckert and co-workers reported that treating HUVECs with lactate for 24 hours dose-dependently increased VEGF protein levels indirectly leading to an increase in HUVEC migration (Beckert et al., 2006). In parallel, increased intracellular lactate induced NF-κB activation leading to IL-8 production that stimulated HUVEC migration (Végran et al., 2011).

Vegran and co-workers showed that elevated lactate concentrations can also trigger reactive oxygen species (ROS) production by HUVECs. Cytosolic inactive NF-κB translocates into the nucleus of the cells regulating gene transcription when it is activated by various stimuli. Hence, increased ROS levels due to elevated lactate levels led to NF-κB activation through IκBα phosphorylation which further stimulated IL-8 production (Vegran et al., 2011). However, the reported effects of glucose on VEGF expression are not consistent. Several studies reported variable results depending on the cell type and experimental conditions (Qian et al., 2011, Yang et al., 2008). Qian and co-workers reported an increase in VEGF protein levels in human microvascular endothelial cells after 48 h high-glucose (30 mM) treatment (Qian et. al., 2011). On the other hand, Yang and co-workers reported

that high-glucose (25 mM) treatment of HUVECs for 72 h significantly reduced VEGF expression at both mRNA and protein levels, and increased cellular apoptosis. However, spiking the medium with 20 ng/ml VEGF protected the cells against apoptosis (Yang et al., 2008).

High-glucose was previously reported to increase intracellular lactate concentration and this was related to decreased flux of pyruvate to the Krebs cycle (Selva et al., 1996). They showed also that thiamine (vitamin B_1) overcame the effect of glucose reducing the lactate concentration. The authors suggested that thiamin achieved this either by favouring pyruvate flux towards the Krebs cycle or increased glucose 6-phosphate flux towards the pentose-phospate pathway. However, they did not provide data in support of these mechanisms. On the other hand, a more recent study reported reductions in intracellular lactate concentrations in AGE1.HN cells induced by quercetin treatment (10 μM) (Niklas et al., 2011). Observations of increased pyruvate flux into mitochondria also indicated that the cells might become less reliant on the glycolytic pathway and switch to the Krebs cycle for energy production after quercetin treatment. Similarly, the present report shows an increased intracellular lactate concentration with high-glucose treatment (28.5 mM), which was reduced ≈15% ($p<0.01$) by quercetin pre-treatment (10 μM). The loading plot (Figure 4.1B) shows that pyruvate had contributed to the separation of treatments from each other. Although it was not statistically significant, reductions in intracellular pyruvate (11.5%) concentrations with quercetin pre-treatment supported the hypothesis that quercetin directs pyruvate into the Krebs cycle to be used up in HUVEC energy production. Likewise, intracellular pyruvate levels were significantly reduced ($p<0.05$) also with quercetin pre-treatment (2 h) that was followed by TNF-α stimulation (6 h) of HUVECs. These data were further supported with the significant reduction in intracellular NAD^+ levels after quercetin pre-treatment followed by high-glucose stimulation. Reductions in intracellular NAD^+ concentrations indicated that NAD^+ was being reduced to NADH in the Krebs cycle which was likely to be activated after quercetin pre-treatment. Incubating HUVECs with medium containing quercetin (10 μM) for 20 h also led to a reduction (24.5%, $p<0.01$) in intracellular NAD^+ concentrations. Therefore, the observation of increased extra- and intracellular lactate concentrations, and their reduction with quercetin pre-treatment is likely to indicate both anti-atherogenic and anti-carcinogenic (Warburg

effect- cancer cells requires increased aerobic glycolysis to produce energy) properties of quercetin due to its effects on HUVEC primary metabolism.

The other significant alterations were observed primarily in the HUVEC purine metabolism. After quercetin treatments significant increases in intracellular adenosine, inosine and AMP concentrations and reductions in intracellular ATP and ADP concentrations were observed. Likewise, increases in extracellular inosine and adenosine concentrations were observed after quercetin treatments. Inosine and adenosine possess anti-inflammatory functions whereas ATP and ADP are pro-inflammatory metabolites. Also, quercetin pre-treatment prior to high-glucose stimulation caused increases in both intra- and extracellular inosine concentrations and reductions in intracellular ATP and ADP concentrations. On the other hand, after TNF-α stimulation of HUVECs reductions in intracellular NAD^+ and adenosine concentrations were observed. Nevertheless, quercetin pre-treatment prior to TNF-α caused elevations in intra- and extracellular inosine and intracellular adenosine concentrations, and reductions in intracellular ATP concentrations.

Previously published reports indicated that inflammatory stimuli including TNF-α affect cellular NAD^+ metabolism, and this effect is cell-type dependent. IFN-γ increased intracellular NAD^+ concentrations in RAW264.7 cells (Grant et al., 1999) whereas a mixture of IL-1β/IFN-γ/TNF-α and TNF-α alone decreased NAD^+ concentrations in Caco-2 cells (Khan et al., 2002) and macrophages (Iqbal and Zaidi, 2006), respectively. In the present study, TNF-α (10 ng/ml for 6 h) caused a significant decrease ($p<0.01$) in intracellular NAD^+ concentrations. Furthermore, it was shown that restoring NAD^+ concentrations diminishes the inflammation (Osar et al., 2004). In the present study, quercetin did not restore NAD^+ concentrations most likely due to its effect of enhancing the Krebs cycle activity caused increased utilization of NAD^+ reducing it to NADH. Quercetin treatment alone and quercetin pre-treatment followed by high-glucose stimulation led to time-dependent reductions in intracellular NAD^+ concentrations in HUVECs. Energy accumulation due to excess cellular fuel have been linked to a decrease in cellular longevity due to elevated ROS levels and disturbed cellular metabolism (Finkel and Holbrook, 2000). These changes were related to high-glucose concentrations in several studies. High-glucose concentrations were reported to reduce the activity of SIRT1

in endothelial cells (Mortuza et al., 2013, Zheng et al., 2012). SIRT1 is a nuclear member of the sirtuin family. Sirtuin protein family deacetylates proteins using NAD^+ as a substrate, and possess important functions to regulate cellular longevity and metabolism (Adams and Klaidman, 2007, Taylor et al., 2008). Previously published reports suggested elevation in SIRT1 activity due to the effects of several polyphenols including resveratrol (Adams and Klaidman, 2007, Chung et al., 2010, Gertz et al., 2012). However, De Bour and co-workers reported that quercetin did not have an effect on SIRT1 activity in HT29 (colon carcinoma cell line) cells although quercetin increased the recombinant SIRT1 activity. The authors related that to the instability of the polyphenol in cell culture medium since they observed a small but not significant increase in the SIRT1 activity when they tested the effect of the main quercetin metabolite, quercetin 3-O-glucuronide (Q 3-O-GlcA) (de Boer et al., 2006). Nevertheless, the present study showed that quercetin was metabolized into quercetin 3-O-sulfate and methyhlated quercetin (refer to chapter 5), which may still bear the capacity to induce SIRT1 activity explaining the decreases in intracellular NAD^+ concentrations observed after quercetin treatments.

Endothelial cell damage bears great importance during early events of acute inflammation. Elevated ATP concentrations were observed at the site of inflammation (Verghese et al., 1996). Budin and Burnstock worked with HUVECs demonstrating an elevation in extracellular ATP concentrations during LPS induced acute inflammation of HUVECs (Bodin and Burnstock, 1998). ATP contributes to the inflammation process in several different ways. After treating human microvascular endothelial cells with hydrolysis resistant ATP (adenosine 5'-O-(3-thiotriphosphate), elevations in the release of pro-inflammatory agents IL-1, IL-8, monocyte chemoattractant protein-1 and growth regulated oncogene α together with the increases in the surface expression of ICAM-1 by the cells were observed (Seiffert et al., 2006). ATP also induced VCAM-1 expression in human coronary artery endothelial cells (HCAEC) enhancing adhesion of monocytic U937 cells to HCAECs indicating that the increased ATP concentrations are likely to be important in the monocyte accumulation at atherosclerotic lesions.

ATP degradation is a constant process. CD39 (ectonucleoside triphosphate diphosphorylase 1, ENTPD1) and CD73 (5'-nucleotidase, ecto-5'-NT) are two

important enzymes present on cell membranes which sequentially convert ATP, ADP and AMP into adenosine (refer to Figure 5.1 for purine metabolism). CD39 hydrolyses ATP and ADP into AMP. AMP is then further hydrolyzed to adenosine by CD73. In several cell types including HUVECs, extracellular adenosine is cleared up and converted to inosine by adenosine deaminase (ecto-ADA) (Yegutkin, 2008b). Likewise, ADP is another metabolite with the potent pro-inflammatory activities. ADP has been known to be a regulator of platelet reactivity in vascular injury sites (Woulfe et al., 2001). Birk and co-workers showed that ADP but not ATP bears pro-aggregatory activity (Birk et al., 2002). However, they observed inhibition of platelet aggregation with ATP treatment in plasma due to the direct hydrolysis of ATP to AMP without yielding ADP. AMP is further hydrolysed to adenosine, and it is a potent inhibitor of platelet aggregation. Therefore, in the present study, the reductions observed in ATP and ADP concentrations after quercetin treatments are associated with the anti-inflammatory activities of quercetin on the endhotelial cell metabolism.

Adenosine is a potent inhibitor of the inflammatory process. Extracellular adenosine concentrations are responsible for its anti-inflammatory properties as its effects are initiated by the activation of G-protein-coupled P1 purinergic receptors ($A_{2A/2B}AR$) that activate intracellular cAMP production leading to a range of effects (Riksen et al., 2003) (Figure 4.5). For example, extracellular adenosine was reported to reduce the expression of VCAM-1 and E-selectin (Bouma et al., 1996). HUVECs were stimulated with TNF-α (0.01 ng/ml) for 5 h to induce E-selectin and VCAM-1 expression, and 20 h to induce ICAM-1 expression that provided maximal expression of these adhesion molecules on HUVEC surface. The presence of adenosine (250 μM) during the stimulation period caused inhibition of E-selectin and VCAM-1 expression but not ICAM-1 expression by HUVECs. Majumdar and Aggarwal investigated the effects of adenosine on NF-κB activation using several different agents to activate various cell types (Majumdar and Aggarwal, 2003). They revealed that the adenosine pre-treatment inhibited NF-κB activation after inflammatory stimuli by TNF-α in human monocytic cell line KBM-5, lymphoid cells (Jurkat), epithelial cells (HeLa), and embryonic kidney cells demonstrating that the effect of adenosine was not cell-type dependent. Nevertheless, adenosine did not inhibit NF-κB activation induced by phorbol ester, LPS, hydrogen peroxide, okadaic acid and ceramide in KBM-5 cells showing selectivity for blocking TNF-α

induced signal transduction pathway. Richard and co-workers assessed the effects of adenosine on endothelium permeability by measuring Even's dye-labeled albumin clearance from cell culture medium. Adenosine enhanced both basal endothelial barrier function and prevented increase in permeability due to the oxidant stimuli after xanthine and xanthine oxidase addition into cellular medium caused oxygen radical production (Richard et al., 1998).
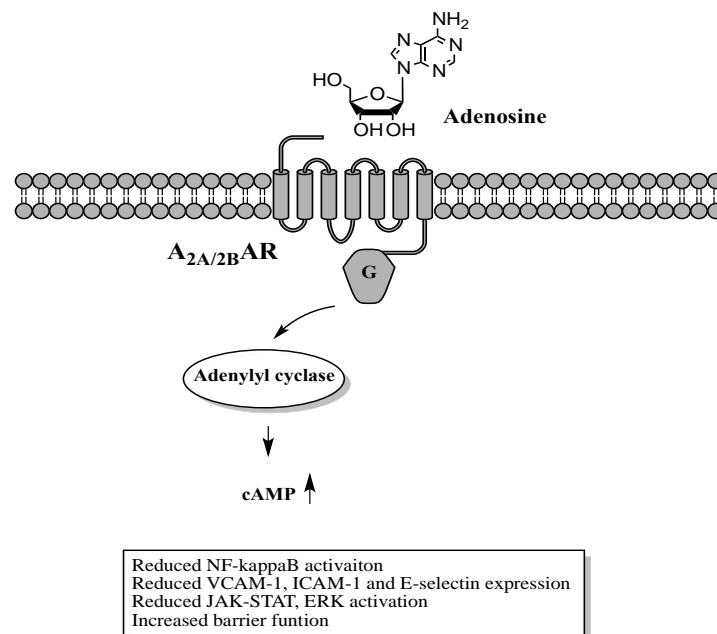
Figure 4.5: Activation of adenosine receptors by adenosine leads to anti-inflammatory responses

On the other hand, inosine has been known as an inert end product in purine metabolism for a long time. However, recent studies showed that inosine may exert anti-inflammatory effects potentially through adenosine A_2 receptors (Liaudet et al., 2002, Hasko et al., 2000, Lapa et al., 2012, Haskó et al., 2004). Hasko and co-workers assessed the effects of inosine both in vitro on macrophages and spleen cells, and in vivo in a mouse model (Hasko et al., 2000). The in vitro study reported that inosine was a potent inhibitor of pro-inflammatory cytokine production including TNF-α, IL-1, IL-12, macrophage-inflammatory protein-1α, and IFN-γ, but not anti-inflammatory IL-10 through the activation of adenosine $A_{1 \text{ and }} A_2$ subtype receptors. These data were further supported by the results obtained after injecting mice with inosine which was followed by challenging the animals with

LPS. In parallel with afore mentioned in vitro study, they observed inhibition in the production of TNF-α, IL-1, IL-12, macrophage-inflammatory protein-1α, and IFN-γ and additionally an increase in the production of anti-inflammatory IL-10 that indicated potent anti-inflammatory characteristics of the metabolite inosine. In a more recent study, Lapa and co-workers demonstrated that adenosine and inosine act synergistically to prevent acute inflammatory responses in carrageenan-induced pleurisy in a mouse model most likely through the activation of adenosine A_2 subtype receptor and the inhibition of inflammatory cytokine production or release (Lapa et al., 2012). Therefore, observation of increased adenosine and inosine concentrations after quercetin treatments in the present study provided evidence to the quercetin associated anti-inflammatory responses by endothelial cells.

It was previously reported that hyperglycaemic conditions (25 mM glucose, 24 h) caused increases in extracellular adenosine concentrations in endothelial cells (not observed in the present study) (Puebla et al., 2008). Likewise, HUVECs from gestational diabetes pregnancies were shown to have higher concentrations of extracellular adenosine due to the reduced transport (San Martín and Sobrevia, 2006). Extracellular adenosine concentrations in HUVECs from normal pregnancies were measured as 0.05 μM whereas extracellular adenosine concentrations for HUVECs from diabetic pregnancies were measured as 2.7 μM (Vásquez et al., 2004). The difference is likely to be an anti-inflammatory response in diabetic patients since adenosine was shown to increase L-arginine level followed by the increased NO production. However, increased NO due to the elevated adenosine concentrations during gestational diabetes may affect the fetus. An impaired nutrient transport to fetus due to vascular endothelial dysfunction may have adverse effects on "fetal programming" leading to increased risk of CVD and diabetes in the later life of progeny (Yajnik et al., 2007). Hence, possible elevations in extracellular adenosine concentrations after consumption of quercetin rich food or supplement may have different consequences in diabetic patients and in diabetic pregnancies.

In conclusion, after the effects of inflammatory conditions and quercetin on HUVEC metabolome were explored, several alterations in HUVEC metabolome were revealed which have biological significances that may be explained with

several different mechanisms. For example, increases in intra- and extracellular lactate concentrations with high-glucose treatments reflect a pro-inflammatory activity in HUVEC metabolism in response to the stimuli, whereas quercetin pre-treatment attenuated these responses by preventing the elevation in lactate concentrations as well as reducing the concentrations of pro-inflammatory metabolites ATP and ADP and in parallel increasing the concentrations of anti-inflammatory metabolites adenosine and inosine. The alterations in HUVEC metalome were observed mainly in the energy metabolism. However, the changes in lactate and pyruvate concentrations were most likely to be mediated through the effects of quercetin on glycolysis and the Krebs cycle, whereas the changes observed in ATP, ADP, AMP, adenosine and xanthine concentrations were most likely to be mediated through the effects of quercetin on the enzymes which are involved in the purine metabolism. Therefore, it was hypothesized that the quercetin-induced changes in metabolism were due to interactions between quercetin or its metabolites and the enzymes involved in energy metabolism. This hypothesis was tested in the next chapter by measuring the effects of quercetin and its metabolites on the activities of the major enzymes involved in purine metabolism, in tubo and using intact HUVECs.

CHAPTER 5: How does quercetin exert its anti-inflammatory effects?

5.1 Abstract

<u>Background:</u> In the previous chapter quercetin was shown to reduce the concentrations of pro-inflammatory metabolites ATP and ADP and in parallel increase the concentrations of anti-inflammatory metabolites adenosine and inosine. Purine nucleotides and their metabolites act as the signalling molecules yielding various biological responses via their specific receptors. ATP and ADP induce pro-inflammatory responses, whereas adenosine has been shown to have extensive anti-inflammatory potential. Therefore, clearance of ATP and ADP from extracellular milieu is a critical process due to the pro-inflammatory effects of these two molecules. There are 5 major enzymes involved in the conversion of ATP and ADP sequentially to uric acid which is the end-product of purine metabolism. Assessing the effects of quercetin on the activities of these enzymes and determining the concentration of quercetin inside the cells and whether it is metabolised by HUVECs will provide valuable data towards the explanation of the alterations observed in HUVEC energy metabolism after quercetin treatments.

<u>Aim:</u> To investigate the potential for quercetin and for its metabolites to modulate the activities of a series of enzymes involved in purine metabolism in HUVECS.

<u>Approaches/Methods:</u> In order to determine the concentration of quercetin and whether it was metabolised, cell and media samples from quercetin-treated HUVECs were analysed using LC-DAD and LC-MS. Single HUVEC volume was estimated using a flow cytometric method in order to calculate intracellular quercetin concentrations after the treatments. The effects of quercetin and individual conjugates were tested on the activities of CD39/ENTPD1, CD73/5'-nucleotidase, adenosine deaminase (ADA), purine nucleoside phosphorylase (PNP) and xanthine oxidase using commercial pure enzymes, HUVEC protein extracts in tubo and using intact HUVECs.

<u>Results:</u> After 10 µM quercetin treatments for 2 h, 8 h or 20 h, quercetin was quickly taken up by HUVECs and metabolized into quercetin, quercetin 3'-O-sulfate (Q 3'-O-S), methylquercetin and 2 other metabolites which could not be

precisely identified. Quercetin aglycone and methylquercetin were present inside the cells up to 8 hours, whereas no flavonols were detected inside the cells after 20 h quercetin treatment. On the other hand, quercetin, methylquercetin and putative quercetin and methylquercetin dimers were identified in the culture media after 2 h, 8 h and 20 h quercetin treatments. Quercetin aglycone was shown to be a strong inhibitor of all the 5 purine metabolism enzymes when its effects on recombinant enzymes were tested (IC_{50}= 0.574 - 55.6 µM) whereas its conjugates had different effects on the activities of the enzymes depending on the position of the conjugation and nature of the conjugated chemical group. However, neither quercetin nor its metabolites inhibited PNP and CD39 activity in the HUVEC extracts or intact HUVECs respectively, and quercetin was only a weak inhibitor of the CD73 activity in intact HUVECs.

Conclusions: The present study assisted to explain the anti-inflammatory alterations observed in HUVEC energy metabolism after quercetin treatments. The most significant changes observed were the reductions in ATP and ADP and the elevations observed in AMP, adenosine and inosine concentrations. The inhibition of ADA and CD73 activities with physiological cellular concentrations was in keeping with the elevations observed in adenosine and AMP levels. At the same time, CD39 and PNP activities were not affected indicating that the reductions in ATP and elevations in inosine levels were likely to be due to the altered levels of CD39 and PNP proteins after quercetin treatments, respectively.

5.2 Introduction

In recent years, the importance of the purinergic signalling cascade has been emphasised by several studies that led to the identification of particular targets for the development of new therapeutic applications in inflammation (Yegutkin, 2008a, Burnstock, 2002). Purine nucleotides and their metabolites act as the signalling molecules yielding various biological responses via their specific receptors. ATP and ADP modulate their effects through P2 receptors whereas adenosine activates P1 receptors (Ralevic and Burnstock, 1998, Bours et al., 2006). ATP was shown to induce cell adhesion molecule expression (Goepfert et al., 2000), and release of cytokines and chemokines (Seiffert et al., 2006) whereas ADP was shown to regulate platelet reactivity (Woulfe et al., 2001, Birk et al., 2002) which were explained in detail in the previous chapter. Therefore, clearance of ATP and ADP from the extracellular milieu is a critical process due to the pro-inflammatory effects of these two molecules, and that is achieved by the activities of the ecto-enzymes present on the cell surface (Bours et al., 2006).

Figure 5.1 shows that CD39 (ectonucleoside triphosphate diphosphohydrolase 1, E-NTPDase1) and CD73 (5'-nucleotidase, ecto-5'-NT) act sequentially converting ATP and ADP to AMP and then AMP to adenosine. CD73 has both membrane bound and soluble forms inside the cells (Antonioli et al., 2013). Goepfert and co-workers had transfected HUVECs with an adenoviral vector, rAdCD39, to increase the CD39 activity in the cells (Goepfert et al., 2000). In parallel, they showed that increased CD39 activity reduced ATP-induced surface expression of E-selectin by HUVECs. On the other hand, Grunewald and Ridley assessed the effects of CD73 depletion in HUVECs. According to the results they had observed, CD73 depletion in HUVECs diminished extracellular adenosine levels showing that CD73 activity is necessary to produce extracellular adenosine by HUVECs (Grunewald and Ridley, 2010). They also observed increased surface expression of ICAM-1, VCAM-1 and E-selectin by HUVECs through the activation of NF-κβ pathway. In contrast to the pro-inflammatory activities of ATP and ADP, adenosine had been shown to possess anti-inflammatory potential modulated through adenosine receptors (Riksen et al., 2003). Adenosine deaminase (ADA) which converts adenosine irreversibly to inosine regulates the activation of the adenosine receptors by eliminating the extracellular adenosine (Cristalli et al., 2001). ADA

protein had been shown to carry out its activities both inside the cells as a soluble enzyme and in the extracellular milieu bound to surface receptor CD26 (Eltzschig et al., 2006). IMP hydrolysis by 5'-NT is another source of inosine. Inosine is converted to hypoxanthine by the activity of the PNP enzyme. Hypoxanthine is further converted to xanthine, and then xanthine is converted to uric acid. Both of the reactions are catalysed by xanthine oxidase, and uric acid is the end-product of purine metabolism.
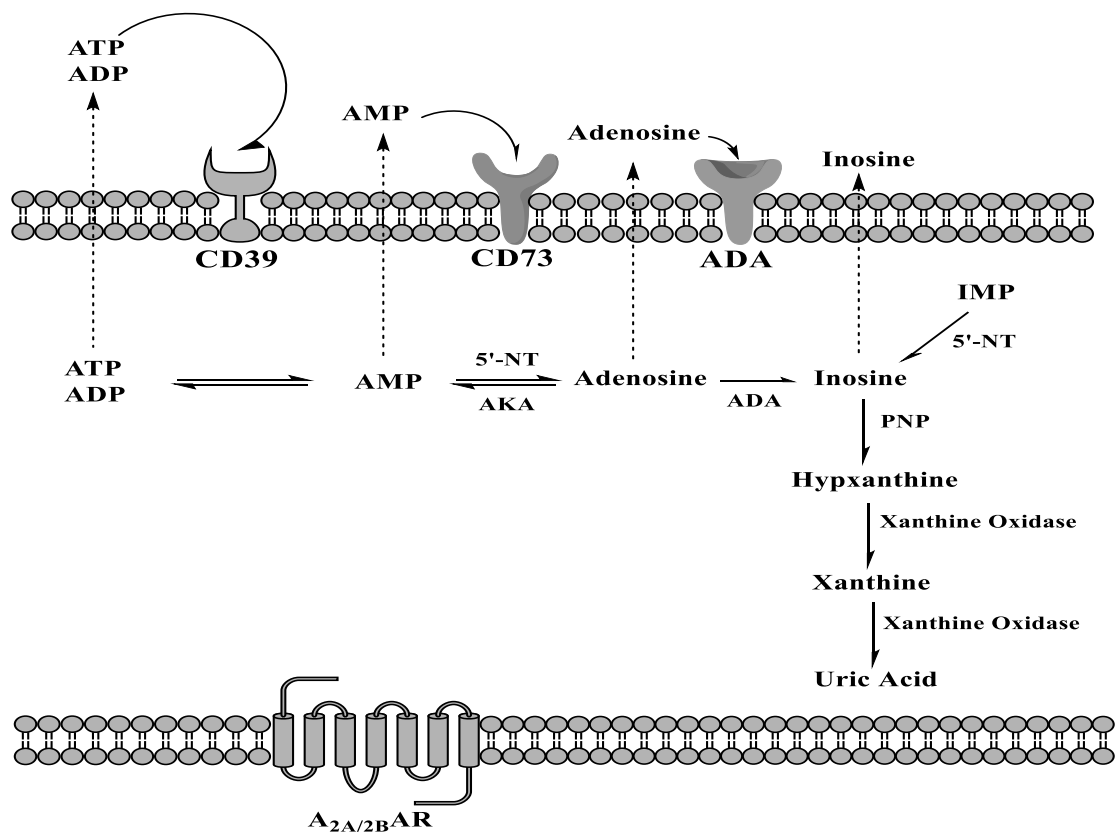
Figure 5.1: Major enzymes involved in purine nucleotide/nucleoside metabolism. ATP and ADP are sequentially converted to AMP, adenosine, inosine, hypoxantine, xanthine and finally to uric acid. Extracellular adenosine activates adenosine receptors initiating anti-inflammatory activities. CD39: ectonucleoside triphosphate diphosphohydrolase 1 (E-NTPDase1), CD73: 5'-nucleotidase (ecto-5'-NT), 5'-NT: 5'-nucleotidase, AKA: adenosine kinase, ADA: adenosine deaminase, PNP: purine nucleoside phosphorylase.

Dietary flavonoids are found in glycosylated forms in plants and food and beverages (Manach et al., 2004), and they are deglycosylated during absorption from the gut (Németh et al., 2003). It was concluded that quercetin glycosylates are further metabolized into different forms by the time they reach the systemic circulation as the quercetin aglycone has not been detected in human plasma (Manach et al., 2005). Mullen and co-workers fed volunteers with lightly fried onions and the analysis showed that quercetin was sulfated, glucuronidated or methylated by the time it reached the systemic circulation (Mullen et al., 2006). Quercetin 3'-O-sulfate (Q 3'-O-S), quercetin 3-O-glucuronide (Q 3-O-GlcA) and 3'-methylquercetin 3-O-glucuronide (IsoR 3-O-GlcA) were the major quercetin metabolites identified in the plasma of volunteers. Nevertheless, the fate of quercetin in HUVECs is unknown.

According to the results obtained in Chapter 4 (metabolomics study), it was hypothesized that the quercetin-induced changes in the HUVEC metabolism were due to interactions between quercetin and the enzymes involved in energy metabolism. This hypothesis was tested in this chapter by investigating the ability of quercetin to interact with the enzymes involved in purine metabolism. Furthermore, the fate of quercetin inside the HUVECs was investigated in order to address important related questions- do HUVECs metabolise quercetin, and do its metabolites accumulate in the cells?

5.3 Materials & Methods

5.3.1 Materials

Isorhamnetin, tamarixetin, rhamnetin and quercetin 3-O-sulfate were purchased from Extrasynthase (Genay, France). Rutin and tetramisole HCl were purchased from Sigma-Aldrich (Poole, UK). Quercetin 3'-O-sulfate, quercetin 3-glucuronide, quercetin 3'-glucuronide, isorhamnetin 3-glucuronide were chemically synthesized by Dr Paul Needs in the Kroon Lab using a previously published method (Needs and Kroon, 2006). 7-Methyl-6-thioguanosine was purchased from Carbosynth Ltd, UK. Biomol Green™ Reagent was purchased from Enzo Life Sciences UK LTD. All the other chemicals used were purchased from Sigma-Aldrich (Poole, UK).

5.3.2 Identification of Flavonol Metabolites in the Intracellular Extracts and the Culture Medium Samples

5.3.2.1 Quercetin Treatments and Harvesting Cells

HUVECs were grown either on 6-well plates or 10-cm dishes until they reached confluency. Then, the culture media were replaced with quercetin (10 µM) containing media for 2 h, 8 h or 20 h. At the end of the treatments, 950 µl of media aliquots were removed from the plates and added into Eppendorf tubes containing 25 µl HPLC grade acetonitrile and 25 µl acetic acid in order to lower the pH and preserve flavonol metabolites. Consequently, the media were removed from the plates and the cells were washed three times with phosphate buffered saline (room temperature). Cells were scraped free. 450 µl MilliQ water was then added onto the cells and the resulting cell suspension was pipetted into Eppendorf tubes containing 25 µl HPLC grade acetonitrile and 25 µl acetic acid. Samples were stored at -20°C when necessary.

5.3.2.2 Sample Preparation

Media samples were mixed using a bench top vortex, and centrifuged at 13,000 rpm for 10 min at 4°C using a bench top centrifuge (Thermo Scientific™ Heraeus™ Fresco 17). Supernatants were removed and pipetted into HPLC vials for analysis

using either LC-DAD or LC-MS. Intracellular extracts were mixed using a bench top vortex, and ultra-sonicated in a sonic water bath (Ultrawave) for 10 min. This was followed by centrifuging samples in the microfuge at 13.000 rpm for 10 min at 4°C. Supernatants were removed and pipetted into HPLC vials for analysis with either LC-DAD or LC-MS.

5.3.2.3 LC-DAD and LC-MS Analyses

Reverse phase HPLC (Agilent HP1100 system, Agilent Technologies, Waldbronn, Germany) with UV diode array detection was used for routine analyses and quantitation. During chromatographic runs, autosampler temperature was set to 4°C, temperature of the column compartment was 30°C and injection volume was 20-100 µl. Metabolites were separated using a Phenomenex$^{\circledR}$ Luna$^{\circledR}$ 5-C18(2) (250 × 4.60 mm, 5 µm) column at a flow rate of 1 ml/min. Mobile phases were (A) 50 mM ammonium acetate in H_2O (adjusted to pH 5) and (B) 2% tetrahydrofuran (THF) and 0.1% acetic acid in acetonitrile. Gradient elution was performed as in Table 5.1.

Table 5.1: Gradient profile of mobile phase for quercetin metabolite detection.

Time (min)	A %	B %
0	83	17
2	83	17
7	75	25
15	65	35
20	50	50
25	0	100
30	0	100
35	83	17
50	83	17

An Agilent 1100 HPLC system coupled to an Agilent LC/MSD SL spectrometer was used for LC-MS analyses. The same gradient elution (Table 5.1) was used for the LC-MS analyses. Flavonol metabolites were monitored using MS in full scan in both positive and negative ion modes with electrospray ionisation.

Individual standards for quercetin, isorhamnetin, rhamnetin, tamarixetin, quercetin 3' -O-sulfate (Q 3'-O-S), quercetin 3 -O-sulfate (Q 3-O-S), quercetin 3'-glucuronide (Q 3'-O-GlcA), quercetin 3-glucuronide (Q 3-O-GlcA), isorhamnetin 3-glucuronide (IsoR 3'GlucA) were analysed using HPLC and LC-MS methods in order to help the metabolite identification process and for quantification.

5.3.2.4 Solid Phase Extraction (SPE)

The aliquoted culture medium sample was centrifuged, and then the supernatant was pumped through a C18 SPE cartridge (Waters Sep-Pak Cartidges Vac C18 3cc) which had been activated by flushing with 4 ml of methanol. Sample was run through the cartridge in 3 ml of acidified water. Another 3 ml of acidified water was used to flush the cartridge to remove all the remaining traces of medium, and the flavonol metabolites were then eluted with 3 ml of acidified methanol. The sample dried until 100-200 μl of sample was left using a centrifugal evaporator placed in HPLC vial for MS analysis.

5.3.2.5 Chemical Synthesis of Quercetin Dimer

The procedure for the quercetin dimer synthesis procedure was adopted from those of Gulsen et al. (2007) and Pham et al. (2012). It involved the oxidation of quercetin with potassium ferricyanide. Quercetin (340 mg) was dissolved in 80 ml of acetonitrile, and mixed with a 20 ml solution of 50 mM potassium ferricyanide and 50 mM sodium carbonate over 30 min. The solution was stirred for 3 h in the dark. Concentrated hydrochloric acid was used to adjust the pH to 2. The solution was then concentrated under vacuum to remove the acetonitrile which was followed by extraction four times with 40 ml of ethyl acetate:diethyl ether (8:2 v/v). The combined extracts were dried using magnesium sulphate ($MgSO_4$). Then

remaining solvents were removed using a rotary evaporator in vacuo (Butchi Rotavapor R-20 coupled to Butchi Vacuum Pupm V-700).

5.3.2.6 Prep-HPLC for Purifying Quercetin Dimer

The final product of the quercetin dimer synthesis was purified using Gilson prep-HPLC. The sample was run through a Phenomenex® Prodigy™ ODS3 guard column (60 × 21.30 mm, 5 µm, 100 Å) connected to Phenomenex® Prodigy™ ODS3 column (250 × 21.2 mm, 5 µm, 100 Å), and fractions were collected using a fraction collector (Gilson Model 120). Collected fractions were analysed by LC-MS and the fractions with the desired quercetin dimer were pooled. Solvents in the pooled samples were removed using the rotary evaporator in vacuo.

5.3.2.7 HUVEC Volume Determination by Flow Cytometry

HUVECs were cultured in 6-well plates at 3500 cells/cm^2 using basal medium (5.5 mM glucose). After the treatments, confluent monolayers were washed with PBS and harvested using Trypsin (0.025%)/EDTA (0.01%) or 2 mM EDTA only. Cells were re-suspended in PBS (pH 7.4) containing 0.1% BSA and propidium iodide (PI) (2 µg/ml). Flow cytometric analysis was carried out using an iCyt Eclipse EC 800 flow cytometer (Sony Biotechnology Inc.) with 405 nm, 488 nm, 561 nm and 642 nm excitation lasers available. The flow rate was adjusted to 10 µl/min and data were acquired for 2.5 min. The FL6 detector was used for electric volume determination and the FL3 detector with a 780/40 filter was used to detect PI stained cells. The PMT setting was 6 and it was 1 for electric volume. The threshold was set on side scatter (SS).

5.3.2.8 Enzymatic Assays

Adenosine Deaminase (ADA)

The effects of quercetin and its metabolites on adenosine deaminase activity were tested using both commercial pure enzymes and crude HUVEC protein extracts. Adenosine deaminase converts the substrate adenosine to inosine (Figure 5.2).

$$\text{Adenosine} \quad + \quad H_2O \quad \xrightarrow{\text{Adenosine deaminase}} \quad \text{Inosine} \quad + \quad NH_3$$
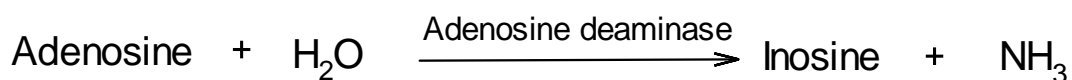
Figure 5.2: Adenosine deaminase catalyzes the conversion of adenosine to inosine.

The enzymatic activity and the inhibition studies for recombinant human adenosine deaminase expressed in *E. coli* (Sigma-Aldrich®) were performed using the continuous spectrophotometric rate determination procedure adapted and modified from the procedure Sigma-Aldrich® provided. Adenosine absorbs UV-light at 265 nm and, in this assay the reduction in adenosine levels in the experimental mix which was reflected as a reduction in the absorbance was measured using a spectrophotometer (Uvikon$_{XS}$). The experimental mixture, containing substrate solution (1.35 mM adenosine solution, pH 7.0 at 25°C), reaction buffer (100 mM potassium phosphate buffer, pH 7.5 at 25°C) and H_2O was incubated in a 3 ml quartz cuvette at 37°C for 1 min to equilibrate the temperature. The reaction was initiated by the addition of the adenosine deaminase enzyme solution (0.20-0.40 unit/ml) making a reaction mix which contained 53.3 mM potassium phosphate, 0.045 mM adenosine and 0.02-0.04 unit of adenosine deaminase (final concentrations). In the inhibition studies quercetin or its metabolites were included in the experimental mix. Quercetin and isorhamnetin were dissolved in DMSO, and the maximum amount of DMSO in the experimental mix was 0.16% (v/v) and 2.2% (v/v) respectively. Decrease in absorbance at 265 nm was measured at 30 s intervals over 5 min. In the blanks, adenosine deaminase was replaced with bovine serum albumin (BSA), and the absorbance values subtracted from experimental readings. Results were plotted as a graph representing adenosine consumption by the enzyme per unit time.

Adenosine deaminase activity was also tested using HUVEC protein extracts. The confluent HUVECs were washed three-times with PBS (room temperature). The cells were then incubated on dry ice for 15 min. 400 µl MilliQ water was added onto the cells, and cell membranes were disrupted using a cell scraper. The solution was transferred into Eppendorf tubes, and centrifuged at 4°C for 15 min. The supernatant was removed, protein concentration in the extract was determined by bicinchoninic acid (BCA) assay and an extract containing 30 µg protein used to replace the pure enzyme in the experimental mix to determine

enzymatic adenosine deaminase activity, and inhibitory effects of quercetin or its metabolites.

5.3.2.9 Xanthine Oxidase

The effects of quercetin and its metabolites on xanthine oxidase activity were tested using a commercial pure enzyme. The enzymatic activity and inhibition studies for the xanthine oxidase from bovine milk (Sigma-Aldrich$^{®}$) were performed using the continuous spectrophotometric rate determination procedure adapted and modified from the procedure Sigma-Aldrich$^{®}$ provided. Xanthine oxidase catalyses the reaction where xanthine is converted into uric acid (Figure 5.3).

$$\text{Xanthine} + \text{H}_2\text{O} + \text{O}_2 \xrightarrow{\text{Xanthine Oxidase}} \text{Uric acid} + \text{H}_2\text{O}_2$$
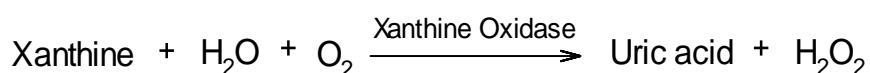
Figure 5.3: Xanthine oxidase catalyzes the conversion of xanthine to uric acid.

Production of uric acid was detected by measuring absorbance at 290 nm. The experimental mixture, containing potassium phosphate buffer (50 mM, pH 7.5), xanthine 0.15 mM), was incubated in a 3 ml quartz cuvette at 37°C for 1 min. The reaction was initiated by xanthine oxidase (0.1-0.2 unit) addition, and the increase in absorption at 290 nm was recorded at 30 s intervals for 5 min at 37°C. The procedure was repeated with the addition of various concentrations of flavonols dissolved in DMSO (final concentration, 0.16% for quercetin and 2.2% for isorhamnetin) and H$_2$O. The blank samples contained the experimental mixtures without xanthine oxidase.

5.3.2.10   Purine Nucleoside Phosphorylase (PNP)

PNP metabolizes adenosine into adenine, inosine into hypoxanthine and guanosine into guanine. The effects of quercetin and its metabolites on PNP activity were tested using both commercial pure enzyme and HUVEC protein extract. The enzymatic activity and inhibition studies for *Geobacterium sp.* PNP

expressed in *E. coli* (Sigma-Aldrich®) were performed using the continuous spectrophotometric rate determination procedure. A guanosine analogue, 7-methyl-6-thioguanosine (MESG) which is widely used in PNP activity assays was used as the substrate for PNP (Webb et al., 1992) (Figure 5.4).

$$7\text{-Methyl-6-thioguanosine} + P_i \xrightarrow{\text{PNP}} 7\text{-Methyl-6-thioguanine} + \text{Ribose 1-phosphate}$$
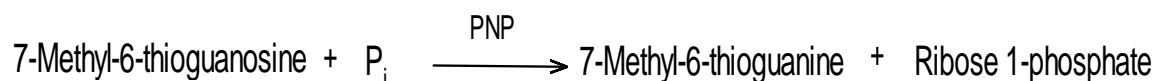
Figure 5.4: PNP catalyzes the conversion of MESG to 7-methyl-6-thioganine and ribose 1-phopshate.

The experimental mixtures, containing potassium phosphate buffer (50 mM, pH 7.5) and PNP (0.02/0.04 unit) were incubated in the wells of a microplate at 37°C for 1 min. The reaction was initiated by substrate addition (800 μM), and the increase in absorption at 360 nm was recorded at 30 s intervals for 5 min at 37°C measuring the formation of the product. The procedure was repeated with the addition of various concentrations of flavonols dissolved in DMSO (final concentration, 0.2%) and H_2O. The blank samples contained the experimental mixtures without the enzyme.

PNP activity was also tested using HUVEC protein extracts by replacing pure commercial PNP in the assay with HUVEC protein extract (30 μg protein).

5.3.2.11   CD39/ENTDP1

CD39 is an ecto-enzyme bound to cell membrane that hydrolyses ATP and ADP to AMP. In this assay, the CD39 activity and inhibitory effects of quercetin and its metabolites were measured using both recombinant human (rh) CD39 (R&D Systems) and intact HUVECs.

The assay procedure provided by R&D Systems was used to measure rhCD39 activity. ATP was used as the substrate, and the free phosphate liberated after hydrolysis of ATP was measured using the Biomol Green™ Reagent kit that is based on a colourimetric phosphate quantification method. First of all, a standard

curve (0-2 nm phosphate) was prepared using the phosphate standard (800 µM phosphate in H_2O) provided in the phosphate detection kit. Then, 25 µl of the 0.04 µg/ml enzyme diluted in assay buffer (25 mM Tris, 5 mM $CaCl_2$, pH 7.5) was mixed with 25 µl of the 100 µM ATP diluted in assay buffer in the wells of a microplate. The microplate was covered with parafilm and incubated at 37°C for 30 min. After the incubation period, the reaction was stopped by the addition of 100 µl of Biomol Green™ Reagent to each well. The microplate was incubated at room temperature for 20 min allowing the formation of green colour, and the absorbance was read at 620 nm. The amount of phosphate liberated in the reaction was calculated using a standard curve prepared with known concentrations of phosphate. The procedure was repeated with the addition of various concentrations of flavonols dissolved in DMSO (final concentration, 0.2% v/v) or H_2O. The blank samples contained the experimental mixtures without CD39.

The CD39 activity in intact HUVECs was measured using an adapted and optimized method (Goepfert et al., 2000, Kawashima et al., 2000). HUVECs were grown in 6-well plates until confluency. Cell medium was removed from the wells and the confluent HUVECs were washed three-times with the assay buffer (25 mM Tris, 5 mM $CaCl_2$, pH 8). The cells were then incubated with 2 ml of substrate buffer (25 mM Tris, 5 mM $CaCl_2$, 5 mM tetramisole HCl,100 µM ATP, pH 8) at 37°C for 15 min. Tetramisole HCl which is an alkaline phosphatase inhibitor was used in the assay to prevent ecto-alkaline phosphatase activity. Liberated phosphate levels were then measured using Biomol Green™ reagent. The procedure was repeated with the addition of various concentrations of flavonols dissolved in DMSO (final concentration, 0.1% v/v) or H_2O into the substrate buffer. For the blanks, 25 mM Tris, 5 mM $CaCl_2$, 5 mM tetramisole HCl and individual flavonols/metabolites were incubated with the cells and the experimental buffer containing substrate was incubated without the cells. The blank values were subtracted from the sample values.

5.3.2.12   CD73/5'-Nucleotidase

CD73 is an enzyme that has the ability to hydrolyse both intra- and extracellular AMP to adenosine. In this assay, CD73 activity and inhibitory effects of quercetin and its metabolites were measured using both rhCD73 (R&D Systems) and intact

HUVECs. CD73 activity assay procedures for both rhCD73 and intact HUVECs were nearly same with the CD39 activity assays performed except few modifications. AMP (50 µM) was used as the substrate, and the free phosphate liberated after hydrolysis of AMP was measured using the Biomol Green™ Reagent kit. A standard curve (0-2 nm phosphate) was prepared using the phosphate standard (800 µM phosphate in distilled water) provided in the phosphate detection kit. Then, 25 µl of the 0.04 µg/ml rhCD73 diluted in assay buffer (25 mM Tris, 5 mM $MgCl_2$, pH 7.5) was mixed with 25 µl of the 50 µM AMP diluted in assay buffer in the wells of a microplate. The microplate was covered with parafilm and incubated at 37°C for 20 min. After the incubation period reaction was stopped by the addition of 100 µl of Biomol Green™ Reagent to each well. The microplate was incubated at room temperature for 20 min allowing the formation of green colour, and the absorbance was read at 620 nm. Phosphates liberated in the reactions were quantified using the standard curve prepared with known concentrations of phosphate. The procedure was repeated with the addition of various concentrations of flavonols dissolved in DMSO (final concentration, 0.2% v/v) or H_2O. The blank samples contained the experimental mixture without CD39.

The CD73 activity in intact HUVECs was measured using the same procedure with CD39 assays where 100 µM ATP and $CaCl_2$ in the assay buffer were replaced with 50 µM AMP and $MgCl_2$ which are essential for CD73 activity. For the blanks, 25 mM Tris, 5 mM $MgCl_2$, 5 mM tetramisole HCl and particular flavonol were incubated with the cells and the experimental buffer containing substrate was incubated without the cells. The blank values were subtracted from the sample values.

5.3.2.13   BCA Assay for Total Protein

BCA assay was used to determine protein concentrations in cellular extracts where necessary. Assay components were bicinchoninic acid and copper(II) sulfate. Samples were diluted 1:15 with sodium phosphate (Na- P_i) buffer. A working reagent was prepared by mixing bicinchoninic acid and copper(II) in the ratio of 50:1. A standard curve was generated using bovine serum albumin diluted in Na-P_i buffer. 25 µl of sample or standard was mixed with 200 µl of working reagent and incubated for 30 min at 37°C. Absorbance was read at 550 nm, and

protein concentrations were calculated using a standard curve prepared with known concentrations of bovine serum albumin.

5.3.2.14 Statistical Analysis

The difference in the enzyme activities after treatments were statistically analyzed using one-way analysis of variance (one-way ANOVA) with the aid of GraphPad Prism 5.01 software. Once it was determined that differences exist among the means, Tukey post hoc tests determined which means differed. P values less than 0.05 (p< 0.05) were accepted as a significant difference.

The IC_{50} values were estimated by the non-linear regression analyses of the residual enzyme activities and the log transformed flavonoid concentrations using GraphPad Prism 5.01 software.

5.4 Results

First, quercetin metabolites present inside the cells and in the culture media after the quercetin treatments were identified. That was followed by measuring the effects of quercetin and its metabolites on the activities of the enzymes, in tubo and using intact HUVECs. Figure 5.5 shows the quercetin conjugates tested in these studies.
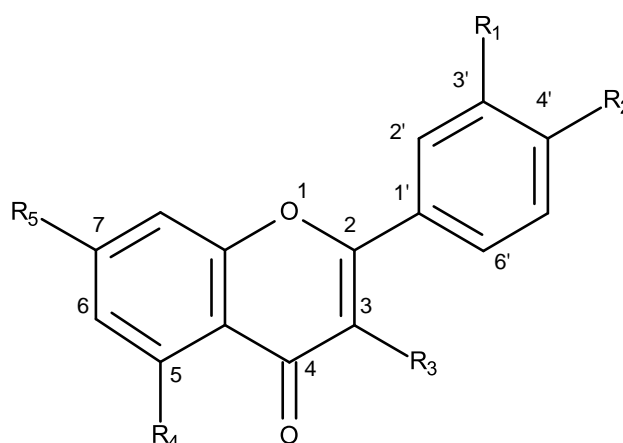
	R_1	R_2	R_3	R_4	R_5
Quercetin	OH	OH	OH	OH	OH
Isorhamnetin	OCH_3	OH	OH	OH	OH
Tamarixetin	OH	OCH_3	OH	OH	OH
Rhamnetin	OH	OH	OH	OH	OCH_3
Q 3'-O-GlcA	OCH_3	OH	OH	OH	OH
Q 3'-O-S	OSO_3	OH	OH	OH	OH
Q 3-O-GlcA	OH	OH	OCH_3	OH	OH
Q 3-O-S	OH	OH	OSO_3	OH	OH
IsoR 3-O-GlcA	OH	OH	OCH_3	OH	OH
Rutin	OH	OH	ORutinoside	OH	OH

Figure 5.5: Quercetin conjugates tested in the study.

5.4.1 Fate of Quercetin in the HUVEC Model and the Nature of Putative Metabolites

Previous human studies showed that quercetin is metabolized in vivo, and only its metabolites were present in circulation after consumption of quercetin rich food (Mullen et al., 2006, Egert et al., 2012) or supplements (Cialdella-Kam et al., 2013). There are also studies that have been reported in the literature with regards to the intracellular quercetin metabolism including the studies which used human dermal fibro blasts (Spencer et al., 2003), Caco-2 cells (Murota and Terao, 2003) and HT29 cells (de Boer et al., 2006). However, there is no information with regards to metabolism of quercetin in HUVECs.

Therefore, the fate of quercetin in the HUVEC model was assessed prior to the investigation of the inhibitory effects of quercetin on certain purine metabolism enzymes. In order to do that, HUVECs were incubated with 10 µM quercetin for 2 h, 8 h and 20 h which allowed to analyse uptake kinetics and intracellular quercetin levels (Figures 5.6 and 5.7). Figures 5.6 and 5.7 shows that quercetin was quickly taken up by HUVECs and metabolized into quercetin, quercetin 3'-O-sulfate (Q 3'-O-S), methylquercetin and 2 other metabolites which could not be precisely identified. There was no free quercetin aglycone left in the culture medium after 20 h. Intracellular extracts contained only quercetin and methylquercetin after 2 h - 8 h, but there were no polyphenols left inside the cells after 20 h that could be detected by LC-DAD. Q 3'-O-S was present in culture media after 2 h treatment. However, it was not present in intracellular extracts indicating that quercetin was metabolized quickly in the cells and most likely the Q 3'-O-S was rapidly removed from the HUVECs. Likewise, methyquercetin was present in culture media after 2 h, and its concentrations were highest in culture media after 8 h. However, its presence in the intracellular extracts after 2 h and 8 h of the quercetin treatment indicated that unlike Q 3'-O-S, it was not removed from the HUVECs quickly. The culture medium samples and intracellular extracts were analysed also with LC-MS (Table 5.2). After LC-MS analysis, the unknown peaks observed in the LC-DAD analyses were believed to represent oxidation products of quercetin and methylquercetin. Therefore, they were likely to be produced in the culture medium rather than being cellular products.

LC-MS analysis confirmed the identities of the labelled peaks in LC-DAD chromatogram (Figure 5.6A, Table 5.2). The culture medium samples were analysed by LC-MS after a solid-phase extraction process to concentrate quercetin conjugates and remove other cell culture medium components that interfere with the analysis. Standards prepared were also analysed to assist the identification process of the quercetin conjugates. The peak with the retention time of 16.56 min in culture medium samples was identified as a quercetin sulfate (M - H of 380.8 and M + H of 382.9). Both Q 3'-O-S and quercetin 3-O-sulfate (Q 3-O-S) standards were analysed with the LC-MS method. Retention time for Q 3-O-S standard was 10.66 min whereas it was 16.85 min for Q 3'-O-S standard which was similar to the retention time for quercetin sulfate identified in culture medium samples (16.56 min) indicating that it was representing Q 3'-O-S. Unknown 1 peak had a retention time of 17.73 min. After the LC-MS analysis, it was assumed to be a quercetin dimer (M - H of 600.8). The peak with retention time of 19.95 min was identified as quercetin (M –H of 300.9 and M + H of 302.9). Unknown 2 peak had a retention time of 21.357 min was assumed to be a methylquercetin dimer (M – H of 628.8). The peaks with retention times of 22.55 and 22.60 in the culture medium samples were identified as methylquercetin (M - H of 314.9 and M - H of 317.0). Isorhamnetin (3'-OCH$_3$-quercetin), tamarixetin (4'-OCH$_3$-methylquercetin) and rhamnetin (7-OCH$_3$-methylquercetin) standards were analysed in order to identify the site of the methyl group conjugation. Isorhamnetin and tamarixetin had retention times of 22.77 min and 22.90 min respectively, and rhamnetin had a retention time of 24.42 min. Therefore, the peaks in culture medium samples which were identified as methylquercetin likely to be representing isorhamnetin and tamarixetin. The exact molecular structures for unknown conjugates and other identified conjugates can be confirmed with NMR spectroscopy analysis after isolating the fractions which would contain each flavonol separately. The peak that represented unknown 3 disappeared after the SPE process, and also its UV spectrum in LC-DAD analysis indicated that it was not representing a polyphenol.

A.
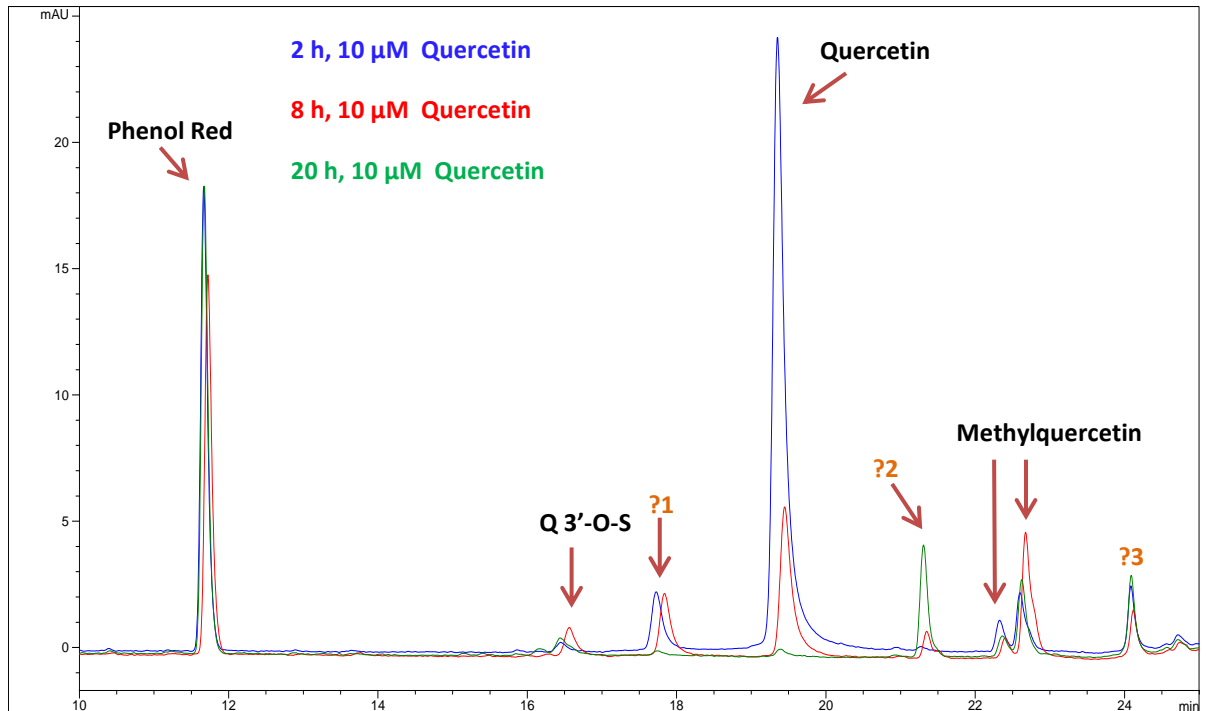
B.
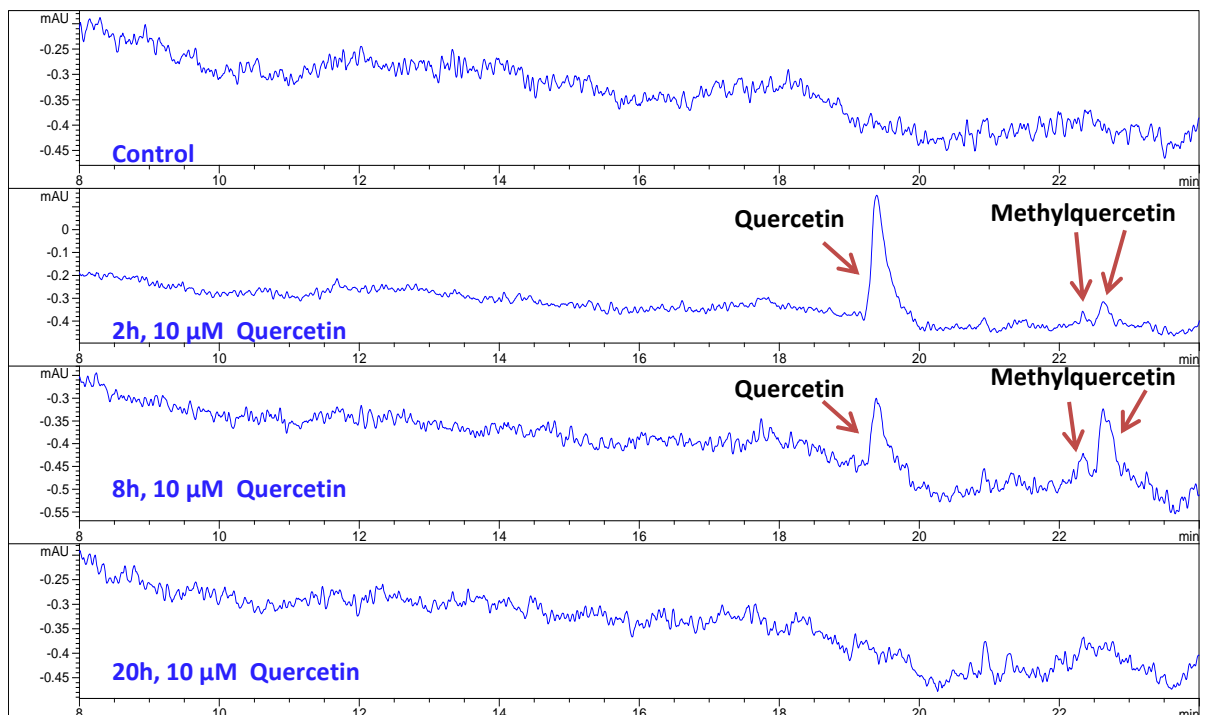
Figure 5.6: LC-DAD chromatograms. **A.** Culture medium samples collected at 3 different time points after quercetin treatment. Phenol red, Q 3'-O-S, quercetin and methylquercetin could be identified using standards. However, peaks labelled as ?1, ?2 and ?3 remained as unknowns that could not be precisely identified by HPLC analysis. **B.** Intracellular extracts obtained from control cells (without quercetin treatment), 2 h, 8 h and 20 h quercetin treated cells.

A. Culture medium samples
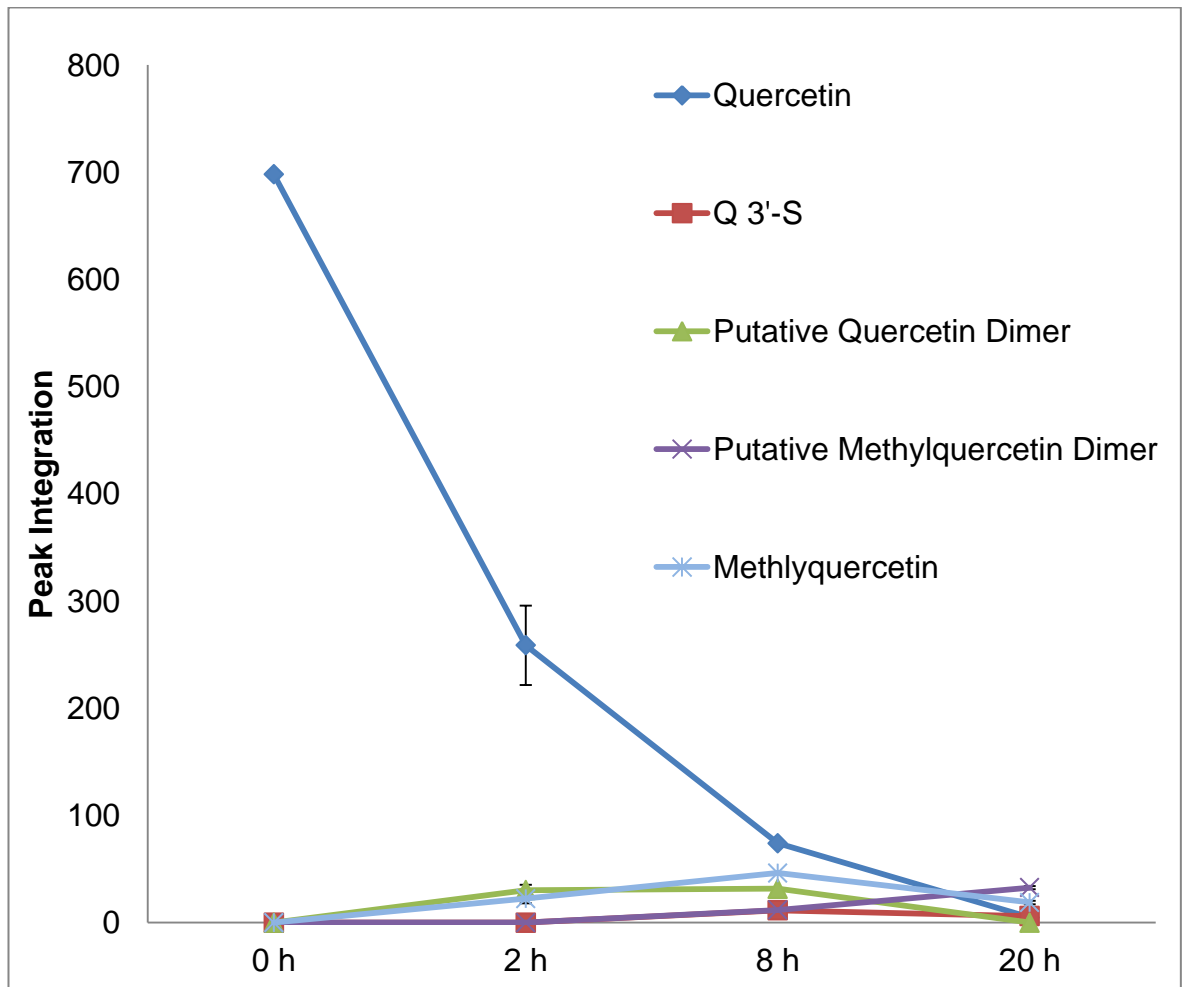
B. Intracellular Extracts
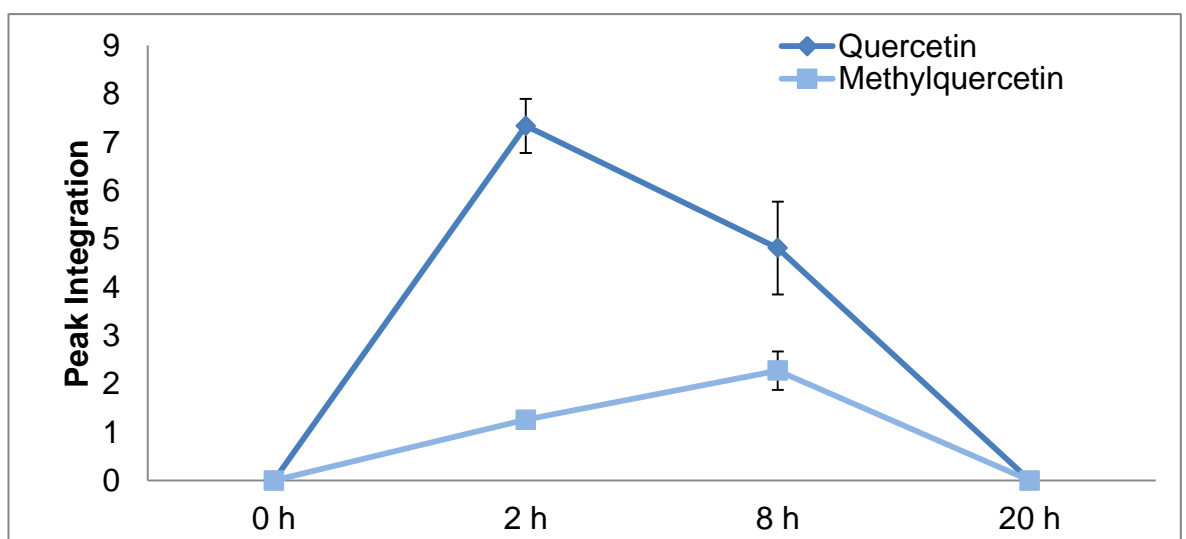
Figure 5.7: Quercetin uptake and metabolism kinetics by HUVECs. **A.** Levels of quercetin and its metabolites produced in culture medium with time (n=3). **B.** Levels of quercetin and merhylquercetin in intracellular extracts with time (n=3).

Table 5.2: M-Z values values for the flavonols detected in the medium samples.

Retention Time (min)	M-H	M+H	Identity
16.56	380.8	382.9	Q 3'-O-S
17.73	600.8	-	(Quercetin Dimer)
19.95	300.9	302.9	Quercetin
21.36	628.8	-	(Methylquercetin Dimer)
22.55 and 22.67	314.9	317.0	Methyquercetin

Interestingly, when the fresh culture medium was spiked with 10 µM or 100 µM quercetin and incubated at 37°C without the cells, free quercetin aglycone disappeared with time, and two new peaks were observed (Figure 5.8). According to the LC-MS analysis results, these two peaks were assumed to be quercetin dimers   (M – H of 600.8) likely produced after oxidation of quercetin in the culture medium.
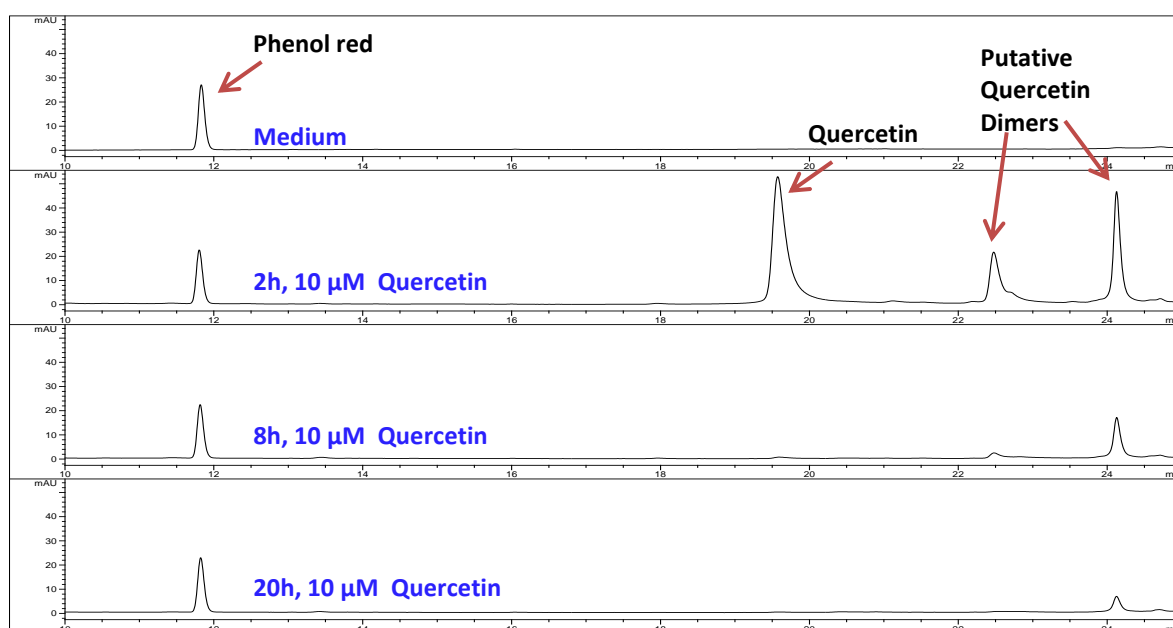
Figure 5.8: HPLC chromatogram for fresh culture medium samples spiked with 10 µM quercetin and incubated for 2 h, 8 h or 20 h at 37°C.

Further investigations showed that quercetin oxidation was due to a component of the culture medium since the incubation of quercetin (100 µM) spiked into PBS at 37°C did not cause any modifications on of the quercetin aglycone (Figure 5.9). Also, supplementing culture medium with additional ascorbic acid, reduced the rate of quercetin oxidation (data not shown).
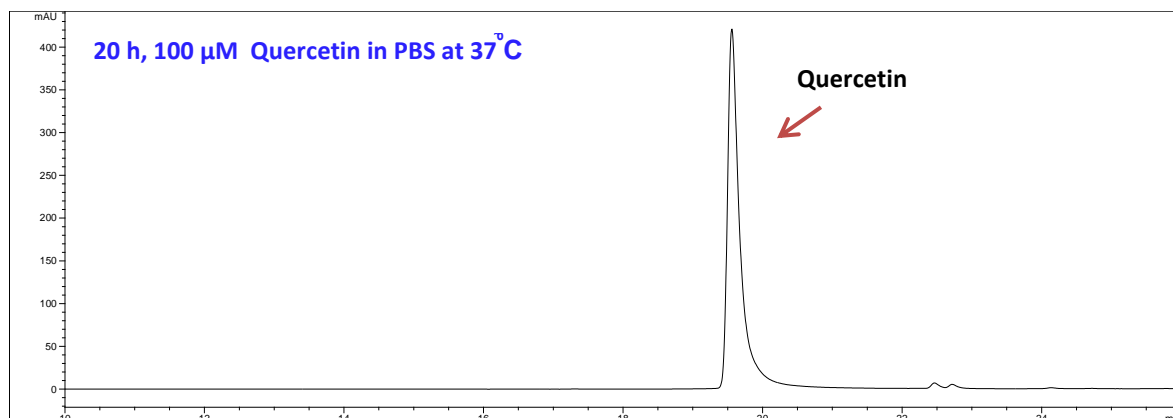
Figure 5.9: HPLC chromatogram of quercetin (100 µM) spiked PBS at 37°C for 20 h.

Previously, Pham and co-workers reported the presence of a quercetin dimer (M + H of 603.0769) in culture medium after the incubation of quercetin (100 µM) spiked medium at 37°C for 24 h, and they had revealed the structure of the dimer using [1]NMR and LC-MS analyses (Pham et al., 2012). They had also confirmed that their dimer had the same molecular structure with a previously reported synthetic quercetin dimer (Gülşen et al., 2007). In the present study, a synthetic dimer was synthesized using the procedure Pham and co-workers had used to aid the elucidation of the molecular structures of quercetin dimers observed after treating the cells or spiking the culture medium with quercetin. The reaction mixture contained three major peaks (Figure 5.10). The required product, quercetin dimer, was shown to have a retention time of 24.06 min and M − H of 600.8 and M + H of 602.8. Hence, it had the same retention time and mass as one of the two quercetin dimers observed here in the quercetin spiked culture medium incubated without the cells (Figure 5.8). The peak representing quercetin dimer was isolated using prep-HPLC to be analysed by NMR to elucidate its molecular structure. The

product was successfully isolated with a negligible amount of quercetin aglycone impurity as it could be seen in Figure 5.11. The final step prior to NMR analysis to elucidate quercetin dimer structure involved removing the solvents using a rotary evaporator in vacuo. Unfortunately, in the final step the purity of the product was lost (Figure 5.12). The newly formed products had a similar profile to the initial product mixture, but with an interesting new peak observed with a retention time of 18.03 and M - H of 600.8 (Figure 5.12). Hence, it had same retention time and M – H with the quercetin dimer (unknown 1) identified after treating HUVECs with quercetin (Figures 5.6 and 5.12).
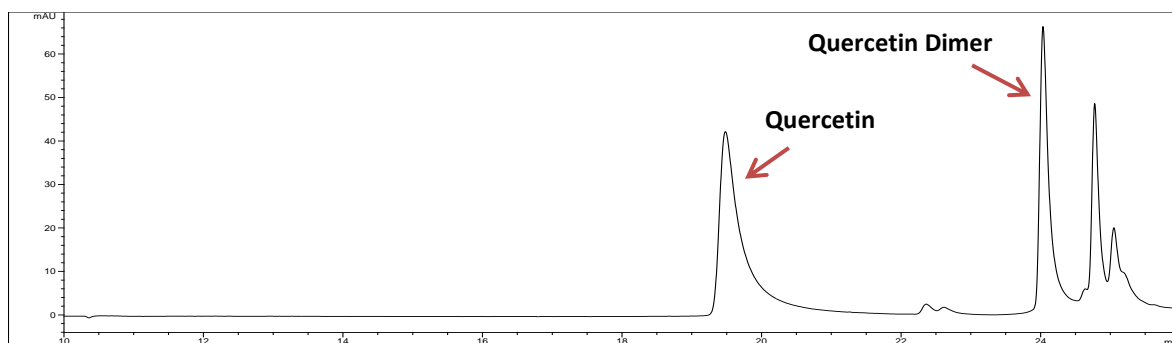
Figure 5.10: HPLC chromatogram for reaction mixture produced during chemical synthesis of quercetin dimer.
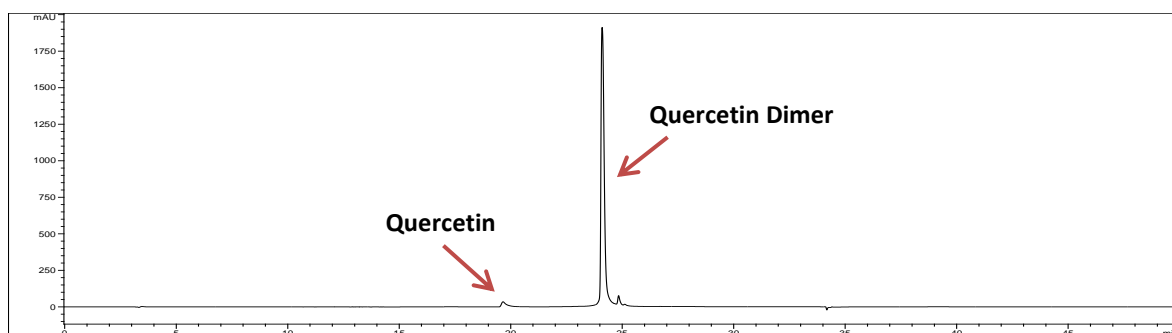
Figure 5.11: HPLC chromatogram representing the purity check for the isolated fraction (isolated from the mixture represented in Figure 5.10) containing quercetin dimer after prep-HPLC application.
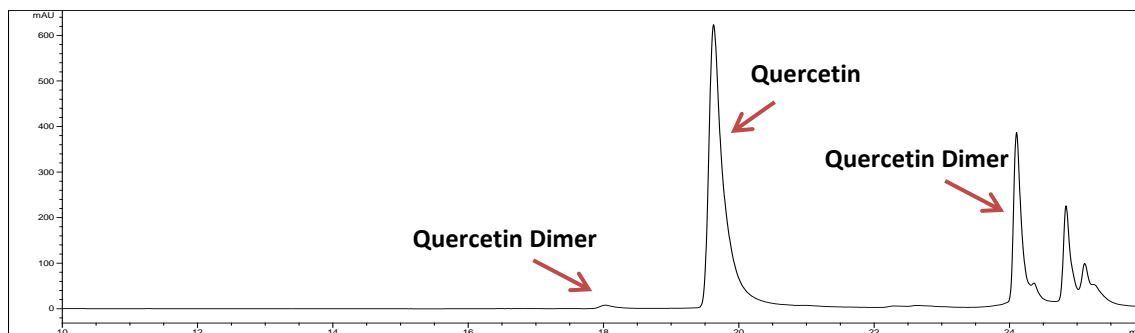
Figure 5.12: HPLC chromatogram representing the purity check for the isolated fraction containing quercetin dimer after removal of solvents prior to NMR analysis.

5.4.2 Estimation of Single HUVEC Volume and Intracellular Quercetin Concentrations

Single HUVEC volume was estimated using a flow cytometric approach. First, the effects of cell harvesting methods on HUVEC volume were assessed in order to have confidence that the volume estimates were not affected by the processing of the cells. In Figure 5.13, it can be observed that the live cells and propodium iodide stained dead cells were gated. Only live cells were analysed for their volumes. Trypsin/EDTA treatment yielded a higher percentage of live cells (n=3, p<0.05). However, it seemed to be a more aggressive method since higher variability in the cell volume was observed compared to the cells harvested using EDTA only. Since it is necessary to work with a method that would not affect cell volume, EDTA was used to harvest cells in the subsequent experiments.
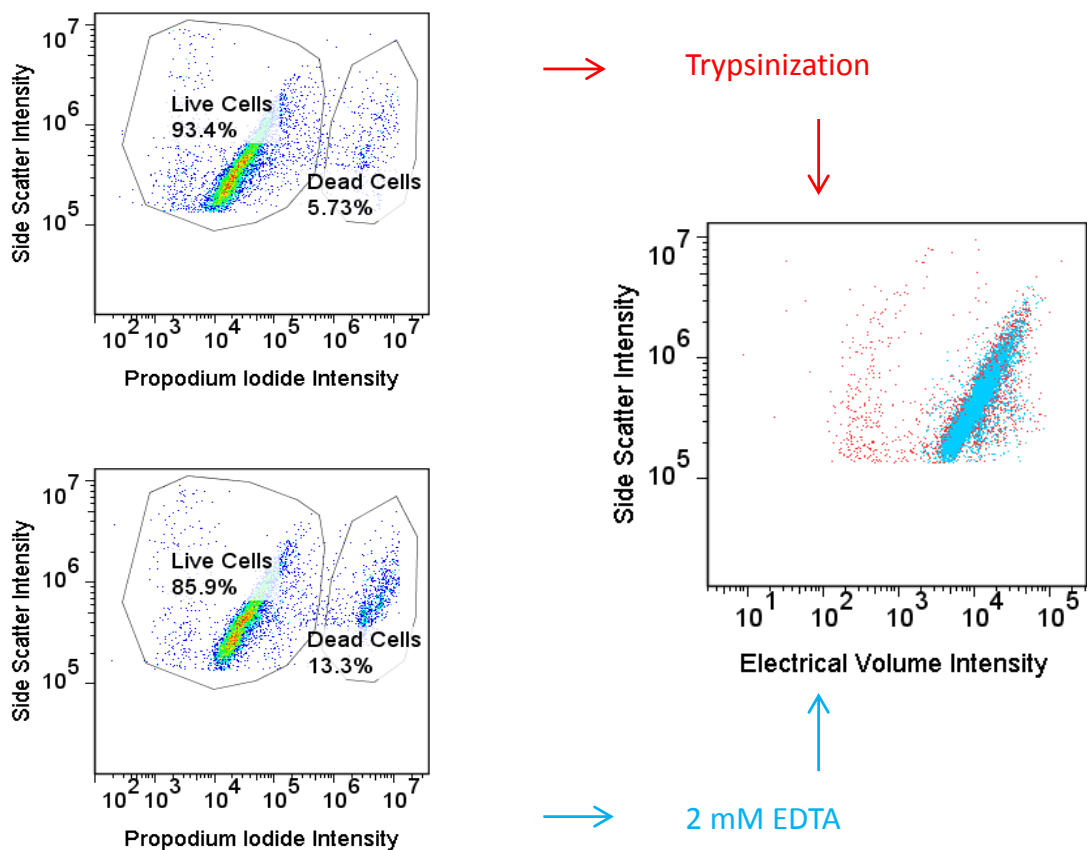
Figure 5.13: Effects of cell harvesting methods on HUVEC volume. Live cells were gated for electric volume analysis.

Next, the volume of normal resting HUVECs and of treated HUVECs was estimated using flow cytometry. High-glucose concentrations increased HUVEC volume to 113.6% ± 8.490% of the unstimulated HUVEC volume, but this change was not statistically significant (Figure 5.14A). However, both quercetin and quercetin pre-treatment followed by glucose treatment significantly reduced HUVEC volume compared to high-glucose treated cells ($p < 0.05$ and $p < 0.01$ respectively). Similarly, TNF-α alone did not have a significant effect on HUVEC volume (Figure 5.14B). Nevertheless, reductions in HUVEC volumes to 64.77% ± 5.963% ($p < 0.01$) and 70.68% ± 9.880% ($p < 0.01$) of the unstimulated HUVEC volume were observed after quercetin treatment and quercetin pre-treatment followed by TNF-α, respectively. Therefore, these results indicated that quercetin treatment led to a reduction in HUVEC volume in the presence or absence of high-glucose concentrations and TNF-α treatment.

A.

B.
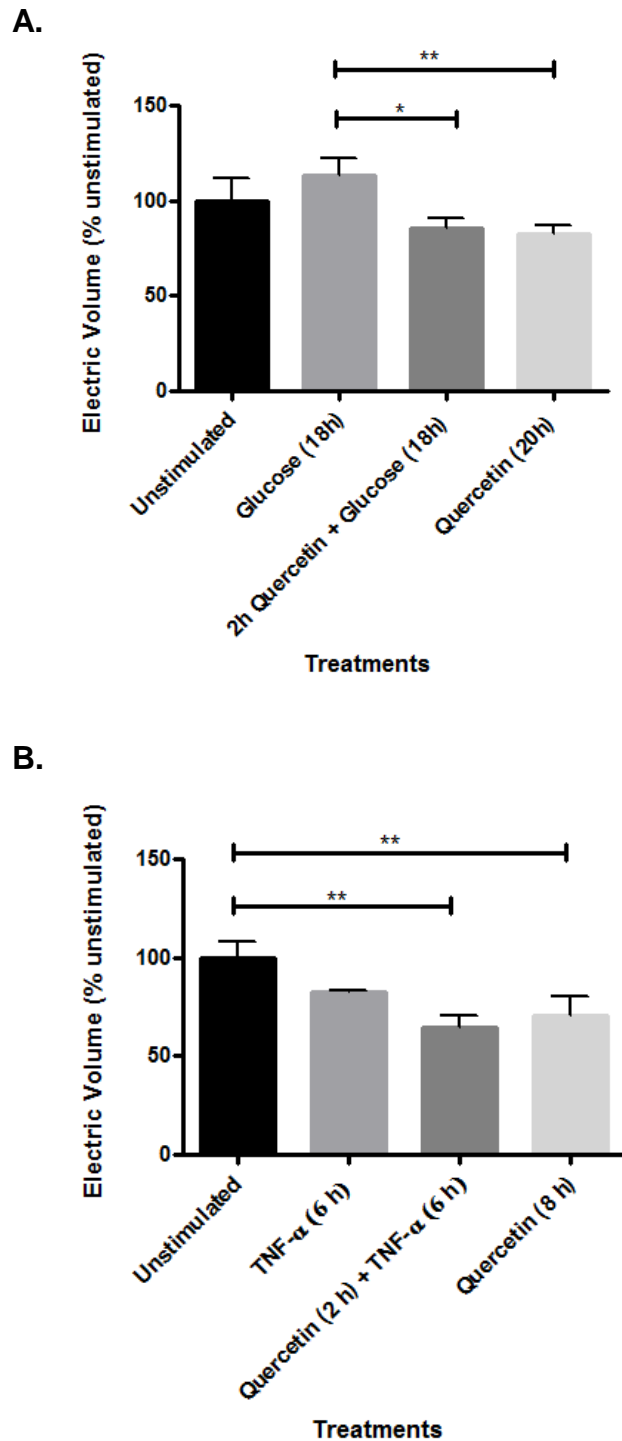
Figure 5.14: HUVEC volume estimation after particular treatments using flow cytometry (n=3). **A.** Mean HUVEC volumes measured after particular treatments with quercetin (10 µM) and glucose (28.5 mM). **B.** Mean HUVEC volumes measured after particular treatments with quercetin (10 µM) and TNF-α (10 ng/ml).

The average quercetin concentration in a single HUVEC was calculated using an equation that was defined by three variables. The amount of quercetin (moles) in a given extract was divided by the volume of a single HUVEC and the total number of cells in order to determine the quercetin concentration in a single HUVEC (Equation 5.1).

Equation 5.1:

$$[quercetin]\ in\ a\ single\ HUVEC = \frac{moles\ of\ quercetin}{volume\ of\ a\ single\ cell\ \times\ cell\ number}$$

An example calculation was carried out to show how the intracellular quercetin concentration for a single HUVEC was calculated after 2 h quercetin (10 µM) treatment. Previously, intracellular extracts for quercetin treated cells were analysed using a HPLC method (Figure 5.6B). A standard curve used to calculate the quercetin concentration in the extract ([quercetin]= 0.4587 µM), and the volume of the extract was 500 µl. Therefore, the amount of quercetin present in the extract could be calculated using "Equation 5.2":

Equation 5.2:

$$M = \frac{number\ of\ moles}{volume}$$

$$0.4587\ \mu M = \frac{number\ of\ moles}{0.0005\ L}$$

$$Quercetin = 2.29 \times 10^{-4}\ \mu moles$$

Average cell number in a single well of a culture plate was calculated as 268750 cells/9.4 cm^2 (n=6). Mean HUVEC volume was measured as 9128 µm^3 (9.13 × 10^{-12} L, n=3) after 2 h quercetin (10 µM) treatment. This value was used to calculate quercetin concentration in a single HUVEC. After obtaining all of the three variables, it was possible to estimate quercetin concentration in a single cell by applying "Equation 5.1":

$$[quercetin]\ in\ a\ single\ HUVEC = \frac{moles\ of\ quercetin}{volume\ of\ a\ single\ cell\ \times\ cell\ number}$$

$$[quercetin] \ in \ a \ single \ HUVEC = \frac{2.2935 \times 10^{-4} \ \mu moles}{9.13 \ \times \ 10^{-12} \ \times \ 268750}$$

$$[quercetin] \ in \ a \ single \ HUVEC = 93.47 \ \mu M$$

Furthermore, two studies were reported in the literature that attempted to calculate single HUVEC volume. Hillebrand and co-workers used atomic force microscopy (AFM) to assess the effects of estrogens on HUVEC volume (Hillebrand et al., 2005). They measured single HUVEC volume as 2408 ± 94.1 fl/cell. This value was used in "Equation 1" to calculate quercetin concentration in a single HUVEC by replacing the HUVEC volume value measured using flow cytometry.

$$2408 \ fl = 2.408 \ \times \ 10^{-12} \ L$$

$$= \frac{2.2935 \times 10^{-4} \ \mu moles}{2.408 \ \times \ 10^{-12} \ \times \ 268750}$$

$$= 354.4 \ \mu M$$

The other study was carried out by Leunig and co-workers where they had tested effects of Photofrin® treatment and laser light on HUVEC volume (Leunig et al., 2996). They had employed scanning electron microscopy (SEM) to measure endothelial cell volume. They had provided a scanning electron micrograph showing both unstimulated and PF treated HUVECs. HUVEC volume was calculated using the scale on the scanning electron micrograph, and then "Equation 1" was applied to calculate quercetin concentration in a single HUVEC.

$$2.8 \ mm \ in \ micrograph = 1 \ \mu m$$

$$HUVEC \ diameter \ measured = 30 \ mm \quad \therefore 30 \ mm \ represents \ 10.7 \ \mu m,$$

$$radius = \frac{10.7}{2} = 5.35 \ \mu m$$

$$volume \ of \ sphere = \frac{4}{3}.\pi.r^3 = \frac{4}{3}.\pi.(5.35)^3 \ = 641.4 \ \mu m^3 = 6.41 \times 10^{-13} \ L$$

$$[quercetin] \ in \ a \ single \ cell = \frac{2.2935 \times 10^{-4} \ \mu moles}{6.41 \times 10^{-13} \ \times \ 268750}$$

$$[quercetin] \ in \ a \ single \ cell = 1331 \ \mu M = 1.3 \ mM$$

Hence, 3 different HUVEC volume estimations used to calculate intracellular quercetin concentration yielding 3 different values; 93.47 µM with flow cytometry, 354.4 µM with AFM and 1331 µM SEM methods.

5.4.3 The Effects of Quercetin and Its Metabolites on Purine Metabolising Enzymes in HUVECs

Quercetin, methylated quercetin and quercetin sulfate were identified in the culture medium samples whereas quercetin and methylated quercetin were identified in the intracellular extracts after treating the cells with quercetin. Therefore the effects of quercetin, isorhamnetin and Q 3'-O-S were tested on HUVEC energy metabolism enzymes. Also, the effects of other flavonols were tested on these enzymes to provide a broader knowledge of the potential of flavonols to inhibit the activity of these enzymes.

5.4.3.1 Adenosine Deaminase (ADA)

The effects of quercetin, isorhamnetin, quercetin 3'-O-sulfate and quercetin 3'-glucuronide were tested on the activity of adenosine deaminase. The results were plotted as a graph representing adenosine consumption by the enzyme per time, where the gradient of the line reflected the rate of the reaction (A_{265nm}/min) (Figure 5.15). The linear phase of the reaction was used to calculate the rate of adenosine deamination. Therefore, the initial step was to test several parameters in the enzymatic activity measurement procedure to eliminate any bias in the results. First of all, the linear phase of the reaction was determined by allowing the reaction to continue for 20 min. Figure 5.15 shows that during the first 5 min, the reaction rate is roughly linear.
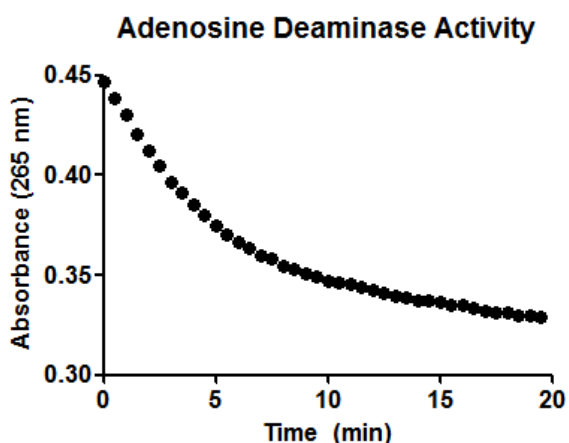
Figure 5.15: Adenosine deaminase activity was represented as adenosine consumption per unit time.

After the optimum reaction time was determined, an absorbance linearity test was performed to determine that the absorbance value did not fall in the plateau, but in the linear phase of the reaction for the adenosine concentration suggested in the test procedure. The initial concentration of adenosine was 45 µM in the assay. When the absorbance values were plotted for the experimental mix containing reaction buffer, increased concentrations of adenosine substrate, quercetin (10 µM) and enzyme (heat de-activated at 70°C) against the adenosine concentrations, it was observed that 90 µM adenosine and the lower concentrations fall in the range of the linearity (Figure 5.16). Therefore, 45 µM adenosine was selected to be a suitable concentration to measure the enzymatic activity of ADA.
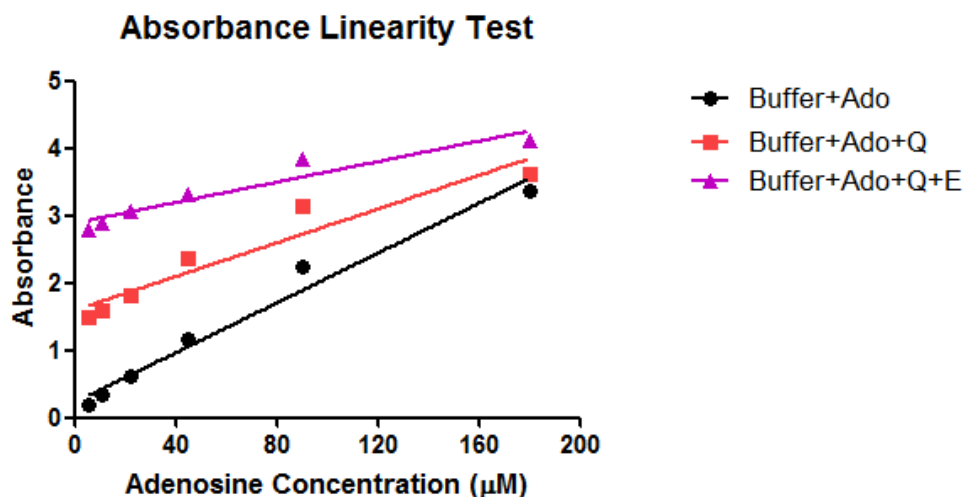
Figure 5.16: Absorbance linearity test. Increasing concentrations of adenosine were tested for their effects on the linearity of the reaction. Purple line which contained the experimental buffer with increased concentrations of adenosine, enzyme and quercetin indicated that 45 μM adenosine is suitable for the assay.

Finally, different DMSO concentrations were tested in experimental mix to test any possible effects on the inhibitory activities of quercetin and isorhamnetin since DMSO may affect the hydrophobic interactions between polyphenols and the enzyme. Increased DMSO concentrations (0.1%-3% (v/v)) did not alter the inhibitory effects of quercetin (30 μM) and isorhamnetin (30 μM) on ADA enzymatic activity (Figure 5.17A & 5.17B).

A.

B.
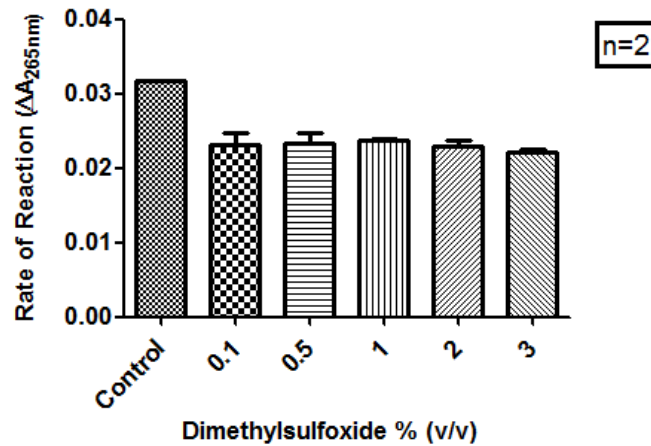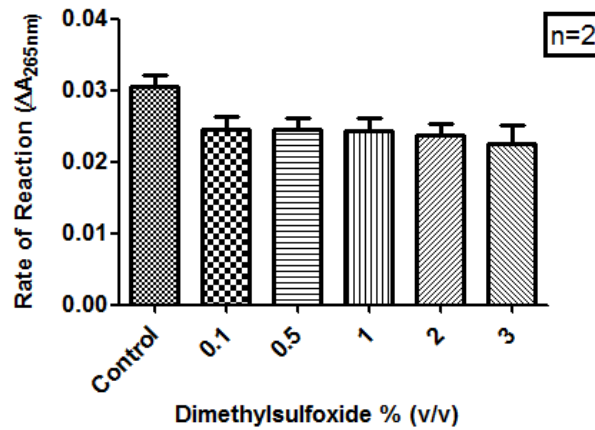
Figure 5.17: Assessing effects of DMSO on enzyme activity inhibition.

Two different protein extraction methods were tested for obtaining the highest yield of protein extracts from HUVECs. A commercial lysis buffer (Cell Signalling Technology) and mechanical disruption methods were compared for their efficiencies. Protein concentrations in the extracts were determined by a BCA assay, and both of the methods yielded similar amounts of protein (data not shown) and ADA activity (Figure 5.18A). However, the lysis buffer contains several chemicals that may affect the inhibitory activity of polyphenols. Therefore, mechanical disruption of the cell membranes was preferred as the method used to obtain protein extracts. When the heat-treated HUVEC protein extracts were used in the experiment, there was only a negligible reduction in A_{265nm} (Figure 5.18B). The reduction was most likely to be the reflection of adenosine auto-degradation in the experimental mix.

A.

Protein Extraction Methods

B.

Heating the enzyme solution at 70°C for 15 min
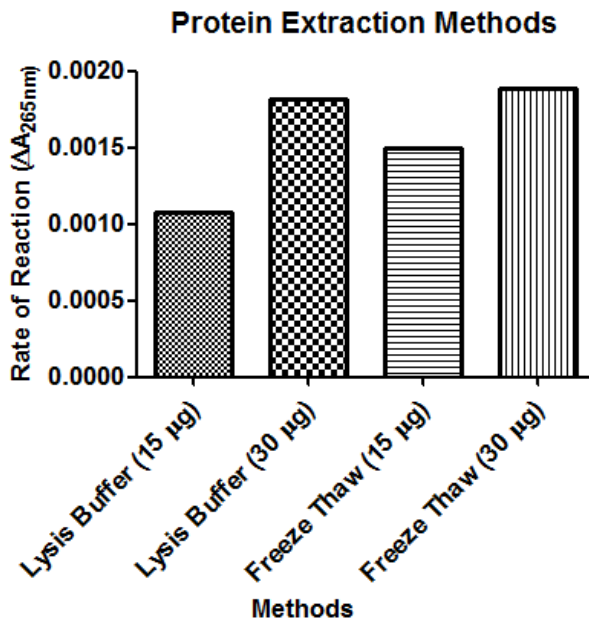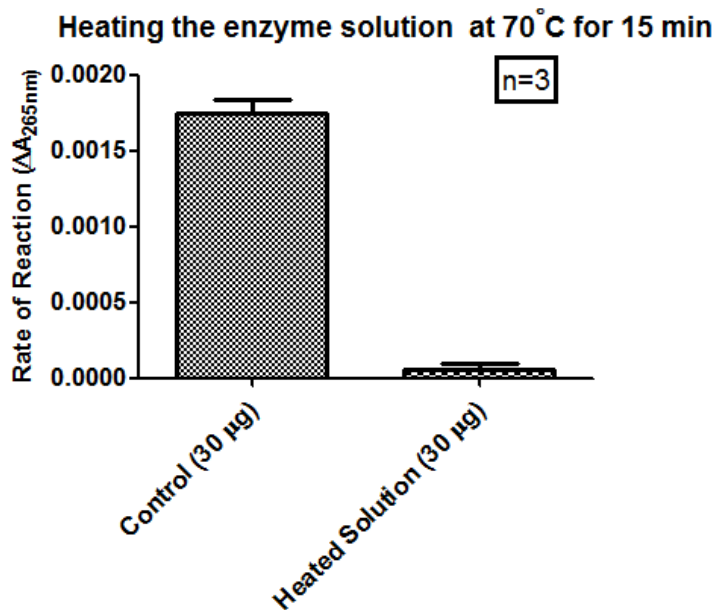
Figure 5.18: HUVEC protein extracts for ADA activity assays. **A.** Assessing the effects of protein extraction methods on enzyme activity. **B.** Heat treatment of the HUVEC extracts almost completely abrogates the reduction in A_{265nm} which shows that the loss of adenosine was enzyme dependent.

The inhibitory effects of quercetin, isorhamnetin, Q 3'-O-S and Q 3'-O-GlcA were tested on ADA activity (2 µM - 50 µM). All of these flavonols significantly inhibited ADA activity. Analysis of the inhibitory effects of quercetin on ADA activity was given as an example to show how the calculation of IC_{50} (half maximal inhibitory concentration) estimates was performed. Figure 5.19A shows the dose-dependent inhibition of ADA activity by quercetin, and Figure 5.19B shows the calculation of an IC_{50} value for inhibition of ADA activity using the rate of the reaction values from Figure 5.19A.

A.
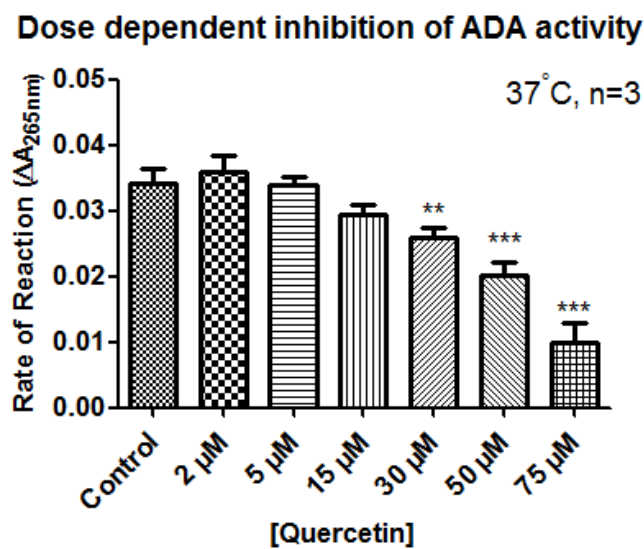
B.
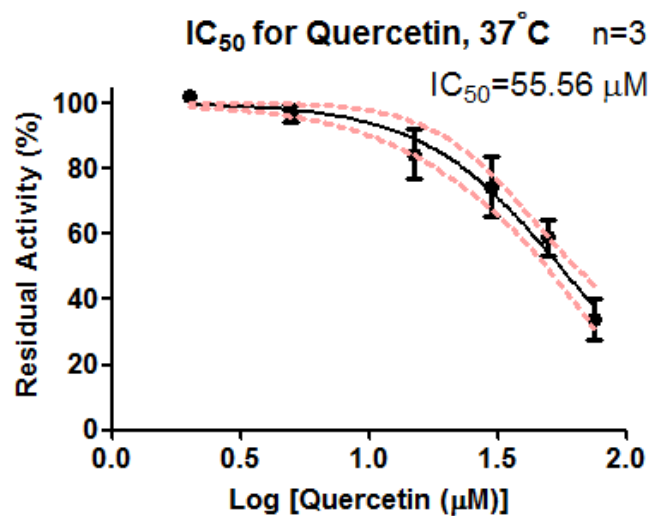
Figure 5.19: Determination of IC_{50} value for quercetin. **A.** Quercetin dose-dependently inhibited ADA activity. **B.** IC_{50} value for quercetin was determined as 55.6 µM. Red-dashed line shows 95% confidence interval.

The strongest inhibitory activity (=most potent inhibitor) was observed with isorhamnetin, and it was followed by quercetin, Q 3'-O-S and Q 3-O-GlcA (Table 5.3). Quercetin, isorhamnetin and Q 3'-O-S showed dose-dependent inhibitory effects. However, Q 3-O-GlcA significantly inhibited ADA activity at 2 µM (p<0.01, n=3), but increasing its concentration did not further alter the residual activity (Figure 5.20). Hence, it was not possible to calculate an IC_{50} value for the Q 3-O-GlcA. Interestingly, the IC_{50} values for isorhamnetin, quercetin and Q 3'-O-S were lower for the ADA activity in HUVEC protein extracts, and the inhibition strength by each flavonol was ordered in parallel with the results obtained for the commercial pure enzyme (Table 5.3).
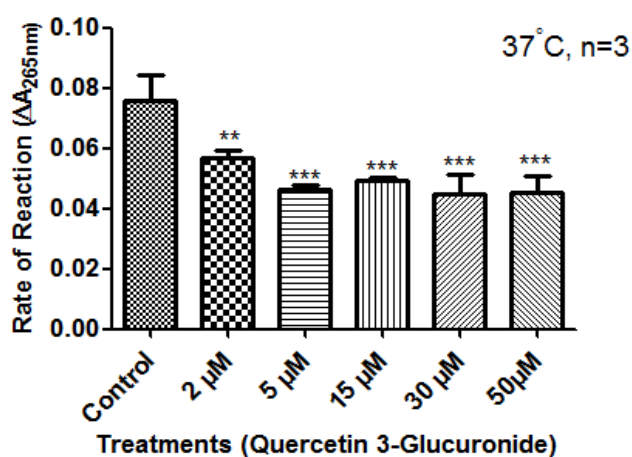
Figure 5.20: Q 3-O-GlcA significantly inhibited ADA activity with concentrtions starting at 2 µM. The strongest inhibition was obtained with 50 µM Q 3-GlcA (37.3% inhibition)

Table 5.3: Effects of quercetin and its metabolites on ADA activity (n=3 minimum for each treatment).

Enzyme	Treatment	Method		Literature
		Pure Human Enzyme IC_{50} (μM)	HUVEC Extract IC_{50} (μM)	
Adenosine Deaminase	Isorhamnetin	48.94	15.67	Intact calf aortic endothelial cells were used to test several flavonoids. IC_{50} for quercetin was 26 μM (Melzig et al., 1995).
	Quercetin	55.56	20.04	
	Quercetin 3'-O-Sulfate	194.6	55.65	
	Quercetin 3-O-Glucuronide	-	Not tested	

5.4.3.2 Xanthine Oxidase

Quercetin, isorhamnetin and Q 3'-O-S were strong inhibitors of the xanthine oxidase activity (Table 5.4). Likewise the ADA inhibition, isorhamnetin was the most potent inhibitor of xanthine oxidase activity (IC_{50}=0.31 μM, n=3) followed by Q 3'-O-S (IC_{50}=0.45 μM, n=3), and quercetin (IC_{50}=3.04 μM, n=3) (Figure 5.21). However, no xanthine oxidase activity was observed when the HUVEC protein extract (30-100 μg protein content) was used in the assay instead of the commercial pure enzyme. This remained the case even when the extracts were de-salted and concentrated using spin columns (Millipore Microcon®) to remove any substances potentially interfering with the assay.

A.
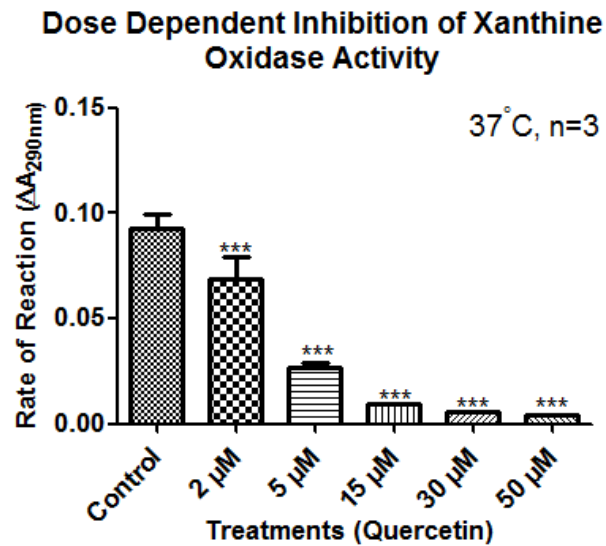
B.
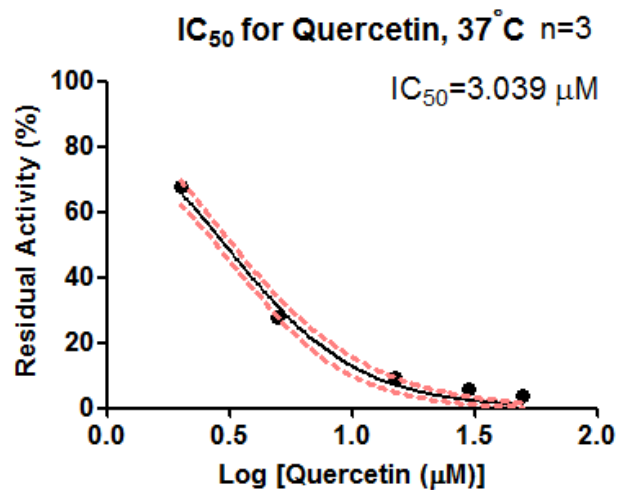
Figure 5.21: Determination of IC_{50} value for inhibition of xanthine oxidase by quercetin. **A.** Quercetin dose-dependently inhibited xanthine oxidase activity. **B.** IC_{50} value for quercetin was determined as 3.04 µM. Red-dashed line shows 95% confidence interval.

Table 5.4: Effects of quercetin and its metabolites on xanthine oxidase activity (n=3 minimum for each treatment).

Enzyme	Treatment	Method		Literature
		Pure Human Enzyme IC$_{50}$ (µM)	HUVEC Extract IC$_{50}$ (µM)	
Xanthine Oxidase	Isorhamnetin	0.31	Enzyme activity could not be detected	Quercetin and its metabolites are strong inhibitors of xanthine oxidase. Day et al. (2000) used xanthine oxidase (from buttermilk).
	Quercetin 3'-O-sulfate	0.45	Enzyme activity could not be detected	
	Quercetin	3.04	Enzyme activity could not be detected	

5.4.3.3 Purine Nucleoside Phosphorylase (PNP)

Inhibitory effects of quercetin, isorhamnetin, Q 3'-O-S, Q 3-O-S, IsoR 3-O-GlcA, rhamnetin, Q 3-O-GlcA and Q 3'-O-GlcA were tested on PNP activity (2 µM - 50 µM) (Table 5.5). Quercetin and Q 3'-O-S were the only flavonols which inhibited the activity of bacterial purine nucleosidase with IC$_{50}$ values of 36.9 µM (Figure 5.22) and 48.3 µM (n=3) respectively. The inhibitory effect of quercetin became significant at 30 µM whereas this value was 15 µM for Q 3'-O-S. Furthermore, the effects of increased phosphate and sulphate ion concentrations on PNP activity were tested. Neither phosphate nor sulphate affected PNP activity or the inhibitory activity of Q 3'-O-S (Figure 5.23).

Quercetin and quercetin 3'-O-S were tested for their inhibitory effects on the PNP activity using HUVEC protein extracts. Interestingly, neither quercetin aglycone nor Q 3'-O-S inhibited PNP activity.

A.
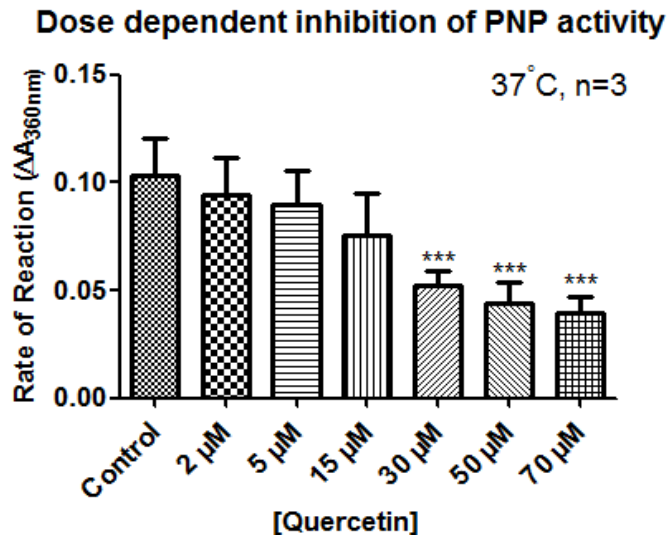
B.
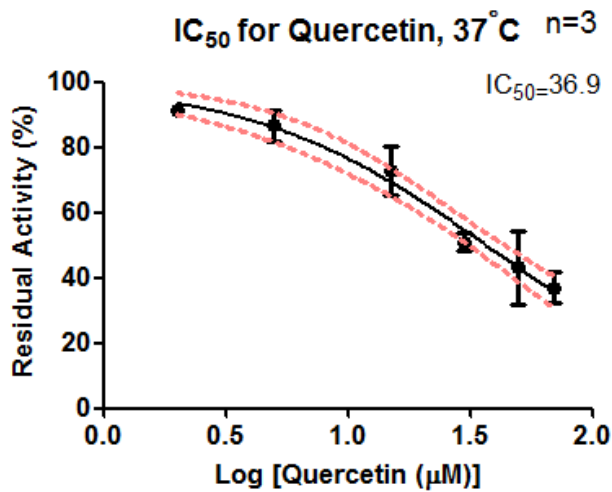
Figure 5.22: Determination of IC_{50} value for quercetin. **A.** Quercetin dose-dependently inhibited PNP activity. **B.** IC_{50} value for quercetin was determined as 36.9 µM. Red-dashed line shows 95% confidence interval.

Table 5.5: Effects of quercetin and its metabolites on PNP activity (n=3 minimum for each treatment).

Enzyme	Treatment	Method		Literature
		Pure Bacterial Enzyme IC_{50} (µM)	HUVEC Extract IC_{50} (µM)	
Purine Nucleoside Phosphorylase	Quercetin	36.9	No inhibition	No literature about flavonoid inhibition. However, the effects of sulfate on the bacterial enzyme was tested since it was shown that sulfate and P_i can compete for the binding site (Kierdaszuk et al., 1997; Modrak-wojcik et al., 2008).
	Quercetin 3'-O-sulfate	48.3 µM	No inhibition	
	Isorhamnetin	No inhibition	Not tested	
	Quercetin 3-O-sulfate	No inhibition	Not tested	
	Isorhamnetin 3-O-Glucuronide	No inhibition	Not tested	
	Rhamnetin	No inhibition	Not tested	
	Quercetin 3'-O-Glucuronide	No inhibition	Not tested	
	Quercetin 3-O-Glucuronide	No inhibition	Not tested	

Figure 5.23: Effects of sulfate **(A.)** and phosphate **(B.)** on PNP activity.

5.4.3.4 CD39/ENTDP1

The activity of a recombinant human CD39 enzyme (rhCD39) was inhibited by Q 3'-O-S (IC_{50}=0.183 µM), quercetin (IC_{50}=0.574 µM), Q 3'-O-GlcA (IC_{50}= 10.1 µM) (Figure 5.24), Q 3-O-GlcA (IC_{50}= 52.5 µM) and IsoR 3-O-GlcA (IC_{50}= 75.2 µM) but not by isorhamnetin, tamarixetin or rhamnetin (Table 5.6). The inhibition became significant at 2 µM ($p<0.001$) with Q 3'-O-S, quercetin and Q 3'-O-GlcA (Figure 5.24) whereas the inhibition became significant at 15 µM with quercetin, IsoR 3-O-GlcA and Q 3-O-GlcA.

Prior to the experiments using intact HUVECs as a source of CD39, different substrate concentrations were tested. As the ATP concentration was increased, the amount of phosphate liberated with the CD39 activity was increased (Figure 5.25). 100 µM ATP was shown to be a suitable substrate concentration. Quercetin, Q 3'-O-S and isorhamnetin were tested for their inhibitory effects on CD39 activity using intact HUVECs. In contrast to the inhibitory effects of quercetin and Q 3'-O-S observed with rhCD39, quercetin and Q 3'-O-S did not inhibit the CD39 activity in the intact HUVECs. Isorhamnetin was also tested to confirm that the flavonols which did not inhibit rhCD39 also do not inhibit CD39 activity in the intact HUVECs.

A.

Dose dependent inhibition of CD39 activity

37°C, n=3

Y-axis: Phoshate (nmol), ranging 0.0 to 1.5
X-axis: Treatments (Quercetin 3'-Glucuronide) — Control, 2 µM, 5 µM, 15 µM, 30 µM, 50 µM, 70 µM (*** above treated bars)
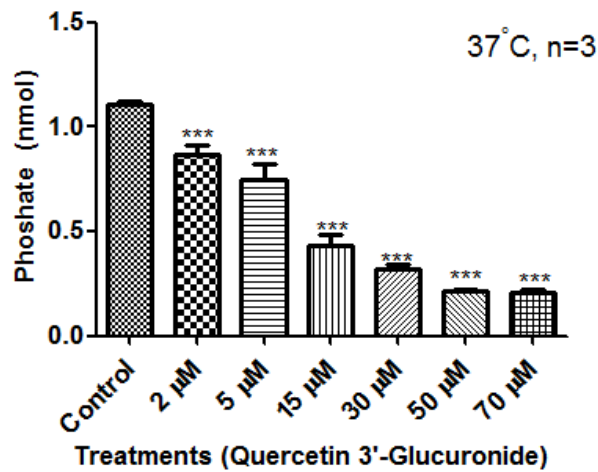
B.

IC$_{50}$ for Quercetin 3'-O-Glucuronide, 37°C n=3

IC$_{50}$= 10.11 µM

Y-axis: Residual Activity (%), 0 to 100
X-axis: Log [Quercetin (µM)], 0.0 to 2.0
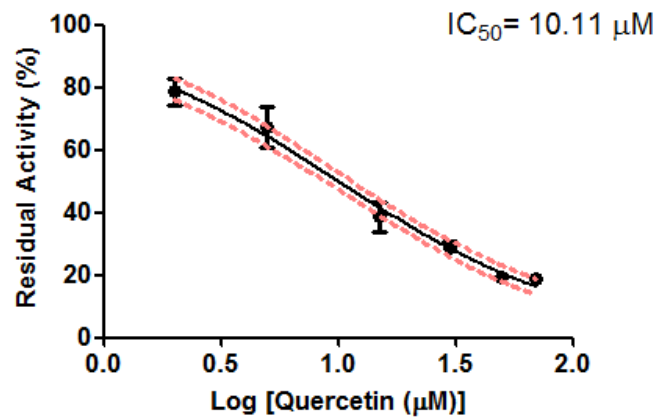
Figure 5.24: Determination of IC$_{50}$ value for Q 3'-O-GlcA. **A.** Q 3'-O-GlcA dose-dependently inhibited rhCD39 activity. **B.** IC$_{50}$ value for Q 3'-O-GlcA was determined as 10.11 µM.

Y-axis: Phophate (nmol), 0.0 to 2.5
X-axis: [ATP] — 5 mM, 10 mM, 25 mM, 50 mM, 100 mM
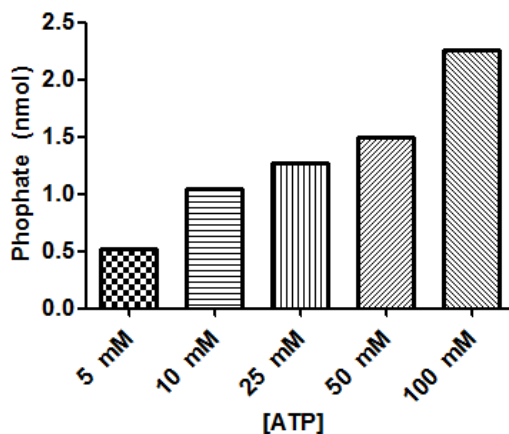
Figure 5.25: Determination of the optimum substrate concentration for the CD39 assay.

Table 5.6: Effects of quercetin and its metabolites on CD39 (n=3 minimum for each treatment).

Enzyme	Treatment	Method		Literature
		Pure Human Enzyme IC_{50} (µM)	Intact HUVECs IC_{50} (µM)	
CD39/ENTPD1	Quercetin 3'-O-sulfate	0.183	No inhibition	Quercetin and resveratrol restored the reduced CD39 activity in HUVECs, in response to thrombin (Kaneider et al., 2004)
	Quercetin	0.574	No inhibition	
	Quercetin 3'-O-Glucuronide	10.1	Not tested	
	Quercetin 3-O-Glucuronide	52.5	Not tested	
	Isorhamnetin 3-O-Glucuronide	71.2	Not tested	
	Isorhamnetin	No inhibition	No inhibition	
	Tamarixetin	No inhibition	Not tested	
	Rhamnetin	No inhibition	Not tested	

5.4.3.5 5'-Nucleotidase/CD73 Activity

rhCD73 activity was inhibited by quercetin ($IC_{50}=1.69$ µM), isorhamnetin ($IC_{50}=$ 8.29 µM) and Q 3'-O-S ($IC_{50}=160$ µM) but not by rutin, Q 3'-O-GlcA, Q 3-O-GlcA or IsoR 3-O-GlcA (Table 5.7). Quercetin (Figure 5.26) and isorhamnetin were strong inhibitors of the CD73 activity where the inhibition became significant at 1 µM ($p<0.01$) and 2 µM ($p<0.001$) respectively whereas Q 3'-O-S was a weak inhibitor where the inhibition became significant at 30 µM ($p<0.01$).

Prior to the experiments where intact HUVECs were used as a source of CD73, different substrate concentrations were tested. As the AMP concentration was increased (5 µM- 200 µM), the amount of phosphate liberated (due to CD73 activity) was increased (Figure 5.27). 50 µM was found to be a suitable substrate concentration to be used in the assays.

CD73 activity in intact HUVECs was weakly inhibited by quercetin (50 µM, 13% inhibition, n=3), but not by isorhamnetin or Q 3'-O-S.

A.
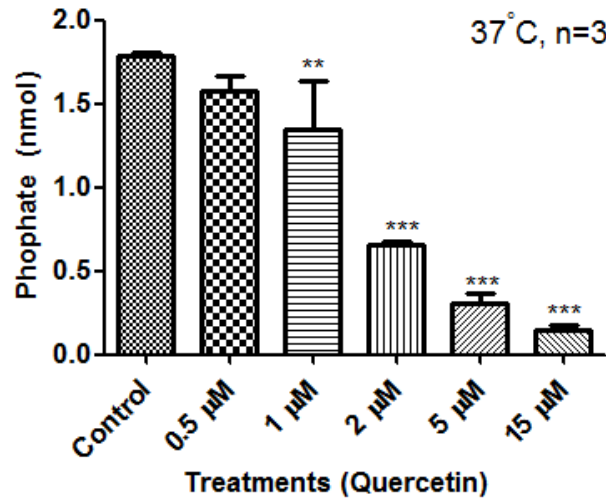
B.
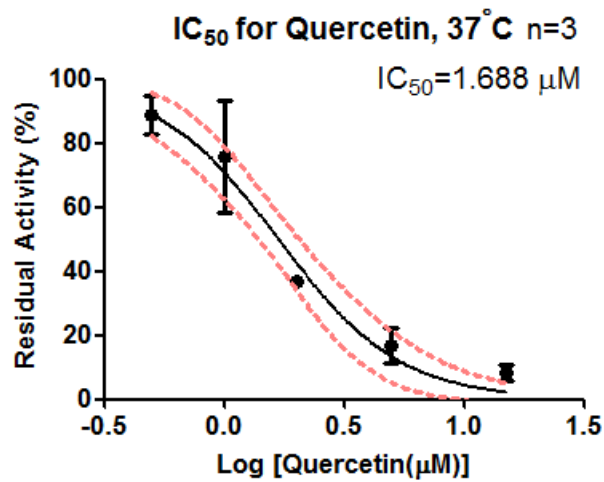
Figure 5.26: Determination of quercetin IC$_{50}$ value for quercetin. **A.** Quercetin dose-dependently inhibited rhCD73activity. **B.** IC$_{50}$ value for quercetin was determined as 1.69 µM.
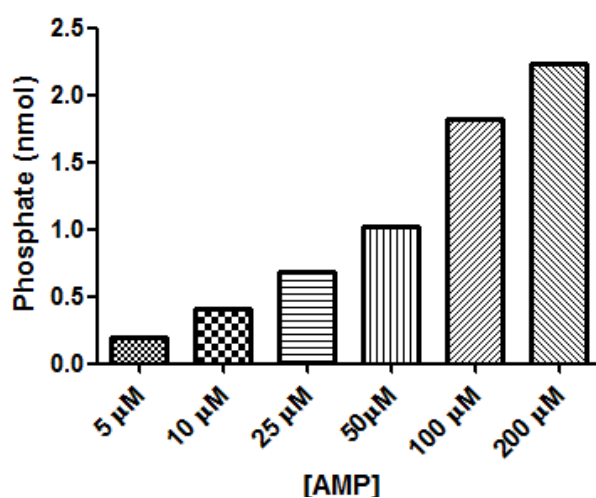
Figure 5.27: Determination of the optimum substrate concentration for the CD73 assay.

Table 5.7: Effects of quercetin and its metabolites on CD73 (n=3 minimum for each treatment).

Enzyme	Treatment	Method		Literature
		Pure Human Enzyme IC_{50} (μM)	Intact HUVECs IC_{50} (μM)	
5'-Nucleotidase/CD73	Quercetin	1.69	13% inhibition with 50 μM quercetin	Quercetin was able to inhibit the ecto-5'-NT/CD73 activity and modulate its expression in human U138MCG glioma cell line (Braganhol et al., 2007). Flavonids inhibits 5'-nucleotisase activity. Pure enzyme cell-free assay. 5'-NT from *Crotalus atrox* venom (Kavutcu & Melzig, 1999). Quercetin IC_{50}= 1.4 μM, no inhibition with rutin.
	Isorhamnetin	8.29	No inhibition	
	Quercetin 3'-O-sulfate	160	No inhibition	
	Quercetin 3-O-Glucuronide	No inhibition	Not tested	
	Isorhamnetin 3-O-Glucuronide	No inhibition	Not tested	
	Quercetin 3'-O-Glucuronide	No inhibition	Not tested	
	Rutin	No inhibition	Not tested	

NMR spectroscopy was also used to check the activity of the enzyme by measuring the substrate AMP and the product adenosine levels directly, rather than measuring free-phosphate levels. Figure 5.28 shows that the HUVECs converted AMP to adenosine indicating that the assay was working, and that topical quercetin (2-15 µM) additions did not have an effect on CD73 activity.
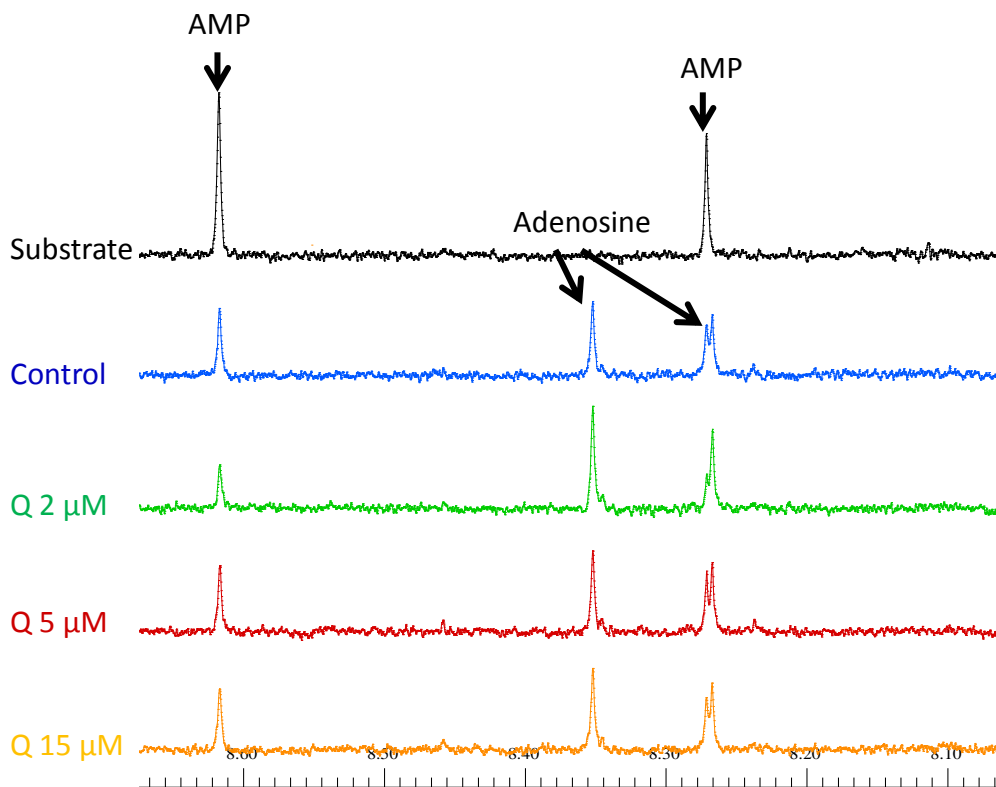
Figure 5.28: NMR analysis of intact HUVEC CD73 activity experimental mixture. Presence of signals belonging to adenosine showed that CD73 was actively converting AMP to adenosine.

5.5 Discussion

In the previous chapter, it was shown that quercetin treatments altered HUVEC energy metabolism, and the changes observed in ATP, ADP, AMP, adenosine and xanthine concentrations were most likely to be mediated through the effects of quercetin on the enzymes which are involved in the purine metabolism. Therefore, the interactions between quercetin and quercetin metabolites and the major enzymes involved in purine metabolism were investigated.

The main findings presented here revealed that HUVECs metabolize quercetin to Q 3'-O-S and methylquercetin. Also, dimers of quercetin and methylquercetin were produced in the culture medium. The effects of quercetin aglycone, isorhamnetin and Q 3'-O-S together with other quercetin and methylquercetin conjugates were tested on the activities of the 5 major enzymes involved in HUVEC energy metabolism. Quercetin aglycone was observed to be a strong inhibitor when its effects on recombinant enzymes were tested whereas its conjugates had different effects on the activities of the enzymes depending on the position of the conjugation and nature of the conjugated chemical group. However, neither quercetin nor its metabolites inhibited PNP and CD39 activities in HUVEC extracts or intact HUVECs respectively, and quercetin was only a weak inhibitor of CD73 activity in intact HUVECs.

There are numerous published studies describing quercetin metabolism in cellular systems, but hardly anything for HUVECs. Awad and co-workers identified glutathionyl quercetin in culture medium which also indicated the formation of intermediate quercetin quinone/quinone methide metabolites after treating B16F-10 melanoma cells with 10-100 µM quercetin (Awad et al., 2002). Spencer and co-workers worked with dermal fibroblasts in order to explore the intracellular metabolism of quercetin. Similarly, they reported the presence of quercetin aglycone, a 2'-glutathionyl quercetin adduct and an unidentified product (which they believed to be quercetin quinone/quinone methide) after treating the cells with quercetin (Spencer et al., 2003). In another study, Murota and co-workers assessed the efficiency of absorption and metabolic conversion of quercetin in human intestinal cell line Caco-2 (Murota and Terao, 2003). They found quercetin, isorhamnetin and their conjugated forms present inside the cells. However they did not identify the conjugated forms of quercetin and isorhamnetin. In the present

study, quercetin aglycone and methylquercetins were identified inside the cells whereas quercetin aglycone, Q 3'-O-S, methylquercetins and also putative quercetin and methylquercetin dimers were identified in culture medium after treating the cells with 10 µM quercetin. Formation of quercetin dimers after spiking the culture medium with quercetin aglycone alone indicated that it was not stable in the culture medium. Pham and co-workers isolated a quercetin dimer formed after incubating quercetin in complete culture medium (DMEM), and they identified its molecular structure using ^{1}H NMR and LC-MS (Pham et al., 2012). However, the present study showed that two different quercetin dimers were formed in complete culture medium (EGM-2). Also, after treating the HUVECs with quercetin, there was only one dimer observed in the culture medium most certainly with a different molecular structure since all these dimers had the same molecular weights, but different retention times. Pham and co-workers assessed the effects of the quercetin dimer they had identified on MDA-MB-231 (human breast adenocarcinoma) cells by treating the cells with the culture medium which was incubated with quercetin for 24 h prior to the treatment to allow the quercetin dimer formation. That treatment (72 h) did not have an effect on cell death, but fresh quercetin aglycone treatment significantly increased cell death, and they concluded that the quercetin aglycone was responsible for the observed cell death. However, the appearance of structurally different quercetin dimers in the present study in culture media only in the presence of cells indicates that a quercetin dimer might be responsible for the increased cell death observed in the previously reported studies with MDA-MB-231 cells. In the present study, it was aimed to isolate, structurally define and chemically synthesize the quercetin and methylquercetin dimers produced after the quercetin treatments and test their effects on the enzymes. However, it was not possible to obtain enough material for the structural analysis with [1]NMR due to the low quantities produced by cultured cells.

In this study, single HUVEC volume was estimated using a flow cytometric method in order to calculate intracellular flavonol concentrations. This was important because flavonol concentrations in the physiological range could be used while testing their effects on the purine metabolism enzymes. According to the calculations where single HUVEC volume was estimated using the flow cytometric method, intracellular quercetin concentrations after 2 h quercetin treatment (10

µM) was calculated as 93.5 µM. However, in this method, beads with known sizes (5 µm, 10 µm and 15 µm) were used for calibration which is not directly comparable with the live cells. Hence, it is important to understand that the measured HUVEC volume provided just an estimate. The estimates of single HUVEC volumes reported previously (two different studies) were also used as references to calculate the intracellular quercetin concentration. Intracellular quercetin concentrations after 2 h quercetin treatment were calculated as 354 µM and 1330 µM using AFM and SEM methods to estimate cell volumes, respectively (Hillebrand et al., 2006, Leunig et al., 1996). All three values reflected enough intracellular quercetin concentrations to inhibit intracellular ADA, 5'-NT and xanthine oxidase activities. The estimates of cell volume reported here are the highest, and consequently the intracellular concentrations the lowest to date.

Energy metabolites such as ATP, ADP and adenosine play important roles in cellular signalling cascades. Several polyphenols have been shown to have inhibitory effects on the individual enzymes involved in energy metabolism (Kaneider et al., 2004, Wu et al., 2010). The present study is integrated in investigating all major purine metabolism enzymes with quercetin aglycone and its metabolites.

CD39 is the first enzyme in the overall pathway where ATP is converted by a series of enzyme-catalysed reactions into uric acid (Figure 5.29). CD39 hydrolyses ATP and ADP into AMP. Thrombin was previously shown to reduce CD39 activity leading to increased ATP and ADP levels (Kaneider et al., 2002). Kaneider and co-workers assessed the effects of quercetin and resveratrol on CD39 activity in thrombin-activated HUVECs (Kaneider et al., 2004). They treated HUVECs with thrombin (0.1 mU/ml) and quercetin or resveratrol (1 pM to 100 µM) for 45 min which was followed by the addition of 100 µM ATP or ADP (20 min) into the environment that allowed measurement of the CD39 activity. They reported that both quercetin and resveratrol pre-treatments restored the thrombin-induced decreased rate of ATP and ADP hydrolysis dose-dependently which could be measured as the elevations in AMP and adenosine levels. In the present study, rhCD39 activity was strongly inhibited by Q 3'-O-S, quercetin, Q 3'-O-GlcA, Q 3-O-GlcA and IsoR 3-O-GlcA, whereas isorhamnetin, tamarixetin and rhamnetin did not inhibit CD39 activity. According to these results, the inhibitory activity of

quercerin was affected by the conjugation of a single methyl group regardless the conjugation site. Interestingly, isorhamnetin with a conjugated glucuronide group at 3-position still had the inhibitory effect but with a higher IC_{50} value compared to the other flavonols which inhibited CD39 activity. On the other hand, quercetin, Q 3'-O-S and isorhamnetin were tested for their effects on CD39 activity in the intact HUVECs, and they did not have an effect on the CD39 enzymatic activity. In chapter 4, decreased ATP (70.7% of control, $p<0.01$) and ADP (71.6%% of control, $p<0.05$) and elevated intracellular AMP (196.10% of control, $p<0.01$) and adenosine (162 % of control, $p<0.05$) levels were observed after quercetin treatments (20 h). Therefore, the observation of no inhibitory effects of quercetin and its conjugates on CD39 activity when the intact HUVECs were used in the assays is in line with the results observed in metabolomics analysis. The decreased ATP and ADP levels after quercetin (20 h) treatments were most likely due to the increased expression of CD39 protein by HUVECs.
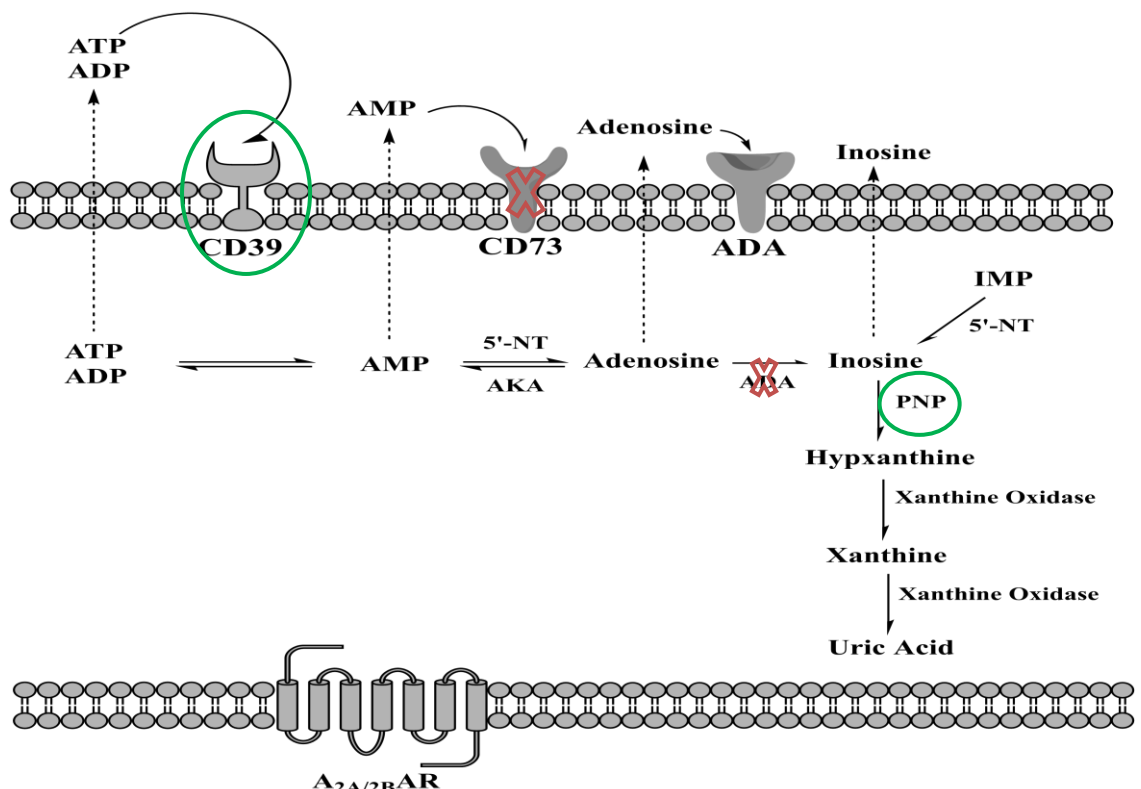
Figure 5.29: Effects of quertin and its conjugates on the enzymes involved in purine nucleotide/nucleoside metabolism. The red crosses shows the enzymes inhibited by quercetin and its particular conjugates and the green circles shows the enzymes which were not affected in this study.

rhCD73 activity was inhibited strongly by quercetin and isorhamnetin. Q 3'-O-S was a weak inhibitor of rhCD73 activity, whereas Q 3-O-GlcA, Q 3'-O-GlcA, IsoR 3-O-GlcA and rutin did not have an effect on rhCD73 activity. Therefore, it was observed that the hydroxyl group at the 3-position is likely to be important for the inhibitory activity, and Q 3'-O-GlcA did not have an effect most likely due to the relatively large size of the glucuronic acid group at the 3'-position. On the other hand, quercetin was a weak inhibitor of CD73 activity in the intact HUVECs. The other flavonols tested did not exert an effect on CD73 activity in the intact HUVECs. In the literature, there are two reports regarding the effects of flavonoids on CD73 activity. Kavutcu and Melzig assessed the inhibitory activities of several flavonoids on purified 5'-NT obtained from *Crotalus atrox* venom. They revealed that quercetin and myricetin strongly inhibited 5'-NT activity, and that several other flavonoids were also inhibitors but with weaker inhibitory activities depending on the hydroxylation patterns. Rutin was one of the flavonoids which did not inhibit 5'-NT activity (Kavutcu and Melzig, 1999). Therefore, the strong inhibition with quercetin and lack of inhibitory activity with rutin is in parallel with the results obtained in the present study where rhCD73 was used. On the other hand, Braganhol and co-workers assessed the effects of quercetin on CD73 activity in U138MG human glioma cell line (Braganhol et al., 2007). They reported that quercetin inhibited AMP hydrolysis by the cells with an IC_{50} value of 45.3 µM. The assay involved incubating the cells with the substrate AMP and different concentrations of quercetin (0.1 to 500 µM). They also treated the cells with quercetin (10, 30 and 100 µM) for 24 h, 48 h or 72 h, and then assessed CD73 activity in the cells. After 72 h quercetin treatment, they observed a reduction in CD73 activity, which might be due to decreased CD73 protein expression by the cells since they observed decreased CD73 mRNA expression after 24 h quercetin treatment. Therefore, the strong inhibitory effects of quercetin on CD73 activity in the U138MG human glioma cell line was in contrast with the minor inhibitory activity of quercetin on CD73 activity in HUVECs reported here. The weak inhibition of CD73 by quercetin is likely to explain the time-dependent increase in AMP levels observed after quercetin treatment in the metabolomics study (Table 4.6). Nevertheless, a possible increase in CD39 protein expression by HUVECs, the minor inhibition of CD73 with quercetin or both might be responsible for the increase observed in AMP levels in HUVECs after quercetin treatments.

Isorhamnetin, quercetin and Q 3'-O-S inhibited both recombinant human ADA and ADA activity in HUVEC extracts. Q 3-O-GlcA was tested with only recombinant human ADA, and it inhibited ADA activity. Several flavonols including quercetin, myricetin, kaempferol, morin and rutin were shown to inhibit ADA activity in calf aortic endothelial cells (Melzig, 1996). Therefore, the inhibitory activity of quercetin observed in the present study is consistent with the previously reported study. Furthermore, the demonstration of inhibition of ADA activity by isorhamnetin and Q 3'-O-S is important because it was also shown that quercetin aglycone was metabolized by HUVECs yielding quercetin aglycone and methylquercetin inside the HUVECs and quercetin, methylquercetin and Q 3'-O-S in the culture medium after 2 h quercetin treatment. In parallel, increases in intra- and extracellular adenosine (112.5% and 286.2% of control levels, respectively) were observed which were most likely due to the inhibitory activities of the afore mentioned flavonols. Melzig (1996) stated that ADA activity is present only inside the cells. However, a more recent study by Eltzschic and co-workers hypothesized that under inflammatory conditions, ADA is synthesized inside and then released from the endothelial cells, and then binds to the surface receptor CD26 which converts adenosine to inosine (Eltzschig et al., 2006). They inhibited the interaction of ADA with CD26 using the HIV-1 envelope glycoprotein gp120 and showed that this led significant reductions in extracellular ADA activity in human microvascular endothelial cells (HMEC-1s), thus supporting their hypothesis.

The next enzyme on the pathway was PNP. The pure bacterial PNP activity was inhibited by quercetin and Q 3'-O-S. Interestingly, the inhibitory activity was lost in the other conjugates tested. In the literature, it was reported that sulfate competes with P_i for the enzyme active site (Kierdaszuk et al., 1997, Modrak-Wójcik et al., 2008). Therefore, it was hypothesized that the inhibitory effect of Q 3'-O-S was due the conjugated sulfate group. Nevertheless, neither Q 3-O-S nor sulfate alone inhibited the PNP activity and also increased P_i did not diminish the inhibitory effect of Q 3'-O-S indicating that the inhibitory activity of Q 3'-O-S was not due to the conjugated sulphate group. On the other hand, none of the tested flavonols inhibited PNP activity in HUVEC extracts. In the metabolomics study (Chapter 4), it was observed that there was a time-dependent elevation observed in both intra- and extracellular inosine levels after quercetin treatment. Since the activity of PNP was not affected, it can be concluded that the increased inosine levels were most

certainly due to a decrease in the levels of PNP protein after quercetin treatments which might have resulted in decreased inosine conversion to hypoxanthine.

The final enzyme in the pathway was xanthine oxidase. Isorhamnetin, quercetin and Q 3'-O-S were strong inhibitors of the xanthine oxidase from bovine milk. The inhibitory activities of the dietary polyphenols on this particular enzyme were previously reported (Day et al., 2000, Pauff and Hille, 2009, Wu et al., 2010). For example, Day and co-workers tested the effects of quercetin and its glucuronide conjugates on xanthine oxidase activity (from butter milk) (Day et al., 2000). They had observed that quercetin, isorhamnetin, Q 4'-O-GlucA, and Q 3'-O-GlcA inhibited xanthine oxidase activity. In the metabolomics study, intracellular xanthine levels were not altered after treating HUVECs with quercetin. Therefore, this indicated that even though strong inhibition of the enzyme was observed in vitro with quercetin and its conjugates, xanthine oxidase activity in HUVECs might not be affected by quercetin treatments. This could not be tested since the xanthine oxidase activity could not be detected with the assay used in the present study.

A recent study which used a strepozotocin-induced diabetic rat model to investigate the effects of red wine and grape juice consumption on activities of CD39, 5'-NT and adenosine deaminase reported that the diabetic rats had higher CD39, 5'-NT and adenosine deaminase activities (Schmatz et al., 2013). They showed that administration of red wine and grape juice (4.28 ml/kg body weight) to the diabetic rats for 45 days further increased ectonucleotidases activities and inhibited ADA activity. The in vitro effects of resveratrol which is one of the polyphenolic constituents of the red wine and grape juice on these enzyme were consistent with the in vivo study. They observed an increase in ectonucleotidases activities and inhibition in ADA activity by resveratrol in the platelets isolated from the diabetic rats. However, when they tested the effects of another constituent of the red wine and grape juice, quercetin, on the CD39, 5'-NT and adenosine deaminase in platelets isolated from the diabetic rats, they showed that quercetin (5-200 µM) significantly inhibited ATP, ADP and AMP hydrolysis and ADA activity. This is partially consistent with the notion in the present study that quercetin modulates purine metabolism enzymes leading to changes in the endothelial cell energy metabolism.

According to the results obtained in Chapter 4 (metabolomics study), it was hypothesized that the quercetin-induced changes in the HUVEC metabolism were due to interactions between quercetin and the enzymes involved in energy metabolism. The present study which involved integrated investigation of all major purine metabolism enzymes with quercetin aglycone and its metabolites assisted to test this hypothesis. The most significant changes observed after quercetin treatments were the reductions in ATP and ADP concentrations and elevations in AMP, adenosine and inosine concentrations (Table 4.6). Although quercetin and its individual conjugates were potent inhibitors of CD39 and PNP activities in the assays where commercial pure recombinant enzymes were used, the assays performed using intact HUVECs or HUVEC protein extracts showed that neither quercetin nor its conjugates inhibited CD39 and PNP activities in cellular environment. As the CD39 activity was not inhibited by quercetin or its metabolites, a possible elevation in the expression of CD39 protein by HUVECs together with the minor inhibition of CD73 after quercetin treatment was likely to explain the increase in AMP levels. At the same time, quercetin was shown to be a potent inhibitor of ADA activity which is consistent with the observation of elevations in adenosine concentrations after quercetin treatments in the metabolomics study. Nevertheless, PNP activity was not inhibited by quercetin or its conjugates, and inosine was being actively metabolized into hypoxanthine. Therefore, elevated inosine concentrations observed after quercetin treatments in the metabolomics study were most likely due to decreased activity of PNP (converts inosine to hypoxanthine) inside the cells possibly due to the decreased expression of PNP protein after quercetin treatments. Furthermore, the estimated intracellular quercetin concentrations after 10 µM quercetin treatments also indicated that the IC_{50} values obtained for the enzymes tested in the present study were achievable in the cellular environment supporting the notion that increased adenosine and AMP concentrations were due to the inhibition of adenosine deaminase by quercetin and its metabolite Q 3'-O-S and the partial inhibition of CD73 by quercetin, respectively. However, it is necessary to investigate the effects of quercetin and its metabolites on the expression levels of CD39 protein to explain the reductions in ATP and ADP concentrations and the levels of CD73 proteins in order to explain the elevation in inosine concentrations.

Hence, the enzyme activity assays performed in the present study showed that quercetin treatments modulate both endo and ecto-enzyme activities in HUVECS playing an important role in the alterations observed in endogenous metabolites involved in pro- or anti-inflammatory processes.

CHAPTER 6: General Discussion

6.1 Summary of Main Findings

The overall aim of the research project described in this thesis was to investigate the deleterious effects of hyperglycaemia and inflammatory cytokines on vascular endothelial cells, with a particular focus on elucidating underlying mechanisms. The effects of hyperglycaemic conditions and inflammatory cytokines on established physiological markers of endothelial function and the ability of selected polyphenols to prevent these negative changes were assessed.

The main findings were:

- The inflammatory cytokines TNF-α and IL1-β were shown to induce significant changes in CAM surface expression, and the different polyphenols induced different responses, pro- and anti-inflammatory, depending on concentration and period of exposure.

- The protocol developed for metabolomics study facilitated rapid and effective freezing of cellular metabolism and extraction of metabolites. The extracted metabolites were analysed using ^{1}H NMR, which produced non-biased and reproducible results when the effects of several known metabolic effectors on HUVECs were tested in the HUVEC model.

- The prevention of deleterious increases in lactate, reductions in the concentrations of pro-inflammatory metabolites ATP and ADP and, in parallel, increased concentrations of anti-inflammatory metabolites adenosine and inosine were observed after quercetin treatments, and these alterations were associated with anti-inflammatory properties of quercetin that protect vascular endothelial cells against inflammation-induced damage.

- Subsequently, the investigation of purine metabolism assisted to explain the anti-inflammatory alterations observed in HUVEC energy metabolism after quercetin treatments. The inhibition of ADA and CD73 activities with

physiological cellular concentrations of quercetin was consistent with the elevations observed in adenosine and AMP levels.

6.2 Relevance and Importance of the Findings

Before the project started, there have been no studies reported in the literature with regards to the metabolite profile of endothelial cells. Here, it was shown for the first time that non-targeted analysis of endothelial cell metabolite profile can be achieved using ^{1}H NMR. This approach was applied successfully to reveal the alterations in endothelial cell primary metabolism (e.g Krebs cycle, purine metabolism) after malonate, high-glucose, TNF-α and polyphenol treatments showing that the approach is favourable to be used in future studies by scientists to test various biological or chemical effectors on endothelial cell metabolome. For example, consumption of cruciferous vegetables have been associated with the reduced risk of cancer and CVD (Zhang et al., 2011, Bosetti et al., 2012), and a recent intervention study by Armah and co-workers has shown that consumption of a diet rich in high-glucoraphanin broccoli altered plasma metabolite profiles of the subjects providing more evidence that the consumption of cruciferous vegetables is associated with reduced risk of cancer (Armah et al., 2013). Glucosinolates are another type of plant secondary metabolites, and glucoraphanin is a glucosinolate which accumulates in vegetables such as broccoli, kale and calebrese (Traka et al., 2013). The interesting point is that the alterations observed after high-glucoraphanin diet were suggested to be the effect of glucoraphanin on mitochondrial dysfunction via the regulation of fatty acid *β* oxidation (reduced acylcarnitines), and cataplerotic and anaplerotic reactions (altered amino acid profiles) affecting Krebs cycle. Consequently, the effects of glucoraphanin may be explored in HUVEC metabolism using the method developed in the present project and obtaining supplementary data for Krebs cycle metabolites using LC-MS in order to elucidate the mechanism of the glucoraphanin action at cellular levels by confirming its potential effects on mitochondrial activity.

6.2.1 Quercetin and Its Metabolites Altered HUVEC Energy Metabolism

6.2.1.1 Reduction in Lactate Production is Promising in Several Different Aspects

The specific tested markers of vascular endothelial cell function were not significantly affected after high-glucose treatments. However, the hyperglycaemic conditions experienced during diabetes are likely to induce metabolic disturbances. In this project, the effects of high-glucose conditions on endothelial cell metabolome were explored for the first time. Furthermore, quercetin was shown to prevent some of the alterations. The prevention of the increase in lactate concentrations by quercetin was not only associated with improved endothelial cell function, but it is also a remarkable finding for proposing imminent research studies related to cancer biology. Tumour cells were shown to consume relatively higher amounts of glucose and accumulate lactate via glycolysis even in the presence of oxygen (Warburg Effect) (Hirschhaeuser et al., 2011). Lactate induces metastasis through stimulation of tumour-associated fibroblasts to secrete hyaluronan (Stern et al., 2002). Moreover, it induces cell migration and VEGF production which is fundamental for angiogenesis process to produce new blood vessels supplying the tumour with enough oxygen and nutrient to allow proliferation of tumour cells (Goetze et al., 2011, Beckert et al., 2006). Consequently, lactate concentrations in solid tumours can be used to predict metastasis and correlate with survival of patients (Hirschhaeuser et al., 2011, Goetze et al., 2011). Therefore, prevention of the elevation in lactate concentrations by quercetin is likely to be a promising area for future cancer research, and should include effects to elucidate the mechanism at the molecular level.

Another example for the potential use of quercetin would be in pharmaceutical industry rather than being a dietary polyphenol which is again related to its effects on energy metabolism in cells. Niklas and co-workers have been trying to generate an efficient host to produce α_1-antitrypsin in a cost effective way in recent years (Niklas et al., 2012a, Niklas et al., 2012b, Niklas et al., 2013, Niklas et al., 2011). α_1-Antitrypsin is a glycoprotein which is necessary for protection against neutrophil elastase where inherited low serum levels in patients can result in lung emphysema and liver dysfunction leading to death (Petrache et al., 2009, Kelly et

al., 2010, Niklas et al., 2013). The intravenous perfusion of pure α_1-antitrypsin to elevate its serum levels was shown to diminish the rate of mortality in patients (The Alpha-1-Antitrypsin Deficiency Registry Study Group, 1998). The fact that only human plasma-derived products are licenced by US-FDA for augmentation therapy regardless of the attempts to produce recombinant human α_1-proteinase inhibitors in several different host systems has driven Niklas and co-workers to optimize AGE1.HN cell metabolism for α_1-antitrypsin production. AGE1.HN cells are continuous human brain cells. Continuous cell lines play an important role in the pharmaceutical industry, however, they have been known to have disadvantages in that their primary metabolism shares similarities with cancer cells (Irani et al., 1999). For example, the energy demands in continuous cells are similarly supplied mainly via aerobic glycolysis which leads to elevated lactate production (Xu et al., 2005). Consequently, lactate lowers the pH of the extracellular medium causing growth inhibition (Ozturk et al., 1992). Beside the inefficient use of glucose that yields much lower energy via glycolysis (2 mol of ATP versus 36 mol ATP), the generation of ammonia during the compensation of cellular energy demands via anaplerotic reactions (glutuminolysis) that feeds the Krebs cycle represents another drawback. Ammonia has been shown to inhibit cellular growth and induce cell death (Newland et al., 1990), and lower product quality by affecting protein glycosylation (Yang and Butler, 2000). Irani and co-workers showed that continuous mammalian cell metabolism can be improved by transfecting BHK-21A (Syrian baby hamster kidney) cells line with a plasmid containing the cDNA of pyruvate carboxylase (converts pyruvate to oxaloacetate) which increased glucose flux into Krebs cycle. As a result, the consumption of glucose and glutamine for energy production was reduced together with the reduction in lactate concentrations which improved cellular growth. Therefore, this metabolomic engineering study managed to manipulate cellular metabolism, improving the use of energy source and reducing the generation of unfavourable by-products by the cells, and overall demonstrated a promising step for reduced production costs. Similarly, Niklas and co-workers showed that increased pyruvate supplementation to AGE1.HN cells led to elevated lactate concentrations (Niklas et al., 2012b). Consequently, they showed that both reducing the glucose concentrations and ceasing pyruvate supplementation improved cell viability and elevated α_1-antrypsin production by the cells. Therefore their findings also

indicated a weakness in the connection of pyruvate flux into the Krebs cycle. Furthermore, in another study, they showed that supplementing cell culture media with quercetin reduced lactate production by the cells, improved AGE1.HN longevity and increased α_1-antrypsin yield. They suggested that quercetin managed to alter the metabolic phenotype of the cells by channelling pyruvate flux into mitochondria and hence improving Krebs cycle. Therefore, when the afore mentioned mechanisms and effects of quercetin on the manipulation of cellular energy metabolism both in Niklas et al. (2012) and in the present study (reduced pyruvate and lactate concentrations) are taken into account, quercetin has been shown to be an exogenous effector that may improve the cellular metabolic phenotype, specifically by enhancing biopharmaceutical production by the host mammalian cells without the need of metabolic engineering.

Consequently, the fact that quercetin increases the connection between glycolysis and the Krebs cycle made it possible to consider a therapy that will involve quercetin supplementation of pyruvate carboxylase (PC) deficiency patients aiming to minimize detrimental effects of lactic acidosis and related biochemical disturbances. PC replenishes the Krebs cycle by converting pyruvate to oxaloacetate (Figure 3.15). PC deficiency is a rare (1:250,000 live births) autosomal recessive disease, and classified into three forms which are the infantile form (Type A, North American form), neonatal form (Type B, French Form) and benign form (Type C, Benign form) (Wang et al., 2008). PC actively contributes to intermediary metabolism by playing important roles in gluconeogenesis, glycogen synthesis, lipogenesis, glycerogenesis, the synthesis of amino acids and neurotransmitters, and glucose-dependent insulin secretion, and therefore its deficiency may disrupt metabolism in various organs especially where relatively high Krebs cycle activity (oxaloacetate flow) is necessary (e.g. liver and brain) (Wang et al., 2008, Marin-Valencia et al., 2010). PC deficiency manifests itself with the presence of elevated serum lactate concentrations due to increased pyruvate concentrations leading to lactic acidosis (> 5 mmol/L lactic acid). Ahmed and co-workers applied a treatment involving high doses of aspartate and citrate supplementation to a patient with the Type B form of PC deficiency (severe lactic acidosis and ketosis, low aspartate and glutamate, elevated citrulline and proline, and mild hyperammonemia). They showed that feeding anaplerotic reactions to compensate the reductions in oxaloacetate levels

was successful in terms of controlling biochemical disturbances. Nevertheless, the treatment did not affect the neurological complications observed in the patient. Furthermore, Marin-Valencia and co-workers summarised the important therapeutic strategies used so far and concluded that the future therapeutic applications should attempt to activate Krebs cycle using anaplerotic substrates. In summary, there is good evidence showing that quercetin activates the Krebs cycle by directing pyruvate flux towards the Krebs cycle although the exact mechanism has not been elucidated yet. Therefore, it can be hypothesized that quercetin treatment will improve biochemical profiles of patients suffering from pyruvate carboxylase deficiency because of its ability to direct excess pyruvate to the Krebs cycle.

6.2.1.2 Quercetin and Its Metabolites Altered Purine Metabolism by Directly Interacting with the Enzymes Involved In Purine Metabolism

The other remarkable discovery in this project was the ability of quercetin to alter purine metabolism. Both the prevention of increases in lactate concentrations during inflammatory conditions and the alteration in energy metabolites might be due to different properties of quercetin and its metabolites (e.g. inhibition of particular enzymes, alteration of gene expression and effect on signalling pathways). Since several polyphenols are known to interact with proteins (Nozaki et al., 2009, Rawel et al., 2005), and several polyphenols have been shown to inhibit some of the enzymes involved in purine metabolism, the hypothesis that the polyphenols altered energy metabolite concentrations in HUVECs by directly affecting activities of the enzymes (e.g. inhibition of enzyme) involved in purine metabolism was investigated in more details under in vitro conditions. The work presented here is the most comprehensive study reported to date and includes testing the effects of both quercetin and its metabolites on the activities of all the 5 major enzymes involved in purine metabolism so far.

Polyphenol classes differ in structure, and this difference influences the effects of different polyphenols on the purine metabolism enzymes. For example, Schmatz and co-workers showed that quercetin was a potent inhibitor of the hydrolysis of ATP and ADP in platelets from diabetic rats (Schmatz et al., 2013) whereas

quercetin did not affect the hydrolysis of ATP and caused only minor inhibition of ADP in HUVECs. Therefore, this project broadened the literature indicating that more research is needed to elucidate the polyphenol mechanism of action on CD39 enzyme, and it should be noted that the effects of quercetin on the purine metabolism enzymes in different cell types may differ.

6.2.2 HUVECs Metabolized Quercetin Producing Methylated and Sulfated Conjugates

Polyphenols have been shown to be metabolized by a limited number of cell types. The majority of reported studies were with intestinal, colon or kidney cells, and there is no information reported in the literature regarding quercetin metabolism in HUVECs. In this project, quercetin was shown to be taken up and rapidly metabolized by HUVECs. The identified metabolites were then tested for their effects on purine metabolism enzymes to observe whether quercetin or its metabolites were responsible for the alteration observed. The observation of variable effects of quercetin metabolites depending on position and nature of the conjugated group indicated that these metabolites may have specific biological actions. Therefore, it is now logical to suggest that the polyphenol uptake and metabolism should always be investigated as part of cell model-based studies.

6.3 The Use of Venous Endothelial Cells Might be a Limitation to the Study

Atherosclerosis is the disease of arteries (Berliner et al., 1995). However, in this project, venous endothelial cells were used. This may account as a limitation to the study because differences were observed between the two cell types. Apart from the obvious difference that arteries manage oxygenated blood flow whereas veins manage deoxyganeted blood flow, there were several other differences observed between arterial and venous endothelial cells. Deng and co-workers compared both basal and oxLDL-stimulated (atherogenic stimuli) gene expression profiles of human saphenous vein endothelial cells (SVECs) and coronary artery endothelial cells (CAECs) (Deng et al., 2006). Interestingly, the basal gene expression profiles of the two cell types differed significantly and 1129 genes were

differently expressed between them. They revealed that the venous arterial cells over-expressed genes involved in protection against endothelial dysfunction (which is a fundamental process in the initiation of atherosclerosis) compared to coronary artery cells. Consequently, they showed that oxLDL stimulation of the cells increased the expression of the genes involved in cell proliferation and apoptosis in CAECs, whereas these genes were not affected in SVECs after oxLDL stimulation. Therefore, the atheroprotective gene expression patterns in vein endothelial cells might be the reason explaining why high-glucose did not affect endothelial cell proliferation and cell adhesion molecule expression in this project.

6.4 Future Work

One of the major findings of this project was that quercetin treatments modified purine metabolism (ATP, ADP, adenosine and inosine concentrations). This observation was important because alterations in purine metabolism have the potential to alter purinergic signalling which might contribute to the regulation of inflammatory responses in the endothelial cells under hyperglycaemic conditions that mimic the diabetic state. However, this project did not involve targeted studies designed to demonstrate if changes in anti-inflammatory processes were due to altered purinergic signalling. Therefore, the potential of quercetin and its metabolites to alter purinergic signalling directs future research towards the determination of whether the quercetin-induced alterations in purine metabolism modulate ATP and adenosine receptors activation and initiation of anti-inflammatory events.

In this respect, subsequent research would need to involve a series of experimental approaches that would provide a more comprehensive set of observations. First, it would be useful to determine the effects of quercetin on expression of purine metabolising enzymes to confirm whether ATP and ADP hydrolysis and inosine accumulation are due to increased levels of CD39 and 5'-NT proteins. At the same time, a more sensitive LC-MS method needs to be developed so that quantification of extracellular concentrations of ATP, ADP and AMP could be possible. This would facilitate the investigation of the effects of

quercetin on ATP and ADP release from HUVECs. In parallel, the effects of quercetin on adenosine transporters should be assessed in order to elucidate if they contribute to the elevations observed in extracellular adenosine concentrations. Subsequently, the effects of quercetin and high-glucose/TNF-α treatments on the inflammatory status of the cells should be compared in the presence and absence of inhibitors of adenosine receptors. This could be assessed by investigating several factors such as alterations in NF-κB activation, cell adhesion molecule expression and endothelial cell barrier function which have been previously shown to be affected by the activation of adenosine receptors.

More potent inflammatory responses may be observed after high-glucose or pro-inflammatory cytokine treatments when arterial endothelial cells are used because arterial endothelial cells are more vulnerable to atherogenic stimuli compared to vein endothelial cells (Deng et al., 2006). Therefore, it would be useful to investigate the effects of quercetin on the energy metabolite concentrations in human arterial endothelial cells (HAECs). According to the results, the next step could involve investigation of the effects of quercetin and its metabolites on the purine metabolism enzymes in HAECs. After confirming the effects of polyphenol treatments on arterial endothelial cells, a potential animal study would provide extremely valuable data since the reported animal and human studies in the literature have been mostly focused on the effects of quercetin supplementation on selected markers (Dias et al., 2005, Davis et al., 2008, Askari et al., 2012), and there are no reported studies focused on alterations in energy metabolite levels and the activities of the enzymes investigated here, except for xanthine oxidase (Abbey and Rankin, 2011).

Therefore, a comprehensive animal study which would investigate the effects of quercetin supplementation on the levels of energy metabolites and the enzymes involved in purine metabolism and their activities could provide valuable information. In addition, physiological evidence could relate potential alterations in energy metabolites to their biological effects on atherosclerotic plaque formation in animals. For example mouse models of diabetes and atherosclerosis such as streptozotocin (STZ)-induced diabetic mice (Ito et al., 2001) and apolipoprotein E deficient mice (ApoE -/-) (Chatzigeorgiou et al., 2009) both of which are prone to developing atherosclerosis could be used for this purpose. The proposed animal

study would involve supplementing the mice with quercetin which may be in oral or intravenous forms. The dose and duration of the treatment could be determined either by reviewing previously published study reports or performing preliminary treatments to set the optimum dose and duration. After the treatment period, blood would be collected from animals in order to determine the effects of quercetin treatments on plasma concentrations of ATP, ADP, AMP, adenosine, inosine and xanthine, and platelet aggregation. The isolated platelets would be used to measure the activities of purine metabolism enzymes. Furthermore, pro-inflammatory markers which are closely associated with purinergic signalling could be assessed. The effects of quercetin treatment on NF-κB activation could be investigated together with its downstream effects on IFN-γ and inducible nitric oxide synthase (iNOS). Therefore, at this point, another treatment group which would be supplemented by adenosine may be useful to determine whether the changes observed after quercetin treatments were due to adenosine receptor activation. Similarly, treating mice with inhibitors of purinergic receptors would indicate whether the changes are due to altered ATP concentrations.

The reductions in lactate concentrations after quercetin treatments are also interesting because that may have therapeutic potential in cancer and pyruvate carboxylase deficiency disease. Further, this may be useful in pharmaceutical industry with the potential to improve the yield and quality of recombinant proteins produced by mammalian host cells. It is now logical to propose the investigation of the contributions of a potential inhibition in lactate dehydrogenase activity (converts pyruvate to lactate) by quercetin and its metabolites to the reductions observed in lactate concentrations. In parallel, studies should be designed to assess the effects of quercetin on the flux of pyruvate into the Krebs cycle since it is another potential mechanism to explain the observed reductions in lactate concentrations.

Supplementary Information

The metabolite concentrations measured for HUVEC extracts (intracellular metabolites) and cell culture media samples (extracellular metabolites) using HILIC mode LC-MS method are presented below:

Table S 1: Metabolite concentrations for HUVEC extracts after high-glucose and quercetin treatments.

	High-glucose (18 h)	Quercetin (2 h) + High-glucose (18 h)	p-value
ATP	29.3±4.147 µM	12.8±6.662 µM	p<0.01
ADP	2.40±0.273 µM	1.5±0.798 µM	p<0.05
AMP	0.17±0.039 µM	0.21±0.068 µM	p>0.05
Adenosine	0.29±0.055 µM	0.26±0.106 µM	p>0.05
Inosine	0.52±0.091 µM	1.07±0.029 µM	p<0.05
Xanthine	0.55±0.083 µM	0.46±0.149 µM	p>0.05
NAD$^+$	5.42±0.495 µM	3.64±1.492 µM	p<0.01

Table S 2: Metabolite concentrations for extracellular media samples after high-glucose and quercetin treatments.

	High-glucose (18 h)	Quercetin (2 h) + High-glucose (18 h)	p-value
Adenosine	0.05±0.001 µM	0.05±0.002 µM	p>0.05
Inosine	2.23±0.148 µM	6.67±0.545 µM	p<0.01
Xanthine	2.63±0.105 µM	2.48±0.065 µM	P<0.05

Table S 3: Metabolite concentrations for HUVEC extracts after TNF-α and quercetin treatments.

	TNF-α (6 h)	Quercetin (2 h) +TNF-α (6 h)	p-value
AMP	0.33±0.053 µM	0.29±0.056 µM	p>0.05
Adenosine	0.06±0.036 µM	0.12±0.036 µM	p<0.05
Inosine	4.89±0.563 µM	9.07±0.075 µM	p<0.001
Xanthine	0.59±0.046 µM	0.66±0.022 µM	p>0.05
NAD$^+$	2.94±0.265 µM	3.00±0.263 µM	p>0.05

Table S 4: Metabolite concentrations for extracellular media samples after TNF-α and quercetin treatments.

	TNF-α (6 h)	Quercetin (2 h) +TNF-α (6 h)	p-value
Adenosine	0.02±0.006 µM	0.02±0.007 µM	p>0.05
Inosine	22.5±0.852 µM	35.8±1.546 µM	p<0.001
Xanthine	2.13±0.282 µM	2.15±0.173 µM	P>0.05

Table S 5: Metabolite concentrations for HUVEC extracts after quercetin treatment (2 h).

	Unstimulated (2 h)	Quercetin (2 h)	p-value
AMP	0.25±0.036 µM	0.24±0.033 µM	$p>0.05$
Adenosine	0.24±0.130 µM	0.49±0.151 µM	$p<0.05$
Inosine	6.11±1.224 µM	7.33±1.187 µM	$p>0.05$
Xanthine	0.30±0.051 µM	0.29±0.045 µM	$p>0.05$

Table S 6: Metabolite concentrations for extracellular media samples after quercetin treatment (2 h).

	Unstimulated (2 h)	Quercetin (2 h)	p-value
Adenosine	0.03±0.130 µM	0.04±0.151 µM	$p<0.05$
Inosine	37.8±0.756 µM	45.4±1.098 µM	$p<0.01$
Xanthine	2.57±0.047 µM	2.64±0.120 µM	$p>0.05$

Table S 7: Metabolite concentrations for HUVEC extracts after quercetin treatment (8 h).

	Unstimulated (8 h)	Quercetin (8 h)	p-value
AMP	0.24±0.050	0.36±0.045	p<0.05
Adenosine	0.07±0.015 µM	0.05±0.025 µM	p>0.05
Inosine	4.37±0.707 µM	8.56±0.656 µM	p<0.01
Xanthine	0.63±0.126 µM	0.62±0.055 µM	p>0.05
NAD$^+$	3.57±0.495 µM	3.21±1.492 µM	p>0.05

Table S 8: Metabolite concentrations for extracellular media samples after quercetin treatment (8 h).

	Unstimulated (8 h)	Quercetin (8 h)	p-value
Adenosine	0.01±0.003 µM	0.01±0.002 µM	p>0.05
Inosine	21.4±1.563 µM	35.9±0.891 µM	p<0.01
Xanthine	2.15±0.244 µM	2.24±0.229 µM	p>0.05

Table S 9: Metabolite concentrations for HUVEC extracts after quercetin treatment (20 h).

	Unstimulated (20 h)	Quercetin (20 h)	p-value
ATP	29.0±2.978 µM	20.2±3.281 µM	p<0.01
ADP	2.6±0.619 µM	1.87±0.548 µM	p<0.05
AMP	0.19±0.050	0.21±0.045	p<0.05
Adenosine	0.23±0.056 µM	0.37±0.216 µM	p<0.05
Inosine	0.42±0.040 µM	1.147±0.157 µM	p<0.01
Xanthine	0.46±0.039 µM	0.50±0.048 µM	p>0.05
NAD$^+$	5.90±0.346 µM	4.46±0.191 µM	p<0.01

Table S 10: Metabolite concentrations for extracellular media samples after quercetin treatment (20h).

	Unstimulated (20 h)	Quercetin (20 h)	p-value
Adenosine	0.05±0.008 µM	0.054±0.002 µM	p>0.05
Inosine	2.10±0.060 µM	6.38±0.271 µM	p<0.01
Xanthine	2.66±0.049 µM	2.49±0.025 µM	p<0.01

References

ABBEY, E. L. & RANKIN, J. W. 2011. Effect of quercetin supplementation on repeated-sprint performance, xanthine oxidase activity, and inflammation. *International journal of sport nutrition and exercise metabolism,* 21**,** 91-96.

ADAMS, D. J. & KLAIDMAN, L. K. 2007. Sirtuins, Nicotinamide and Aging: A Critical Review. *Letters in Drug Design & Discovery,* 4**,** 44-48.

AGARWAL C., S. R. P., DHANALAKSHMI S., AGARWAL R. 2004. Anti-angiogenic efficacy of grape seed extract in endothelial cells. *Oncology Reports,* 11**,** 681-685.

ALTANNAVCH T. S., R., K., KUCERA P., ANDEL M. 2004. Effect of High Glucose Concentrations on Expression of ELAM-1, VCAM-1 and ICAM-1 in HUVEC with and without Cytokine Activation *Physiological Research***,** 77-82.

ANTONIOLI, L., PACHER, P., VIZI, E. S. & HASKÓ, G. 2013. CD39 and CD73 in immunity and inflammation. *Trends in Molecular Medicine,* 19**,** 355-367.

APPELDOORN, M. M., VINCKEN, J.-P., AURA, A.-M., HOLLMAN, P. C. H. & GRUPPEN, H. 2009. Procyanidin Dimers Are Metabolized by Human Microbiota with 2-(3,4-Dihydroxyphenyl)acetic Acid and 5-(3,4-Dihydroxyphenyl)-γ-valerolactone as the Major Metabolites. *Journal of Agricultural and Food Chemistry,* 57**,** 1084-1092.

ARMAH, C. N., TRAKA, M. H., DAINTY, J. R., DEFERNEZ, M., JANSSENS, A., LEUNG, W., DOLEMAN, J. F., POTTER, J. F. & MITHEN, R. F. 2013. A diet rich in high-glucoraphanin broccoli interacts with genotype to reduce discordance in plasma metabolite profiles by modulating mitochondrial function. *The American Journal of Clinical Nutrition,* 98**,** 712-722.

ARTS, I. C. & HOLLMAN, P. C. 2005. Polyphenols and disease risk in epidemiologic studies. *The American Journal of Clinical Nutrition,* 81**,** 317S-325S.

ASKARI, G., GHIASVAND, R., KARIMIAN, J., FEIZI, A., PAKNAHAD, Z., SHARIFIRAD, G. & HAJISHAFIEI, M. 2012. Does quercetin and vitamin C improve exercise performance, muscle damage, and body composition in male athletes? *Journal of Research in Medical Sciences,* 17**,** 328-331.

AWAD, H. M., BOERSMA, M. G., BOEREN, S., VAN DER WOUDE, H., VAN ZANDEN, J., VAN BLADEREN, P. J., VERVOORT, J. & RIETJENS, I. M. C. M. 2002. Identification of o-quinone/quinone methide metabolites of quercetin in a cellular in vitro system. *FEBS Letters,* 520**,** 30-34.

AZCUTIA, V., ABU-TAHA, M., ROMACHO, T., VÁZQUEZ-BELLA, M., MATESANZ, N., LUSCINSKAS, F. W., RODRÍGUEZ-MAÑAS, L., SANZ, M. J., SÁNCHEZ-FERRER, C. F. & PEIRÓ, C. 2010. Inflammation Determines the Pro-Adhesive Properties of High Extracellular D-Glucose in Human Endothelial Cells *In Vitro* and Rat Microvessels *In Vivo*. *PLoS ONE,* 5**,** e10091.

BABA, S., OSAKABE, N., NATSUME, M. & TERAO, J. 2002. Absorption and urinary excretion of procyanidin B2 [epicatechin-(4[beta]-8)-epicatechin] in rats. *Free Radical Biology and Medicine,* 33**,** 142-148.

BARTOLOMÈ, B., HERN·NDEZ, T., BENGOECHEA, M. L., QUESADA, C., GÛMEZ-CORDOVÈS, C. & ESTRELLA, I. 1996. Determination of some structural features of procyanidins and related compounds by photodiode-array detection. *Journal of Chromatography A,* 723**,** 19-26.

BASU, A., NEWMAN, E. D., BRYANT, A. L., LYONS, T. J. & BETTS, N. M. 2013. Pomegranate Polyphenols Lower Lipid Peroxidation in Adults with Type 2 Diabetes but Have No Effects in Healthy Volunteers: A Pilot Study. *Journal of Nutrition and Metabolism,* 2013**,** 7.

BAUMGARTNER-PARZER, S. M., WAGNER, L., PETTERMANN, M., GESSL, A. & WALDHÄUSL, W. 1995. Modulation by high glucose of adhesion molecule expression in cultured endothelial cells. *Diabetologia,* 38**,** 1367-1370.

BAUR, J. A., PEARSON, K. J., PRICE, N. L., JAMIESON, H. A., LERIN, C., KALRA, A., PRABHU, V. V., ALLARD, J. S., LOPEZ-LLUCH, G., LEWIS, K., PISTELL, P. J., POOSALA, S., BECKER, K. G., BOSS, O., GWINN, D., WANG, M., RAMASWAMY, S., FISHBEIN, K. W., SPENCER, R. G., LAKATTA, E. G., LE COUTEUR, D., SHAW, R. J., NAVAS, P., PUIGSERVER, P., INGRAM, D. K., DE CABO, R. & SINCLAIR, D. A. 2006. Resveratrol improves health and survival of mice on a high-calorie diet. *Nature,* 444**,** 337-342.

BECKERT, S., FARRAHI, F., ASLAM, R. S., SCHEUENSTUHL, H., KÖNIGSRAINER, A., HUSSAIN, M. Z. & HUNT, T. K. 2006. Lactate stimulates endothelial cell migration. *Wound Repair and Regeneration,* 14**,** 321-324.

BECKMAN, J. A., CREAGER, M. A. & LIBBY, P. 2002. Diabetes and Atherosclerosis: Epidemiology, Pathophysiology, and Management. *JAMA,* 287**,** 2570-2581.

BENDINELLI, B., MASALA, G., SAIEVA, C., SALVINI, S., CALONICO, C., SACERDOTE, C., AGNOLI, C., GRIONI, S., FRASCA, G., MATTIELLO, A., CHIODINI, P., TUMINO, R., VINEIS, P., PALLI, D. & PANICO, S. 2011. Fruit, vegetables, and olive oil and risk of coronary heart disease in Italian women: the EPICOR Study. *The American Journal of Clinical Nutrition,* 93**,** 275-283.

BENNETT, B. D., YUAN, J., KIMBALL, E. H. & RABINOWITZ, J. D. 2008. Absolute quantitation of intracellular metabolite concentrations by an isotope ratio-based approach. *Nat. Protocols,* 3**,** 1299-1311.

BERLINER, J. A., NAVAB, M., FOGELMAN, A. M., FRANK, J. S., DEMER, L. L., EDWARDS, P. A., WATSON, A. D. & LUSIS, A. J. 1995. Atherosclerosis: Basic Mechanisms: Oxidation, Inflammation, and Genetics. *Circulation,* 91**,** 2488-2496.

BIRK, A. V., BROEKMAN, M. J., GLADEK, E. M., ROBERTSON, H. D., DROSOPOULOS, J. H. F., MARCUS, A. J. & SZETO, H. H. 2002. Role of extracellular ATP metabolism in regulation of platelet reactivity. *Journal of Laboratory and Clinical Medicine,* 140**,** 166-175.

BLADÈ, C., AROLA, L. & SALVADÛ, M.-J. 2010. Hypolipidemic effects of proanthocyanidins and their underlying biochemical and molecular mechanisms. *Molecular Nutrition & Food Research,* 54**,** 37-59.

BLANKENBERG, S., BARBAUX, S. & TIRET, L. 2003. Adhesion molecules and atherosclerosis. *Atherosclerosis,* 170**,** 191-203.

BOBRYSHEV, Y. V. 2006. Monocyte recruitment and foam cell formation in atherosclerosis. *Micron,* 37**,** 208-222.

BODE, L. M., BUNZEL, D., HUCH, M., CHO, G.-S., RUHLAND, D., BUNZEL, M., BUB, A., FRANZ, C. M. & KULLING, S. E. 2013. In vivo and in vitro metabolism of trans-resveratrol by human gut microbiota. *The American Journal of Clinical Nutrition,* 97**,** 295-309.

BODIN, P. & BURNSTOCK, G. 1998. Increased release of ATP from endothelial cells during acute inflammation. *Inflammation Research,* 47**,** 351-354.

BOGIN, L., PAPA, M. Z., POLAK-CHARCON, S. & DEGANI, H. 1998. TNF-induced modulations of phospholipid metabolism in human breast cancer cells. *Biochimica et Biophysica Acta (BBA) - Lipids and Lipid Metabolism,* 1392**,** 217-232.

BÖHM, F. & PERNOW, J. 2007. The importance of endothelin-1 for vascular dysfunction in cardiovascular disease. *Cardiovascular Research,* 76**,** 8-18.

BOSETTI, C., FILOMENO, M., RISO, P., POLESEL, J., LEVI, F., TALAMINI, R., MONTELLA, M., NEGRI, E., FRANCESCHI, S. & LA VECCHIA, C. 2012. Cruciferous vegetables and cancer risk in a network of case–control studies. *Annals of Oncology.*

BOUMA, M. G., VAN DEN WILDENBERG, F. A. & BUURMAN, W. A. 1996. Adenosine inhibits cytokine release and expression of adhesion molecules by activated human endothelial cells. *American Journal of Physiology - Cell Physiology,* 270**,** C522-C529.

BOURS, M. J. L., SWENNEN, E. L. R., DI VIRGILIO, F., CRONSTEIN, B. N. & DAGNELIE, P. C. 2006. Adenosine 5′-triphosphate and adenosine as endogenous signaling molecules in immunity and inflammation. *Pharmacology & Therapeutics,* 112**,** 358-404.

BRAGANHOL, E., TAMAJUSUKU, A. S. K., BERNARDI, A., WINK, M. R. & BATTASTINI, A. M. O. 2007. Ecto-5'-nucleotidase/CD73 inhibition by quercetin in the human U138MCG glioma cell line. *Biochimica Et Biophysica Acta-General Subjects,* 1770**,** 1352-1359.

BRASNYÓ, P., MOLNÁR, G. A., MOHÁS, M., MARKÓ, L., LACZY, B., CSEH, J., MIKOLÁS, E., SZIJÁRTÓ, I. A., MÉREI, Á., HALMAI, R., MÉSZÁROS, L. G., SÜMEGI, B. & WITTMANN, I. 2011. Resveratrol improves insulin sensitivity, reduces oxidative stress and activates the Akt pathway in type 2 diabetic patients. *British Journal of Nutrition,* 106**,** 383-389.

BUIJSSE, B., WEIKERT, C., DROGAN, D., BERGMANN, M. & BOEING, H. 2010. Chocolate consumption in relation to blood pressure and risk of cardiovascular disease in German adults. *European Heart Journal.*

BURKON, A. & SOMOZA, V. 2008. Quantification of free and protein-bound trans-resveratrol metabolites and identification of trans-resveratrol-C/O-conjugated diglucuronides – Two novel resveratrol metabolites in human plasma. *Molecular Nutrition & Food Research,* 52**,** 549-557.

BURNSTOCK, G. 2002. Purinergic Signaling and Vascular Cell Proliferation and Death. *Arteriosclerosis, Thrombosis, and Vascular Biology,* 22**,** 364-373.

CEDÓ, L., CASTELL-AUVÍ, A., PALLARÈS, V., BLAY, M., ARDÉVOL, A., AROLA, L. & PINENT, M. 2013. Grape seed procyanidin extract modulates proliferation and apoptosis of pancreatic beta-cells. *Food Chemistry,* 138**,** 524-530.

CERIELLO, A. 2003. New Insights on Oxidative Stress and Diabetic Complications May Lead to a "Causal" Antioxidant Therapy. *Diabetes Care,* 26**,** 1589-1596.

CERSOSIMO, E. & DEFRONZO, R. A. 2006. Insulin resistance and endothelial dysfunction: the road map to cardiovascular diseases. *Diabetes/Metabolism Research and Reviews,* 22**,** 423-436.

CHAO, C.-L., HOU, Y.-C., LEE CHAO, P.-D., WENG, C.-S. & HO, F.-M. 2009. The antioxidant effects of quercetin metabolites on the prevention of high

glucose-induced apoptosis of human umbilical vein endothelial cells. *British Journal of Nutrition,* 101**,** 1165-1170.

CHATELAIN, K., PHIPPEN, S., MCCABE, J., TEETERS, C. A., #39, MALLEY, S. & KINGSLEY, K. 2011. Cranberry and Grape Seed Extracts Inhibit the Proliferative Phenotype of Oral Squamous Cell Carcinomas. *Evidence-Based Complementary and Alternative Medicine,* 2011.

CHATZIGEORGIOU, A., HALAPAS, A., KALAFATAKIS, K. & KAMPER, E. 2009. The Use of Animal Models in the Study of Diabetes Mellitus. *In Vivo,* 23**,** 245-258.

CHEN, A., DONG, L., LEFFLER, N. R., ASCH, A. S., WITTE, O. N. & YANG, L. V. 2011a. Activation of GPR4 by Acidosis Increases Endothelial Cell Adhesion through the cAMP/Epac Pathway. *PLoS ONE,* 6**,** e27586.

CHEN, G., CHEN, Y., CHEN, H., LI, L., YAO, J., JIANG, Q., LIN, X., WEN, J. & LIN, L. 2011b. The effect of NF-κB pathway on proliferation and apoptosis of human umbilical vein endothelial cells induced by intermittent high glucose. *Molecular and Cellular Biochemistry,* 347**,** 127-133.

CHEN, G., ZHANG, D., JING, N., YIN, S., FALANY, C. N. & RADOMINSKA-PANDYA, A. 2003. Human gastrointestinal sulfotransferases: identification and distribution☆. *Toxicology and Applied Pharmacology,* 187**,** 186-197.

CHEN, Y.-H., GUH, J.-Y., CHUANG, T.-D., CHEN, H.-C., CHIOU, S.-J., HUANG, J.-S., YANG, Y.-L. & CHUANG, L.-Y. 2007. High glucose decreases endothelial cell proliferation via the extracellular signal regulated kinase/p15INK4b pathway. *Archives of Biochemistry and Biophysics,* 465**,** 164-171.

CHEN, Y.-W., CHOU, H.-C., LIN, S.-T., CHEN, Y.-H., CHANG, Y.-J., CHEN, L. & CHAN, H.-L. 2013. Cardioprotective Effects of Quercetin in Cardiomyocyte under Ischemia/Reperfusion Injury. *Evidence-Based Complementary and Alternative Medicine,* 2013**,** 16.

CHISOLM, G. M. & STEINBERG, D. 2000. The oxidative modification hypothesis of atherogenesis: an overview. *Free Radical Biology and Medicine,* 28**,** 1815-1826.

CHOI, Y.-J., LIM, H.-S., CHOI, J.-S., SHIN, S.-Y., BAE, J.-Y., KANG, S.-W., KANG, I.-J. & KANG, Y.-H. 2008. Blockade of Chronic High Glucose-Induced Endothelial Apoptosis by Sasa borealis Bamboo Extract. *Exp. Biol. Med.,* 233**,** 580-591.

CHONG, M. F.-F., MACDONALD, R. & LOVEGROVE, J. A. 2010. Fruit polyphenols and CVD risk: a review of human intervention studies. *British Journal of Nutrition,* 104**,** S28-S39.

CHUNG, S., YAO, H., CAITO, S., HWANG, J.-W., ARUNACHALAM, G. & RAHMAN, I. 2010. Regulation of SIRT1 in cellular functions: Role of polyphenols. *Archives of Biochemistry and Biophysics,* 501**,** 79-90.

CIALDELLA-KAM, L., NIEMAN, D. C., SHA, W., MEANEY, M. P., KNAB, A. M. & SHANELY, R. A. 2013. Dose–response to 3 months of quercetin-containing supplements on metabolite and quercetin conjugate profile in adults. *British Journal of Nutrition,* 109**,** 1923-1933.

CORTI, R., FLAMMER, A. J., HOLLENBERG, N. K. & LÜSCHER, T. F. 2009. Cocoa and Cardiovascular Health. *Circulation,* 119**,** 1433-1441.

COSENTINO, F., HISHIKAWA, K., KATUSIC, Z. S. & LUSCHER, T. F. 1997. High Glucose Increases Nitric Oxide Synthase Expression and Superoxide Anion Generation in Human Aortic Endothelial Cells. *Circulation,* 96**,** 25-28.

CRAWFORD, S. O., HOOGEVEEN, R. C., BRANCATI, F. L., ASTOR, B. C., BALLANTYNE, C. M., SCHMIDT, M. I. & YOUNG, J. H. 2010. Association of blood lactate with type 2 diabetes: the Atherosclerosis Risk in Communities Carotid MRI Study. *International Journal of Epidemiology,* 39**,** 1647-1655.

CRESPO, I., GARCÍA-MEDIAVILLA, M. V., GUTIÉRREZ, B., SÁNCHEZ-CAMPOS, S., TUÑÓN, M. J. & GONZÁLEZ-GALLEGO, J. 2008. A comparison of the effects of kaempferol and quercetin on cytokine-induced pro-inflammatory status of cultured human endothelial cells. *British Journal of Nutrition,* 100**,** 968-976.

CRISTALLI, G., COSTANZI, S., LAMBERTUCCI, C., LUPIDI, G., VITTORI, S., VOLPINI, R. & CAMAIONI, E. 2001. Adenosine deaminase: Functional implications and different classes of inhibitors. *Medicinal Research Reviews,* 21**,** 105-128.

CROZIER, A., CLIFFORD, M. N. & ASHIHARA, H. 2006. Plant Secondary Metabolites: Occurance, Structure and Role in the Diet. *Blackwell Publishing.*

CYBULSKY, M. I., IIYAMA, K., LI, H., ZHU, S., CHEN, M., IIYAMA, M., DAVIS, V., GUTIERREZ-RAMOS, J.-C., CONNELLY, P. W. & MILSTONE, D. S. 2001. A major role for VCAM-1, but not ICAM-1, in early atherosclerosis. *The Journal of Clinical Investigation,* 107**,** 1255-1262.

D'ARCHIVIO, M., FILESI, C., BENEDETTO, R. D., RAFFAELLA, G., GIOVANNINI, C. & MASELLA, R. 2007. Polyphenols, dietary sources and bioavailability. *Ann Ist Super Sanità,* 43**,** 348-361.

DANAEI, G., FINUCANE, M. M., LU, Y., SINGH, G. M., COWAN, M. J., PACIOREK, C. J., LIN, J. K., FARZADFAR, F., KHANG, Y.-H., STEVENS, G. A., RAO, M., ALI, M. K., RILEY, L. M., ROBINSON, C. A. & EZZATI, M. 2011. National, regional, and global trends in fasting plasma glucose and diabetes prevalence since 1980: systematic analysis of health examination surveys and epidemiological studies with 370 country-years and 2·7 million participants. *The Lancet,* 378**,** 31-40.

DANIELSSON, A. P. H., MORITZ, T., MULDER, H. & SPÉGEL, P. 2010. Development and optimization of a metabolomic method for analysis of adherent cell cultures. *Analytical Biochemistry,* 404**,** 30-39.

DAVIDSON, S. M. & YELLON, D. M. 2006. Does Hyperglycemia Reduce Proliferation or Increase Apoptosis? *American Journal of Physiology - Heart and Circulatory Physiology,* 291**,** H1486-H1487.

DAVIES, M. J., GORDON, J. L., GEARING, A. J. H., PIGOTT, R., WOOLF, N., KATZ, D. & KYRIAKOPOULOS, A. 1993. The expression of the adhesion molecules ICAM-1, VCAM-1, PECAM, and E-selectin in human atherosclerosis. *The Journal of Pathology,* 171**,** 223-229.

DAVIS, J. M., MURPHY, E. A., MCCLELLAN, J. L., CARMICHAEL, M. D. & GANGEMI, J. D. 2008. Quercetin reduces susceptibility to influenza infection following stressful exercise. *American Journal of Physiology - Regulatory, Integrative and Comparative Physiology,* 295**,** R505-R509.

DAY, A. J., BAO, Y., MORGAN, M. R. A. & WILLIAMSON, G. 2000. Conjugation position of quercetin glucuronides and effect on biological activity. *Free Radical Biology and Medicine,* 29**,** 1234-1243.

DAY, A. J., DUPONT, M. S., RIDLEY, S., RHODES, M., RHODES, M. J. C., MORGAN, M. R. A. & WILLIAMSON, G. 1998. Deglycosylation of flavonoid

and isoflavonoid glycosides by human small intestine and liver β-glucosidase activity. *FEBS Letters,* 436**,** 71-75.

DE BOER, V. C. J., DE GOFFAU, M. C., ARTS, I. C. W., HOLLMAN, P. C. H. & KEIJER, J. 2006. SIRT1 stimulation by polyphenols is affected by their stability and metabolism. *Mechanisms of Ageing and Development,* 127**,** 618-627.

DEL RIO, D., RODRIGUEZ-MATEOS, A., SPENCER, J. P. E., TOGNOLINI, M., BORGES, G. & CROZIER, A. 2013. Dietary (Poly)phenolics in Human Health: Structures, Bioavailability, and Evidence of Protective Effects Against Chronic Diseases. *ANTIOXIDANTS & REDOX SIGNALING,* 18**,** 1819-1893.

DENG, D. X.-F., TSALENKO, A., VAILAYA, A., BEN-DOR, A., KUNDU, R., ESTAY, I., TABIBIAZAR, R., KINCAID, R., YAKHINI, Z., BRUHN, L. & QUERTERMOUS, T. 2006. Differences in Vascular Bed Disease Susceptibility Reflect Differences in Gene Expression Response to Atherogenic Stimuli. *Circulation Research,* 98**,** 200-208.

DEPREZ, S., MILA, I., HUNEAU, J.-F., TOME, D. & SCALBERT, A. 2001. Transport of Proanthocyanidin Dimer, Trimer, and Polymer Across Monolayers of Human Intestinal Epithelial Caco-2 Cells. *Antioxidants & Redox Signaling,* 3**,** 957-967.

DETTMER, K., NÜRNBERGER, N., KASPAR, H., GRUBER, M., ALMSTETTER, M. & OEFNER, P. 2011. Metabolite extraction from adherently growing mammalian cells for metabolomics studies: optimization of harvesting and extraction protocols. *Analytical and Bioanalytical Chemistry,* 399**,** 1127-1139.

DIAS, A. S., PORAWSKI, M., ALONSO, M., MARRONI, N., COLLADO, P. S. & GONZÁLEZ-GALLEGO, J. 2005. Quercetin Decreases Oxidative Stress, NF-κB Activation, and iNOS Overexpression in Liver of Streptozotocin-Induced Diabetic Rats. *The Journal of Nutrition,* 135**,** 2299-2304.

DIETMAIR, S., TIMMINS, N. E., GRAY, P. P., NIELSEN, L. K. & KRÖMER, J. O. 2010. Towards quantitative metabolomics of mammalian cells: Development of a metabolite extraction protocol. *Analytical Biochemistry,* 404**,** 155-164.

DINICOLA, S., CUCINA, A., PASQUALATO, A., D'ANSELMI, F., PROIETTI, S., LISI, E., PASQUA, G., ANTONACCI, D. & BIZZARRI, M. 2012. Antiproliferative and Apoptotic Effects Triggered by Grape Seed Extract (GSE) versus Epigallocatechin and Procyanidins on Colon Cancer Cell Lines. *International Journal of Molecular Sciences,* 13**,** 651-664.

DUARTE, I. F. 2011. Following dynamic biological processes through NMR-based metabonomics: A new tool in nanomedicine? *Journal of Controlled Release,* 153**,** 34-39.

DUARTE, I. F., LAMEGO, I. S., MARQUES, J., MARQUES, M. P. M., BLAISE, B. J. & GIL, A. M. 2010. Nuclear Magnetic Resonance (NMR) Study of the Effect of Cisplatin on the Metabolic Profile of MG-63 Osteosarcoma Cells. *Journal of Proteome Research,* 9**,** 5877-5886.

DULLOO, A. G., DURET, C., ROHRER, D., GIRARDIER, L., MENSI, N., FATHI, M., CHANTRE, P. & VANDERMANDER, J. 1999. Efficacy of a green tea extract rich in catechin polyphenols and caffeine in increasing 24-h energy expenditure and fat oxidation in humans. *The American Journal of Clinical Nutrition,* 70**,** 1040-1045.

DUNN, W. B., BAILEY, N. J. C. & JOHNSON, H. E. 2005. Measuring the metabolome: current analytical technologies. *Analyst,* 130**,** 606-625.

DUNN, W. B. & ELLIS, D. I. 2005. Metabolomics: Current analytical platforms and methodologies. *TrAC Trends in Analytical Chemistry,* 24**,** 285-294.

DUTHIE G. G., P., M. W., GARDNER P. T., MORRICE P. C., JENKINSON M. A., MCPHAIL D. B., STEELE G. M. 1998

The effect of whisky and wine consumption on total phenol content and antioxidant capacity of plasma from healthy volunteers. *Nature,* 52**,** 733-736.

ECKEL, R. H., WASSEF, M., CHAIT, A., SOBEL, B., BARRETT, E., KING, G., LOPES-VIRELLA, M., REUSCH, J., RUDERMAN, N., STEINER, G. & VLASSARA, H. 2002. Prevention Conference VI: Diabetes and Cardiovascular Disease: Writing Group II: Pathogenesis of Atherosclerosis in Diabetes. *Circulation,* 105**,** e138-143.

EDINGER, A. L. & THOMPSON, C. B. 2002. Akt Maintains Cell Size and Survival by Increasing mTOR-dependent Nutrient Uptake. *Molecular Biology of the Cell,* 13**,** 2276-2288.

EGERT, S., BOSY-WESTPHAL, A., SEIBERL, J., KÜRBITZ, C., SETTLER, U., PLACHTA-DANIELZIK, S., WAGNER, A. E., FRANK, J., SCHREZENMEIR, J., RIMBACH, G., WOLFFRAM, S. & MÜLLER, M. J. 2009. Quercetin reduces systolic blood pressure and plasma oxidised low-density lipoprotein concentrations in overweight subjects with a high-cardiovascular disease risk phenotype: a double-blinded, placebo-controlled cross-over study. *British Journal of Nutrition,* 102**,** 1065-1074.

EGERT, S., WOLFFRAM, S., SCHULZE, B., LANGGUTH, P., HUBBERMANN, E. M., SCHWARZ, K., ADOLPHI, B., BOSY-WESTPHAL, A., RIMBACH, G. & MÜLLER, M. J. 2012. Enriched cereal bars are more effective in increasing plasma quercetin compared with quercetin from powder-filled hard capsules. *British Journal of Nutrition,* 107**,** 539-546.

EL-ALFY, A. T., AHMED, A. A. E. & FATANI, A. J. 2005. Protective effect of red grape seeds proanthocyanidins against induction of diabetes by alloxan in rats. *Pharmacological Research,* 52**,** 264-270.

EL GHAZI, I., SHENG, W., HU, S., REILLY, B., LOKENSGARD, J., ROCK, R., PETERSON, P., WILCOX, G. & ARMITAGE, I. 2010. Changes in the NMR Metabolic Profile of Human Microglial Cells Exposed to Lipopolysaccharide or Morphine. *Journal of Neuroimmune Pharmacology,* 5**,** 574-581.

ELTZSCHIG, H. K., FAIGLE, M., KNAPP, S., KARHAUSEN, J., IBLA, J., ROSENBERGER, P., ODEGARD, K. C., LAUSSEN, P. C., THOMPSON, L. F. & COLGAN, S. P. 2006. Endothelial catabolism of extracellular adenosine during hypoxia: the role of surface adenosine deaminase and CD26. *Blood,* 108**,** 1602-1610.

ERK, M. J., ROEPMAN, P., LENDE, T. R., STIERUM, R. H., AARTS, J. M. M. J. G., BLADEREN, P. J. & OMMEN, B. 2005. Integrated assessment by multiple gene expression analysis of quercetin bioactivity on anticancer–related mechanisms in colon cancer cells in vitro. *European Journal of Nutrition,* 44**,** 143-156.

ERLUND, I., KOLI, R., ALFTHAN, G., MARNIEMI, J., PUUKKA, P., MUSTONEN, P., MATTILA, P. & JULA, A. 2008. Favorable effects of berry consumption on platelet function, blood pressure, and HDL cholesterol. *The American Journal of Clinical Nutrition,* 87**,** 323-331.

EVANS, J. L., GOLDFINE, I. D., MADDUX, B. A. & GRODSKY, G. M. 2002. Oxidative Stress and Stress-Activated Signaling Pathways: A Unifying Hypothesis of Type 2 Diabetes. *Endocr Rev,* 23**,** 599-622.

FERRERO, M., BERTELLI, A., FULGENZI, A., PELLEGATTA, F., CORSI, M., BONFRATE, M., FERRARA, F., DE CATERINA, R., GIOVANNINI, L. & BERTELLI, A. 1998. Activity in vitro of resveratrol on granulocyte and monocyte adhesion to endothelium. *Am J Clin Nutr,* 68**,** 1208-1214.

FINKEL, T. & HOLBROOK, N. J. 2000. Oxidants, oxidative stress and the biology of ageing. *Nature,* 408**,** 239-247.

GABETTA, B., FUZZATI, N., GRIFFINI, A., LOLLA, E., PACE, R., RUFFILLI, T. & PETERLONGO, F. 2000. Characterization of proanthocyanidins from grape seeds. *Fitoterapia,* 71**,** 162-175.

GALINDO, P., GONZALEZ-MANZANO, S., ZARZUELO, M. J., GOMEZ-GUZMAN, M., QUINTELA, A. M., GONZALEZ-PARAMAS, A., SANTOS-BUELGA, C., PEREZ-VIZCAINO, F., DUARTE, J. & JIMENEZ, R. 2012. Different cardiovascular protective effects of quercetin administered orally or intraperitoneally in spontaneously hypertensive rats. *Food & Function,* 3**,** 643-650.

GALLEY, H. F. & WEBSTER, N. R. 2004. Physiology of the endothelium. *British Journal of Anaesthesia,* 93**,** 105-113.

GAPPA-FAHLENKAMP, H. & SHUKLA, A. 2009. The effect of short-term, high glucose concentration on endothelial cells and leukocytes in a 3D in vitro human vascular tissue model. *In Vitro Cellular & Developmental Biology - Animal,* 45**,** 234-242.

GARCÍA-CONESA, M.-T., TRIBOLO, S., GUYOT, S., TOMÁS-BARBERÁN, F. A. & KROON, P. A. 2009. Oligomeric procyanidins inhibit cell migration and modulate the expression of migration and proliferation associated genes in human umbilical vascular endothelial cells. *Molecular Nutrition & Food Research,* 53**,** 266-276.

GEE, J. M., DUPONT, M. S., DAY, A. J., PLUMB, G. W., WILLIAMSON, G. & JOHNSON, I. T. 2000. Intestinal Transport of Quercetin Glycosides in Rats Involves Both Deglycosylation and Interaction with the Hexose Transport Pathway. *The Journal of Nutrition,* 130**,** 2765-2771.

GERTZ, M., NGUYEN, G. T. T., FISCHER, F., SUENKEL, B., SCHLICKER, C., FRÄNZEL, B., TOMASCHEWSKI, J., ALADINI, F., BECKER, C., WOLTERS, D. & STEEGBORN, C. 2012. A Molecular Mechanism for Direct Sirtuin Activation by Resveratrol. *PLOS ONE,* 7**,** e49761.

GHANI, Q. P., WAGNER, S., BECKER, H. D., HUNT, T. K. & HUSSAIN, M. Z. 2004. Regulatory Role of Lactate in Wound Repair. *In:* CHANDAN, K. S. & GREGG, L. S. (eds.) *Methods in Enzymology.* Academic Press.

GINSBERG, H. N. 2000. Insulin resistance and cardiovascular disease. *The Journal of Clinical Investigation,* 106**,** 453-458.

GOEPFERT, C., IMAI, M., S, B., CSIZMADIA, E. & KACZMAREK, E. R. 2000. CD39 modulates endothelial cell activation and apoptosis. *Molecular Medicine,* 6**,** 591-603.

GOETZE, K., WALENTA, S., KSIAZKIEWICZ, M., KUNZ-SCHUGHART, L. & MUELLER-KLIESER, W. 2011. Lactate enhances motility of tumor cells and inhibits monocyte migration and cytokine release. *International Journal of Oncology,* 39**,** 453-463.

GOLDIN, A., BECKMAN, J. A., SCHMIDT, A. M. & CREAGER, M. A. 2006. Advanced Glycation End Products: Sparking the Development of Diabetic Vascular Injury. *Circulation,* 114**,** 597-605.

GOMIKAWA, S. & ISHIKAWA, Y. 2002. Effects of catechins and ground green tea drinking on the susceptibility of plasma and LDL to the oxidation in vitro and ex vivo. *Journal of Clinical Biochemistry and Nutrition,* 32**,** 55-68.

GONTHIER, M.-P., DONOVAN, J. L., TEXIER, O., FELGINES, C., REMESY, C. & SCALBERT, A. 2003. Metabolism of dietary procyanidins in rats. *Free Radical Biology and Medicine,* 35**,** 837-844.

GOTTLIEB, E., ARMOUR, S. M. & THOMPSON, C. B. 2002. Mitochondrial respiratory control is lost during growth factor deprivation. *Proceedings of the National Academy of Sciences,* 99**,** 12801-12806.

GRÄBNER, R., TILL, U. & HELLER, R. 2000. Flow cytometric determination of E-selectin, vascular cell adhesion molecule-1, and intercellular cell adhesion molecule-1 in formaldehyde-fixed endothelial cell monolayers. *Cytometry,* 40**,** 238-244.

GRANT, R. S., PASSEY, R., MATANOVIC, G., SMYTHE, G. & KAPOOR, V. 1999. Evidence for Increased de Novo Synthesis of NAD in Immune-Activated RAW264.7 Macrophages: A Self-Protective Mechanism? *Archives of Biochemistry and Biophysics,* 372**,** 1-7.

GRIFFIN, J. L., BOLLARD, M., NICHOLSON, J. K. & BHAKOO, K. 2002. Spectral profiles of cultured neuronal and glial cells derived from HRMAS 1H NMR spectroscopy. *NMR in Biomedicine,* 15**,** 375-384.

GROUP, T. A.-.-A. D. R. S. 1998. Survival and FEV1 Decline in Individuals with Severe Deficiency of α1-Antitrypsin. *American Journal of Respiratory and Critical Care Medicine,* 158**,** 49-59.

GRUNEWALD, J. & RIDLEY, A. 2010. CD73 represses pro-inflammatory responses in human endothelial cells. *Journal of Inflammation,* 7**,** 10.

GU, L., KELM, M., HAMMERSTONE, J. F., BEECHER, G., CUNNINGHAM, D., VANNOZZI, S. & PRIOR, R. L. 2002. Fractionation of Polymeric Procyanidins from Lowbush Blueberry and Quantification of Procyanidins in Selected Foods with an Optimized Normal-Phase HPLC‚àíMS Fluorescent Detection Method. *Journal of Agricultural and Food Chemistry,* 50**,** 4852-4860.

GUERCI , B., KEARNEY-SCHWARTZ, A., BÖHME, B., ZANNAD, F. & DROUIN, P. 2001. Endothelial Dysfunction And Type 2 Diabetes: Part 1: Physiology And Methods For Exploring The Endothelial Function. *Diabetes Metab,* 27**,** 425-434.

GÜLÇIN, İ. 2010. Antioxidant properties of resveratrol: A structure–activity insight. *Innovative Food Science & Emerging Technologies,* 11**,** 210-218.

GULGUN, M., ERDEM, O., OZTAS, E., KESIK, V., BALAMTEKIN, N., VURUCU, S., KUL, M., KISMET, E. & KOSEOGLU, V. 2010. Proanthocyanidin prevents methotrexate-induced intestinal damage and oxidative stress. *Experimental and Toxicologic Pathology,* 62**,** 109-115.

GÜLŞEN, A., MAKRIS, D. P. & KEFALAS, P. 2007. Biomimetic oxidation of quercetin: Isolation of a naturally occurring quercetin heterodimer and evaluation of its in vitro antioxidant properties. *Food Research International,* 40**,** 7-14.

GUO, H., CHEN, Y., LIAO, L. & WU, W. 2013. Resveratrol Protects HUVECs from Oxidized-LDL Induced Oxidative Damage by Autophagy Upregulation via

the AMPK/SIRT1 Pathway. *Cardiovascular Drugs and Therapy,* 27, 189-198.

GUZIK, T. J., MUSSA, S., GASTALDI, D., SADOWSKI, J., RATNATUNGA, C., PILLAI, R. & CHANNON, K. M. 2002. Mechanisms of Increased Vascular Superoxide Production in Human Diabetes Mellitus: Role of NAD(P)H Oxidase and Endothelial Nitric Oxide Synthase. *Circulation,* 105, 1656-1662.

HAFFNER, S. M., LEHTO, S., RONNEMAA, T., PYORALA, K. & LAAKSO, M. 1998. Mortality from Coronary Heart Disease in Subjects with Type 2 Diabetes and in Nondiabetic Subjects with and without Prior Myocardial Infarction. *N Engl J Med,* 339, 229-234.

HAN, J., PAN, X.-Y., XU, Y., XIAO, Y., AN, Y., TIE, L., PAN, Y. & LI, X.-J. 2012. Curcumin induces autophagy to protect vascular endothelial cell survival from oxidative stress damage. *Autophagy,* 8, 812-825.

HAN, L., MA, Q., LI, J., LIU, H., LI, W., MA, G., XU, Q., ZHOU, S. & WU, E. 2011. High Glucose Promotes Pancreatic Cancer Cell Proliferation via the Induction of EGF Expression and Transactivation of EGFR. *PLoS ONE,* 6, e27074.

HANSSON, G. K. 2005. Inflammation, Atherosclerosis, and Coronary Artery Disease. *N Engl J Med,* 352, 1685-1695.

HASKO, G., KUHEL, D. G., CHEN, J.-F., SCHWARZSCHILD, M. A., DEITCH, E. A., MABLEY, J. G., MARTON, A. & SZABÓ, C. 2000. Adenosine inhibits IL-12 and TNF-α production via adenosine A2a receptor-dependent and independent mechanisms. *The FASEB Journal,* 14, 2065-2074.

HASKÓ, G., SITKOVSKY, M. V. & SZABÓ, C. 2004. Immunomodulatory and neuroprotective effects of inosine. *Trends in Pharmacological Sciences,* 25, 152-157.

HERTOG, M. G. L., HOLLMAN, P. C. H., KATAN, M. B. & KROMHOUT, D. 1993. Intake of potentially anticarcinogenic flavonoids and their determinants in adults in the Netherlands. *Nutrition and Cancer,* 20, 21-29.

HILLEBRAND, U., HAUSBERG, M., STOCK, C., SHAHIN, V., NIKOVA, D., RIETHMÜLLER, C., KLICHE, K., LUDWIG, T., SCHILLERS, H., SCHNEIDER, S. W. & OBERLEITHNER, H. 2006. 17β-estradiol increases volume, apical surface and elasticity of human endothelium mediated by Na+/H+ exchange. *Cardiovascular Research,* 69, 916-924.

HINK, U., LI, H., MOLLNAU, H., OELZE, M., MATHEIS, E., HARTMANN, M., SKATCHKOV, M., THAISS, F., STAHL, R. A. K., WARNHOLTZ, A., MEINERTZ, T., GRIENDLING, K., HARRISON, D. G., FORSTERMANN, U. & MUNZEL, T. 2001. Mechanisms Underlying Endothelial Dysfunction in Diabetes Mellitus. *Circ Res,* 88, e14-22.

HIRSCHHAEUSER, F., SATTLER, U. G. A. & MUELLER-KLIESER, W. 2011. Lactate: A Metabolic Key Player in Cancer. *Cancer Research,* 71, 6921-6925.

HO, F. M., LIU, S. H., LIAU, C. S., HUANG, P. J. & LIN-SHIAU, S. Y. 2000. High Glucose-Induced Apoptosis in Human Endothelial Cells Is Mediated by Sequential Activations of c-Jun NH2-Terminal Kinase and Caspase-3. *Circulation,* 101, 2618-2624.

HOLLANDS, W. J., HART, D. J., DAINTY, J. R., HASSELWANDER, O., TIIHONEN, K., WOOD, R. & KROON, P. A. 2013. Bioavailability of epicatechin and effects on nitric oxide metabolites of an apple flavanol-rich extract supplemented beverage compared to a whole apple puree: a

randomized, placebo-controlled, crossover trial. *Molecular Nutrition & Food Research,* 57**,** 1209-1217.

HOLLMAN, P. C., DE VRIES, J. H., VAN LEEUWEN, S. D., MENGELERS, M. J. & KATAN, M. B. 1995. Absorption of dietary quercetin glycosides and quercetin in healthy ileostomy volunteers. *The American Journal of Clinical Nutrition,* 62**,** 1276-82.

HOOPER, L., KROON, P. A., RIMM, E. B., COHN, J. S., HARVEY, I., LE CORNU, K. A., RYDER, J. J., HALL, W. L. & CASSIDY, A. 2008. Flavonoids, flavonoid-rich foods, and cardiovascular risk: a meta-analysis of randomized controlled trials. *The American Journal of Clinical Nutrition,* 88**,** 38-50.

HSIEH, C.-L., HUANG, C.-N., LIN, Y.-C. & PENG, R. Y. 2007. Molecular Action Mechanism against Apoptosis by Aqueous Extract from Guava Budding Leaves Elucidated with Human Umbilical Vein Endothelial Cell (HUVEC) Model. *Journal of Agricultural and Food Chemistry,* 55**,** 8523-8533.

HUG, D. H., ROTH, D. & HUNTER, J. 1968. Regulation of Histidine Catabolism by Succinate in Pseudomonas putida. *Journal of Bacteriology,* 96**,** 396-402.

HUNT, T. K., ASLAM, R. S., BECKERT, S., WAGNER, S., GHANI, Q. P., HUSSAIN, M. Z., ROY, S. & SEN, C. K. 2007. Aerobically Derived Lactate Stimulates Revascularization and Tissue Repair via Redox Mechanisms *Antioxidants & Redox Signaling,* 9**,** 1115-1124. .

IBÁÑEZ, C., SIMÓ, C., GARCÍA-CAÑAS, V., GÓMEZ-MARTÍNEZ, Á., FERRAGUT, J. A. & CIFUENTES, A. 2012. CE/LC-MS multiplatform for broad metabolomic analysis of dietary polyphenols effect on colon cancer cells proliferation. *ELECTROPHORESIS,* 33**,** 2328-2336.

IQBAL, J. & ZAIDI, M. 2006. TNF regulates cellular NAD+ metabolism in primary macrophages. *Biochemical and Biophysical Research Communications,* 342**,** 1312-1318.

IRANI, N., WIRTH, M., VAN DEN HEUVEL, J. & WAGNER, R. 1999. Improvement of the primary metabolism of cell cultures by introducing a new cytoplasmic pyruvate carboxylase reaction. *Biotechnology and Bioengineering,* 66**,** 238-246.

ITO, M., KONDO, Y., NAKATANI, A., HAYASHI, K. & NARUSE, A. 2001. Characterization of low dose streptozotocin-induced progressive diabetes in mice. *Environmental Toxicology and Pharmacology,* 9**,** 71-78.

JEONG, I.-K., OH, D. H., PARK, S.-J., KANG, J.-H., KIM, S., LEE, M.-S., KIM, M.-J., HWANG, Y.-C., AHN, K. J., CHUNG, H.-Y., CHAE, M.-K. & YOO, H.-J. 2011. Inhibition of NF-[kappa]B prevents high glucose-induced proliferation and plasminogen activator inhibitor-1 expression in vascular smooth muscle cells. *Exp Mol Med,* 43**,** 684-692.

KAHLE, K., HUEMMER, W., KEMPF, M., SCHEPPACH, W., ERK, T. & RICHLING, E. 2007. Polyphenols Are Intensively Metabolized in the Human Gastrointestinal Tract after Apple Juice Consumption. *Journal of Agricultural and Food Chemistry,* 55**,** 10605-10614.

KAHLE, K., KRAUS, M., SCHEPPACH, W. & RICHLING, E. 2005. Colonic availability of apple polyphenols - A study in ileostomy subjects. *Molecular Nutrition & Food Research,* 49**,** 1143-1150.

KAN, O., BALDWIN, S. A. & WHETTON, A. D. 1994. Apoptosis is regulated by the rate of glucose transport in an interleukin 3 dependent cell line. *The Journal of Experimental Medicine,* 180**,** 917-923.

KANEIDER, N. C., EGGER, P., DUNZENDORFER, S., NORIS, P., BALDUINI, C. L., GRITTI, D., RICEVUTI, G. & WIEDERMANN, C. J. 2002. Reversal of Thrombin-Induced Deactivation of CD39/ATPDase in Endothelial Cells by HMG-CoA Reductase Inhibition: Effects on Rho-GTPase and Adenosine Nucleotide Metabolism. *Arteriosclerosis, Thrombosis, and Vascular Biology,* 22**,** 894-900.

KANEIDER, N. C., MOSHEIMER, B., REINISCH, N., PATSCH, J. R. & WIEDERMANN, C. J. 2004. Inhibition of thrombin-induced signaling by resveratrol and quercetin: effects on adenosine nucleotide metabolism in endothelial cells and platelet-neutrophil interactions. *Thrombosis Research,* 114**,** 185-194.

KANETO HIDEAKI, N. Y., KAWAMORI DAN, MIYATSUKA TAKESHI, MATSUAKO TAKA-AKI 2004. Involvement of Oxidative Stress and the JNK Pathhway in Glucose Toxicity. *The Review of Diabetic Studies,* 1**,** 165-174.

KAVUTCU, M. & MELZIG, M. F. 1999. In vitro effects of selected flavonoids on the 5'-nucleotidase activity. *Pharmazie,* 54**,** 457-9.

KAWAI, N., FUJIBAYASHI, Y., KUWABARA, S., TAKAO, K.-I., IJUIN, Y. & KOBAYASHI, S. 2000. Synthesis of a Potential Key Intermediate of Akaterpin, Specific Inhibitor of PI-PLC. *Tetrahedron,* 56**,** 6467-6478.

KAWASHIMA, Y., NAGASAWA, T. & NINOMIYA, H. 2000. Contribution of ecto-5′-nucleotidase to the inhibition of platelet aggregation by human endothelial cells. *Blood,* 96**,** 2157-2162.

KELLY, E., GREENE, C. M., CARROLL, T. P., MCELVANEY, N. G. & O'NEILL, S. J. 2010. Alpha-1 antitrypsin deficiency. *Respiratory Medicine,* 104**,** 763-772.

KHAN, A. U., DELUDE, R. L., HAN, Y. Y., SAPPINGTON, P. L., HAN, X., CARCILLO, J. A. & FINK, M. P. 2002. Liposomal NAD+ prevents diminished O2consumption by immunostimulated Caco-2 cells. *American Journal of Physiology - Lung Cellular and Molecular Physiology,* 282**,** L1082-L1091.

KIERDASZUK, B., MODRAK-WÓJCIK, A. & SHUGAR, D. 1997. Binding of phosphate and sulfate anions by purine nucleoside phosphorylase from E. coli: ligand-dependent quenching of enzyme intrinsic fluorescence. *Biophysical Chemistry,* 63**,** 107-118.

KIM, Y. K., LEE, M.-S., SON, S. M., KIM, I. J., LEE, W. S., RHIM, B. Y., HONG, K. W. & KIM, C. D. 2002. Vascular NADH Oxidase Is Involved in Impaired Endothelium-Dependent Vasodilation in OLETF Rats, a Model of Type 2 Diabetes. *Diabetes,* 51**,** 522-527.

KNEKT, P., KUMPULAINEN, J., JÄRVINEN, R., RISSANEN, H., HELIÖVAARA, M., REUNANEN, A., HAKULINEN, T. & AROMAA, A. 2002. Flavonoid intake and risk of chronic diseases. *The American Journal of Clinical Nutrition,* 76**,** 560-568.

KOBUCHI, H., ROY, S., SEN, C. K., NGUYEN, H. G. & PACKER, L. 1999. Quercetin inhibits inducible ICAM-1 expression in human endothelial cells through the JNK pathway. *American Journal of Physiology - Cell Physiolog,* 277**,** C403-C411.

KOVACS, H., MOSKAU, D. & SPRAUL, M. 2005. Cryogenically cooled probes—a leap in NMR technology. *Progress in Nuclear Magnetic Resonance Spectroscopy,* 46**,** 131-155.

KROON, P. A., CLIFFORD, M. N., CROZIER, A., DAY, A. J., DONOVAN, J. L., MANACH, C. & WILLIAMSON, G. 2004. How should we assess the effects

of exposure to dietary polyphenols in vitro? *The American Journal of Clinical Nutrition,* 80**,** 15-21.

KUMAR, V. B. S., VIJI, R. I., KIRAN, M. S. & SUDHAKARAN, P. R. 2007. Endothelial cell response to lactate: Implication of PAR modification of VEGF. *Journal of Cellular Physiology,* 211**,** 477-485.

LAKKA, H., LAAKSONEN, D. E., LAKKA, T. A. & ET AL. 2002. THe metabolic syndrome and total and cardiovascular disease mortality in middle-aged men. *JAMA,* 288**,** 2709-2716.

LANDMESSER, U., HORNIG, B. & DREXLER, H. 2004. Endothelial Function: A Critical Determinant in Atherosclerosis? *Circulation,* 109**,** II-27-33.

LAPA, F., DA SILVA, M., DE ALMEIDA CABRINI, D. & SANTOS, A. 2012. Anti-inflammatory effects of purine nucleosides, adenosine and inosine, in a mouse model of pleurisy: evidence for the role of adenosine A₂ receptors. *Purinergic Signalling,* 1-12.

LECHLEITNER, M., KOCH, T., HEROLD, M., DZIEN, A. & HOPPICHLER, F. 2000. Tumour necrosis factor-alpha plasma level in patients with type 1 diabetes mellitus and its association with glycaemic control and cardiovascular risk factors. *Journal of Internal Medicine,* 248**,** 67-76.

LEE, Y. J., KANG, D. G., KIM, J. S. & LEE, H. S. 2008a. Effect of Buddleja officinalis on High-Glucose-Induced Vascular Inflammation in Human Umbilical Vein Endothelial Cells. *Exp. Biol. Med.,* 233**,** 694-700.

LEE, Y. J., KANG, D. G., KIM, J. S. & LEE, H. S. 2008b. <I>Buddleja officinalis</I> inhibits high glucose-induced matrix metalloproteinase activity in human umbilical vein endothelial cells. *Phytotherapy Research,* 22**,** 1655-1659.

LEUNIG, A., STAUB, F., PLESNILA, N., PETERS, J., FEYH, J. & GOETZ, A. 1996. Effect of photodynamic treatment of human endothelial cells on cell volume and cell viability. *International Journal of Oncology,* 8**,** 1217-1221.

LEVINE, B. & YUAN, J. 2005. Autophagy in cell death: an innocent convict? *The Journal of Clinical Investigation,* 115**,** 2679-2688.

LI, J.-M. & SHAH, A. M. 2003. ROS Generation by Nonphagocytic NADPH Oxidase: Potential Relevance in Diabetic Nephropathy. *J Am Soc Nephrol,* 14**,** S221-226.

LIAUDET, L., MABLEY, J. G., PACHER, P., VIRÁG, L., SORIANO, F. G., MARTON, A., HASKÓ, G., DEITCH, E. A. & SZABÓ, C. 2002. Inosine Exerts a Broad Range of Antiinflammatory Effects in a Murine Model of Acute Lung Injury. *Annals of Surgery,* 235**,** 568-578.

LIBBY, P., RIDKER, P. M. & MASERI, A. 2002. Inflammation and Atherosclerosis. *Circulation,* 105**,** 1135-1143.

LOKE, W. M., PROUDFOOT, J. M., MCKINLEY, A. J., NEEDS, P. W., KROON, P. A., HODGSON, J. M. & CROFT, K. D. 2008. Quercetin and Its In Vivo Metabolites Inhibit Neutrophil-Mediated Low-Density Lipoprotein Oxidation. *Journal of Agricultural and Food Chemistry,* 56**,** 3609-3615.

LOTITO, S. B., ZHANG, W.-J., YANG, C. S., CROZIER, A. & FREI, B. 2011. Metabolic conversion of dietary flavonoids alters their anti-inflammatory and antioxidant properties. *Free Radical Biology and Medicine,* 51**,** 454-463.

LUM, J. J., BAUER, D. E., KONG, M., HARRIS, M. H., LI, C., LINDSTEN, T. & THOMPSON, C. B. 2005. Growth Factor Regulation of Autophagy and Cell Survival in the Absence of Apoptosis. *Cell,* 120**,** 237-248.

LUSH, C. W., CEPINSKAS, G. & KVIETYS, P. R. 2000. LPS tolerance in human endothelial cells: reduced PMN adhesion, E-selectin expression, and NF-kappa B mobilization. *Am J Physiol Heart Circ Physiol,* 278**,** H853-861.

MA, L., GAO, H.-Q., LI, B.-Y., MA, Y.-B., YOU, B.-A. & ZHANG, F.-L. 2007. Grape Seed Proanthocyanidin Extracts Inhibit Vascular Cell Adhesion Molecule Expression Induced by Advanced Glycation End Products Through Activation of Peroxisome Proliferators-Activated Receptor [gamma]. *Journal of Cardiovascular Pharmacology,* 49**,** 293-298 10.1097/FJC.0b013e31803c5616.

MAJUMDAR, S. & AGGARWAL, B. B. 2003. Adenosine suppresses activation of nuclear factor-[kappa]B selectively induced by tumor necrosis factor in different cell types. *Oncogene,* 22**,** 1206-1218.

MANACH, C., SCALBERT, A., MORAND, C., REMESY, C. & JIMENEZ, L. 2004. Polyphenols: food sources and bioavailability. *American Journal of Clinical Nutrition,* 79**,** 727-747.

MANACH, C., WILLIAMSON, G., MORAND, C., SCALBERT, A. & RÉMÉSY, C. 2005. Bioavailability and bioefficacy of polyphenols in humans. I. Review of 97 bioavailability studies. *The American Journal of Clinical Nutrition,* 81**,** 230S-242S.

MANNARINO, E. & PIRRO, M. 2008. Molecular biology of atherosclerosis

Clinical Cases in Mineral and Bone Metabolism, 5**,** 57-62.

MARIN-VALENCIA, I., ROE, C. R. & PASCUAL, J. M. 2010. Pyruvate carboxylase deficiency: Mechanisms, mimics and anaplerosis. *Molecular Genetics and Metabolism,* 101**,** 9-17.

MARTINEAU, E., TEA, I., LOAËC, G., GIRAUDEAU, P. & AKOKA, S. 2011. Strategy for choosing extraction procedures for NMR-based metabolomic analysis of mammalian cells. *Analytical and Bioanalytical Chemistry,* 401**,** 2133-2142.

MARTÍNEZ-MARTÍN, N., BLAS-GARCÍA, A., MORALES, J. M., MARTI-CABRERA, M., MONLEÓN, D. & APOSTOLOVA, N. 2012. Metabolomics of the effect of AMPK activation by AICAR on human umbilical vein endothelial cells. *International journal of molecular medicine,* 29**,** 88-94.

MASSIMI, M., TOMASSINI, A., SCIUBBA, F., SOBOLEV, A. P., DEVIRGILIIS, L. C. & MICCHELI, A. 2012. Effects of resveratrol on HepG2 cells as revealed by 1H-NMR based metabolic profiling. *Biochimica et Biophysica Acta (BBA) - General Subjects,* 1820**,** 1-8.

MAYER, R., STECHER, G., WUERZNER, R., SILVA, R. C., SULTANA, T., TROJER, L., FEUERSTEIN, I., KRIEG, C., ABEL, G., POPP, M., BOBLETER, O. & BONN, G. K. 2008. Proanthocyanidins: Target Compounds as Antibacterial Agents. *Journal of Agricultural and Food Chemistry,* 56**,** 6959-6966.

MCCULLOUGH, M. L., PETERSON, J. J., PATEL, R., JACQUES, P. F., SHAH, R. & DWYER, J. T. 2012. Flavonoid intake and cardiovascular disease mortality in a prospective cohort of US adults. *The American Journal of Clinical Nutrition,* 95**,** 454-464.

MCGINN, S., SAAD, S., PORONNIK, P. & POLLOCK, C. A. 2003. High glucose-mediated effects on endothelial cell proliferation occur via p38 MAP kinase. *Am J Physiol Endocrinol Metab,* 285**,** E708-717.

MELZIG, M. F. 1996. Inhibition of Adenosine Deaminase Activity of Aortic Endothelial Cells by Selected Flavonoids. *Planta Med,* 62**,** 20,21.

MESSANA, I., FORNI, F., FERRARI, F., ROSSI, C., GIARDINA, B. & ZUPPI, C. 1998. Proton nuclear magnetic resonance spectral profiles of urine in type II diabetic patients. *Clinical Chemistry,* 44**,** 1529-1534.

MICCHELI, A. T., MICCHELI, A., DI CLEMENTE, R., VALERIO, M., COLUCCIA, P., BIZZARRI, M. & CONTI, F. 2006. NMR-based metabolic profiling of human hepatoma cells in relation to cell growth by culture media analysis. *Biochimica Et Biophysica Acta-General Subjects,* 1760**,** 1723-1731.

MIDDLETON, E. & ANNE, S. 1995. Quercetin Inhibits Lipopolysaccharide Induced Expression of Endothelial Cell Intracellular Adhesion Molecule-1. *International Archive of Allergy Immunology,* 107**,** 435-436.

MILSTIEN, S. & KATUSIC, Z. 1999. Oxidation of Tetrahydrobiopterin by Peroxynitrite: Implications for Vascular Endothelial Function. *Biochemical and Biophysical Research Communications,* 263**,** 681-684.

MINK, P. J., SCRAFFORD, C. G., BARRAJ, L. M., HARNACK, L., HONG, C.-P., NETTLETON, J. A. & JACOBS, D. R. 2007. Flavonoid intake and cardiovascular disease mortality: a prospective study in postmenopausal women. *The American Journal of Clinical Nutrition,* 85**,** 895-909.

MODRAK-WÓJCIK, A., KIRILENKO, A., SHUGAR, D. & KIERDASZUK, B. 2008. Role of ionization of the phosphate cosubstrate on phosphorolysis by purine nucleoside phosphorylase (PNP) of bacterial (<i>E. coli) and mammalian (human) origin. *European Biophysics Journal,* 37**,** 153-164.

MORTUZA, R., CHEN, S., FENG, B., SEN, S. & CHAKRABARTI, S. 2013. High Glucose Induced Alteration of SIRTs in Endothelial Cells Causes Rapid Aging in a p300 and FOXO Regulated Pathway. *PLoS ONE,* 8**,** e54514.

MULLEN, W., EDWARDS, C. A. & CROZIER, A. 2006. Absorption, excretion and metabolite profiling of methyl-, glucuronyl-, glucosyl- and sulpho-conjugates of quercetin in human plasma and urine after ingestion of onions. *British Journal of Nutrition,* 96**,** 107-116.

MUROTA, K. & TERAO, J. 2003. Antioxidative flavonoid quercetin: implication of its intestinal absorption and metabolism. *Archives of Biochemistry and Biophysics,* 417**,** 12-17.

MUTIN, M., GEORGE, F., LESAULE, G. & SAMPOL, J. 1996. Reevaluation of Trypsin-EDTA for Endothelial Cell Detachment before Flow Cytometry Analysis. *Endothelium: Journal of Endothelial Cell Research,* 4**,** 289 - 295.

NAIR, M. P., MAHAJAN, S., REYNOLDS, J. L., AALINKEEL, R., NAIR, H., SCHWARTZ, S. A. & KANDASWAMI, C. 2006. The Flavonoid Quercetin Inhibits Proinflammatory Cytokine (Tumor Necrosis Factor Alpha) Gene Expression in Normal Peripheral Blood Mononuclear Cells via Modulation of the NF-κβ System. *Clinical and Vaccine Immunology,* 13**,** 319-328.

NEEDS, P. W. & KROON, P. A. 2006. Convenient syntheses of metabolically important quercetin glucuronides and sulfates. *Tetrahedron,* 62**,** 6862-6868.

NÉMETH, K., PLUMB, G. W., BERRIN, J.-G., JUGE, N., JACOB, R., NAIM, H. Y., WILLIAMSON, G., SWALLOW, D. M. & KROON, P. A. 2003. Deglycosylation by small intestinal epithelial cell β-glucosidases is a critical step in the absorption and metabolism of dietary flavonoid glycosides in humans. *European Journal of Nutrition,* 42**,** 29-42.

NEWLAND, M., GREENFIELD, P. F. & REID, S. 1990. Hybridoma growth limitations: The roles of energy metabolism and ammonia production. *Cytotechnology,* 3**,** 215-229.

NICHOLS M, T. N., LUENGO-FERNANDEZ R, LEAL J, GRAY A, SCARBOROUGH P, RAYNER M 2012. European Cardiovascular Disease Statistics 2012. *European Heart Network, Brussels, European Society of Cardiology, Sophia Antipolis.*

NIKLAS, J., NONNENMACHER, Y., ROSE, T., SANDIG, V. & HEINZLE, E. 2012a. Quercetin treatment changes fluxes in the primary metabolism and increases culture longevity and recombinant α1-antitrypsin production in human AGE1.HN cells. *Applied Microbiology and Biotechnology,* 94**,** 57-67.

NIKLAS, J., PRIESNITZ, C., ROSE, T., SANDIG, V. & HEINZLE, E. 2012b. Primary metabolism in the new human cell line AGE1.HN at various substrate levels: increased metabolic efficiency and α$_1$-antitrypsin production at reduced pyruvate load. *Applied Microbiology and Biotechnology,* 93**,** 1637-1650.

NIKLAS, J., PRIESNITZ, C., ROSE, T., SANDIG, V. & HEINZLE, E. 2013. Metabolism and metabolic burden by α1-antitrypsin production in human AGE1.HN cells. *Metabolic Engineering,* 16**,** 103-114.

NIKLAS, J., SANDIG, V. & HEINZLE, E. 2011. Metabolite channeling and compartmentation in the human cell line AGE1.HN determined by 13C labeling experiments and 13C metabolic flux analysis. *Journal of Bioscience and Bioengineering,* 112**,** 616-623.

NILSSON, J., JOVINGE, S., NIEMANN, A., RENELAND, R. & LITHELL, H. 1998. Relation Between Plasma Tumor Necrosis Factor-α and Insulin Sensitivity in Elderly Men With Non–Insulin-Dependent Diabetes Mellitus. *Arteriosclerosis, Thrombosis, and Vascular Biology,* 18**,** 1199-1202.

NOZAKI, A., HORI, M., KIMURA, T., ITO, H. & HATANO, T. 2009. Interaction of Polyphenols with Proteins: Binding of (−)-Epigallocatechin Gallate to Serum Albumin, Estimated by Induced Circular Dichroism. *Chemical and Pharmaceutical Bulletin,* 57**,** 224-228.

OLTHOF, M. R., HOLLMAN, P. C. H., BUIJSMAN, M. N. C. P., VAN AMELSVOORT, J. M. M. & KATAN, M. B. 2003. Chlorogenic Acid, Quercetin-3-Rutinoside and Black Tea Phenols Are Extensively Metabolized in Humans. *The Journal of Nutrition,* 133**,** 1806-1814.

OSAR, Z., SAMANCI, T., #XFC, LAY, DEMIREL, G., #XFC, YANIKKAYA, L., DAMCI, T. & ILKOVA, H. 2004. Nicotinamide Effects Oxidative Burst Activity of Neutrophils in Patients with Poorly Controlled Type 2 Diabetes Mellitus. *Experimental Diabesity Research,* 5**,** 155-162.

OU, H.-C., CHOU, F.-P., SHEEN, H.-M., LIN, T.-M., YANG, C.-H. & HUEY-HERNG SHEU, W. 2006. Resveratrol, a polyphenolic compound in red wine, protects against oxidized LDL-induced cytotoxicity in endothelial cells. *Clinica Chimica Acta,* 364**,** 196-204.

OZTURK, S. S., RILEY, M. R. & PALSSON, B. O. 1992. Effects of ammonia and lactate on hybridoma growth, metabolism, and antibody production. *Biotechnology and Bioengineering,* 39**,** 418-431.

PAN, M., WASA, M. & SOUBA, W. W. 1995. Tumor Necrosis Factor Stimulates System X-AG Transport Activity in Human Endothelium. *Journal of Surgical Research,* 58**,** 659-664.

PANIERI, E., TOIETTA, G., MELE, M., LABATE, V., RANIERI, S. C., FUSCO, S., TESORI, V., ANTONINI, A., MAULUCCI, G., DE SPIRITO, M., GALEOTTI, T. & PANI, G. 2010. Nutrient withdrawal rescues growth factor-deprived cells from mTOR-dependent damage. *Aging,* 2**,** 487-503.

PARK, J. S., KIM, K. M., KIM, M. H., CHANG, H. J., BAEK, M. K., KIM, S. M. & JUNG, Y. D. 2009. Resveratrol Inhibits Tumor Cell Adhesion to Endothelial Cells by Blocking ICAM-1 Expression. *Anticancer Research,* 29**,** 355-362.

PAUFF, J. M. & HILLE, R. 2009. Inhibition Studies of Bovine Xanthine Oxidase by Luteolin, Silibinin, Quercetin, and Curcumin. *Journal of Natural Products,* 72**,** 725-731.

PEARSON, D. A., PAGLIERONI, T. G., REIN, D., WUN, T., SCHRAMM, D. D., WANG, J. F., HOLT, R. R., GOSSELIN, R., SCHMITZ, H. H. & KEEN, C. L. 2002. The effects of flavanol-rich cocoa and aspirin on ex vivo platelet function. *Thrombosis Research,* 106**,** 191-197.

PÉREZ-JIMÉNEZ, J., FEZEU, L., TOUVIER, M., ARNAULT, N., MANACH, C., HERCBERG, S., GALAN, P. & SCALBERT, A. 2011. Dietary intake of 337 polyphenols in French adults. *The American Journal of Clinical Nutrition,* 93**,** 1220-1228.

PEREZ-JIMENEZ, J., NEVEU, V., VOS, F. & SCALBERT, A. 2010. Identification of the 100 richest dietary sources of polyphenols: an application of the Phenol-Explorer database. *Eur J Clin Nutr,* 64**,** S112-S120.

PETERS, K., KAMP, G., BERZ, A., UNGER, R. E., BARTH, S., SALAMON, A., RYCHLY, J. & KIRKPATRICK, J. C. 2009. Changes in Human Endothelial Cell Energy Metabolic Capacities during in vitro Cultivation. The Role of "Aerobic Glycolysis" and Proliferation. *Cellular Physiology and Biochemistry,* 24**,** 483-492.

PETRACHE, I., HAJJAR, J. & CAMPOS, M. 2009. Safety and efficacy of alpha-1-antitrypsin augmentation therapy in the treatment of patients with alpha-1-antitrypsin deficiency. *Biologics: Targets & Therapy,* 3**,** 193-204.

PHAM, A., BORTOLAZZO, A. & WHITE, J. B. 2012. Rapid dimerization of quercetin through an oxidative mechanism in the presence of serum albumin decreases its ability to induce cytotoxicity in MDA-MB-231 cells. *Biochemical and Biophysical Research Communications,* 427**,** 415-420.

PICONI, L., CORGNALI, M., DA ROS, R., ASSALONI, R., PILIEGO, T. & CERIELLO, A. 2004. The protective effect of rosuvastatin in human umbilical endothelial cells exposed to constant or intermittent high glucose. *Journal of Diabetes and its Complications,* 22**,** 38-45.

PINENT, M., BLAY, M., BLADE, M. C., SALVADO, M. J., AROLA, L. & ARDEVOL, A. 2004. Grape Seed-Derived Procyanidins Have an Antihyperglycemic Effect in Streptozotocin-Induced Diabetic Rats and Insulinomimetic Activity in Insulin-Sensitive Cell Lines. *Endocrinology,* 145**,** 4985-4990.

PORTER, K. J., GONIPETA, B., PARVATANENI, S., APPLEDORN, D. M., PATIAL, S., SHARMA, D., GANGUR, V., AMALFITANO, A. & PARAMESWARAN, N. 2010. Regulation of lipopolysaccharide-induced inflammatory response and endotoxemia by β-arrestins. *Journal of Cellular Physiology,* 225**,** 406-416.

PREINERSTORFER, B., SCHIESEL, S., LÄMMERHOFER, M. & LINDNER, W. 2010. Metabolic profiling of intracellular metabolites in fermentation broths from β-lactam antibiotics production by liquid chromatography–tandem mass spectrometry methods. *Journal of Chromatography A,* 1217**,** 312-328.

PRIEUR, C., RIGAUD, J., CHEYNIER, V. & MOUTOUNET, M. 1994. Oligomeric and polymeric procyanidins from grape seeds. *Phytochemistry,* 36**,** 781-784.

PRIOR, R. L. & GU, L. 2005. Occurrence and biological significance of proanthocyanidins in the American diet. *Phytochemistry,* 66**,** 2264-2280.

PUEBLA, C., FARÍAS, M., GONZÁLEZ, M., VECCHIOLA, A., AGUAYO, C., KRAUSE, B., PASTOR-ANGLADA, M., CASANELLO, P. & SOBREVIA, L. 2008. High D-glucose reduces SLC29A1 promoter activity and adenosine

transport involving specific protein 1 in human umbilical vein endothelium. *Journal of Cellular Physiology,* 215**,** 645-656.

QIAN, S., HUO, D., WANG, S. & QIAN, Q. 2011. Inhibition of glucose-induced vascular endothelial growth factor expression by Salvia miltiorrhiza hydrophilic extract in human microvascular endothelial cells: Evidence for mitochondrial oxidative stress. *Journal of Ethnopharmacology,* 137**,** 985-991.

RAJARAJESWARI, D., RAMALINGAM, K., KRISHNAMMA, M. & SHARMILA KRISHNA, T. 2011. ASSOCIATION OF TNF-A WITH OBESITY IN TYPE2-DIABETES MELLITUS. *International Journal of Pharma and Bio Sciences* 2**,** 352-357.

RALEVIC, V. & BURNSTOCK, G. 1998. Receptors for Purines and Pyrimidines. *Pharmacological Reviews,* 50**,** 413-492.

RAMIRO-PUIG, E. & CASTELL, M. 2009. Cocoa: antioxidant and immunomodulator. *British Journal of Nutrition,* 101**,** 931-940.

RAMUSSEN, L. M., SCHMITZ, O. & LEDET, T. 2002. Increased expression of vascular cell adhesion molecule-1 (VCAM-1) in cultured endothelial cells exposed to serum from type 1 diabetic patients: no effects of high glucose concentrations. *Scandinavian Journal of Clinical & Laboratory Investigation,* 62**,** 485-493.

RAWEL, H. M., MEIDTNER, K. & KROLL, J. 2005. Binding of Selected Phenolic Compounds to Proteins. *Journal of Agricultural and Food Chemistry,* 53**,** 4228-4235.

REIN, D., LOTITO, S., HOLT, R. R., KEEN, C. L., SCHMITZ, H. H. & FRAGA, C. G. 2000. Epicatechin in Human Plasma: In Vivo Determination and Effect of Chocolate Consumption on Plasma Oxidation Status. *The Journal of Nutrition,* 130**,** 2109S-2114S.

REUSCH, J. E.-B. & DRAZNIN, B. B. 2007. Atherosclerosis in diabetes and insulin resistance. *Diabetes, Obesity and Metabolism,* 9**,** 455-463.

RICARDO DA SILVA, J. M., RIGAUD, J., CHEYNIER, V., CHEMINAT, A. & MOUTOUNET, M. 1991. Procyanidin dimers and trimers from grape seeds. *Phytochemistry,* 30**,** 1259-1264.

RICE-EVANS, C. A., MILLER, N. J. & PAGANGA, G. 1996. Structure-antioxidant activity relationships of flavonoids and phenolic acids. *Free Radical Biology and Medicine,* 20**,** 933-956.

RICHARD, L. F., DAHMS, T. E. & WEBSTER, R. O. 1998. Adenosine prevents permeability increase in oxidant-injured endothelial monolayers. *American Journal of Physiology - Heart and Circulatory Physiology,* 274**,** H35-H42.

RIETVELD, A. & WISEMAN, S. 2003. Antioxidant Effects of Tea: Evidence from Human Clinical Trials. *J. Nutr.,* 133**,** 3285S-3292.

RIKSEN, N. P., RONGEN, G. A., BLOM, H. J., RUSSEL, F. G. M., BOERS, G. H. J. & SMITS, P. 2003. Potential role for adenosine in the pathogenesis of the vascular complications of hyperhomocysteinemia. *Cardiovascular Research,* 59**,** 271-276.

RIZZA, S., MUNIYAPPA, R., IANTORNO, M., KIM, J.-A., CHEN, H., PULLIKOTIL, P., SENESE, N., TESAURO, M., LAURO, D., CARDILLO, C. & QUON, M. J. 2011. Citrus Polyphenol Hesperidin Stimulates Production of Nitric Oxide in Endothelial Cells while Improving Endothelial Function and Reducing Inflammatory Markers in Patients with Metabolic Syndrome. *Journal of Clinical Endocrinology & Metabolism,* 96**,** E782-E792.

ROBBINS, R. J., LEONCZAK, J., JOHNSON, J. C., LI, J., KWIK-URIBE, C., PRIOR, R. L. & GU, L. 2009. Method performance and multi-laboratory assessment of a normal phase high pressure liquid chromatography-fluorescence detection method for the quantitation of flavanols and procyanidins in cocoa and chocolate containing samples. *Journal of Chromatography A,* 1216**,** 4831-4840.

ROCHE, H. M., PHILLIPS, C. & GIBNEY, M. J. 2005. The metabolic syndrome: the crossroads of diet and genetics. *Proceedings of the Nutrition Society,* 64**,** 371-377.

ROGERS, S. C., ZHANG, X., AZHAR, G., LUO, S. & WEI, J. Y. 2013. Exposure to High or Low Glucose Levels Accelerates the Appearance of Markers of Endothelial Cell Senescence and Induces Dysregulation of Nitric Oxide Synthase. *The Journals of Gerontology Series A: Biological Sciences and Medical Sciences.*

ROMIER, B., SCHNEIDER, Y.-J., LARONDELLE, Y. & DURING, A. 2009. Dietary polyphenols can modulate the intestinal inflammatory response. *Nutrition Reviews,* 67**,** 363-378.

ROSS, R. 1993. The pathogenesis of atherosclerosis: a perspective of the 1990s. *Nature,* 362**,** 801-809.

ROSS, R. 1999. Atherosclerosis -- An Inflammatory Disease. *N Engl J Med,* 340**,** 115-126.

SAN MARTÍN, R. & SOBREVIA, L. 2006. Gestational diabetes and the adenosine/l-Arginine/nitric oxide (ALANO) pathway in human umbilical vein endothelium. *Placenta,* 27**,** 1-10.

SANO, A., YAMAKOSHI, J., TOKUTAKE, S., TOBE, K., KUBOTA, Y. & KIKUCHI, M. 2003. Procyanidin B1 is detected in human serum after intake of proanthocyanidin-rich grape seed extract. *Bioscience Biotechnology and Biochemistry,* 67**,** 1140-1143.

SCALBERT, A., JOHNSON, I. T. & SALTMARSH, M. 2005. Polyphenols: antioxidants and beyond. *The American Journal of Clinical Nutrition,* 81**,** 215S-217S.

SCALBERT, A., MORAND, C., MANACH, C. & RÈMÈSY, C. 2002. Absorption and metabolism of polyphenols in the gut and impact on health. *Biomedecine & Pharmacotherapy,* 56**,** 276-282.

SCALBERT, A. & WILLIAMSON, G. 2000. Dietary Intake and Bioavailability of Polyphenols. *J. Nutr.,* 130**,** 2073S-2085.

SCHMATZ, R., MANN, T., SPANEVELLO, R., MACHADO, M., ZANINI, D., PIMENTEL, V., STEFANELLO, N., MARTINS, C., CARDOSO, A., BAGATINI, M., GUTIERRES, J., LEAL, C. M., PEREIRA, L., MAZZANTI, C., SCHETINGER, M. & MORSCH, V. 2013. Moderate Red Wine and Grape Juice Consumption Modulates the Hydrolysis of the Adenine Nucleotides and Decreases Platelet Aggregation in Streptozotocin-Induced Diabetic Rats. *Cell Biochemistry and Biophysics,* 65**,** 129-143.

SCHWEIGHOFER, B., TESTORI, J., STURTZEL, C., SATTLER, S., MAYER, H., WAGNER, O., BILBAN, M. & HOFER, E. 2009. The VEGF-induced transcriptional response comprises gene

clusters at the crossroad of angiogenesis and inflammation. *Thrombosis and Haemostasis,* 102**,** 544-554.

SEIFFERT, K., DING, W., WAGNER, J. A. & GRANSTEIN, R. D. 2006. ATP[gamma]S Enhances the Production of Inflammatory Mediators by a

Human Dermal Endothelial Cell Line via Purinergic Receptor Signaling. *J Invest Dermatol,* 126**,** 1017-1027.

SELLICK, C. A., HANSEN, R., MAQSOOD, A. R., DUNN, W. B., STEPHENS, G. M., GOODACRE, R. & DICKSON, A. J. 2008. Effective Quenching Processes for Physiologically Valid Metabolite Profiling of Suspension Cultured Mammalian Cells. *Analytical Chemistry,* 81**,** 174-183.

SELVA, M. L., BELTRAMO, E., PAGNOZZI, F., BENA, E., MOLINATTI, P. A., MOLINATTI, G. M. & PORTA, M. 1996. Thiamine corrects delayed replication and decreases production of lactate and advanced glycation end-products in bovine retinal and human umbilical vein endothelial cells cultured under high glucose conditions. *Diabetologia,* 39**,** 1263-1268.

SELVIN, E., CORESH, J., GOLDEN, S. H., BOLAND, L. L., BRANCATI, F. L. & STEFFES, M. W. 2005. Glycemic Control, Atherosclerosis, and Risk Factors for Cardiovascular Disease in Individuals With Diabetes: The Atherosclerosis Risk in Communities study. *Diabetes Care,* 28**,** 1965-1973.

SEN, C. K. & BAGCHI, D. 2001. Regulation of inducible adhesion molecule expression in human endothelial cells by grape seed proanthocyanidin extract. *Molecular and Cellular Biochemistry,* 216**,** 1-7.

SHEU, M. L., HO, F. M., YANG, R. S., CHAO, K. F., LIN, W. W., LIN-SHIAU, S. Y. & LIU, S.-H. 2005. High Glucose Induces Human Endothelial Cell Apoptosis Through a Phosphoinositide 3-Kinase-Regulated Cyclooxygenase-2 Pathway. *Arterioscler Thromb Vasc Biol,* 25**,** 539-545.

SHI, C., WANG, X., WU, S., ZHU, Y., CHUNG, L. W. K. & MAO, H. 2008. HRMAS 1H-NMR measured changes of the metabolite profile as mesenchymal stem cells differentiate to targeted fat cells in vitro: implications for non-invasive monitoring of stem cell differentiation in vivo. *Journal of Tissue Engineering and Regenerative Medicine,* 2**,** 482-490.

SHI, J., YU, J., POHORLY, J. E. & KAKUDA, Y. 2003. Polyphenolics in Grape Seeds‚ÄîBiochemistry and Functionality. *Journal of Medicinal Food,* 6**,** 291-299.

SHIH, S.-C. & STUTMAN, O. 1996. Cell Cycle-dependent Tumor Necrosis Factor Apoptosis. *Cancer Research,* 56**,** 1591-1598.

SHIRAI, M., YAMANISHI, R., MOON, J.-H., MUROTA, K. & TERAO, J. 2002. Effect of Quercetin and Its Conjugated Metabolite on the Hydrogen Peroxide-induced Intracellular Production of Reactive Oxygen Species in Mouse Fibroblasts. *Bioscience, Biotechnology, and Biochemistry,* 66**,** 1015-1021.

SHOJI, T., MASUMOTO, S., MORIICHI, N., KOBORI, M., KANDA, T., SHINMOTO, H. & TSUSHIDA, T. 2005. Procyanidin Trimers to Pentamers Fractionated from Apple Inhibit Melanogenesis in B16 Mouse Melanoma Cells. *Journal of Agricultural and Food Chemistry,* 53**,** 6105-6111.

SJÖSTRAND, M., HOLMÄNG, A., STRINDBERG, L. & LÖNNROTH, P. 2000. Estimations of muscle interstitial insulin, glucose, and lactate in type 2 diabetic subjects. *American Journal of Physiology - Endocrinology And Metabolism,* 279**,** E1097-E1103.

SON, S. M. 2007. Role of vascular reactive oxygen species in development of vascular abnormalities in diabetes. *Diabetes Research and Clinical Practice,* 77**,** S65-S70.

SPENCER, J. P. E., KUHNLE, G. G. C., WILLIAMS, R. J. & RICE-EVANS, C. 2003. Intracellular metabolism and bioactivity of quercetin and its in vivo metabolites. *Biochem. J.,* 372**,** 173-181.

SPRANGER, J., KROKE, A., MÖHLIG, M., HOFFMANN, K., BERGMANN, M. M., RISTOW, M., BOEING, H. & PFEIFFER, A. F. H. 2003. Inflammatory Cytokines and the Risk to Develop Type 2 Diabetes: Results of the Prospective Population-Based European Prospective Investigation into Cancer and Nutrition (EPIC)-Potsdam Study. *Diabetes,* 52**,** 812-817.

STARY, H., CHANDLER, A., GLAGOV, S., GUYTON, J., INSULL, W., JR, ROSENFELD, M., SCHAFFER, S., SCHWARTZ, C., WAGNER, W. & WISSLER, R. 1994. A definition of initial, fatty streak, and intermediate lesions of atherosclerosis. A report from the Committee on Vascular Lesions of the Council on Arteriosclerosis, American Heart Association. *Circulation,* 89**,** 2462-2478.

STEINBERG, D. 2002. Atherogenesis in perspective: Hypercholesterolemia and inflammation as partners in crime. *Nature Medicine,* 8**,** 1211-1217.

STEINBERGER, J. & DANIELS, S. R. 2003. Obesity, Insulin Resistance, Diabetes, and Cardiovascular Risk in Children: An American Heart Association Scientific Statement From the Atherosclerosis, Hypertension, and Obesity in the Young Committee (Council on Cardiovascular Disease in the Young) and the Diabetes Committee (Council on Nutrition, Physical Activity, and Metabolism). *Circulation,* 107**,** 1448-1453.

STERN, R., SHUSTER, S., NEUDECKER, B. A. & FORMBY, B. 2002. Lactate Stimulates Fibroblast Expression of Hyaluronan and CD44: The Warburg Effect Revisited. *Experimental Cell Research,* 276**,** 24-31.

STORNIOLO, C. E. & MORENO, J. J. 2012. Resveratrol metabolites have an antiproliferative effect on intestinal epithelial cancer cells. *Food Chemistry,* 134**,** 1385-1391.

SUN, J., XU, Y., DAI, Z. & SUN, Y. 2009. Intermittent high glucose enhances proliferation of vascular smooth muscle cells by upregulating osteopontin. *Molecular and Cellular Endocrinology,* 313**,** 64-69.

SUN, J., XU, Y., SUN, S., SUN, Y. & WANG, X. 2010. Intermittent high glucose enhances cell proliferation and VEGF expression in retinal endothelial cells: the role of mitochondrial reactive oxygen species. *Molecular and Cellular Biochemistry,* 343**,** 27-35.

SWEET, I., GILBERT, M., MALONEY, E., HOCKENBERY, D., SCHWARTZ, M. & KIM, F. 2009. Endothelial inflammation induced by excess glucose is associated with cytosolic glucose 6-phosphate but not increased mitochondrial respiration. *Diabetologia,* 52**,** 921-931.

TAKI, H., KASHIWAGI, A., TANAKA, Y. & HORIIKC, K. 1996. Expression of intercellular adhesion molecules 1 (ICAM-1) via an osmotic effect in human umbilical vein endothelial cells exposed to high glucose medium. *Life Sciences,* 58**,** 1713-1721.

TANG, Q., LI, G., WEI, X., ZHANG, J., CHIU, J.-F., HASENMAYER, D., ZHANG, D. & ZHANG, H. 2013. Resveratrol-induced apoptosis is enhanced by inhibition of autophagy in esophageal squamous cell carcinoma. *Cancer Letters,* 336**,** 325-337.

TAYLOR, D. M., MAXWELL, M. M., LUTHI-CARTER, R. & KAZANTSEV, A. G. 2008. Biological and Potential Therapeutic Roles of Sirtuin Deacetylases. *Cellular and Molecular Life Sciences,* 65**,** 4000-4018.

TENG, Q., HUANG, W., COLLETTE, T., EKMAN, D. & TAN, C. 2009. A direct cell quenching method for cell-culture based metabolomics. *Metabolomics,* 5**,** 199-208.

TESFAMARIAM, B. 1994. Free radicals in diabetic endothelial cell dysfunction. *Free Radical Biology and Medicine,* 16**,** 383-391.

TRAKA, M. H., SAHA, S., HUSEBY, S., KOPRIVA, S., WALLEY, P. G., BARKER, G. C., MOORE, J., MERO, G., VAN DEN BOSCH, F., CONSTANT, H., KELLY, L., SCHEPERS, H., BODDUPALLI, S. & MITHEN, R. F. 2013. Genetic regulation of glucoraphanin accumulation in Beneforté® broccoli. *New Phytologist,* 198**,** 1085-1095.

TRIBOLO, S., LODI, F., CONNOR, C., SURI, S., WILSON, V. G., TAYLOR, M. A., NEEDS, P. W., KROON, P. A. & HUGHES, D. A. 2008. Comparative effects of quercetin and its predominant human metabolites on adhesion molecule expression in activated human vascular endothelial cells. *Atherosclerosis,* 197**,** 50-56.

TSANG, C., AUGER, C., MULLEN, W., BORNET, A. L., ROUANET, J.-M., CROZIER, A. & TEISSEDRE, P.-L. 2005. The absorption, metabolism and excretion of flavan-3-ols and procyanidins following the ingestion of a grape seed extract by rats. *British Journal of Nutrition,* 94**,** 170-181.

VALDÉS, A., SIMÓ, C., IBÁÑEZ, C., ROCAMORA-REVERTE, L., FERRAGUT, J. A., GARCÍA-CAÑAS, V. & CIFUENTES, A. 2012. Effect of dietary polyphenols on K562 leukemia cells: A Foodomics approach. *ELECTROPHORESIS,* 33**,** 2314-2327.

VARMA, S., LAL, B. K., ZHENG, R., BRESLIN, J. W., SAITO, S., PAPPAS, P. J., HOBSON, R. W., II & DURAN, W. N. 2005. Hyperglycemia alters PI3k and Akt signaling and leads to endothelial cell proliferative dysfunction. *Am J Physiol Heart Circ Physiol,* 289**,** H1744-1751.

VÁSQUEZ-VIVAR, J., KALYANARAMAN, B., MARTÁSEK, P., HOGG, N., MASTERS, B. S. S., KAROUI, H., TORDO, P. & PRITCHARD, K. A. 1998. Superoxide generation by endothelial nitric oxide synthase: The influence of cofactors. *Proceedings of the National Academy of Sciences of the United States of America,* 95**,** 9220-9225.

VÁSQUEZ, G., SANHUEZA, F., VÁSQUEZ, R., GONZÁLEZ, M., SAN MARTÍN, R., CASANELLO, P. & SOBREVIA, L. 2004. Role of adenosine transport in gestational diabetes-induced l-arginine transport and nitric oxide synthesis in human umbilical vein endothelium. *The Journal of Physiology,* 560**,** 111-122.

VÉGRAN, F., BOIDOT, R., MICHIELS, C., SONVEAUX, P. & FERON, O. 2011. Lactate influx through the endothelial cell monocarboxylate transporter MCT1 supports an NF-kappaB/IL-8 pathway that drives tumor angiogenesis. *Cancer Research.*

VERGHESE, M. W., KNEISLER, T. B. & BOUCHERON, J. A. 1996. P2U Agonists Induce Chemotaxis and Actin Polymerization in Human Neutrophils and Differentiated HL60 Cells. *Journal of Biological Chemistry,* 271**,** 15597-15601.

WAHYUDI, S. & SARGOWO, D. 2007. Green Tea Polyphenols Inhibit Oxidized LDL-induced

NF-KB Activation in Human Umbilical Vein Endothelial Cells. *Acta Medica Indonesiana,* 39**,** 66-70.

WAKABAYASHI, I. & TAKEDA, Y. 2013. Inhibitory effects of resveratrol on MCP-1, IL-6, and IL-8 production in human coronary artery smooth muscle cells. *Naunyn-Schmiedeberg's Archives of Pharmacology,* 386**,** 835-839.

WANG, D., YANG, H., DE BRAGANCA, K. C., LU, J., YU SHIH, L., BRIONES, P., LANG, T. & DE VIVO, D. C. 2008. The molecular basis of pyruvate

carboxylase deficiency: Mosaicism correlates with prolonged survival. *Molecular Genetics and Metabolism, 95,* 31-38.

WANG, L., ZHU, L.-H., JIANG, H., TANG, Q.-Z., YAN, L., WANG, D., LIU, C., BIAN, Z.-Y. & LI, H. 2010. Grape seed proanthocyanidins attenuate vascular smooth muscle cell proliferation via blocking phosphatidylinositol 3-kinase-dependent signaling pathways. *Journal of Cellular Physiology,* 223, 713-726.

WESTON, G. C., HAVIV, I. & ROGERS, P. A. W. 2002. Microarray analysis of VEGF-responsive genes in myometrial endothelial cells. *Molecular Human Reproduction,* 8, 855-863.

WEYBRIGHT, P., MILLIS, K., CAMPBELL, N., CORY, D. G. & SINGER, S. 1998. Gradient, high-resolution, magic angle spinning 1H nuclear magnetic resonance spectroscopy of intact cells. *Magnetic Resonance in Medicine,* 39, 337-345.

WILLIAMS, S. B., CUSCO, J. A., RODDY, M.-A., JOHNSTONE, M. T. & CREAGER, M. A. 1996. Impaired nitric oxide-mediated vasodilation in patients with non-insulin-dependent diabetes mellitus. *Journal of the American College of Cardiology,* 27, 567-574.

WILLIAMSON, G. & MANACH, C. 2005. Bioavailability and bioefficacy of polyphenols in humans. II. Review of 93 intervention studies. *The American Journal of Clinical Nutrition,* 81, 243S-255S.

WINTERBONE, M. S., TRIBOLO, S., NEEDS, P. W., KROON, P. A. & HUGHES, D. A. 2009. Physiologically relevant metabolites of quercetin have no effect on adhesion molecule or chemokine expression in human vascular smooth muscle cells. *Atherosclerosis,* 202, 431-438.

WOLFF, S. P. & DEAN, R. T. 1987. Glucose autoxidation and protein modification. The potential role of 'autoxidative glycosylation' in diabetes. *Biochem. J.,* 245, 243-250.

WOULFE, D., YANG, J. & BRASS, L. 2001. ADP and platelets: the end of the beginning. *The Journal of Clinical Investigation,* 107, 1503-1505.

WU, N., ZU, Y., FU, Y., KONG, Y., ZHAO, J., LI, X., LI, J., WINK, M. & EFFERTH, T. 2010. Antioxidant Activities and Xanthine Oxidase Inhibitory Effects of Extracts and Main Polyphenolic Compounds Obtained from Geranium sibiricum L. *Journal of Agricultural and Food Chemistry,* 58, 4737-4743.

XU, R.-H., PELICANO, H., ZHOU, Y., CAREW, J. S., FENG, L., BHALLA, K. N., KEATING, M. J. & HUANG, P. 2005. Inhibition of Glycolysis in Cancer Cells: A Novel Strategy to Overcome Drug Resistance Associated with Mitochondrial Respiratory Defect and Hypoxia. *Cancer Research,* 65, 613-621.

YAJNIK, C. S., GODBOLE, K., OTIV, S. R. & LUBREE, H. G. 2007. Fetal Programming of Type 2 Diabetes. *Diabetes Care,* 30, 2754-2755.

YANG, M. & BUTLER, M. 2000. Effects of ammonia on CHO cell growth, erythropoietin production, and glycosylation. *Biotechnology and Bioengineering,* 68, 370-380.

YANG, Z., MO, X., GONG, Q., PAN, Q., YANG, X., CAI, W., LI, C., MA, J.-X., HE, Y. & GAO, G. 2008. Critical effect of VEGF in the process of endothelial cell apoptosis induced by high glucose. *Apoptosis,* 13, 1331-1343.

YAO, L. H., JIANG, Y. M., SHI, J., TOMÁS-BARBERÁN, F. A., DATTA, N., SINGANUSONG, R. & CHEN, S. S. 2004. Flavonoids in Food and Their Health Benefits. *Plant Foods for Human Nutrition (Formerly Qualitas Plantarum),* 59, 113-122.

YAWATA, I., TAKEUCHI, H., DOI, Y., LIANG, J., MIZUNO, T. & SUZUMURA, A. 2008. Macrophage-induced neurotoxicity is mediated by glutamate and attenuated by glutaminase inhibitors and gap junction inhibitors. *Life Sciences,* 82**,** 1111-1116.

YEGUTKIN, G. 2008a. Nucleotide- and nucleoside-converting ectoenzymes: Important modulators of purinergic signalling cascade. *Biochim Biophys Acta,* 1783**,** 673 - 694.

YEGUTKIN, G. G. 2008b. Nucleotide- and nucleoside-converting ectoenzymes: Important modulators of purinergic signalling cascade. *Biochimica et Biophysica Acta (BBA) - Molecular Cell Research,* 1783**,** 673-694.

YU, C., SHIN, Y., CHOW, A., LI, Y., KOSMEDER, J., LEE, Y., HIRSCHELMAN, W., PEZZUTO, J., MEHTA, R. & VAN BREEMEN, R. 2002. Human, Rat, and Mouse Metabolism of Resveratrol. *Pharmaceutical Research,* 19**,** 1907-1914.

ZHANG, F.-L., GAO, H.-Q., WU, J.-M., MA, Y.-B., YOU, B.-A., LI, B.-Y. & XUAN, J.-H. 2006. Selective Inhibition by Grape Seed Proanthocyanidin Extracts of Cell Adhesion Molecule Expression Induced by Advanced Glycation End Products in Endothelial Cells. *Journal of Cardiovascular Pharmacology,* 48**,** 47-53 10.1097/01.fjc.0000242058.72471.0c.

ZHANG, X., SHU, X.-O., XIANG, Y.-B., YANG, G., LI, H., GAO, J., CAI, H., GAO, Y.-T. & ZHENG, W. 2011. Cruciferous vegetable consumption is associated with a reduced risk of total and cardiovascular disease mortality. *The American Journal of Clinical Nutrition,* 94**,** 240-246.

ZHENG, Z., CHEN, H., LI, J., LI, T., ZHENG, B., ZHENG, Y., JIN, H., HE, Y., GU, Q. & XU, X. 2012. Sirtuin 1–Mediated Cellular Metabolic Memory of High Glucose Via the LKB1/AMPK/ROS Pathway and Therapeutic Effects of Metformin. *Diabetes,* 61**,** 217-228.